

THE ROLE OF MICRO-ORGANISMS IN THE PRODUCTION
OF SEMIOCHEMICALS IN THE INTERDIGITAL SECRETION
OF THE BONTBOK, *DAMALISCUS PYGARGUS*
PYGARGUS.

by

GARY TERRI SCOTT

Thesis presented in partial fulfillment of the requirements for the degree



of
MASTER OF SCIENCE

in Chemistry

at the

University of Stellenbosch

Promoter: Dr. M. le Roux

Stellenbosch

Co-promoter: Prof. B. V. Burger

March 2004

DECLARATION

I, the undersigned, hereby declare that the work contained in this thesis is my own original work and that I have not previously in its entirety or in part submitted it at any other university for a degree.

G. T. Scott

SUMMARY

Bontebok, *Damaliscus pygargus pygargus*, formerly classified as *D. dorcas dorcas*, are territorial animals with interdigital glands between the toes of the forelegs. Males regularly defecate on dung heaps, on which they often lie, to communicate with other members of their species. They also communicate by means of visual displays, scent marking and occasionally with scraping or pawing of dung heaps. It is assumed that scent marking with the interdigital secretion serves to define territories frequented by these antelope. These glands secrete a complex mixture of volatile and non-volatile compounds and the volatile compounds in the secretion serve as a chemical signal for other bontebok.

It has been suggested that the interdigital secretion is not produced in its final composition by the interdigital gland alone, but that microbial activity is responsible for many of the compounds present in the secretion. In general, many compounds can be attributed to the by-products of microbial hydrolysis of triglycerides, a common characteristic of sebum. It is well documented that micro-organisms inhabit the deep recesses of sebaceous glands and the presence of micro-organisms has been found to be consistent in all antelope exocrine glandular areas.

This study involved the chemical characterisation of the volatile metabolites produced *in vitro* by micro-organisms from the interdigital cavity of the bontebok.

Various comparative studies were made, one of which was comparison of the metabolites produced by the individual microbial species as well as the total community of bacteria incubated in different media. A comparison of the

compounds identified in the interdigital secretion and the metabolites produced by the micro-organisms in the different media was also made.

The volatile metabolite extracts of the individual bacterial species and of the total community were chemically characterised by low-resolution gas chromatography–mass spectroscopy. Classes of compounds identified from the volatile metabolite extracts include:

- Acids – Aliphatic (saturated and unsaturated)
- Alcohols – Aliphatic (saturated and unsaturated)
- Aldehydes – Aliphatic (saturated and unsaturated)
- Aromatic compounds
- Ketones – Aliphatic (saturated and unsaturated)
- Pyrazines
- Dimethyldisulphide
- Squalene and cholesterol

Several qualitative differences were found between the compounds identified in the volatile metabolite extracts of the micro-organisms when incubated in tryptic soy broth (TSB) and minimal salt medium (MSM). In particular, when the microbes were incubated in TSB medium a number of pyrazines were found that were not present when utilising MSM as a medium.

Additional qualitative differences were found between the compounds identified in the metabolite extracts of the individual bacterial species and the total community of bacteria, when incubated in both TSB and MSM media.

A comparison of the interdigital secretion and the metabolite extracts of the microbial communities incubated in TSB and MSM revealed that many

compounds produced in MSM corresponded to the compounds identified in the interdigital secretion. These corresponding compounds were found to be saturated and unsaturated acids, aldehydes and squalene. Furthermore, there was only one corresponding compound in the case of TSB as medium.

OPSOMMING

Die bontebok, *Damaliscus pygargus pygargus*, voorheen geklassifiseer as *D. dorcas dorcas*, is 'n territoriale dier met interdigitale kliere tussen die kloutjies van die voorpote. Ramme ontlaas gereeld op mishope, waarop hulle dikwels lê, om met ander lede van die spesie te kommunikeer. Hulle kommunikeer ook deur middel van visuele seine, reukmerking en soms deur mishope met die voorpote te kap of te skraap. Reukmerking met die interdigitale afskeiding dien klaarblyklik om gebiede wat deur hierdie diere bewoon word, af te baken. Die interdigitale kliere skei 'n komplekse mengsel van vlugtige en nie-vlugtige verbindings af en die vlugtige verbindings dien as chemiese sein vir ander bontebokke.

Die vermoede bestaan dat die interdigitale klier nie alleen verantwoordelik is vir die finale samestelling van die interdigitale afskeiding nie, maar dat die mikrobiële aktiwiteit bydra tot die produksie van baie van die verbindings wat in die afskeiding aanwesig is. Sekere verbindings kan in die algemeen toegeskryf word aan die vorming van die nuweprodukte van mikrobiële hidrolise van trigliseriede, 'n algemene eienskap van sebum. Dit is bekend dat die diep holtes van vetkliere 'n goeie teelaarde is vir mikroörganismes en daar is gevind dat mikroörganismes feitlik deurgaans voorkom in alle anteloop eksokriene klierareas.

Hierdie studie behels die chemiese karakterisering van die vlugtige metaboliete wat *in vitro* deur mikroörganismes van die interdigitale klierholte van die bontebok geproduseer word.

Verskeie vergelykende studies is uitgevoer waarvan een die vergelyking was van die metaboliete wat deur die individuele mikrobiële spesies sowel as die

totale gemeenskap van bakterieë geproduseer word tydens inkubasie in verskillende media. Vergelyking van die verbindings wat in die interdigitale afskeiding geïdentifiseer is met die metaboliete wat in verskillende media geproduseer is, het ook deel van die studie uitgemaak.

Die vlugtige metaboliet ekstrakte van die individuele bakteriese spesies en van die totale gemeenskap is chemies gekarakteriseer deur middel van lae-resolusie gaschromatografie-massaspektrometrie. Die volgende groepe verbindings is onder andere in die vlugtige metaboliet ekstrakte geïdentifiseer:

- Sure – Alifaties (versadig en onversadig)
- Alkohole – Alifaties (versadig en onversadig)
- Aldehiede – Alifaties (versadig en onversadig)
- Aromatiese verbindings
- Ketone – Alifaties (versadig en onversadig)
- Pirasiene
- Dimetieldisulfied
- Skwaleen en cholesterol

Verskeie kwalitatiewe verskille is gevind tussen die verbindings wat geïdentifiseer is in die vlugtige metaboliet ekstrakte van die mikroörganismes onderskeidelik in TSB medium en MSM geïnkubeer. Opvallend was byvoorbeeld die voorkoms van pirasiene in gevalle waar mikroörganismes in TSB medium geïnkubeer is, terwyl hierdie groep verbindings afwesig was wanneer MSM gebruik is.

Onderlinge kwalitatiewe verskille is ook gevind tussen die verbindings wat geïdentifiseer is in die metaboliet ekstrakte van die individuele bakteriese

spesies en die totale gemeenskap van bakterieë, wanneer in TSB medium sowel as in MSM geïnkubeer is.

Vergelyking van die verbindings in die interdigitale afskeiding en in die metaboliet ekstrakte van die mikrobiële gemeenskappe, het getoon dat 'n aantal verbindings wat in MSM geproduseer is, ooreenstem met verbindings wat in die interdigitale afskeiding geïdentifiseer is. Daar is gevind dat hierdie verbindings versadigde en onversadigde sure en aldehyde en skwaleen is. Met TSB as medium was daar slegs een ooreenstemmende verbinding.

ACKNOWLEDGEMENTS

Sincere thanks and appreciation to following persons:

- Dr. M. le Roux for the patience and guidance in the many fields of her expertise and most importantly her belief in me and the project.
- Prof. B.V. Burger for the willingness to share his experience in and devotion to the field of ecological chemistry.
- Mrs. W.J.G. Burger, the kind hands that manufactured the gas chromatographic columns and the kind heart that always lifted my spirits.
- Prof. G.M. Wolfaardt, Elana, Keith, Venessa, Murray and everyone else in the ecological microbiology lab for their advice and unwavering characters that made all the microbiology possible.
- Mr. Steve Mitchell for his time and capture of bontebok.
- Brenda Marx and Ngassi for friendship.
- My family, Reneze and friends for their steadfast support.

*Something is right when it preserves
the integrity, stability and beauty of
the biotic community*

Aldo Leopoldt

CONTENTS

CHAPTER 1

INTRODUCTION AND OBJECTIVES

1.1	OLFACTION	3
1.1.1	General physiology of olfaction	3
1.1.1.1	The trigeminal sense in the olfactory epithelium	6
1.1.1.2	Chemical olfactory stimulation - Theories on olfaction	7
1.1.1.2.1	The Steric Theory of Odour	7
1.1.1.2.2	The Vibrational Theory of Odour	8
1.2	SEMIOCHEMICAL COMMUNICATION	9
1.2.1	What is Semiochemical Communication?	9
1.2.2	Intraspecific Communication	10
1.2.3	Interspecific Communication	10
1.3	THE BONTEBOK	12
1.3.1	The histology of the interdigital gland	13
1.4	THE ROLE OF MICRO-ORGANISMS IN THE PRODUCTION OF SEMIOCHEMICALS	17

1.5	OBJECTIVES OF THIS STUDY	19
-----	--------------------------	----

	References: Chapter 1	21
--	------------------------------	----

CHAPTER 2

ISOLATION OF THE VOLATILE METABOLITES OF MICRO-ORGANISMS FROM THE INTERDIGITAL CAVITY OF THE BONTÉBOK

2.1	ISOLATION OF BACTERIA AND CULTIVATION IN DIFFERENT GROWTH MEDIA	24
-----	---	----

2.2	DETERMINATION OF GROWTH CURVES FOR EACH INDIVIDUAL MICRO-ORGANISMS	27
-----	--	----

2.3	EXTRACTION OF MICROBIAL METABOLITES	34
-----	-------------------------------------	----

	References: Chapter 2	35
--	------------------------------	----

CHAPTER 3

CHEMICAL CHARACTERISATION OF THE VOLATILE METABOLITES OF MICRO-ORGANISMS FROM THE INTERDIGITAL CAVITY OF THE BONTEBOK

3.1	STRUCTURAL DETERMINATION OF THE MICROBIAL METABOLITES PRODUCED IN TSB AS GROWTH MEDIUM	38
3.1.1	Alcohols	38
3.1.2	Aldehydes	42
3.1.3	Ketones	47
3.1.4	Aromatic compounds	51
3.1.5	Pyrazines	58
3.2	IDENTIFICATION OF THE MICROBIAL METABOLITES PRODUCED IN MSM AS GROWTH MEDIUM	65
3.2.1	Alcohols: Aliphatic	65
3.2.2	Aldehydes: Aliphatic (Saturated)	66
3.2.3	Aldehydes: Aliphatic (Unsaturated)	70
3.2.4	Acids: Aliphatic (Saturated)	72
3.2.5	Acids: Aliphatic (Unsaturated)	75
3.2.6	Ketones: Aliphatic	76
3.2.7	Aromatic compounds	77
3.2.8	Squalene	77
	References: Chapter 3	126

CHAPTER 4

DISCUSSION AND COMPARISON OF RESULTS

4.1	COMPARISON OF THE RESULTS OBTAINED WITH DIFFERENT GROWTH MEDIA	129
4.2	COMPARISON OF THE METABOLITE PROFILES PRODUCED BY THE INDIVIDUAL INTERDIGITAL MICRO-ORGANISMS AND BY THE TOTAL COMMUNITY OF MICRO-ORGANISMS	130
4.2.1	TSB as growth medium	130
4.2.2	MSM as growth medium and glucose as carbon source	134
4.3	COMPARISON OF THE COMPOUNDS PRESENT IN THE INTERDIGITAL GLAND SECRETION AND THE METABOLITES PRODUCED BY THE TOTAL COMMUNITY OF MICRO-ORGANISMS (IN TSB AND MSM)	138
	References: Chapter 4	141

CHAPTER 5

EXPERIMENTAL

5.1	GENERAL	142
5.2	INSTRUMENTATION	142
5.3	SAMPLING OF BIOLOGICAL MATERIAL	143
5.4	ISOLATION OF MICRO-ORGANISMS AND INOCULATION OF MICRO-ORGANISMS INTO LIQUID BROTHS	143
5.5	ISOLATION OF MICROBIAL METABOLITES	145
5.5.1	Incubation in tryptic soya broth (TSB) medium	145
5.5.2	Incubation in minimal salts medium (MSM) with glucose as the carbon source	146
5.6	DETERMINATION OF THE GROWTH CURVES	147
5.7	SYNTHESIS OF REFERENCE COMPOUNDS	148
5.7.1	Preparation of phenylacetamide	149
5.7.2	Preparation of 3-methyl-3-buten-2-ol	149
5.7.3	Preparation of alkylpyrazines	150

References: Chapter 5	152
------------------------------	-----

ADDENDUM A	153
-------------------	-----

CHAPTER 1

INTRODUCTION AND OBJECTIVES

Man has always been fascinated by smell. It has been one of our greatest fascinations and we express this fascination by masking our own scents by the use of other "more desirable" scents. Perfumes are used on our bodies, our clothes, in our surroundings, many of our commercial products are scented to make them more appealing and one product may have a variety of scents to provide man more choices to suit his sense of smell. Odours that are considered as bad or as unpleasant are masked with ones that are more pleasant and consequently all the valuable information that could have been transmitted by a particular odour is lost.

The sense of smell is almost unutilised by humans when compared to other organisms of the animal kingdom. Many organisms have adapted their sense of smell in various ways to function, *inter alia*, in the detection of danger, the recognition of a member of the same species, the recognition of their young and the distinguishing and detecting of food. Motile micro-organisms, the smallest living creatures, have adapted to their surroundings by being able to respond to chemical stimuli such as certain amino acids, sugars and chemical products of the Krebs's cycle¹. Predatory microbes prey on other microbes in much the same way white corpuscles respond to alien cells in the body. It has been established that certain microbes respond to compounds in their environment, which they do not require for metabolism², by means of chemoreceptors on the surface of the microbe. When these are not triggered, the microbe instinctively swims away. This ability to respond to external chemical stimuli is called chemotaxis and has been considered the simplest form of smell. An acute sense of smell is one of the many abilities man has lost

since he took upon himself the task of becoming civilised. It is quite evident that, with some exceptions, man cannot gather information or interpret his environment by smell.

However, man became interested in the ability of other organisms to gather information by simply smelling the surrounding environment and now man seeks means to translate what the individual scents mean to the respective organisms. The study of semiochemistry has developed from this fascination and in the same manner has been fuelled by the interests of man to understand the signals produced by organisms. It is thought of as a relatively simple task by most, but many organisms use complex mixtures of compounds to convey messages to other organisms. The scent or signal may be used interspecifically, that is between organisms from different species, or intraspecifically, that is, between organisms of the same species. To make it even more complex, the scents may convey specific messages and the signals may change due to a change in season or a change in habitat. Female white mice remain sterile if no male is present and in approximately three days after the introduction of a virile male, the females become fertile due to an androgen-dependent component in the male's urine³. Female white mice make male members of the species aware that they are fertile by emitting hormones in their urine and if an alien male mouse is present in the population, the females emit a hormone which prevents fertilisation. This complexity makes it increasingly difficult to interpret the meaning of the scents. If these messages were understood, it could be possible to regulate organisms by preparing a mixture of the correct composition and inducing the desired response. As most organisms do not readily procreate in captivity, animals that struggle to breed in captivity could, for example, be induced into their respective breeding cycles. In zoos, for instance, certain females are artificially inseminated, a very stressful procedure which could be avoided in this way. Pest control in crops

could be possible without the use of pesticides, which also harm and kill useful insects. Another important application would be the use of semiochemicals in the regulation of animals considered by farmers as vermin. Every year, farmers kill many animals that destroy crops and if semiochemic control were possible, a more humane method could be used to regulate the reproduction of these animals. These possibilities are the driving force behind the study of compounds involved in chemical communication, namely semiochemistry.

1.1 OLFACTION

The sense of smell is a primal sense for animals⁴. From an evolutionary viewpoint, it is one of the most ancient of senses. Smell (or olfaction) allows vertebrates and other organisms with olfactory receptors to identify food, mates, predators, and provides both sensual pleasure (the odour of flowers and perfume, for example) as well as danger warnings (spoiled food, chemical pollutants). For animals, it is one of the most important means by which they communicate with their environment.

1.1.1 General physiology of olfaction

Odouriferants are volatile chemical compounds that are carried by inhaled air to the Regio olfactoria (olfactory epithelium) located in the roof of the two nasal cavities of the mammalian nose, just below and between the eyes (see Fig. 1.1).

The odouriferant must possess certain molecular properties in order to provide sensory stimulus. It must have a degree of water solubility, a sufficiently high

vapour pressure, the ability to dissolve in fat (lipophilicity), surface activity and a molecular weight not exceeding a molecular mass of approximately 290 Da.

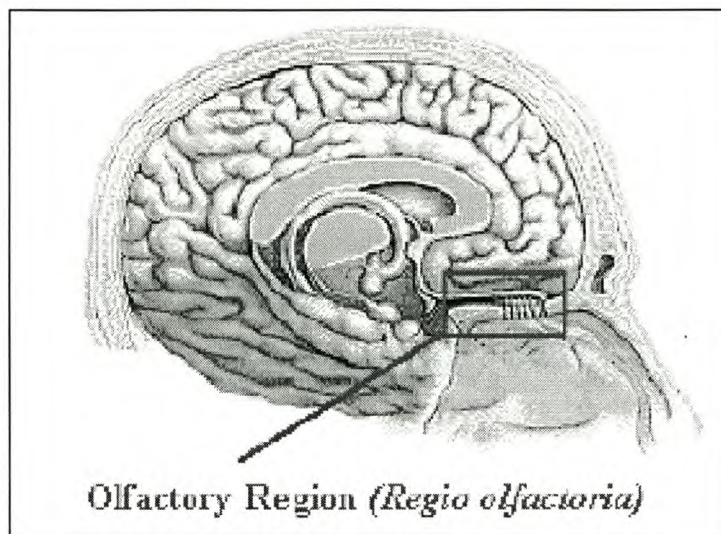


Fig. 1.1: The olfactory region⁴

The mammalian olfactory system is able to distinguish among a practically infinite number of chemical compounds at very low concentrations. The olfactory region of each of the two nasal passages in mammals is a small area of about 2.5 square centimetres containing in total approximately 50 million primary sensory receptor cells. It consists of cilia projecting down out of the olfactory epithelium into a layer of mucus, which is about 60 microns thick (see Fig. 1.2). This mucous layer is a lipid-rich secretion that bathes the surface of the receptors at the epithelium surface and the layer is produced by the Bowman's glands, which reside in the olfactory epithelium. The mucous lipids assist in transporting the odouriferant molecules, as only volatile materials that are soluble in the mucus can interact with the olfactory receptors and produce the signals that the brain interprets as odour. Each olfactory receptor neuron has 8-20 cilia that are whip-like extensions 30-200 microns in length. The olfactory cilia are the sites where molecular reception of the odouriferant and sensory transduction (transmission) starts.

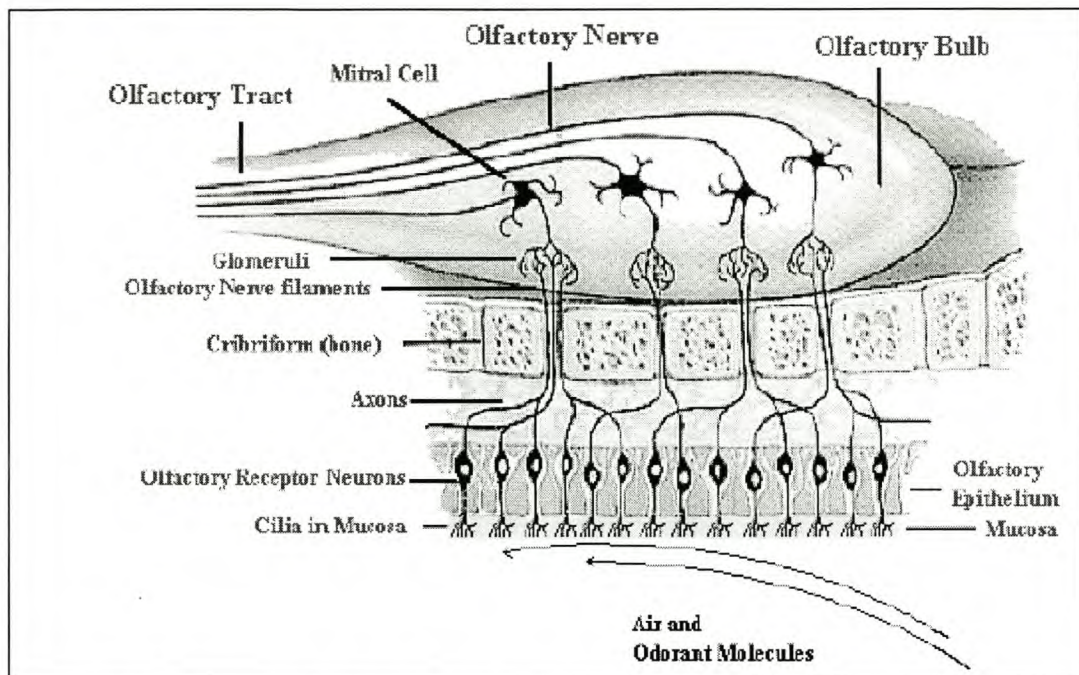


Fig. 1.2: A magnified, sectional view of the olfactory region⁴

Above the mucous layer is the base olfactory epithelium, which consists partially of basal cells located in the lowest cellular layer of the olfactory epithelium, which are capable of mitotic cell division to form olfactory receptor neurons when functionally mature. The olfactory receptor neurons replicate approximately every 40 days. The epithelium also contains pigmented cells that are light yellow in humans and dark yellow to brown in dogs. The intensity of colour seems to be correlated with olfactory sensitivity. While the olfactory receptor neurons extend through the epithelium to contact odouriferants in the atmosphere, on the opposite side within the epithelium, the neuronal cells form axons that are bundled in groups of 10-100. These bundles penetrate the ethmoidal cribriform plate of bone, reaching the olfactory bulb of the brain where they converge to terminate with post-synaptic cells to form synaptic structures called glomeruli. The glomeruli are connected in groups that converge into mitral cells. (Note that in Fig. 1.2 above this convergence is not clearly depicted). For example, in rabbits, there are 26,000 receptor neurons

converging onto 200 glomeruli, which then converge at 25:1 onto each mitral cell. The total convergence is estimated to be about 1000:1.

Physiologically, this convergence increases the sensitivity of the olfactory signal sent to the brain. From the mitral cells, the message is sent directly to the higher levels of the central nervous system in the corticomедial amygdala portion of the brain (via the olfactory nerve tract). Here the signalling process is decoded and olfactory interpretation and response occurs.

1.1.1.1 The trigeminal sense in the olfactory epithelium

Whereas the olfactory receptor system is highly localised in mammals, it must also be noted that the olfactory epithelium contains another sensory system in the form of trigeminal nerve receptors. The fifth cranial or trigeminal nerve, which is the largest cranial nerve, is the nerve responsible for sensing of stimuli in the face, teeth, mouth, most of the scalp, and it is the motor nerve of the muscles used for mastication. The nerve provides a second set of nerve endings, which are responsible for tactile, pressure, pain and temperature sensations in the areas of the mouth, eyes and nasal cavity. A number of chemical trigeminal stimulants produce effects described as hot, cold, tingling or irritating. For example, (-)-menthol produces the trigeminal feeling of "cold" at moderate concentrations and "hot" at high concentrations in the nasal cavity. This type of sensory "description" is often not just limited to the areas of the nose, mouth and eyes. It also occurs on skin areas not served by the fifth cranial nerve (especially, the genitalia) and thus such stimulants may affect a variety of nerve endings. Similarly, camphor, which possesses markedly more aroma than menthol, also produces the "cold" sensation via interaction with trigeminal receptors. According to Ohloff, about 70% of all odours are said to

stimulate the trigeminal nerve although, in general, they may be several times less sensitive than olfactory receptors⁵.

Other commonly encountered trigeminal stimulants include chemicals like allyl isothiocyanate (mustard, mustard oil), capsiacin (hot Chile powder, mace spray) and diallyl sulphide (onion) (see Fig. 1.3).

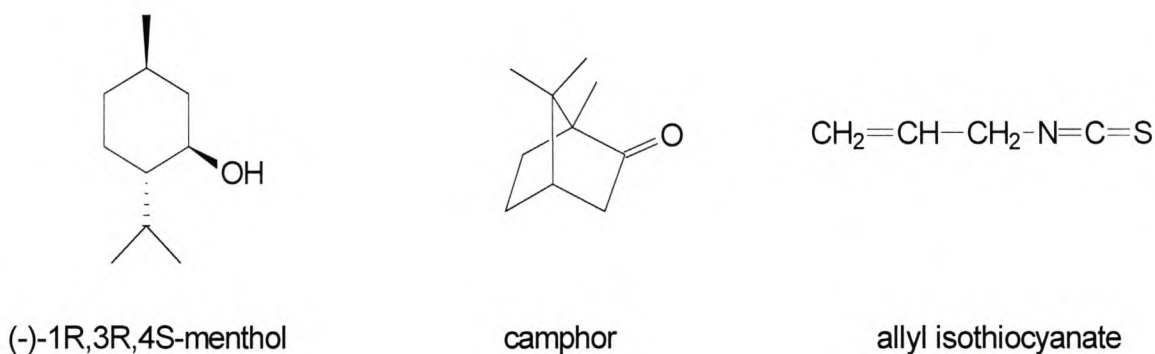


Fig. 1.3: Examples of molecules that affect the trigeminal sensory nerve.

1.1.1.2 Chemical olfactory stimulation - Theories on olfaction

Over the years, a number of theories relating odouriferant quality to molecular structure have been proposed. The two most prominent theories will be discussed briefly.

1.1.1.2.1 The steric theory of odour

In 1946, future Nobel laureate, Linus Pauling⁶ indicated that a specific odour quality is due to the molecular shape and size of the chemical. Similarly, in his book, "Molecular Basis of Odour", John Amoore⁷ extended the idea of a "Steric Theory of Odour" originally proposed by R.W. Moncrieff in 1949⁸. Amoore

stated that air-borne chemical molecules are smelled when they fit into certain complimentary receptor sites on the olfactory nervous system. This "lock and key" approach was an extension from enzyme kinetics. Amoore proposed the term primary odours (ethereal, camphoraceous, musky, floral, minty, pungent and putrid). The molecular volume and shape similarity of various odour chemicals were compared by making hand-prepared molecular models and physically measuring volume and creating silhouette patterns. The steric theory is well suited to the idea that the odouriferant receptor proteins accept only certain odouriferants at a specific receptor site.

1.1.1.2.2 The vibrational theory of odour

In 1938, Dyson⁹ suggested that the infrared resonance (IR), which is a measurement of a molecule's vibration, might be associated with odour. This idea was popularised by R.H. Wright¹⁰ in the mid-1950's when infrared spectrophotometers became generally available for such spectral measurements, which Wright was able to correlate with certain odouriferants.

During the 60's and early 70's, vigorous debate raged as to the validity of each theory for classifying chemical odouriferants. By the mid-70's, it appeared that Wright's theory had failed a critical test. The optical enantiomers of menthol¹¹ and of carvone¹² smelled distinctly different, although the corresponding infrared spectra were identical. An extensive site that provides over 100 enantiomeric pairs of odouriferants that have differing odour properties was recently published on the internet by Leffingwell. This site provides both 2-D and 3-D molecular structures along with odour descriptors, odour thresholds and original references.

1.2 SEMIOCHEMICAL COMMUNICATION

1.2.1 What is semiochemical communication?

The word semiochemical is derived from the Greek words *semeion* (sign or signal) and *chemeceia* (alchemic). Many organisms use organic compounds to convey messages to other organisms¹³. This type of communication is called semiochemical communication and the compounds or mixtures of compounds involved are named semiochemicals. In other words, semiochemicals are compounds that carry signals between organisms.

A whole spectrum of chemicals that act as semiochemicals exists and thus further distinctions are made based on the areas or senses they affect (see Fig. 1.4). The first group of semiochemicals are those compounds that act intraspecifically in the communication between members of the same species while the second group represents those that act interspecifically, that is, between members of different species. It is important to note that hormones and nucleic acids are distinguished from semiochemicals because hormones and nucleic acids communicate within an organism.

An important advantage of semiochemical communication lies in the fact that, unlike speech, chemical information can remain behind for days or even weeks. The receiving organism could therefore detect the semiochemical signal long after the emitting organism has left the area. Another advantage is that in some cases the emitting organism does not need to reproduce the chemical signal frequently. The ability of the chemical signal to remain in its surroundings for a long duration of time makes it possible for certain mammals to have large territories because the perimeter of the territory does not have to be marked with high frequency.

1.2.2 Intraspecific communication

The compounds responsible for intraspecific communication, more commonly known as pheromones, are sub-divided into two groups, namely releasers and primers, based on the behaviour of the receiving organism. Releasers are responsible for communication when the receiving organism shows an immediate response and primer pheromones are noted to first affect a physiological change in the recipient before it manifests a response in the recipient. An example of a releaser pheromone would be a sex attractant used by female insects upon which the male reacts and exhibits sexual behaviour. The action of a primer pheromone is delayed and a response only occurs sometime after initial reception of the semiochemical. An example of a primer pheromone is the blockage of the ova in female mice after an alien male is introduced into the population.

1.2.3 Interspecific communication

In interspecific semiochemical communication two types of signals exist, namely those that favour the transmitter of the scent and those favouring the receiver. Interspecific communicating compounds are collectively known as allelomones and if an allelomone favours the transmitter and promotes a response in the receiver, whether physiological or behavioural, it is called an allomone. An example of this type is the response of organisms to the foul smell of a skunk when it ejects its secretion into the air. An allelomone that benefits the receiving organism is known as a kairomone, for example when the predator becomes aware of its prey.

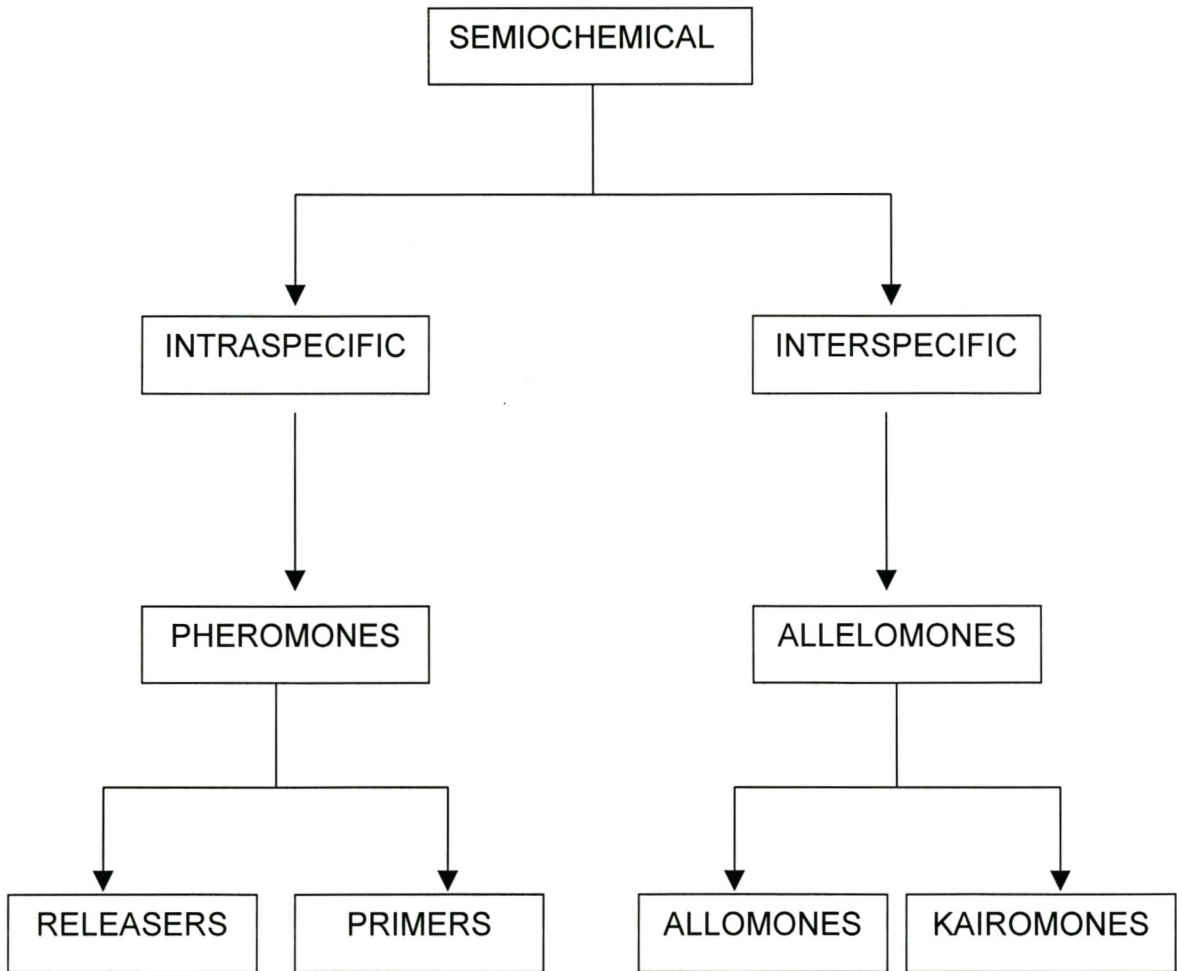


Fig. 1.4: The semiochemical concept

1.3 THE BONTEBOK

The name bontebok is derived from *bont* (Afrikaans), meaning multicoloured and *bok* (Afrikaans), meaning buck¹³. There has been some confusion with respect to its scientific classification in the past. The former name *Damaliscus dorcas dorcas* has since been changed to *Damaliscus pygargus pygargus*, from *Damalis* (Greek) meaning a young cow, *iscus* (Latin) diminutive suffix, *puge* (Greek) meaning the rump and *argos* (Greek) meaning shining; hence *pugargos*, meaning white rump. The bontebok is an antelope from the subfamily *Acelaphinae*, the members of which all have interdigital glands between the toes of their forelegs. Bontebok were first observed as early as 1652 in herds so large that it took days to pass on horseback. However, two years later the early farmers who established farms in the area described the herds as being between twelve and twenty¹⁵ due to extensive hunting. Once the early European farmers established themselves in the bontebok habitat, they cleared vast lands for agriculture and the bontebok were considered as intruders. The result was that the bontebok was hunted to the brink of extinction by 1931, with as few as 17 animals left in the country. With careful conservation, their numbers have increased to between 2000-3000. Most bontebok now flourish in private reserves and on private game farms.

The hair of the bontebok is soft and has an iridescent sheen¹⁶. The body colour is a deep purple-brown with a white blaze on the buttocks and is distinguished from blesbok by the solid white blaze on the face. The horns are strongly ridged, lyre shaped and grow to approximately 35-50 cm. Territorial males defecate on the limited number of dung heaps, on which they often lie, to communicate with other members of their species¹⁷. They also communicate by means of visual displays, scent marking and occasionally with scraping or pawing of dung heaps¹⁸. Both sexes have preorbital, pedal or interdigital

glands. These glands secrete a complex mixture of volatile and non-volatile compounds and the volatile compounds in the secretion serve as a chemical signal for other bontebok^{19,20,21}. It has been suggested that the non-volatile compounds in the mixture serve as a controlled-release agent for the volatile components which makes it possible for the scent of the markings to linger long after the antelope has departed from that section of the territory.

1.3.1 The histology of the interdigital gland

The interdigital gland of the bontebok is situated between the hoofs on the front leg. The gland itself can be described as a sheath enclosing the interdigital cavity, but it should be noted that the sheath has an opening in its length²². In adult members of the species, the sheath is approximately 55 mm in length with an approximate diameter of 20 mm and a wall-thickness of approximately 3 mm (see Figures 1.5 and 1.6). Long, single hairs grow in the cavity on the inner surface of the sheath and due to the secretion, the hairs have a distinct yellow-brown colouration. It has been proposed that the hairs aid the emission of the volatile components present in the interdigital cavity.

The tissue of the gland (described above as the sheath) is a modified skin appendage derived from downgrowths of epidermal epithelium during development²³. These appendages (see Fig. 1.7) can be classed as

- Hair follicles and their products, *hair*.
- Sebaceous glands and their products, *sebum*.
- Eccrine sweat glands and their products, *sweat*.
- Apocrine sweat glands and their products, *serous secretion*.

As previously mentioned, the hairs could be an aid for the emission of volatiles and grows from the follicle. The follicle is responsible for the production of a hair and the ducts of sebaceous and apocrine glands open into the follicle (see Fig. 1.7).

The follicle is of nearly uniform diameter except at the base, where it expands to form the bulb. The outermost part of the follicle is a downgrowth of the epidermis called the external or outer root sheath. Other cells forming the bulb, including those that surround the connective tissue are collectively called the matrix. The cells that make up the matrix are aptly named the matrix cells.

The sebaceous glands develop as an outgrowth of the external root sheath of the hair follicle, usually producing several glands per follicle. The oily substance produced in the gland is called sebum and is the product of holocrine secretion. In this, secretory cells develop on the periphery of the glandular lobule and are slowly displaced towards the centre of the lobule by newly developing cells. As the cells move toward the centre they fill with lipids and simultaneously degenerate. Ultimately, the secretory product and the cell debris are discharged from the gland into the pilosebaceous canal.

The function of sebum is not clearly defined²⁴. Various investigators have ascribed bacteriostatic, emollient, barrier and pheromone functions to sebum. What is known is that the triglyceride content of sebum is broken down by micro-organisms on the surface, to liberate free fatty acids²⁵.

Sweat glands are classified based on their structure and the nature of their secretion. The two types of sweat glands recognised are eccrine sweat glands and apocrine sweat glands.



Fig. 1.5: The yellow colouration of secretion indicating the entrance to the interdigital gland cavity.



Fig. 1.6: Bontebok interdigital gland. The gland is in the form of a pouch with a wall-thickness of 2-3 mm.

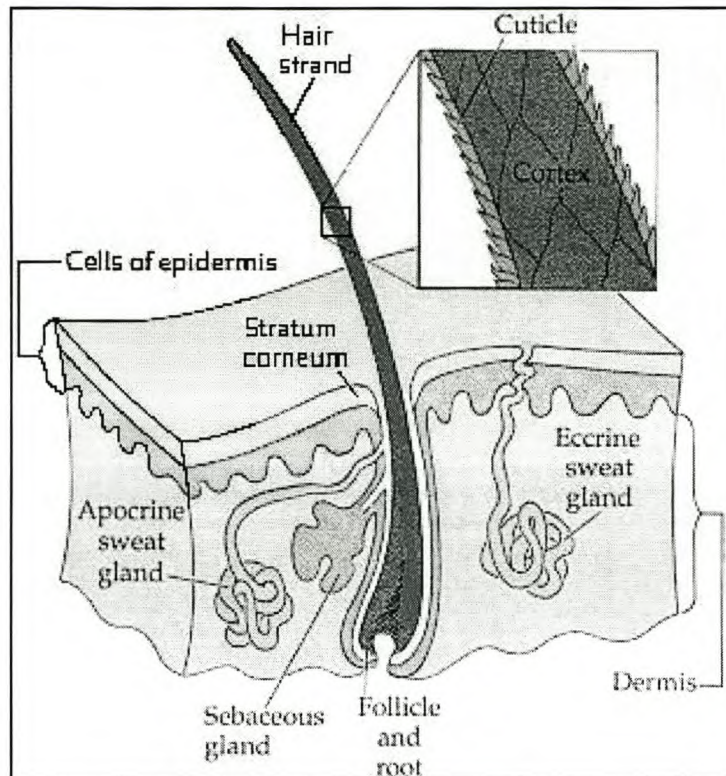


Fig. 1.7: Illustration of skin appendages.

The term apocrine glands encompasses a variety of structures which were once thought to share a common secretory mechanism in which the apical portions of secretory cells are shed leaving the remainder of the cell intact. The glands occur throughout the hairy skins of most carnivores and many other mammals and their main function is thought to aid thermoregulation. In contrast to eccrine glands, human apocrine glands are usually associated with hair follicles, discharging into the pilosebaceous canal, above the sebaceous duct. The gland consists of a tube and an inner coiled part, which is lined with secretory tissues. With exception of a relatively straight duct, which opens into the pilosebaceous canal, the entire structure is embedded deep in the dermis (see Fig. 1.7).

The eccrine gland is a simple, coiled secretory tube embedded in the dermis and a duct leading directly to the skin surface. Eccrine sweat is the most dilute of the body fluids consisting of approximately 99% water. Sweating can occur in response to emotional stress, however such sweating exhibits characteristics that distinguish it from sweating caused by exercise.

1.4 THE ROLE OF MICRO-ORGANISMS IN THE PRODUCTION OF SEMIOCHEMICALS

It appears that each organism (even within a species) is unique in the details of the microbial ecology of its skin²⁶. Not only are there variations in the strains of bacteria present but the distribution of the micro-organisms over the skin surface differs from individual to individual.

The major bacterial contributors are members of the Micrococcaceae and various aerobic diptheroids. These micro-organisms inhabit the deep recesses of the sebaceous glands, but although these organisms are normally inhibited by oxygen, substances present in the skin surface appear to enable them to grow aerobically²⁷. Many glands and even the human skin surface are characterised by high levels of long-chain free fatty acids. These are derived by microbial hydrolysis from triglycerides, the occurrence of which in large quantities is a characteristic of human sebum^{28,29}.

The role micro-organisms play in the production of semiochemicals have been reported in human studies, but very little research has been done for non-human species. It has been suggested³⁰ that all mammalian glands are microbiologically active because glands provide surface lipids, proteins, carbohydrates, water and minerals and these conditions are suitable for microbial growth. More specifically, the presence of micro-organisms is

consistent in all the glands of antelope from the pedal gland to the pre-orbital gland³¹.

The mammalian body surface provides a variety of habitats where microbial species can flourish, utilising and converting the mammal's secretion and excretions by the microbes' metabolic pathways. The microbes convert these exudates into primary metabolites (which never leave the cell) and into secondary metabolites, which are excreted. These excreted metabolites could serve as mammalian semiochemicals, but it must be noted that not all secondary metabolites would act as semiochemicals. Therefore, it is immaterial that these mammalian semiochemicals may be produced by the microbes, which its body supports³². The chemical compound only needs to be stable enough to be potentially useful to the mammal. Many important odouriferants identified in mammalian chemical communication are known microbial products.

Strict anaerobes (bacteria that flourish in environments without oxygen) are often important odour producers. Although aerobes (microbes that flourish in oxygen-rich environments) themselves are important odour producers, aerobes serve as an important means of removing oxygen from the immediate environment, allowing anaerobes to flourish in the environment, where they normally would wither, thus sustaining symbiosis by this interaction. The different organisms providing one another with metabolites in a nutrient limited environment could further extend the symbiosis, thus the symbiosis could be considered mutualistic. It must be noted that for the two groups of microbes (aerobes and anaerobes) to survive in the same environment, the environment cannot be closed off from air entirely. On the other hand, the environment cannot be entirely open to air, as the aerobes would not be able to effectively remove all the oxygen. Therefore, they would have to exist in a micro-

environment such as a sac, pouch, invagination or crevice. Due to the complexity and the difficulties in studying a micro-environment of this nature, namely an anaerobic growth environment and the strict anaerobic microbes of a mammalian scent organ, this can be a considerable task to undertake.

The interest in the role of microbes arose when chemical characterisations of glandular secretions were studied and some of the compounds identified in the secretion were not found to be present in the glandular tissue³³. Therefore, the existence of another entity had to be present to produce the compounds, which were not observed in the glandular tissue. Further research led to the conclusion that microbes were present and in most cases, the metabolites of these microbes corresponded to the compounds of unknown origin in the glandular secretion³⁴.

1.5 OBJECTIVES OF THIS STUDY

As previously mentioned in Section 1.3, bontebok males mark their territory by various methods, one of which is scent marking. It has been suggested that scent marking with the exudate of the interdigital gland serves to define territories frequented by these animals¹⁷. Importantly it has also been suggested that micro-organisms contribute to the complexity of the secretion¹⁷.

In order to study the role played by the bacteria present in the interdigital cavity of the bontebok in the production of semiochemicals, a first objective was the isolation of the individual microbial species (isolates) from the interdigital gland and the determination of the most suitable growth medium for enrichment of the bacterial cultures and for the production of metabolites. A further objective of this study was the characterisation of the metabolites produced by the

microbes and the comparison of the results with the compounds identified in a previous study of the interdigital secretion³⁵.

An additional aim of the study was to compare the metabolites produced by the individual species of bacteria to the metabolites produced by the total community of bacteria. This was done to determine to what extent the metabolite profiles of the total community and those of the isolates differ, which may be indicative of mutualism (synergism) between the micro-organisms or the inhibition of one micro-organism by another in the interdigital cavity.

References: Chapter 1

1. C. Weibull, *The Bacteria*, Vol. 1, Academic Press, New York (1960), p. 153.
2. J. Alder, Chemoreceptors in bacteria, *Science* **166**, 1588 (1969).
3. E.S. Albone, *Mammalian Semiochemistry: The investigation of chemical signals between mammals*, John Wiley & Sons, New York (1984), pp. 13-28 and 201-225.
4. J.C. Leffingwell and Associates, *Leffingwell Reports*, Olfaction-Update No. 5, **2** (1), pp. 1 – 34 (2002).
5. G. Ohloff, *Scent and Fragrances*, Springer-Verlag, Berlin Heidelberg (1994), p 6.
6. L. Pauling, Molecular Architecture and Biological Reactions, *Chem. Eng. News* **24**, 1375 (1946) (referenced by Ref 4).
7. J.E. Amoore, *Molecular Basis of Odor*, C.C. Thomas, Publ., Springfield (1970).
8. R.W. Moncrieff, What is Odour. A New Theory, *Am. Perfumer* **54**, 453 (1949).
9. G.M. Dyson, The Scientific Basis of Odour, *Chem. Ind.* **57**, 647 (1938).
10. R.H. Wright, *The Sense of Smell*, CRC Press, Boca Raton, Florida (1982).
11. J.C. Leffingwell, *Comment in Gustation and Olfaction*, G. Ohloff and A. Thomas, Ed, Academic Press, New York (1971), p. 144.
12. E.E. Langenau, *Olfaction and Taste*, C. Pfaffman, Ed., Rockefeller University Press, New York (1967).
13. F.E. Regnier, *Biology of Reproduction* **4**, 309 (1971).

14. D.E. Wilson and D.M. Reeder (Ed), *Mammal Species of the World* (second edition), Smithsonian Institution Press, Washington (1993).
<http://nmnhwww.si.edu/msw/> and
<http://www.ultimateungulate.com/artiodactylia>
15. P. Hopkins, Back from the brink, *Timbila* (South African National Parks) **1** (8), 24 (1998). www.southafricanartist.co.za/cochnotes/bontebok.htm
16. Ref. 13, and <http://www.ultimateungulate.com/artiodactylia>
17. B.V. Burger, A.E. Nell, H.S.C. Spies, M. le Roux, R.C. Bigalke and P. A. J. Brand, Mammalian exocrine secretions XII: Constituents of interdigital secretions of bontebok, *Damaliscus dorcas dorcas*, and blesbok, *D. d. phillipsi*, *J. Chem. Ecol.* **25** (9), 2057 (1999).
18. Ref. 3, pp. 74 – 109.
19. W.B. Quay and Dietland Müller-Schwarze, *J. Mammology* **52**, 670 (1971).
20. L.M. Prescott, J.P. Harley and D.A. Klein, *Microbiology* (fourth edition), McGraw-Hill, New York (1999).
21. A.E. Nell, *Reuksintuiglike Kommunikasie: Chemiese Karakterisering van die Bontebok, Damaliscus dorcas dorcas en die Blesbok, Damaliscus dorcas phillipsi*, Ph. D. Thesis, Stellenbosch University (1992), pp. 176-202.
22. Ref. 20, pp. 170 and 183
23. M.H. Ross, L.J. Romrell, G.I. Kaye, *Histology: A text and atlas* (third edition), Williams & Wilkins, Baltimore, USA, pp. 382-390 (1995).
24. Ref. 23, p. 383
25. Ref. 3, pp. 42 - 54.
26. Ref. 3, pp. 135 -164.

27. C.M. Evans and K.L. Mattern, The aerobic growth of *Propionibacterium acnes* in primary cultures from skin, *J. Investig. Dermatol.* **72**, 143 (1979).
28. R.R. Marples, The microflora of the face and acne lesions, *J. Investig. Dermatol.* **62**, 326 (1974)
29. J.H. Cove, K.T. Holland and W.J. Cunliffe, An analysis of sebum excretion rate, bacterial population and the production rate of free fatty acids on human skin, *Br. J. Dermatol.* **103**, 383 (1980).
30. V.E Sokolov, N.A. Ushakova, V.I. Prikhod'ko, T.I. Neklyudova, V.S. Gromov and I.P. Belousova, *Microbiology (Russian, Mikrobiologiya)* **59**, 472 (1990).
31. Ref. 3, p. 135.
32. Ref. 3, p. 135.
33. Ref. 20, pp. 191 -192.
34. Ref 21, pp. 176 - 190. Microbiology conducted by Prof P.A.J. Brand (Univ. Potchefstroom).
35. Ref. 21, pp. 163-169.

CHAPTER 2

ISOLATION OF THE VOLATILE METABOLITES OF MICRO-ORGANISMS FROM THE INTERDIGITAL CAVITY OF THE BONTBOK

The methods employed for the collection of the secretion from the interdigital cavity, the isolation of the microbes from the secretion and their inoculation in different growth media, as well as the extraction of the volatile metabolites for chemical analysis, will be discussed below. The experimental detail is reported in Chapter 5.

2.1 ISOLATION OF BACTERIA AND CULTIVATION IN DIFFERENT GROWTH MEDIA

For the purpose of this study, interdigital secretion was collected from a bontebok that had been darted with a tranquilliser before relocation from AE&CI near Somerset West to a guest farm nearby. Samples were taken from both left and right forelegs of the bontebok for the purpose of comparing the microbial communities of the right and left interdigital cavities. Samples were also taken from the surrounding soil, to assess potential contribution of environmental microbes and reveal contamination.

Samples collected from the interdigital cavity with sterile swabs were diluted and streaked out on agar plates, which contained a suitable nutrient for microbial growth. The inoculated plates were then incubated for the enrichment of the microbial samples.

Initially, different media were used to plate the secretion to determine which medium would be best for plating the microbes. Certain micro-organisms prefer selective media due to their specific growth requirements and may not grow on complex (non-selective) media. This method of isolation therefore attempted to eliminate the possibility of missing microbes that may be present, but are unable to grow on complex media. All the isolates were plated using the streak-plate technique¹.

Six bacterial strains were isolated from the interdigital cavity of the bontebok and they were respectively labelled R1.1, R1.2, R2.1, R3.1, R4.2 and L2.2. After incubation, a number of different colonies of bacteria were obtained and each individual colony was once more plated onto its respective agar plate and incubated overnight, thus purified cultures of the bacteria present in the interdigital cavity were obtained.

Once sufficient enrichment of the isolated micro-organisms was attained, the next step was to determine a suitable growth medium, and the media employed were tryptic soya broth (TSB) and minimal salt solution (MSM). TSB is a complex medium and does not require the addition of a carbon source as it is rich in various nutrient sources². MSM is a defined medium (synthetic medium) which contains only the essential elements required to maintain the functioning of a bacterial cell with the exception of a carbon source. Glucose, was added in this case³. Due to MSM's nutritional content, it is considered to be a starvation medium, therefore it might be expected that the growth of certain bacteria might be favoured because some bacteria have the ability to flourish under stressed conditions whilst its competition cannot.

In preparing a broth, no agar was included, as agar is an agent used to solidify media and for the purpose of analysis, extraction of the bacterial metabolites from a liquid medium is preferred. Inoculation of each individually isolated

bacterium into each of the two respective sterilised broths was performed utilising the hot needle method⁴. The total community of the bacteria was also inoculated into both TSB and MSM broth.

All the inoculated media were incubated with stirring and samples were eventually taken from the respective broths at varying intervals. Sampling at various intervals was utilised for the following reasons:

- This method would not discriminate between those microbes with a rapid and those with a slow growth rate, by allowing sufficient time to produce metabolites.
- A thorough representation of the microbial growth curves could be obtained and any change in the microbial metabolite profile with sample age could thus be determined.
- Micro-organisms, depending on their respective growth phases (Fig. 2.1), may produce metabolites only in a certain phase, therefore sampling at various intervals would statistically improve the assessment of microbial metabolites.

The phases of the growth curve are characterised as follows⁵:

- Lag Phase: when microbes are introduced into medium, no immediate increase in cell number or mass.
- Log or Exponential Growth Phase: bacteria are growing and dividing at maximal rate.
- Stationary Phase: population growth ceases and curve becomes horizontal.
- Death Phase: detrimental environmental changes like nutrient depletion and build up of toxins lead to the decline in viable cells. The death phase, like the log phase, is logarithmic because as the bacteria die, their cells undergo lysis.

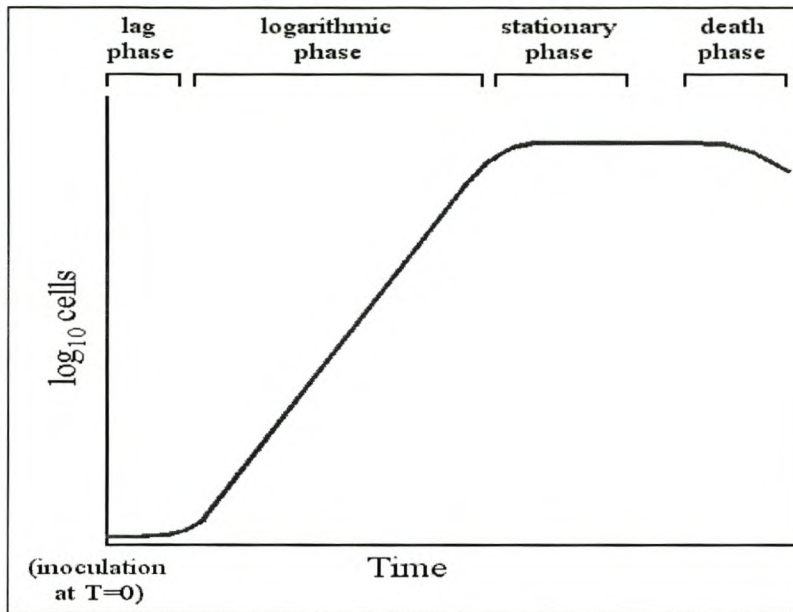


Fig. 2.1: Schematic representation of microbial growth and its different phases.

2.2 DETERMINATION OF GROWTH CURVES FOR EACH INDIVIDUAL MICRO-ORGANISMS

Many methods exist to compare different species of bacteria and a growth curve is only one method of doing so⁶. Bacteria can be compared based on their taxonomic characteristics, namely:

- *Morphological characteristics:* Differentiation based on structural features, as these features depend on expression of many genes in their genome and the expressions thereof normally do not vary greatly with environmental changes.
- *Physiological and metabolic characteristics:* Differentiation based on *inter alia*, utilisation of energy sources (nutrient source), the ability to ferment,

general nutritional type, osmotic tolerance, sensitivity to metabolic inhibitors, motility and differences in secondary metabolites produced.

- *Ecological characteristics*: Many properties are ecological in nature since they affect the relation of micro-organisms to their environment. Some examples of taxonomically important ecological properties are life cycle patterns, the nature of symbiotic relationships and habitat requirements such as temperature, oxygen and pH.
- *Genetic Analysis*: As most eucaryotes are able to reproduce sexually, genetic analysis has been of considerable usefulness in the classification of these organisms. Although procaryotes do not reproduce sexually, the study of chromosomal gene exchange through transformation and conjugation is sometimes useful in their classification.

The utilisation of a growth curve as a method for comparing micro-organisms would be beneficial as it would encompass the physiological and metabolic characteristics. The study of the growth curve would be a visual method of observing the individual species of micro-organisms utilising their energy source which is related to their ability to produce and use the metabolites required for growth. The growth rate of any microbe is dependent on the use of its energy source and therefore analysis of metabolite production of a micro-organism would be dependent on the growth phase at the time of sampling. The logarithmic (log) phase is the period when cell growth is at its maximum. Thus, the determination of the log phase for each micro-organism would reveal the most appropriate interval to sample the particular microbe. Therefore, metabolic profiles of the individual microbes could be compared to one another.

With the information gained from this study, the growth rate of each microbial species could be determined as well as the most favourable interval to sample the individual species. In addition, the most favourable time to sample the total community could be postulated.

Another important factor that had to be noted before commencing with the study of the growth curves was that once micro-organisms undergo a few cycles of incubation under laboratory conditions they may lose their protective slime layer. This phenomenon is due to the absence of any competition for the energy source from other microbes, as they are incubated as isolates in the laboratory. Therefore, to gain the most accurate growth curve, fresh samples from the interdigital cavity of the bontebok had to be obtained.

Fresh interdigital secretion was collected from a bontebok kept in a camp on the Welgevallen experimental farm in Stellenbosch, and sampling of the secretion, isolation and incubation of the individual microbes was accomplished in the same manner as previously described. Seven bacterium species were isolated from the fresh secretion and they were respectively labelled 3A – 3G.

Prior to commencing with the determination of the growth curves, all the micro-organisms had to be replated to obtain fresh colonies of bacteria. These microbes were subsequently inoculated into replicate test tubes, which were then incubated overnight to obtain enrichment of the micro-organisms in the medium before inoculation into Erlenmeyer flasks with larger quantities of the medium.

After inoculation of the bacterial cultures into individual Erlenmeyer flasks was performed, the respective Erlenmeyer flasks were incubated by stirring. Samples were taken from the Erlenmeyer flasks after predetermined intervals and the optical density (OD) or absorbance of light by bacterial growth was determined by ultra violet or visible light (UV/Vis) spectrophotometry. The values obtained at these intervals (e.g. Table 2.1) were plotted against time and thus growth curves (Fig. 2.2 – 2.5) were obtained for all the individual bacterium species.

Table 2.1: An extract of the measurements obtained during a growth curve experiment, used to plot the respective graphs.

Absorbance ($\lambda = 600 \text{ nm}$)							
Time (Hrs)	Micro-organism						
	3A	3B	3C	3D	3E	3F	3G
24	0.058		0.022		0.590	0.117	
25	0.070		0.030		0.738	0.156	
26	0.086		0.048		0.921	0.180	
27	0.103		0.067		1.096	0.248	
28	0.108		0.089		1.110	0.280	
29	0.128		0.183		1.042	0.353	
30	0.144		0.262		1.020	0.414	
31	0.177		0.359		1.000	0.492	
32	0.202		0.487		1.005	0.588	
33	0.240		0.589		1.010	0.700	
34	0.278		0.739		0.992	0.785	
35	0.328		0.912		0.970	0.808	
36	0.399		1.024		0.963	0.794	
37	0.452		1.112		0.946	0.789	
38	0.535		1.230		0.968	0.781	
39	0.615		1.314		0.964	0.775	
40	0.600		1.547		0.967	0.768	
41	0.589		1.568				
42	0.585		1.450				

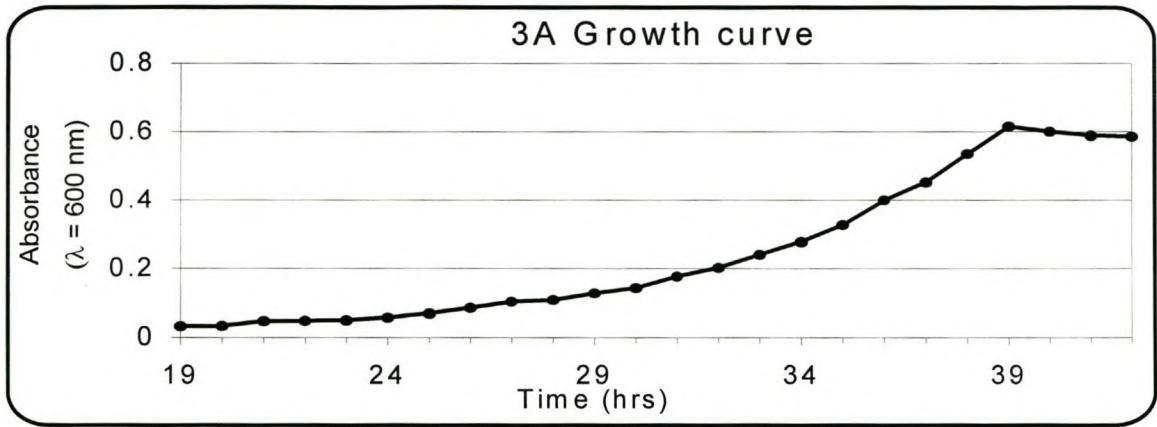


Fig. 2.2: Growth curve of micro-organism 3A.

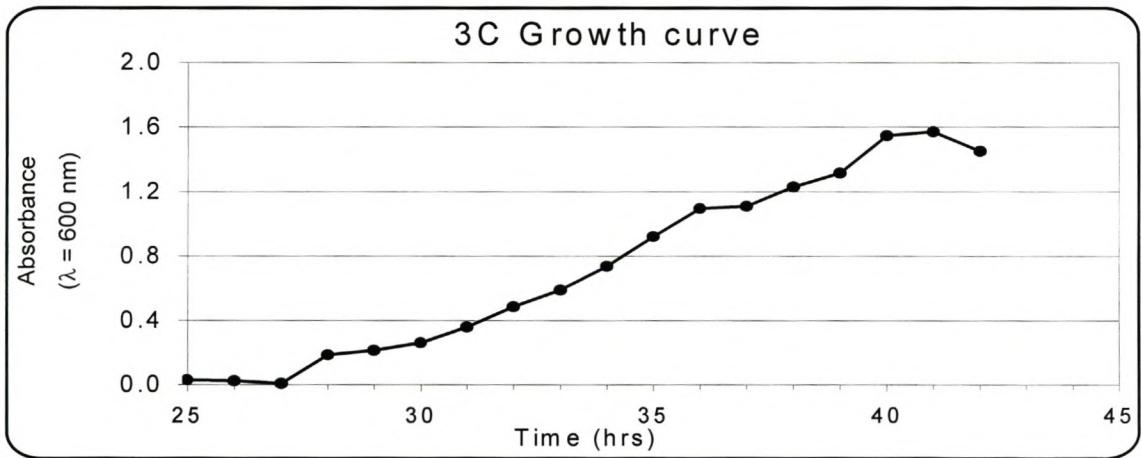


Fig. 2.3: Growth curve of micro-organism 3C.

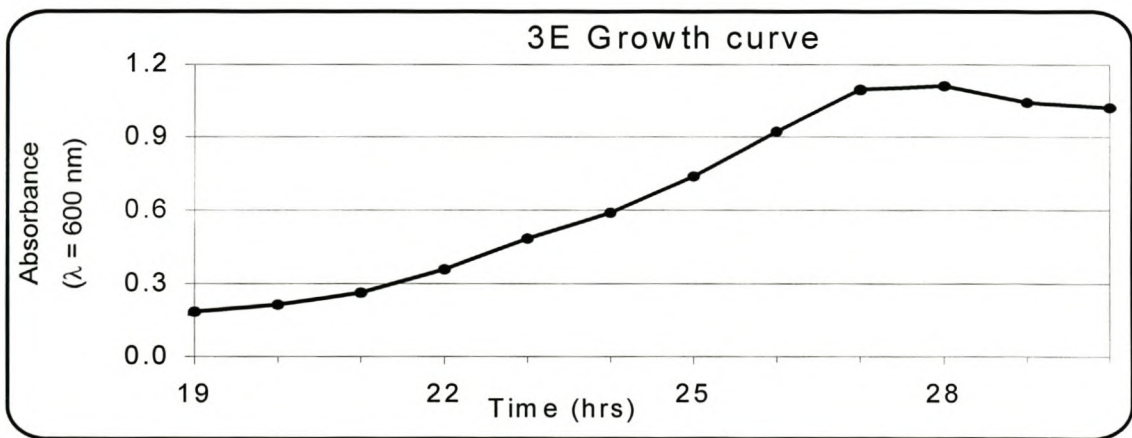


Fig. 2.4: Growth curve of micro-organism 3E.

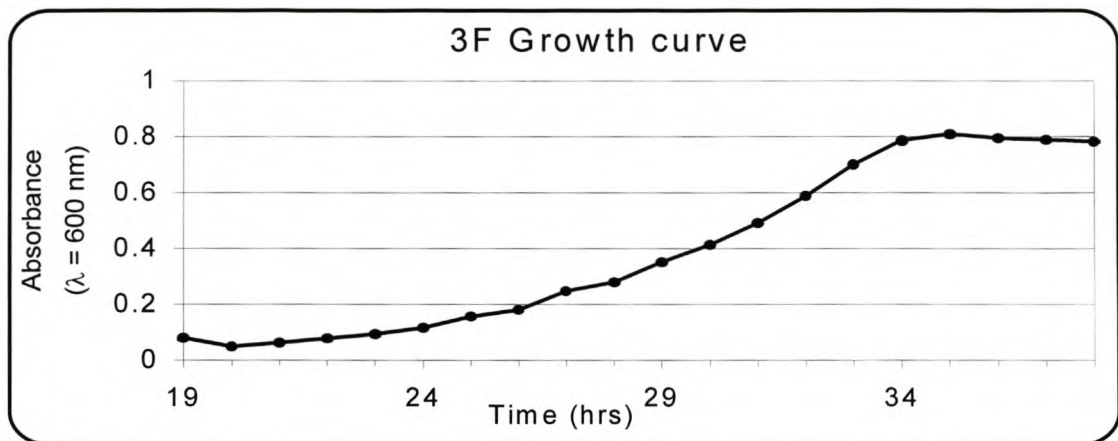


Fig. 2.5: Growth curve of micro-organism 3F.

From the graphs above (Fig. 2.2 – 2.5) it appears that the microbes in the interdigital cavity generally grow very slowly when compared, for example, to a *Pseudomonas* sp. in which a completed growth curve can be obtained in 14 hours⁷. The first organism (3E) only enters its logarithmic (log) phase after 19 hours. The beginning of each isolate's log phase and the end of its log phase have been tabulated below (Table 2.2).

Table 2.2: The time noted at the start of each isolate of the interdigital cavity entering the logarithmic phase and the time noted at completion of the logarithmic phase.

Micro-organism	Start of log phase (hrs)	End of log phase (hrs)
3A	21	39
3C	28	41
3E	19	28
3F	21	35

The prominent feature of Table 2.2 is that the overnight cultures of microbes 3B and 3G did not grow at the low concentration of glucose used in the experiment. The experiment was repeated several times and incubating these microbes at a higher temperature (37°C) did not facilitate their growth. The experiment could not be repeated at higher concentrations of glucose due to concerns that higher nutrient concentrations would not provide a realistic representation of the conditions present in the interdigital gland of the bontebok. Thus, inaccurate growth curves would be obtained.

Micro-organism 3D grew extremely slowly, exhibiting visible growth only after 8 days and completion after 10 days. As a result of its long logarithmic phase, accurate determination of the growth curve of 3D was difficult.

Having determined the individual growth curves, this information was then applied to the planning of all sampling procedures (see Section 5.5). Based on the information obtained from the graphs, it appeared that sampling all the isolates at three days would be a favourable interval for the extraction of metabolites, particularly for the microbes with a faster growth rate. Samples of all the microbes, also those that grew slower, were however to be taken for the sake of consistency. For the same reason, all the isolates were also to be sampled at 10 days.

Taking into consideration those microbes that did not grow, samples of all the isolates were to be taken at 30 days as well, because an additional investigation of 3B and 3G at a higher concentration of glucose and larger volumes did in fact exhibit growth.

2.3 EXTRACTION OF MICROBIAL METABOLITES

The samples taken at different intervals for each micro-organism as well as the total community in each medium were centrifuged to separate the bacteria from the broth. The resulting supernatant was decanted from the microbes and was then extracted by liquid-liquid extraction with minute quantities of dichloromethane. The dichloromethane extracts were then naturally evaporated to concentrate the samples prior to GC-MS analysis.

Dichloromethane was used as the organic solvent of choice for the following reasons:

- It can be bought in a residue analysis grade that is pure enough for capillary GC-MS purposes.
- Has a relatively low boiling point, thus not superimposing any of the metabolite peaks in the chromatogram because it elutes at the start of the chromatographic analysis.
- Dichloromethane can dissolve a wide range of organic compounds.

It should be noted that most of the samples were incubated, extracted and sampled in duplicate to avoid misleading results on account of, for example, the presence of a contaminant in a sample, a sudden or an unexplainable lack of growth of a sample, or the presence of metabolites in a gas chromatographic analysis in concentrations too low to obtain unequivocal identification.

References: Chapter 2

1. L.M. Prescott, J.P. Harley and D.A. Klein, *Microbiology* (fourth edition), McGraw-Hill, New York (1999), pp. 107-108.
2. Ref. 1, pp. 106–107.
3. Ref. 1, pp. 105–106.
4. B. Prior, *General microbiology*, Dept. Microbiology, Stellenbosch University (1999), p. 17
5. Ref. 1, pp. 114-115.
6. Ref. 1, pp. 400–405.
7. E. Bester, *Differential response of sessile and planktonic bacterial populations following exposure to antimicrobial treatment*, MSc Thesis, Stellenbosch University (2004), p. 54

CHAPTER 3

CHEMICAL CHARACTERISATION OF THE VOLATILE METABOLITES OF MICRO-ORGANISMS FROM THE INTERDIGITAL CAVITY OF THE BONTEBOK

The following samples were subjected to analysis by gas chromatography-mass spectrometry (GC-MS) after extraction of the organic material from the medium with dichloromethane and concentration of the extract by partial evaporation of the solvent:

Table 3.1: Samples analysed by GC-MS.

A. With TSB as growth medium			
Micro-organism	Inoculation period (days)	TIC Fig. No.	Compounds identified in Table No.
Total Community	3	Fig. 3.3	3.4
	10	Fig. 3.4	3.5
	30	Fig. 3.1	3.2
R1.1	3	Fig. 3.5	3.6
	10	Fig. 3.6	3.7
	30	Fig. 3.7	3.8
R1.2	3	Fig. 3.8	3.9
	10	Fig. 3.9	3.10
	30	Fig. 3.10	3.11
R2.1	3	Fig. 3.11	3.12
	10	Fig. 3.12	3.13
	30	Fig. 3.13	3.14
R3.1	3	Fig. 3.14	3.15
	10	Fig. 3.15	3.16
	30	Fig. 3.16	3.17
R4.2	3	Fig. 3.17	3.18
	10	Fig. 3.18	3.19
	30	Fig. 3.19	3.20
L2.2	3	Fig. 3.20	3.21
	10	Fig. 3.21	3.22
	30	Fig. 3.22	3.23

Table 3.1 continued

B. With MSM as growth medium (glucose as nutrient source)			
Micro-organism	Inoculation period (days)	TIC Fig. No.	Compounds identified in Table No.
Total Community	3	Fig. 3.2	3.3
	10	Fig. 3.23	3.24
	30	Fig. 3.24	3.25
R1.1	3	Fig. 3.25	3.26
	10	Fig. 3.26	3.27
	30	Fig. 3.27	3.28
R1.2	3	Fig. 3.28	3.29
	10	Fig. 3.29	3.30
	30	nmo	nmo
R2.1	3	Fig. 3.30	3.31
	10	Fig. 3.31	nmo
	30	nmo	nmo
R3.1	3	Fig. 3.32	nmo
	10	Fig. 3.33	3.32
	30	nmo	nmo
R4.2	3	Fig. 3.34	nmo
	10	Fig. 3.35	3.33
	30	Fig. 3.36	3.34
L2.2	3	Fig. 3.37	nmo
	10	Fig. 3.38	3.35
	30	nmo	nmo

nmo: No metabolites observed in the TIC of the respective micro-organism.

Although the metabolites of each individual bacterium strain, as well as of the total community of bacteria have been characterised by GC-MS analysis, only the analyses of the total community of bacteria in each medium will be used for the purpose of the discussion of the chemical characterisation of the volatile metabolites, since these analyses were found to be representative of the results in general. The results obtained for each individual bacterium species produced in the two media have been reported in the respective tables (Tables 3.4 – 3.39, Addendum A).

3.1 STRUCTURAL DETERMINATION OF THE MICROBIAL METABOLITES PRODUCED IN TSB AS GROWTH MEDIUM

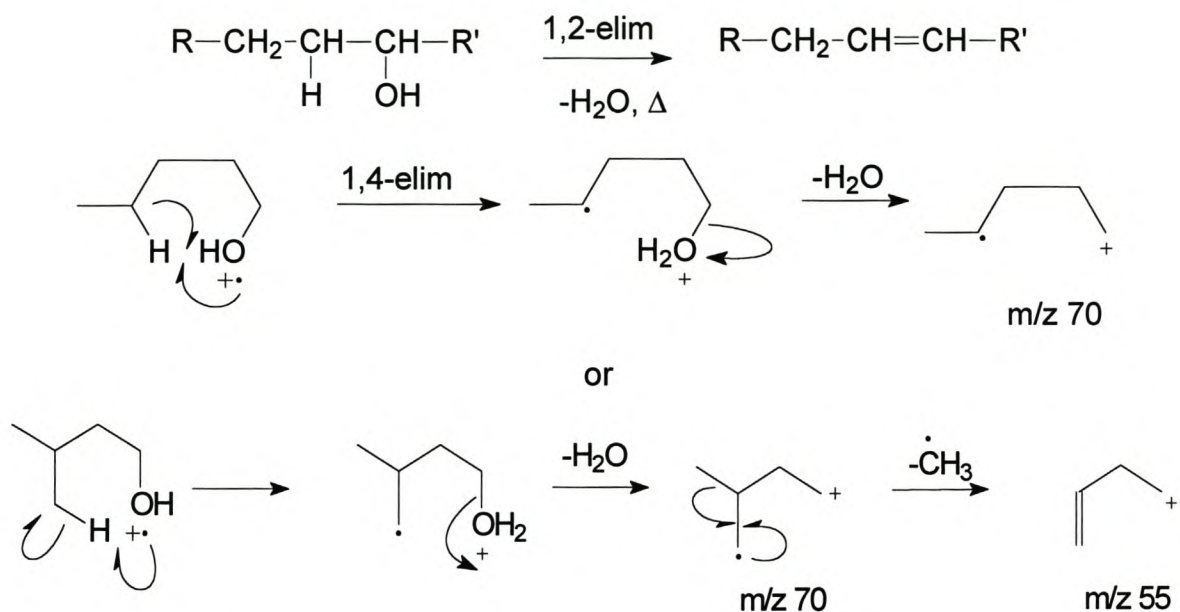
The total ion chromatogram (TIC) (Fig. 3.1) of the extract of the microbial metabolites produced by the total community of bacteria in TSB will be used as reference in the discussion of the structural elucidation of the metabolites. Each component will be referred to by its number in this chromatogram.

Individual compounds were identified by interpreting their low resolution electron impact (EI) mass spectra and this was confirmed by gas chromatographic retention time comparison with either synthetic, commercially available compounds or compounds synthesised from synthetic material in the laboratory. Computer-aided comparison of each component's mass spectrum with mass spectrometric library data served as further evidence and confirmation in the structural elucidation of the component.

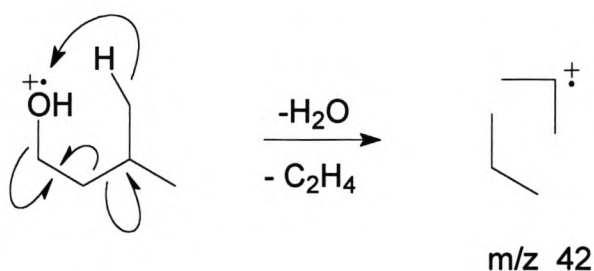
3.1.1 Alcohols

In the EI mass spectrum (Fig. 3.43) of component 337, the peaks at m/z 42, 55 and 70 are the most abundant ions, of which the one at m/z 55 is the base peak. A library search using these ions indicated that possible structures for component 337 were 1-pentanol or 3-methyl-1-butanol.

With this information, the ion at m/z 70 $[M-18]^+$ could be attributed to the loss of water due to a 1,4- or 1,2- elimination as follows:

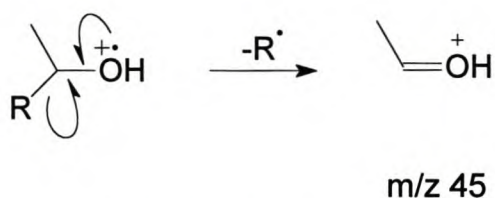


The base peak at m/z 55 is formed by rearrangement after the loss of water and a methyl radical as shown above in the 1-4-elimination of the branched aliphatic alcohol. The ion at m/z 42 $[\text{M}-46]^+$ occurs due to the loss of a neutral fragment of water and ethylene as follows:



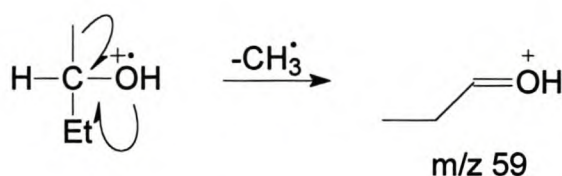
As 1-pentanol and 3-methyl-1-butanol have very similar spectra, synthetic samples of both were analysed by GC-MS and it was found that the retention time of 1-pentanol was too long. Component 337 was confirmed to be 3-methyl-1-butanol.

In the spectrum of component 190 (Fig. 3.44), the ion at m/z 45 suggests the possibility of an α -cleavage of a secondary methylcarbinol ion (2-alkanol) as follows¹:



In general a larger substituent ($\text{R} > \text{CH}_3$) will be expelled more readily, since the single electron of the neutral radical can be stabilised more effectively in a longer chain by rearrangement or by further decomposition².

Although the largest substituent is readily expelled from the molecular ion of secondary alcohols, less favourable α -cleavages do occur. The relative abundance of the ion formed by the less favourable cleavage would be lower than that formed by the favoured cleavage and the larger the substituent, the lower the abundance would be. With respect to the ion at m/z 45, an ion of lower relative abundance is observed at m/z 59 which was a good indication that component 190 could be a secondary ethylcarbinol.

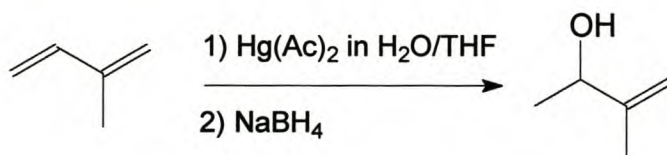


The presence of the base peak at m/z 71 and the absence of a molecular ion lead to the assumption that component 190 could possibly be a tertiary alcohol. A library search was performed³, which gave three candidate structures, namely 3-penten-2-ol, 4-penten-2-ol and 2-methyl-3-buten-2-ol. The possibility of 4-penten-2-ol was eliminated because its mass spectrum does not possess

a m/z 59 fragment and it has a base peak at m/z 45. The possibility of 3-penten-2-ol was eliminated on account of the absence of ions at m/z 59 and m/z 45 and it has a molecular ion at m/z 86 which was further reason to discard it as a possibility.

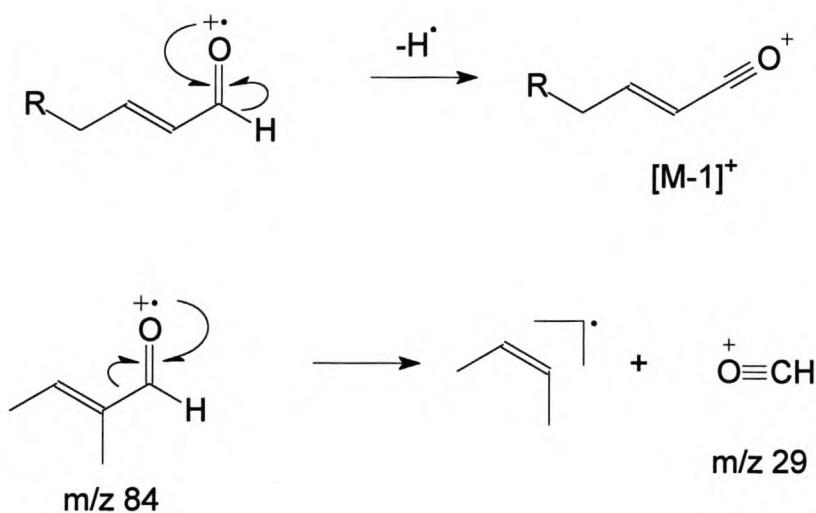
Based on this information, and further confirmation by retention-time comparisons, component 190 was identified as 2-methyl-3-buten-2-ol.

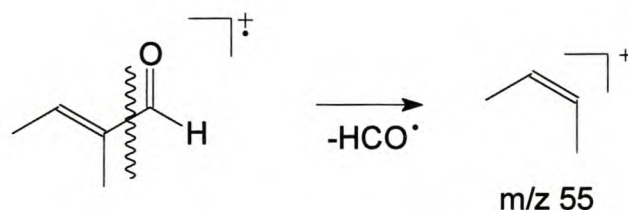
Component 261 has a molecular ion at m/z 86 and a base peak at m/z 43. The EI mass spectrum (Fig. 3.45) also has ions at m/z 71 $[M-CH_3]^+$ (80%) and m/z 45 (28%). This information was used in a computer library search, which gave three possibilities, namely 3-penten-2-ol, 2-methyl-3-buten-2-ol and 4-penten-2-ol. 2-Methyl-3-buten-2-ol was eliminated because of the presence of an m/z 59 ion in the mass spectrum of this tertiary alcohol, which not present in the mass spectrum of component 261. Synthetic 3- and 4-penten-2-ol were tested and it was found that the retention times of both compounds were too long. The computer search was repeated and this time m/z 71 was not included in the search parameters. This gave one additional candidate structure, namely 3-methyl-3-buten-2-ol, which was synthesised according to the reaction scheme below (see Section 5.x and Fig. 5.x) and GC-MS analysis of this compound confirmed that component 261 is in fact 3-methyl-3-buten-2-ol.



3.1.2 Aldehydes

An ion at m/z 84 that could possibly be the molecular ion is the most prominent ion (base peak) in the EI mass spectrum of component 343 (Fig. 3.46). On the basis of such an assumption the ions at m/z 83 $[M-1]^+$ and m/z 29 $[\text{CHO}]^+$ could be accepted as evidence that component 343 was an unsaturated aldehyde. The abundant ion at m/z 55 is most likely due to simple fission of the alpha bond with charge retention on the alkyl moiety of the aldehyde, which then has to be a butyl group. The candidate structures for component 343 were 3-methyl-2-butenal, 2-pentenal and 2-methyl-2-butenal. As all three candidates' mass spectra have the same intense molecular ion and very prominent ion at m/z 55 as well as an ion at m/z 29⁴, eliminating any of the candidates based on their respective mass spectra was not possible. Therefore, co-injection of all three of these compounds was required to determine the identity of component 343. It was found that the retention times of both 3-methyl-2-butenal and 2-pentenal were too long, whilst the retention time of 2-methyl-2-butenal corresponded to that of component 343.

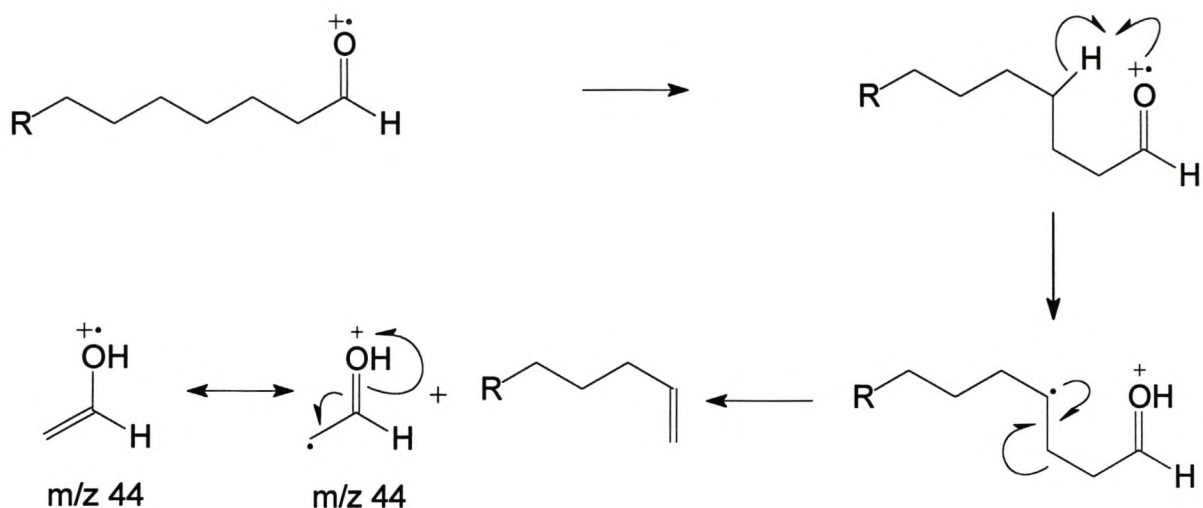




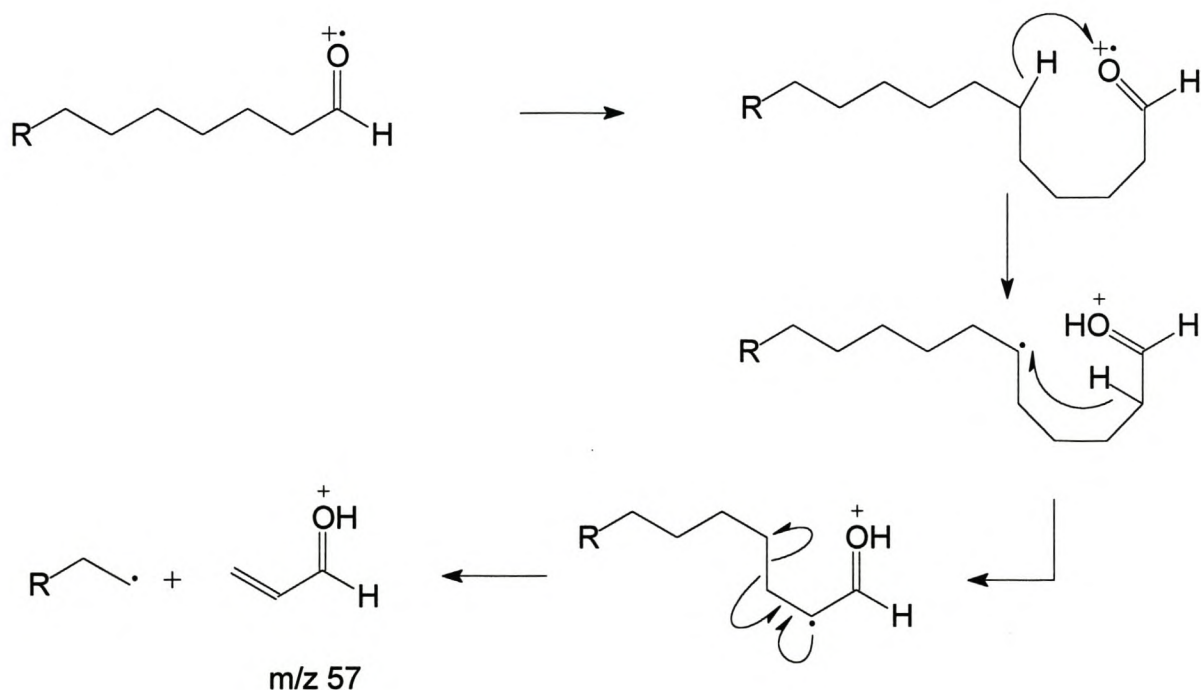
The presence of a base peak which is apparently also the molecular ion at m/z 84 in the EI mass spectrum of component 416 (Fig. 3.47) and prominent peaks at m/z 29, 55 and 83 is similar in this respect to the spectrum of 2-methyl-2-butenal. The main difference in this spectrum, when compared to that of 2-methyl-2-butenal, is that the ion at m/z 55 is not as abundant, whereas the ion at m/z 83 $[\text{M}-1]^+$ is more abundant. Component 414 was therefore accepted also to be an aldehyde and thus the same candidate structures 3-methyl-2-butenal, 2-pentenal and 2-methyl-2-butenal, were considered as possibilities.

2-Pentenal and 2-methyl-2-butenal were eliminated as possibilities, based on their respective retention times. The retention time of 2-pentenal was too long and that of 2-methyl-2-butenal was shown to be shorter than that of component 414. GC-MS comparison with synthetic material confirmed component 414 in the extract of the metabolites of the total microbial community to be 3-methyl-2-butenal

The base peak at m/z 44 in the EI mass spectra of components 1085 (Fig. 3.48) and 1264 (Fig. 3.49) is a characteristic ion formed due to the McLafferty rearrangement that occurs in the mass spectra of long-chain aliphatic aldehydes:

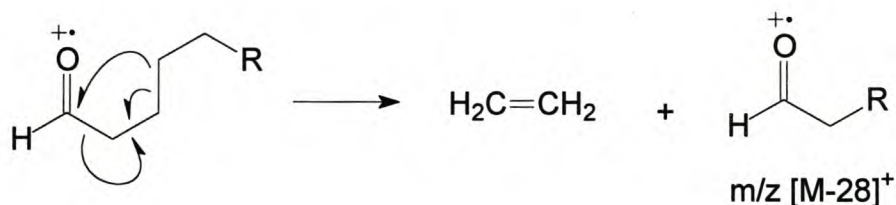


The ion at m/z 57 is observed in both mass spectra of the respective components and is ascribed to a [McLafferty + 13] ion, the formation of which is postulated to proceed as follows:

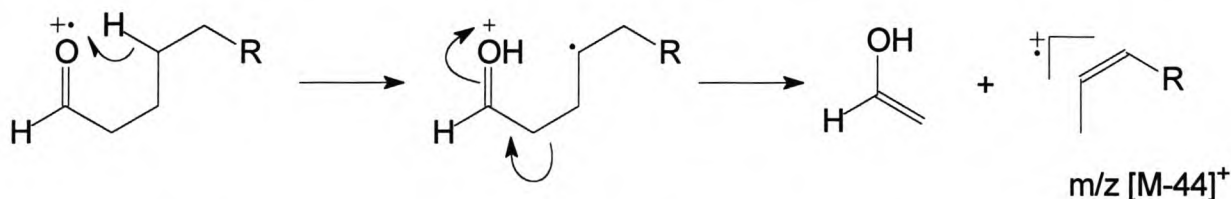


Characteristically, the mass spectra of long chain aliphatic aldehydes often have weak molecular ions, which can be identified by the presence of characteristic $[\text{M}-28]^+$ and $[\text{M}-44]^+$ ions⁵. Assuming that both components are in fact aldehydes,

the respective ions at m/z 114 and 128 are formed by the expulsion of ethylene from the molecular ion^{6,7}:

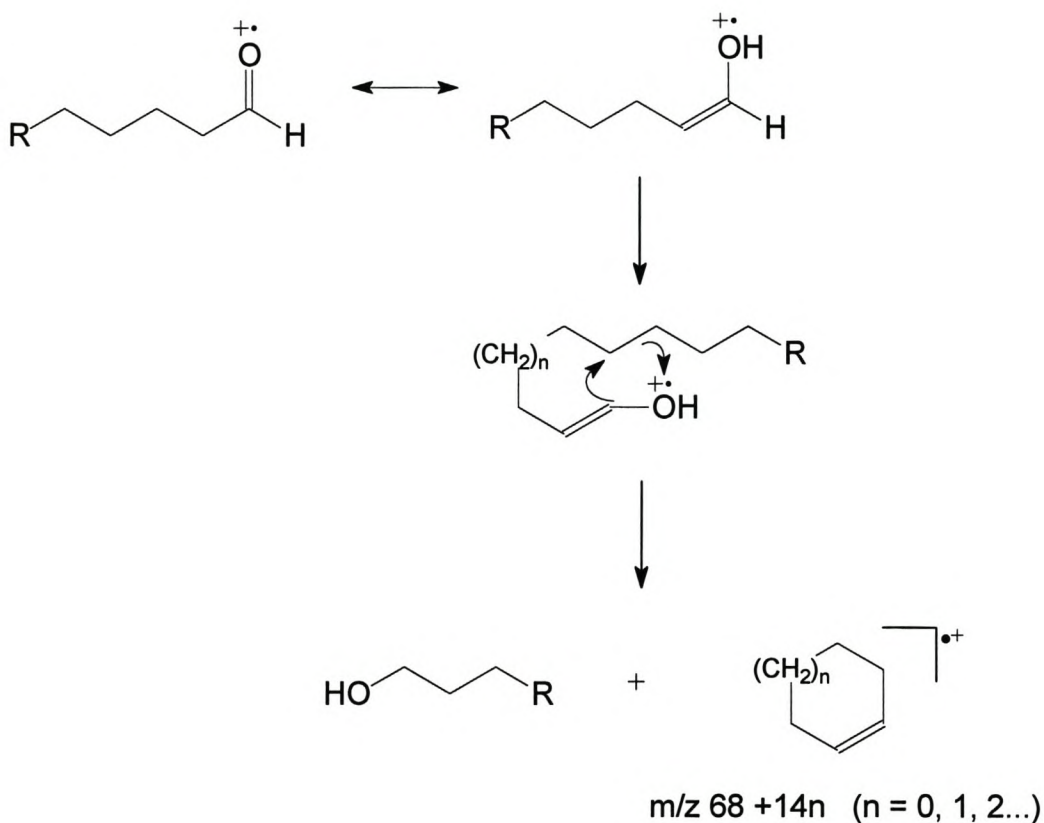


The ions at m/z 98 and 112 in the mass spectra of components 1084 and 1264 are due to the loss of a neutral $[C_2H_4O]$ fragment as shown below⁶. This loss of 44 mass units is an important characteristic of aldehydes without α -branching. Labelling experiments with ^{18}O show that ions resulting from this process have the general formula $[C_nH_{2n}]^+$. This implies β -cleavage with hydrogen atom transfer as in a McLafferty rearrangement, but with charge-retention on the alkene fragment⁸:



In the mass spectra of the higher aliphatic aldehydes an interesting series of even-mass ions is observed corresponding to the general formula m/z 68 + 14n ($n=0,1,2,\dots$)⁹. The elemental composition of these ions has been determined by high-resolution studies of octadecanal to be of the general formula $[C_nH_{2n-2}]^+$. From the spectra of a complete series of isomeric *vic*-dideutero aldehydes, it became clear that the carbon atoms involved in this series of fragments are the carbon atoms near the functional group. These ions result from the loss of a hydrogen atom from C2, whereby the enol form of the aldehyde in a 4-membered ring transition state expels an alcohol (ROH) group.

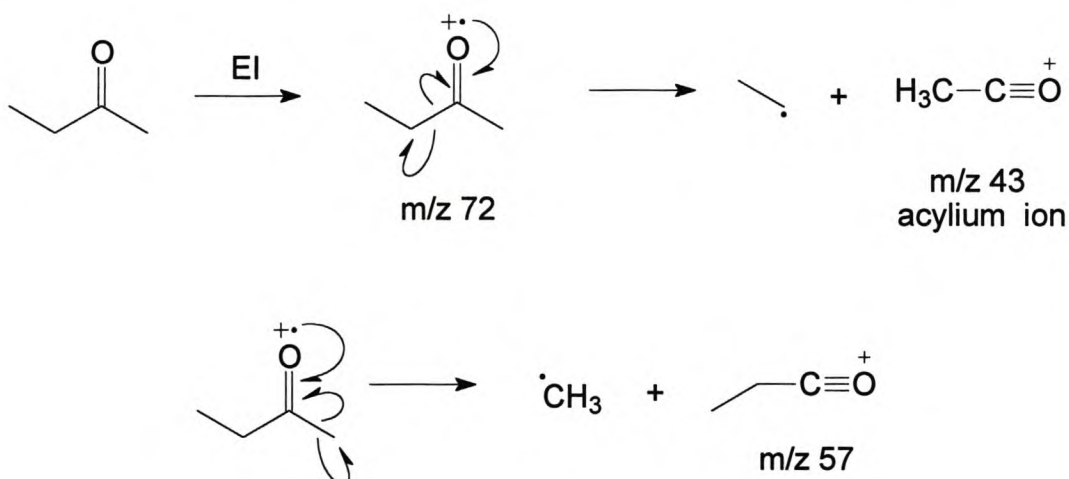
The most intense ions are m/z 68, 82 and 96, which are due to higher probability of 5-, 6- and 7-membered ring formation. The genesis of the ions at m/z 82 ($n = 1$) in the mass spectrum of component 1084 and the ions at m/z 82 and 96 ($n = 2$) in that of component 1264 can therefore be postulated as follows:



For the final identification of components 1084 and 1264, a homologous series of aliphatic aldehydes, namely hexanal through octadecanal, was used for retention-time comparison and components 1084 and 1264 were identified as nonanal and decanal respectively.

3.1.3 Ketones

The EI mass spectrum of component 179 (Fig. 3.50) has a base peak at m/z 43, the molecular ion at m/z 72 and a prominent ion at m/z 57 [$M-CH_3$]. It has been shown that m/z 43 [CH_3CO]⁺ (acylium ion) is the base peak in the mass spectra of a series of branched and unbranched methyl ketones¹⁰ and since the molecular ion of ketones can normally be observed¹¹, it was assumed that component 179 could be a methyl ketone. Considering the molecular ion, it would suggest that the component could be 2-butanone and the retention time of 2-butanone was compared by GC-MS analyses, confirming component 179 to be 2-butanone.



The EI mass spectrum of component 228 (Fig. 3.51) exhibits a fragmentation pattern very similar to that of component 179, with ions at m/z 43 (base peak, acylium ion), m/z 71 [$M-CH_3$]⁺ and the molecular ion peak at m/z 86. On account of this similarity component 227 was concluded to be a 2-alkanone as well and therefore the candidate structures were 2-pentanone and 3-methyl-2-butanone.

The retention-time of the two candidate compounds were compared to those of the metabolites found in the extract of the total microbial community and it was determined that the retention time of 2-pentanone was too long and component 227 was confirmed to be 3-methyl-2-butanone.

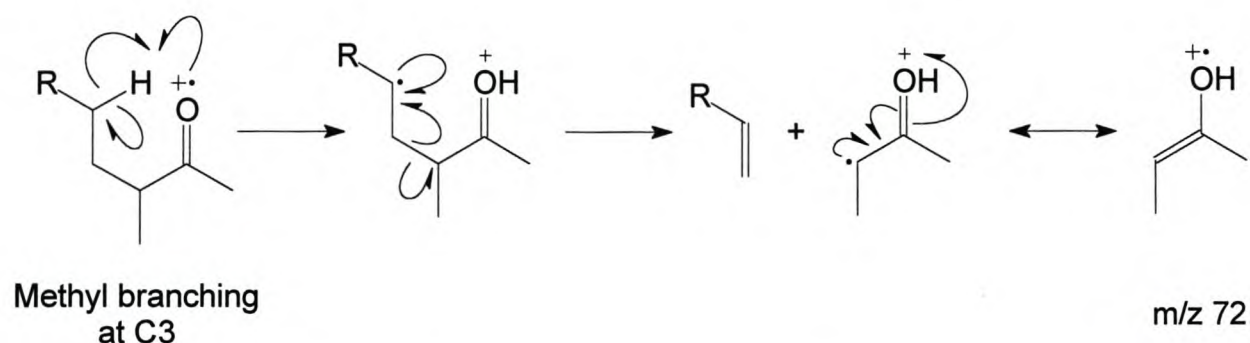
The molecular ion in the EI mass spectrum of component 364 (Fig. 3.52) is present at m/z 100 and other diagnostic ions are present at m/z 43 (base peak), 57, 72 and 85 $[M-15]^+$. The characteristic base peak at m/z 43 suggested that component 364 could also be a 2-alkanone.

When a chain of three or more carbon atoms is attached to the carbonyl group, McLafferty rearrangement (β -fission with transfer of a γ -hydrogen atom) becomes important¹⁰. In the case of ketones the situation with respect to this rearrangement is complex:

1. Even with unbranched ketones, the mass of the rearrangement ion will vary with the size of the alkyl group which is not involved in the rearrangement. Unbranched methyl ketones or those branched beyond the third carbon atom give the rearrangement ion at m/z 58. Ethyl and propyl or isopropyl ketones, with the same reservations as to the branching, give the ion at m/z 72 and m/z 86 respectively.
2. When there is a chain of three or more carbon atoms in each alkyl group, a second McLafferty rearrangement becomes possible, since the enolic product of the primary rearrangement can again fragment through a six-membered ring state to produce an m/z 58 ion.

The ion at m/z 72 is the result of a possible McLafferty rearrangement and can be explained if one were to consider the statement 1 made above. A

McLafferty rearrangement of a methyl ketone forms an ion at m/z 58 if there is no branching at C3. If a 2-alkanone is branched at C3, the ion formed will follow the general formula of $58 + 14n$ (where n is 1, 2 or 3 for a methyl, ethyl or propyl branching) and will therefore be m/z 72, 86 or 100, respectively. The McLafferty rearrangement for the ion at m/z 72 can, therefore, be explained as follows:



Guided by the available information, component 364 was assumed to be an aliphatic methyl ketone, with a methyl branching in the α -position, because the McLafferty rearrangement gives an m/z 72 ion. The possibility of two McLafferty rearrangements was ruled out due to the relatively low molecular weight of the component. Possible candidate structures for component 364 were 2-hexanone, 3-methyl-2-pentanone and 4-methyl-2-pentanone. Retention time comparison of 2-hexanone proved that its retention time was too long, whilst that of 4-methyl-2-pentanone was too short. Component 364 was confirmed, by GC-MS analysis, to be 3-methyl-2-pentanone

The base peak at m/z 45 in the EI mass spectrum of component 283 (Fig. 3.53) is the result of a characteristic α -cleavage of a secondary alcohol, more specifically a methyl carbinol (see Section 3.1.1). Other ions of significance in the mass spectrum of component 283 are the molecular ion at m/z 88, the ion at m/z 43 and the weak ion at m/z 73.

The ions at m/z 43 and 73 $[M-15]^+$ suggest the presence of a methyl ketone, and furthermore the masses of these two ions add up to 88, the mass of the molecular ion. Therefore, only one possible structure was postulated for component 283, namely 3-hydroxy-2-butanone, which was confirmed by a retention time study.

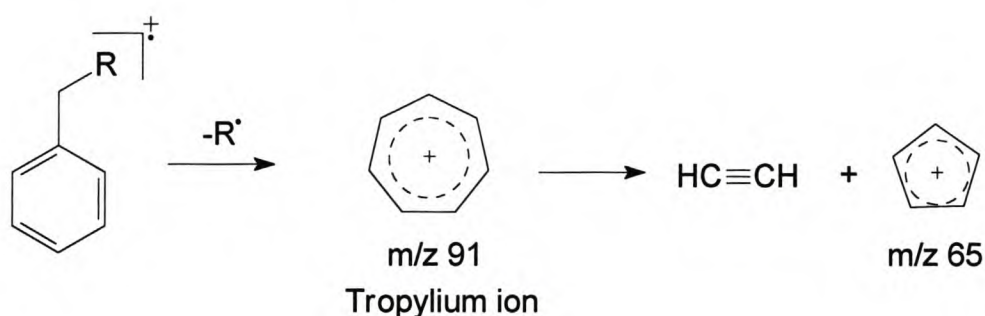
In the EI mass spectrum of component 536 (Fig. 3.54) prominent ions are present at m/z 101 (16%), 59 (39%) and 43 (100%). According to a computer library search three possible structures, namely 2-methyl-2-hexanol, 2,4-dimethyl-2-pentanol and 4-hydroxy-4-methyl-2-pentanone, had to be considered. Of these 2-methyl-2-hexanol and 2,4-dimethyl-2-pentanol were eliminated as possibilities, as both components have a base peak at m/z 59. A retention time study proved that component 536 is in fact 4-hydroxy-4-methyl-2-pentanone.

The base peak at m/z 43 in the EI mass spectrum of component 243 (Fig. 3.55) suggested that it could be a 2-alkanone and based on the presence of the molecular ion at m/z 84 the assumption was made that component 243 was an unsaturated ketone. The ion at m/z 69 also strengthened the proposal that component 243 could be unsaturated.

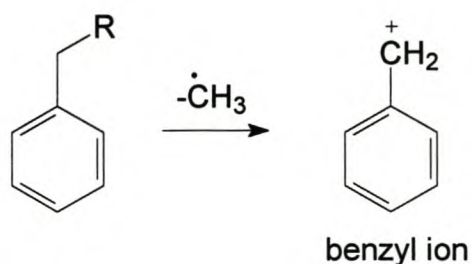
The structures 3-penten-2-one and 3-methyl-3-buten-2-one were considered for component 243. GC-MS comparison revealed that the retention time of 3-penten-2-one was too long and component 243 was confirmed to be 3-methyl-3-buten-2-one.

3.1.4 Aromatic compounds

In the EI mass spectrum of component 1094 (Fig. 3.56) the peak at m/z 91 represents a characteristic ion formed by the fragmentation of alkyl substituted benzene structures to form a tropylium ion¹². Further evidence suggesting an aromatic ring structure is the ion at m/z 65, which is formed by further decomposition of an aromatic ring structure as follows:

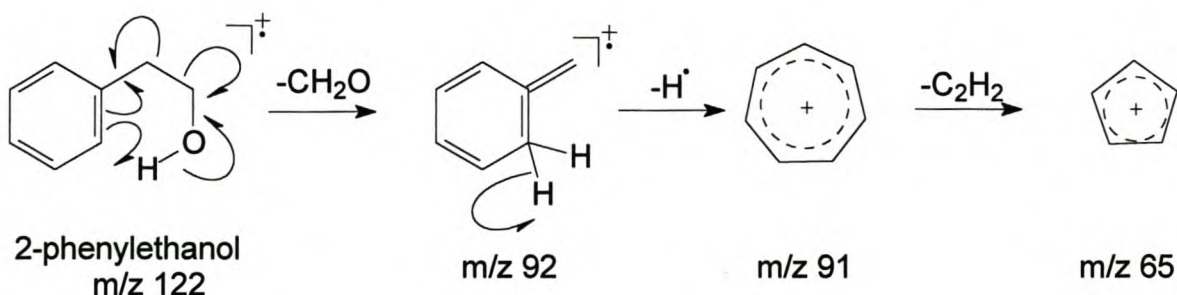


The procession of reactions, as in the scheme above, can be explained as follows. Aromatic ring cleavage usually requires high energies and significant hydrogen and carbon skeleton rearrangements are possible¹³. Normally, ionisation will take place in the π -electron system because it is generally easier to remove a π -electron than it is to remove a σ -electron. For example, in toluene the base peak at 91 is due to the tropylium ion. The tropylium ion is known to be very stable and is formed in preference to the benzyl ion isomer. The tropylium ion is resonance stabilised, with seven resonance structures. Deuterium labelling experiments provided further evidence in this direction¹². Ethylbenzene labelled in various positions showed that the methyl group (in scheme below $\text{R} = \text{CH}_3$) was lost without any preceding rearrangement in accordance with a mechanism leading to the proposed benzyl ion.

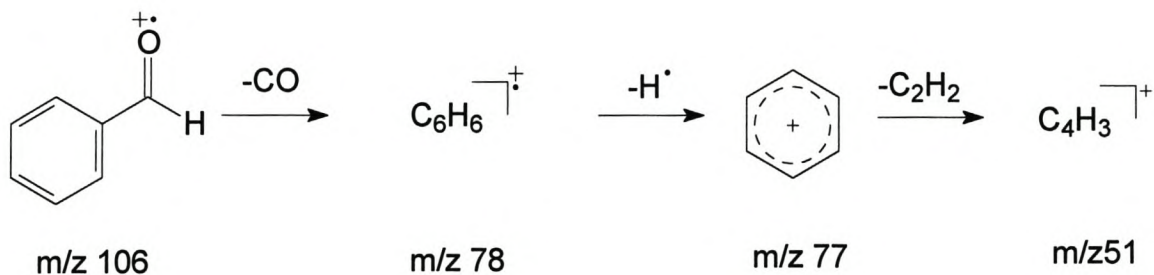
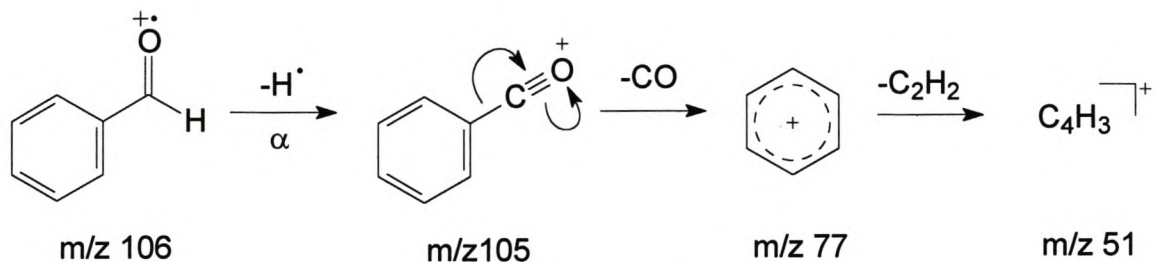


However, prior to further decomposition of the $[\text{C}_7\text{H}_7]^+$ species through loss of acetylene, all seven hydrogen atoms had become equivalent. This strongly suggested a symmetrical structure for this ion, most likely represented by the tropylium ion.

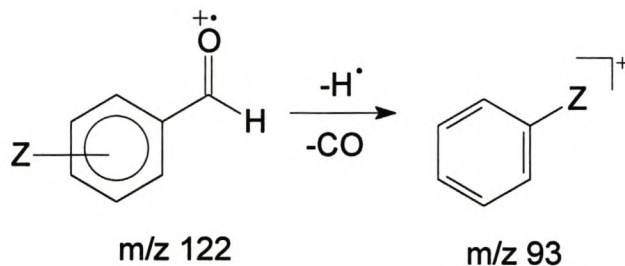
Other significant ions in the mass spectrum of component 1094 are the molecular ion at m/z 122 and the ion at m/z 92. A computer library search was performed and only one acceptable candidate structure was obtained namely 2-phenylethanol. Retention-time comparison with a synthetic sample confirmed component 1094 to be 2-phenylethanol.



The EI mass spectrum of component 788 (Fig. 3.57) has prominent ions at m/z 51, 77 (base peak), 78, 105 and 106 (molecular ion). The two ions at m/z 105 and 106 are of almost identical relative abundance, indicating that component 788 could be benzaldehyde¹⁴. A retention time study of benzaldehyde confirmed the identity of component 788. The formation of the prominent ions in its mass spectrum can be formulated as follows:

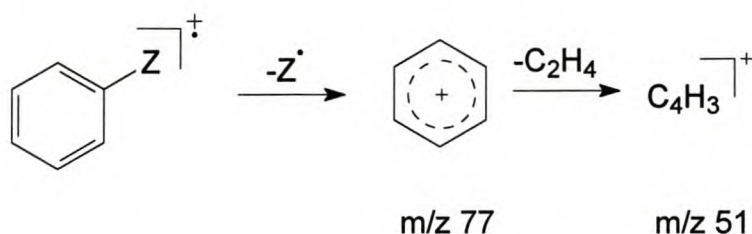


The EI mass spectrum of component 957 (Fig. 3.58) also displays two very prominent ions, with comparable relative abundance, at m/z 121 and m/z 122 (the base as well as molecular ion peak). If it is assumed that these two peaks (m/z 121 and 122) analogous to those of benzaldehyde (m/z 105 and 106), it can be assumed that component 957 is a substituted aldehyde. If the assumption is valid, the formation of an $[M-29]^+$ ion can be explained as follows:



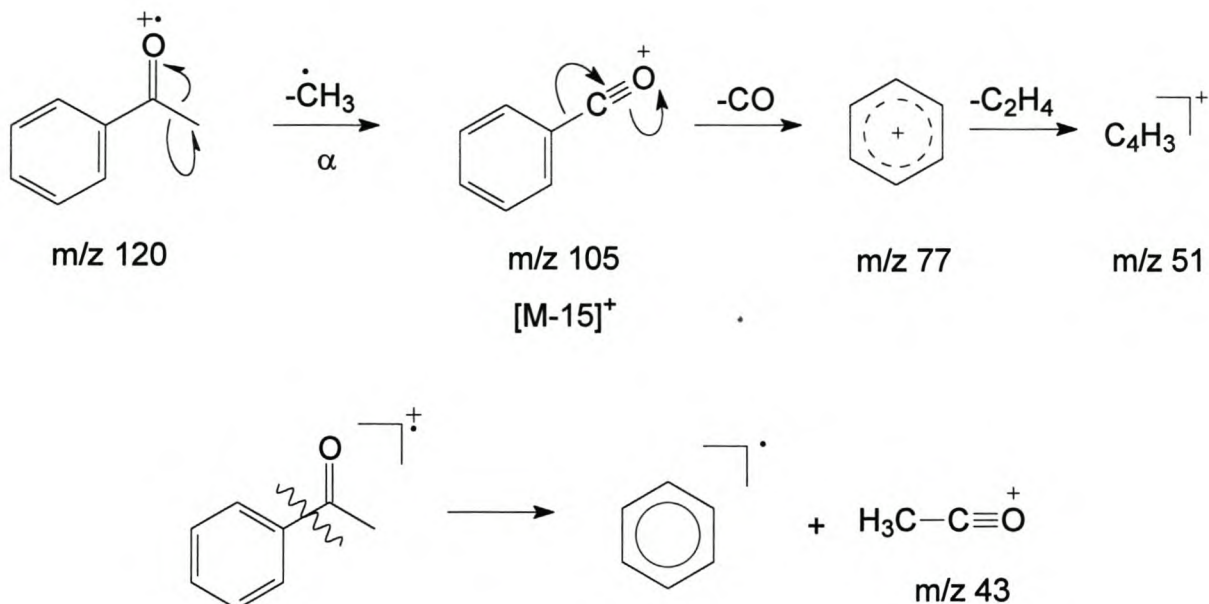
The molecular formula of the ion at m/z 93 is $[C_6H_4Z]^+$, therefore Z must be a hydroxyl group and thus possible candidate structures for component could be 2-, 3- or 4-hydroxybenzaldehyde. 4-Hydroxybenzaldehyde was eliminated as a possibility because it has its base peak at m/z 121, whereas 2- and 3-hydroxybenzaldehyde have a base peak at m/z 122. Retention-time comparisons revealed that component 954 was in fact 2-hydroxybenzaldehyde while the retention time of 3-hydroxybenzaldehyde was too long.

In the EI mass spectrum of component 1001 (Fig. 3.59) prominent ions are observed at m/z 51, 77, 105 (base peak) and 120 (molecular ion). The ions at m/z 51 and 77 are indicative of a monosubstituted benzene in which a tropylium ion cannot be formed, due to the type of substituent on the ring, namely a “non-alkyl” functional group.



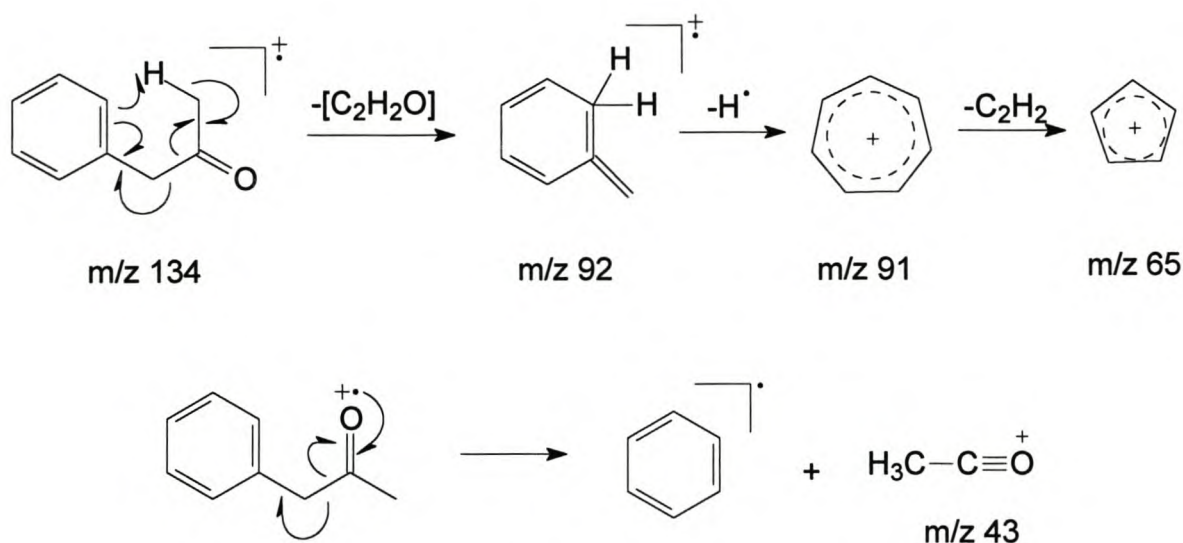
If it is assumed that the base peak at m/z 105 fragments to form the ion at m/z 77, a loss of 28 mass units is involved. This corresponds to the loss of the elements of a carbonyl group. This assumption is further strengthened by a loss of 15 mass units from the molecular ion at m/z 120. This $[M-15]^+$ ion (m/z 105) is the result of typical α -cleavage of alkyl aryl ketones^{15,16}. The presence of a weak ion at m/z 43 is also indicative of an alkyl aryl ketone, as this ion could form due to the alternative α -fission of the phenyl-carbonyl bond.

Therefore, the ions in the mass spectrum of component 1001 can be formulated as follows:



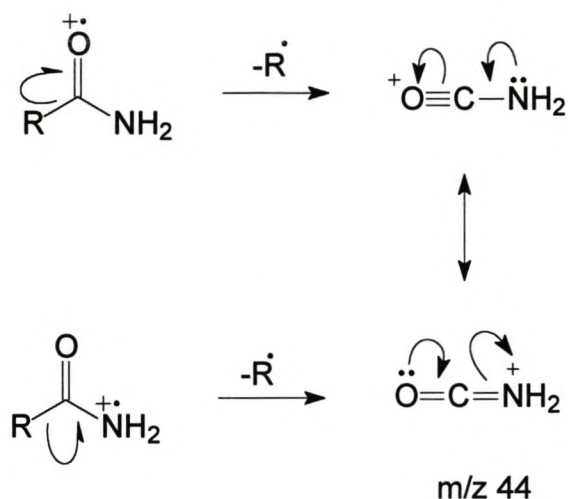
As suggested by the schemes above, the only possible structure for component 1001 was acetophenone and retention-time comparison confirmed this.

The base peak at m/z 43 in the EI mass spectrum of component 1117 (Fig. 3.60) is indicative of a methyl ketone. The ions at m/z 91 (tropylium ion) and 65 suggested that component 1117 possesses a benzyl group and it was therefore derived that the carbonyl group of the ketone was not adjacent to the benzene ring. In addition to these peaks, the molecular ion of component 1117 is observable at m/z 134 and it was noted that the sum of the m/z values of the ions at m/z 43 and 91 equalled that of the molecular ion. This left one possible candidate for component 1117, namely 1-phenyl-2-propanone and retention-time comparison confirmed that component 1117 is 1-phenyl-2-propanone. The formation of ions in the mass spectrum of this compound can be formulated as follows:

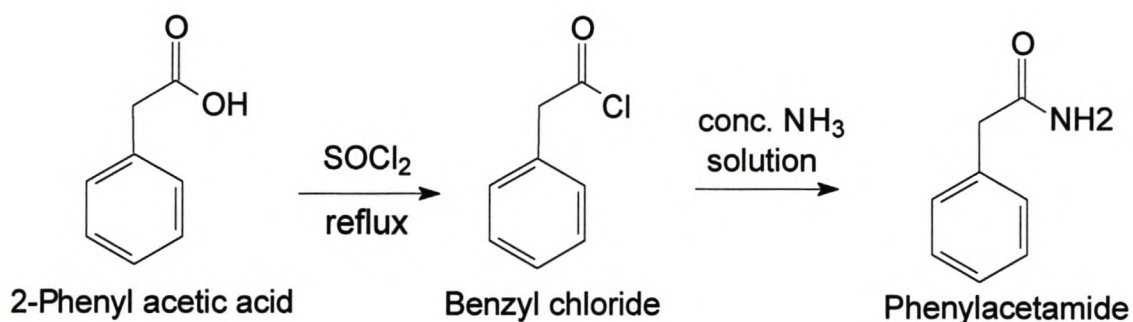


In the EI mass spectrum of component 1550 (Fig. 3.61) significant ions are observed at m/z 44, 65, 91, 92, 135. The familiar ions at m/z 91 (the base peak) and 65 respectively indicated the presence of a tropylium ion and the further decomposition thereof by expulsion of acetylene. Another ion of important diagnostic value is the molecular ion at the odd m/z 135, indicating the presence of an odd number of nitrogen atoms.

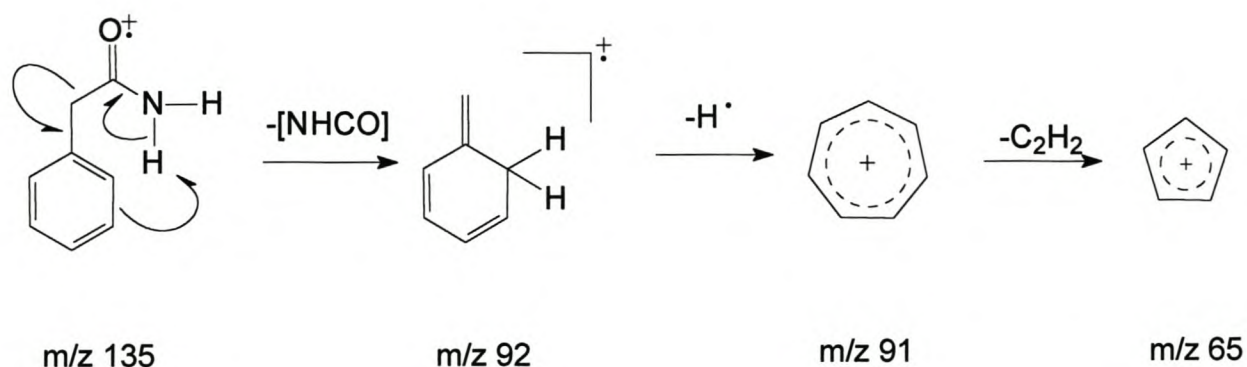
The ion at m/z 44 is due to the characteristic fragmentation of a primary amide, involving the removal of one of the lone pair electrons of either oxygen or nitrogen, which directs α -fission to form the resonance stabilised ion at m/z 44¹⁷. The possibility of the ion at m/z 44 originating from an aliphatic aldehyde was ruled out due to the typical aromatic fragmentation in the mass spectrum and the relatively low mass of the molecular ion. Also, the possibility of component 1548 being an amine was ruled out due to the absence of ions at m/z 58 and 72, characteristic for amines²⁰.



Based on this information, possible candidate structures for component 1548 were N-methylbenzamide and phenylacetamide. N-methylbenzamide was eliminated as a possibility due to the absence of a substituent on the aromatic ring that would allow the formation of a tropylium ion at m/z 91. Phenylacetamide was synthesised (see scheme below and Section 5.7.1) for GC-MS comparison with the natural substance and was confirmed to be phenylacetamide.

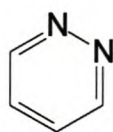


The formation of the ions present in the mass spectrum of phenylacetamide can be explained as follows:

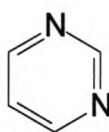


3.1.5 Pyrazines

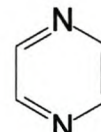
In the EI mass spectrum of component 321 (Fig. 3.62) three prominent ions are observed at m/z 26, 53 and 80. A computer library search gave three probable structures, namely pyridazine (1,2-diazine), pyrimidine (1,3-diazine) and pyrazine (1,4-diazine).



Pyridazine



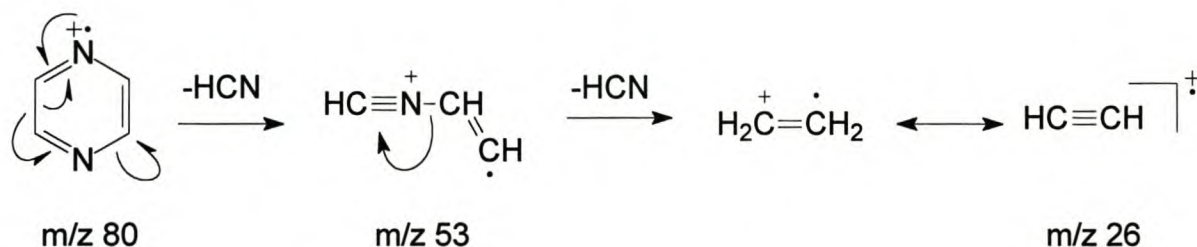
Pyrimidine



Pyrazine

The mass spectra of these compounds are quite similar, but pyridazine could be eliminated because its mass spectrum has a prominent ion at m/z 51, which is absent from the mass spectrum of component 320. Retention-time and mass-spectral comparison of authentic synthetic samples of these two compounds (pyrimidine and pyrazine) with compound 320 showed that the retention-time of pyrimidine was longer than that of the natural substance and confirmed component 320 to be pyrazine.

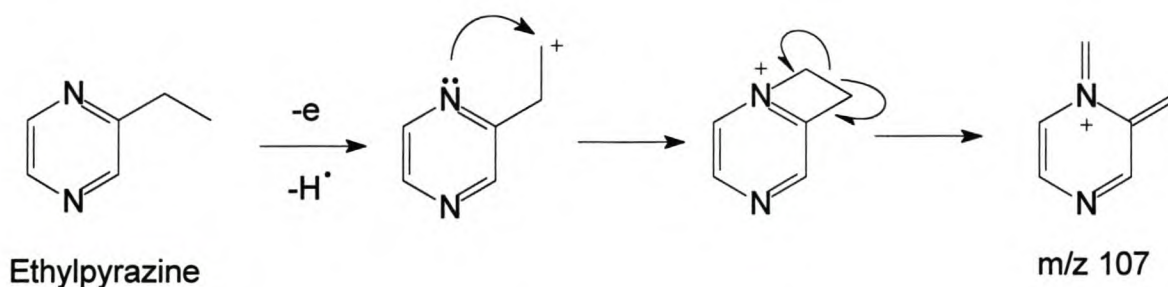
The molecular ion of pyrazine (m/z 80) is very stable and also forms the base peak of the spectrum. The ions at m/z 53 [M-27] and 26 can be explained in terms of the sequential expulsion of hydrogen cyanide from the molecular ion as follows:



The EI mass spectrum of component 494 (Fig. 3.63) with the molecular ion at m/z 94 and an ion at m/z 67 [M-27], is very similar to the mass spectrum of pyrazine. The main difference is that these ions are 14 mass units higher than the corresponding ions in the spectrum of pyrazine (m/z 80 and 53), indicating that component 493 could be a methylpyrazine. Evidence supporting the presence of a substituted pyrazine or pyrimidine is the presence of ions at m/z 53 and 26, indicating a fragmentation pattern similar to that of pyrazine. Therefore, methylpyrazine, 2-methylpyrimidine and 4-methylpyrimidine were considered as possible structures for this constituent. Retention-time comparison of the candidate compounds showed that the retention times of 2- and 4-methylpyrimidine were too long and the retention time of methylpyrazine was the same as that of component 493.

The base peak at m/z 108 in the EI mass spectrum of component 689 (Fig. 3.64) is also the molecular ion. The ion at m/z 81 [M-27] suggested that component 685 could be a pyrazine, because as seen in the case the pyrazine (component 320), the elimination of hydrogen cyanide is of significant diagnostic value.

Based on the molecular ion, component 685 would have to be 1,4-disubstituted to be able to eliminate hydrogen cyanide, or component 685 would have to be an ethyl pyrazine. The possibility of this constituent having an ethyl substituent was eliminated due to the presence in the mass spectrum of ethylpyrazine of an $[M-1]^+$ ion as the base peak, the formation of which can be explained as follows¹⁸:

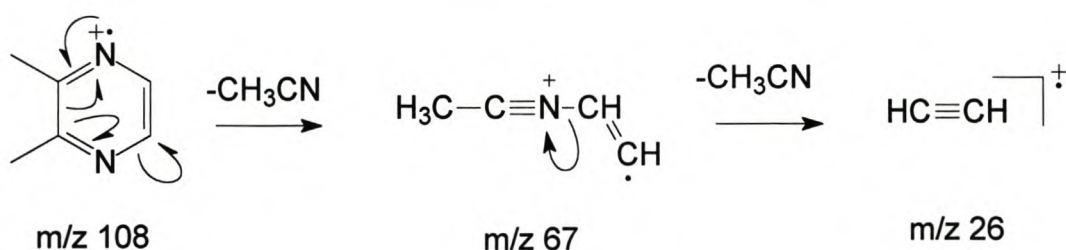


Another significant ion in the mass spectrum of component 685 is the intense ion at m/z 42, which can be explained for pyrazines as a protonated acetonitrile ion. The stability of such a species (protonated acetonitrile) is supported by the presence of a prominent $[M+1]^+$ in the spectra of aliphatic nitriles¹⁸.

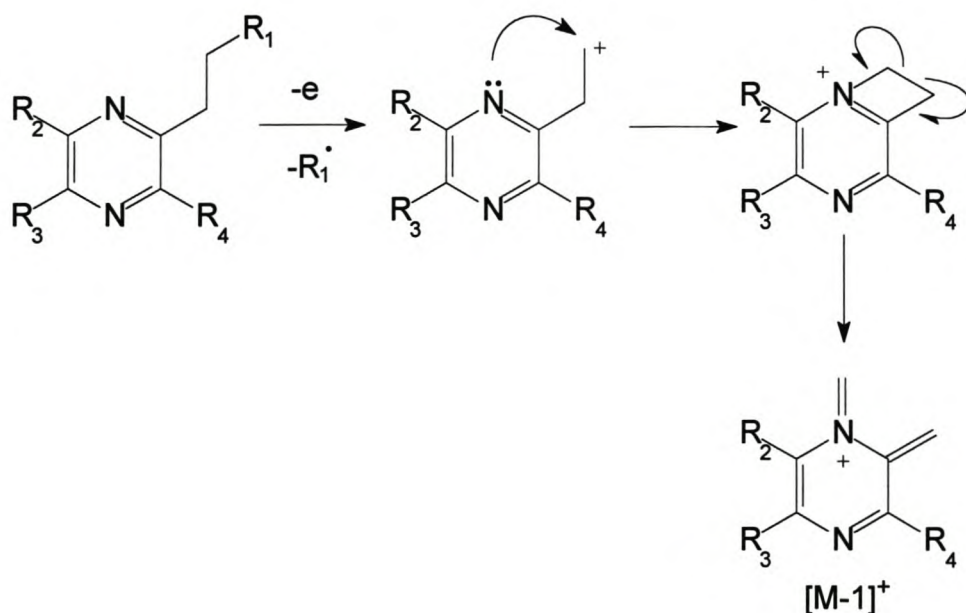
A computer library search was performed and the results obtained provided one possible candidate, namely 2,5-dimethylpyrazine. The identification of component 685 as that of 2,5-dimethylpyrazine was confirmed by retention-time comparison.

In the EI mass spectrum of component 703 (Fig. 3.65) only two abundant ions are observed at m/z 67 (the base peak) and at m/z 108 (the molecular ion). A computer library search yielded only two possible structures for component 703, namely 2,3-dimethylpyrazine and 2-ethoxypyridine. 2-Ethoxypyridine was eliminated as a possibility due the presence of a molecular ion at m/z 123. Retention-time confirmed component 702 to be 2,3-dimethylpyrazine.

The ion at m/z 67 in the mass spectrum of 2,3-dimethylpyrazine could therefore be explained in terms of the elimination of acetonitrile and this elimination occurs in the same manner as the elimination of hydrogen cyanide in pyrazine.

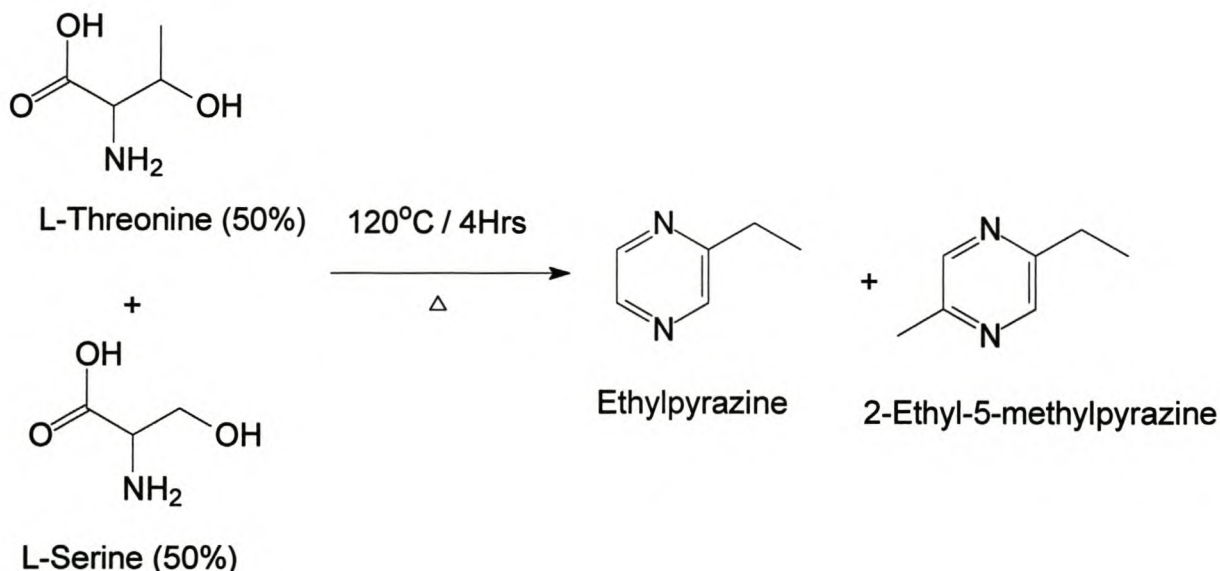


The EI mass spectra of components 697 (Fig. 3.66) and 879 (Fig. 3.67) exhibit prominent molecular ions at m/z 108 and 122 respectively, as well as base peaks at m/z 107 and 121 respectively. The presence of an abundant molecular ion and the base peak at $[\text{M}-1]^+$ in both mass spectra suggested that both components 697 and 878 could be alkylated pyrazines¹⁸. The respective base peaks are probably formed in a similar manner as they both represent an $[\text{M}-1]^+$ ion. The loss of a hydrogen atom can be explained as follows¹⁹:



Evidence supporting the formation of alkylated pyrazines are the ions formed at m/z 80 and 94 for component 697 and 878 respectively, due to an α -cleavage with a hydrogen rearrangement followed by the elimination of ethylene²⁰. A computer library search was performed and the proposed structures for component 878 were 2-ethyl-6-, 2-ethyl-3- and 2-ethyl-5-methylpyrazine and only one compound was suggested for component 697, namely ethylpyrazine.

Taking into consideration that the mass spectrum of 2-ethyl-3-methylpyrazine contains prominent ions at m/z 67 and 80, it was subsequently eliminated as a possible structure of component 878. Similarly 2-ethyl-6-methylpyrazine was discarded due to the presence of a significant ion at m/z 108. Therefore the candidate structures for components 697 and 878 were ethylpyrazine and 2-ethyl-5-methylpyrazine respectively. These two compounds were synthesised (see Section 5.7.3) simultaneously as shown in the scheme below:



The resulting mixture of the two pyrazines was compared with the natural substance by GC-MS and the study confirmed components 697 and 878 to be ethylpyrazine and 2-ethyl-5-methylpyrazine respectively.

The identified metabolites produced by the interdigital micro-organisms in TSB are listed in Table 3.2.

Table 3.2: Volatile metabolites of the interdigital microbial community produced in TSB medium.

In TIC Fig. 3.1	Compound	EI mass spectrum Fig. No.
179	2-butanone	Fig. 3.50
190	2-methyl-3-buten-2-ol	Fig. 3.44
228	3-methyl-2-butanone	Fig. 3.51
243	3-methyl-3-buten-2-one	Fig. 3.55
261	3-methyl-3-buten-2-ol	Fig. 3.45
283	3-hydroxy-2-butanone	Fig. 3.53
321	pyrazine	Fig. 3.62
337	3-methyl-1-butanol	Fig. 3.43
343	2-methyl-2-butenal	Fig. 3.46
364	3-methyl-2-pentanone	Fig. 3.52
416	3-methyl-2-butenal	Fig. 3.47
494	methylpyrazine	Fig. 3.63
536	4-hydroxy-4-methyl-2-pentanone	Fig. 3.54
689	2,5-dimethylpyrazine	Fig. 3.64
697	ethylpyrazine**	Fig. 3.66
703	2,3-dimethylpyrazine	Fig. 3.65
788	benzaldehyde	Fig. 3.57
879	2-ethyl-5-methylpyrazine**	Fig. 3.67
957	2-hydroxybenzaldehyde	Fig. 3.58
1001	acetophenone	Fig. 3.59
1085	nonanal	Fig. 3.48
1094	2-phenylethanol	Fig. 3.56
1117	1-phenyl-2-propanone	Fig. 3.60
1264	decanal	Fig. 3.49
1550	phenylacetamide	Fig. 3.61

3.2 IDENTIFICATION OF THE MICROBIAL METABOLITES PRODUCED IN MSM AS GROWTH MEDIUM

The total ion chromatogram (TIC) (Fig. 3.2) of the extract of the microbial metabolites produced by the total community of bacteria in MSM with glucose as nutrient source, will be used as reference in this discussion. Identification of the volatile organic components of an extract of the medium, containing the total microbial community, was done by interpretation of their low-resolution EI mass spectra and confirmation by comparison with computer library data, as well as by gas chromatographic retention time comparison.

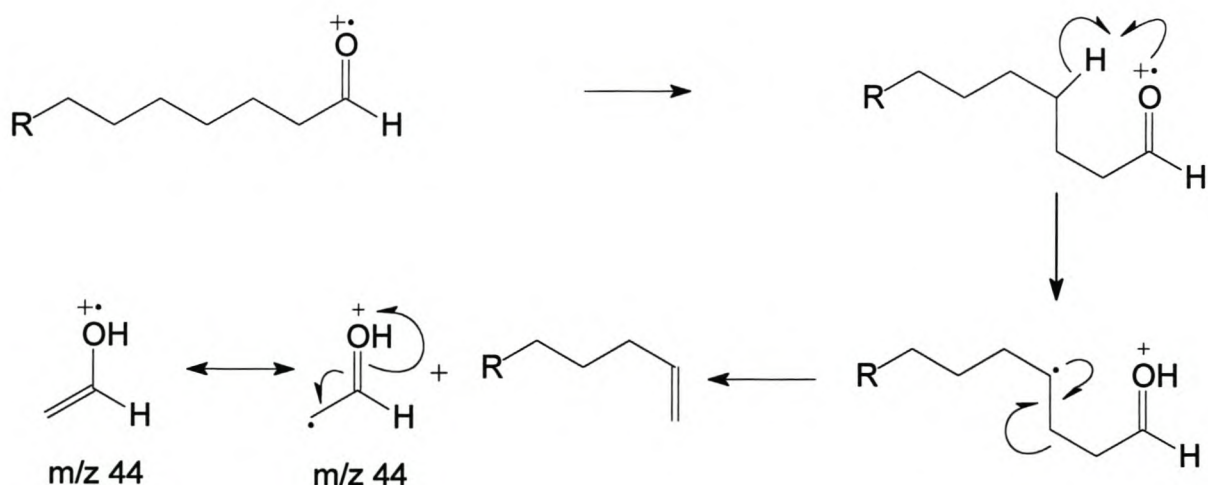
3.2.1 Alcohols: Aliphatic

In the EI mass spectrum of component 1544 (Fig. 3.68), two series of prominent ions appear at m/z 41, 55, 69... and m/z 43, 57, 71... These ion series correspond to the general formulae $[C_nH_{2n-1}]^+$ and $[C_nH_{2n+1}]^+$, respectively, and show a decreasing relative abundance with increasing fragment mass, typically found in the spectra of long chain unbranched 1-alkanols²¹ and 1-alkenes.

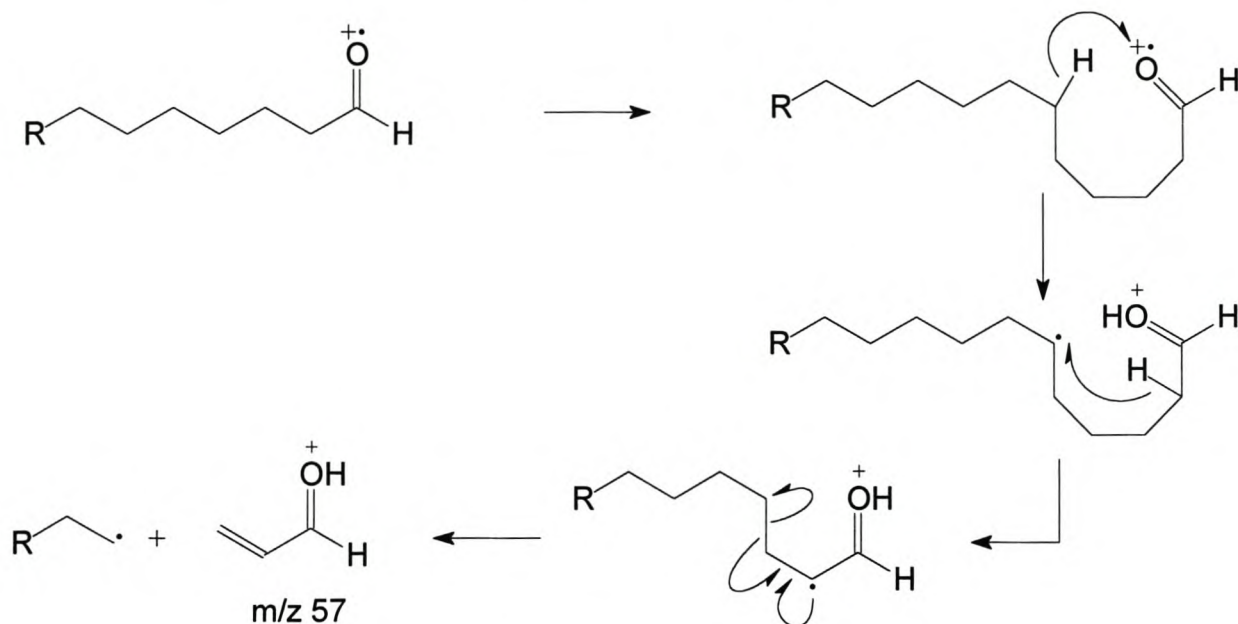
A computer library search was performed and 1-heptene through 1-nonene and 1-heptanol through 1-octanol were suggested as possible structures for component 1544. A retention time analysis of all the compounds revealed that the retention time of 1-octanol matched that of component 1544, thus confirming the structure of component 1544 to be 1-octanol.

3.2.2 Aldehydes: Aliphatic (Saturated)

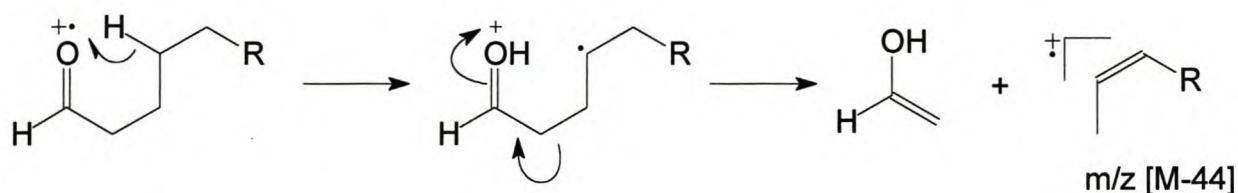
The EI mass spectra of components 1276 (Fig. 3.69), 1646 (Fig. 3.70), 1937 (Fig. 3.71), 2196 (Fig. 3.72), 2433 (Fig. 3.73), 2656 (Fig. 3.73) and 2866 (Fig. 3.75) all have prominent ions at m/z 44 and m/z 57, and they exhibit clusters of ions 14 mass units apart, at m/z 29, 43, 57, 85..., which can be ascribed to the formation of $[C_nH_{2n+1}CO]^+$ and $[C_nH_{2n+1}]^+$ ions. This is characteristic of unbranched aliphatic aldehydes²². Since unbranched aldehydes, containing four to seven carbon atoms, have an ion at m/z 44²³, it was assumed that these components were aldehydes with more than four carbon atoms. The ion at m/z 44 must be a rearrangement peak as it occurs at an even mass, and can be attributed to the characteristic McLafferty rearrangement, resulting in the elimination of an olefin:



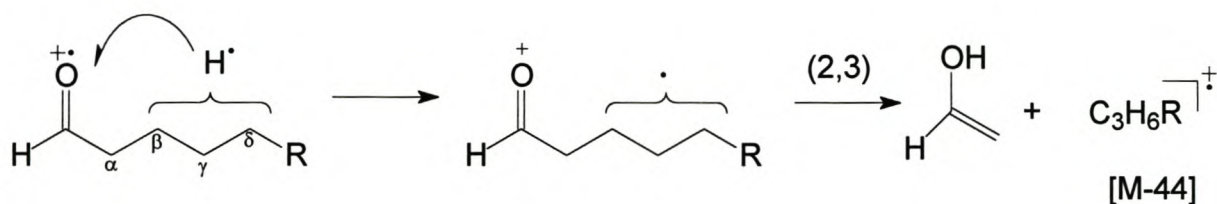
The accompanying [McLafferty + 13] ion at m/z 57 is formed as follows:



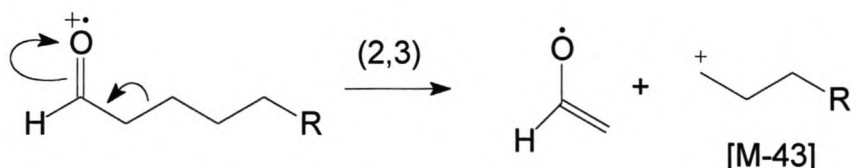
Another characteristic feature of aldehydes without α -branching, is the presence of an ion at $[M-44]^+$. Labelling experiments with ^{18}O show that fragments resulting from this loss are ions with the general formula $[C_nH_{2n}]^+$. This implies β -cleavage with hydrogen atom transfer as in McLafferty rearrangement, but with charge-retention on the alkene fragment⁹:



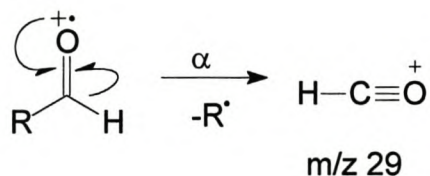
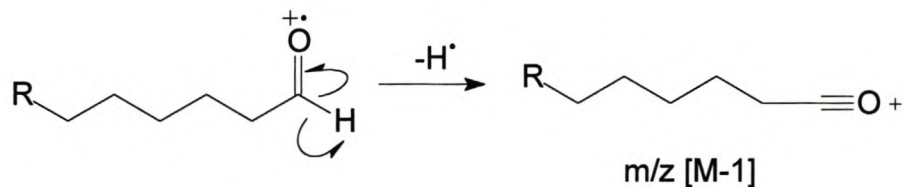
Data obtained with deuterated hexanals, however, demonstrate that this process is in fact not of the site-specific McLafferty rearrangement type⁷. Of the total transfer of hydrogen atoms, 81% originate from the β -, γ - or δ -positions, and therefore the following formulation is more realistic:



Another type of β -cleavage also occurs in which no hydrogen atom transfer takes place and the positive charge is retained on an alkyl fragment⁷ with general formula $[C_nH_{2n+1}]^+$:

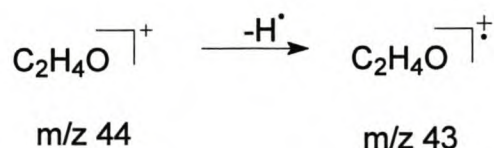


Both possible α -cleavage reactions occur, namely elimination of either an alkyl radical or a hydrogen atom, with the charge remaining on the oxygen-containing fragment. The loss of the larger alkyl radical is favoured. The formation of these ions can be rationalised as follows:

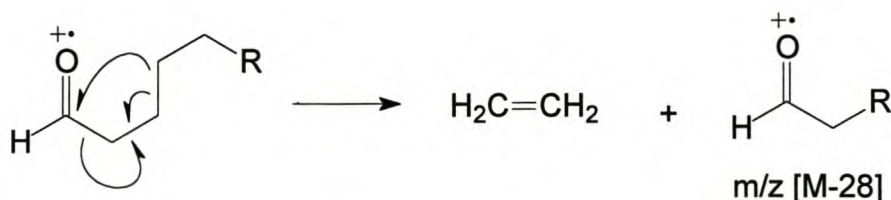


Another fairly prominent ion in the mass spectra of unbranched aldehydes appears at m/z 43. This ion has been shown to be an oxygen-containing

fragment with elemental composition $[C_3H_3O]^+$, and evidence exists that it is formed as a result of the loss of a hydrogen atom from the m/z 44 ion²⁴:



On the basis of the above, a series of synthetic unbranched aldehydes, heptanal through tetradecanal and hexadecanal, were analysed by GC-MS and components 1276, 1664, 1937, 2196, 2433, 2656 and 2866 were identified as octanal, nonanal, decanal, undecanal, dodecanal, tridecanal and tetradecanal, respectively. The molecular ions of the larger aliphatic aldehydes often have a low abundance, but the presence of characteristic $[M-H_2O]^+$ and $[M-C_2H_4]^+$ fragments can be used for identification⁵. Deuterium-labelling experiments have shown that the favoured site of transfer for the hydrogen atoms in the elimination of water, is the C3 carbon atom. Data from deuterated hexanals indicate that the C2 and C3 carbon atoms are eliminated as a unit in the expulsion of ethylene⁷.



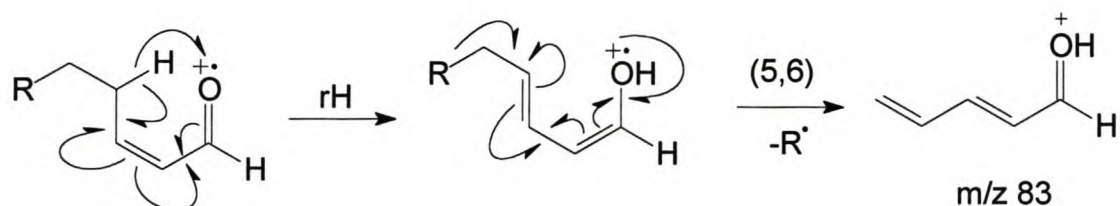
The $[M-H_2O]^+$ and $[M-C_2H_4]^+$ ions are present at m/z 138 and m/z 128, respectively, in the mass spectrum of decanal (component 1937, Fig. 3.71).

In the spectra of these aliphatic aldehydes, especially the larger aliphatic aldehydes, an ion series following the general formula of $68 + 14n$ ($n = 0, 1, 2, \dots$) is observed. This unique series of ions are formed due a rearrangement,

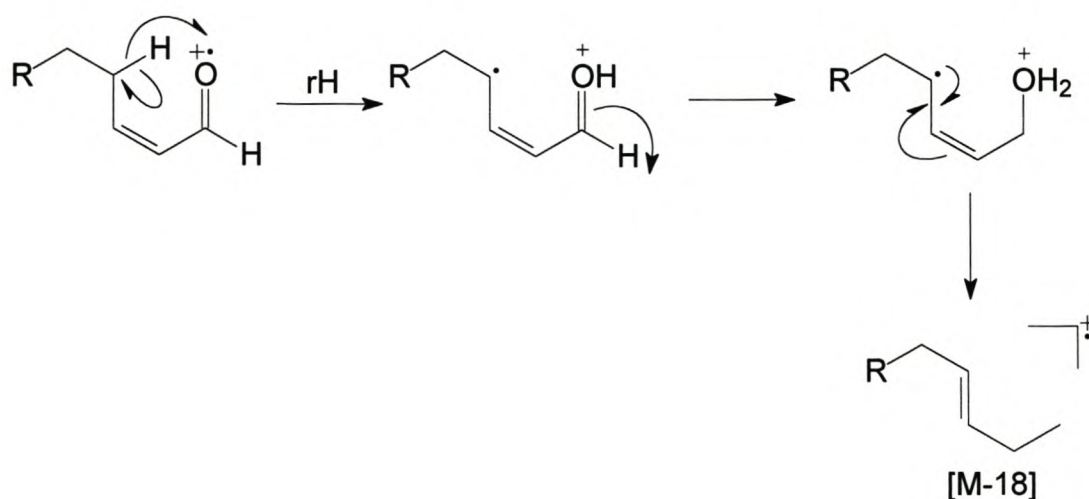
whereby expulsion of an alcohol causes ring closure of the aldehyde. This mechanism is discussed in Section 3.1.2.

3.2.3 Aldehydes: Aliphatic (Unsaturated)

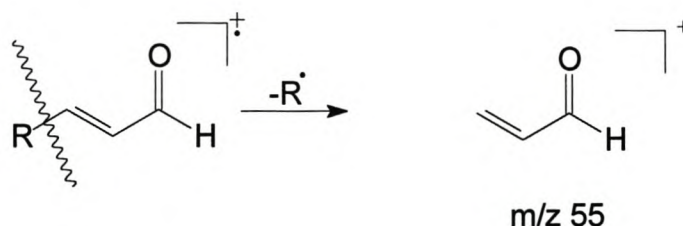
The EI mass spectra of components 1034 (Fig. 3.76), 1804 (Fig. 3.77), 2080 (Fig. 3.78) and 2329 (Fig. 3.79) exhibit the common ion at m/z 83, which is a characteristic nonallylic loss of δ -alkyl radicals from α,β -unsaturated aldehydes, proceeding via a γ -hydrogen rearrangement to form a more stable dienol ion^{25,26}. This ion then loses the δ -alkyl group by cleavage of the newly allylic bond as follows:



Therefore, it was assumed that components 1034, 1804, 2080 and 2329 belong to a homologous series of α,β -unsaturated aldehydes. The molecular ions of the components are either very weak or in the case of component 2329, completely absent. Other significant ions present in the mass spectra of these components are the ions formed at $[M-18]^+$ (m/z 94, 122, 136 and 150, respectively) and the very weak ion at $[M-28]^+$, formed by the expulsion of ethylene from the aldehyde.



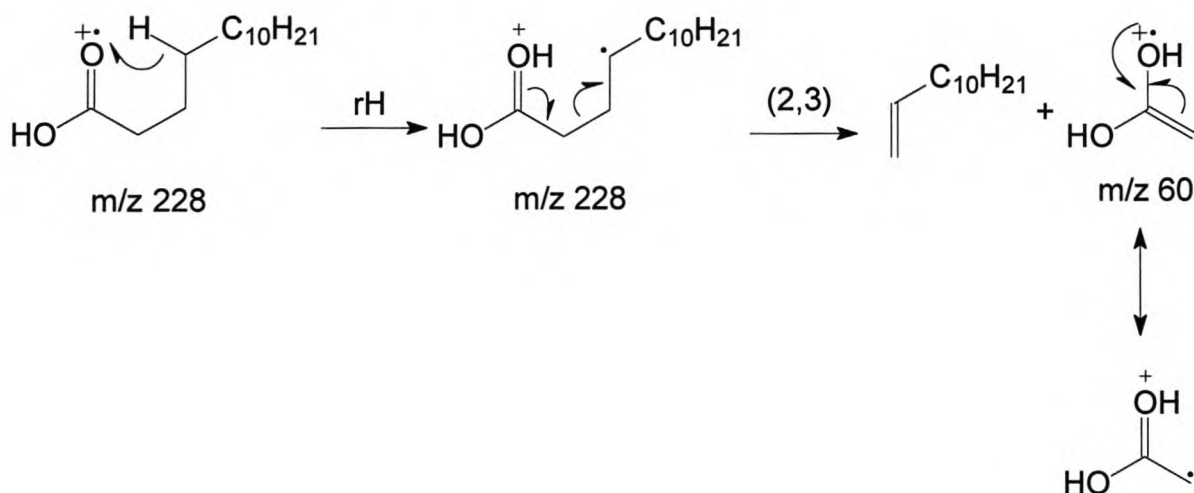
The very prominent ion formed at m/z 55 can be attributed to the simple fission of the bond between C3 and C4. Its high abundance and its presence in all of the mass spectra under discussion can be interpreted as evidence that this ion is formed by simple fission. The ion at m/z 55 can be formulated of as follows:



Based on this information components 1034, 1804, 2080 and 2329 were assumed to be 2-heptenal, 2-nonenal, 2-decenal and 2-undecenal, respectively. Retention-time comparison of a homologous series of 2-unsaturated aldehydes, 2-hexenal through 2-tetradecenal, concluded that components 1034, 1804, 2080 and 2329 were 2-heptenal, 2-nonenal, 2-decenal and 2-undecenal, respectively.

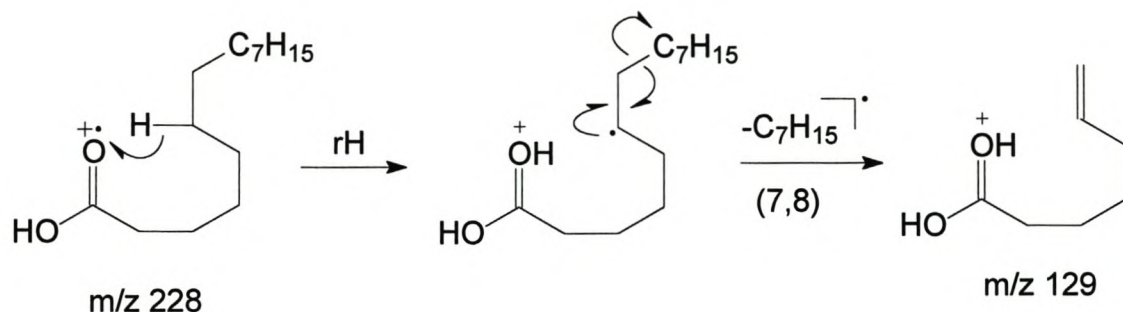
3.2.4 Acids: Aliphatic (Saturated)

The EI mass spectra of components 1234 (Fig. 3.80), 1565 (Fig. 3.81), 2090 (Fig. 3.82), 2750 (Fig. 3.83), 3137 (Fig. 3.84), 3317 (Fig. 3.85), 3495 (Fig. 3.86), 3657 (Fig. 3.87), 3818 (Fig. 3.88), 4121 (Fig. 3.89) and 4470 (Fig. 3.90) are characterised by the presence of a prominent ion at m/z 60, indicating that all these components could be aliphatic acids²⁷, probably belonging to the same homologous series. The EI mass spectrum of component 3137 will be discussed as representative of this series of compounds. Acids generally have reasonably prominent molecular ions, the relative abundance of which increases with molecular mass for unbranched aliphatic acids containing more than six carbon atoms²⁸. For this reason, the ion at m/z 228 in the mass spectrum of component 3137 was assumed to be the molecular ion and this component was therefore presumed to be tetradecanoic acid ($C_{14}H_{28}O_2$, 228 Da). The ion at m/z 60 is formed by the following McLafferty rearrangement²⁹:

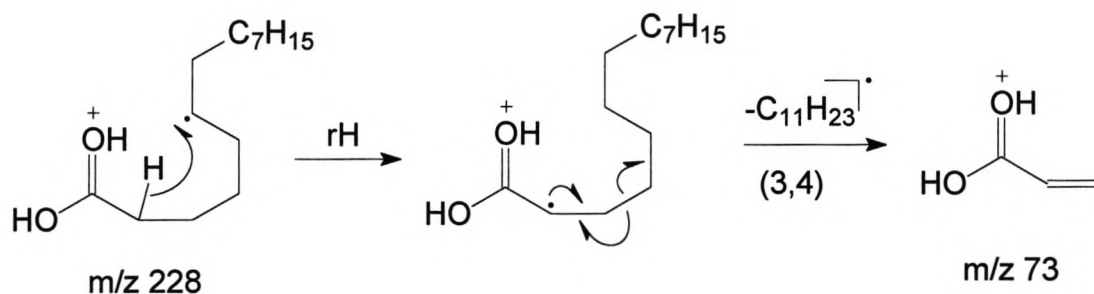


A prominent series of ions in this EI mass spectrum occurs at m/z 73 and 115, 129, 143, 157... These ions are formed by hydrogen transfer from carbon atoms along the carbon chain of the acid, in conjunction with homolysis of one

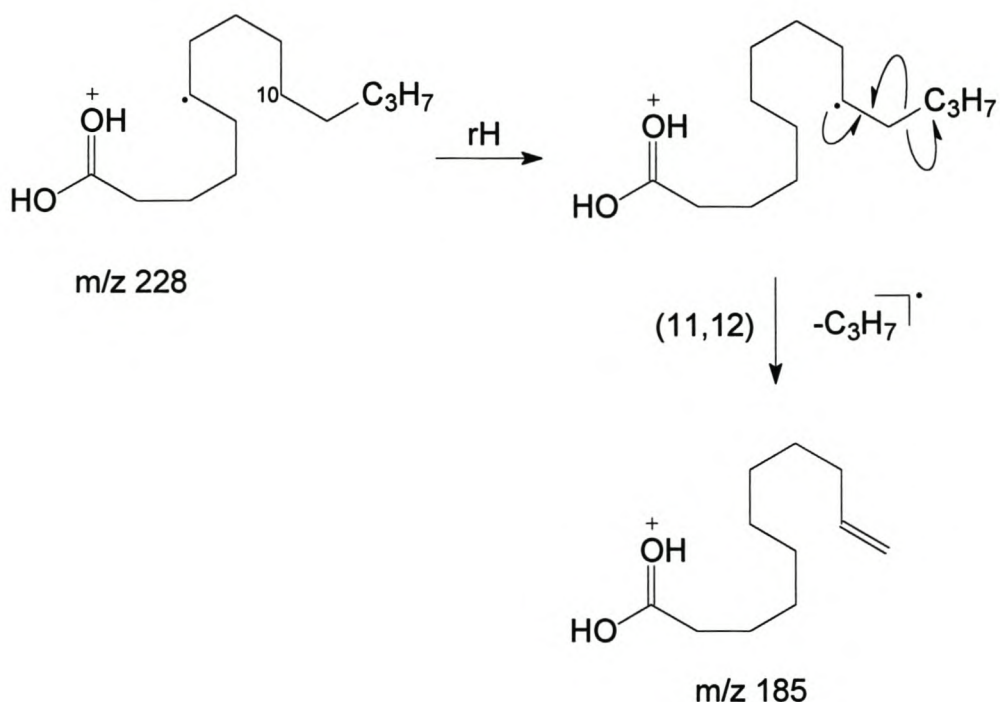
of the bonds beta to these hydrogen-depleted carbon atoms. In the case of the m/z 129 ion, the process can be illustrated as follows³⁰:



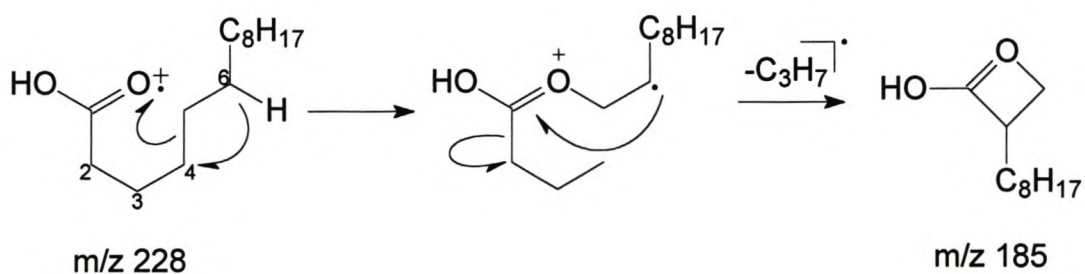
Of these, the transfer of a hydrogen atom from the α -position and β -cleavage is the most favoured reaction. The driving force for this reaction is the high stability of the α,β -unsaturated protonated carbonyl system. The resulting [McLafferty + 13] ion often accompanies the normal McLafferty rearrangement ion³¹:



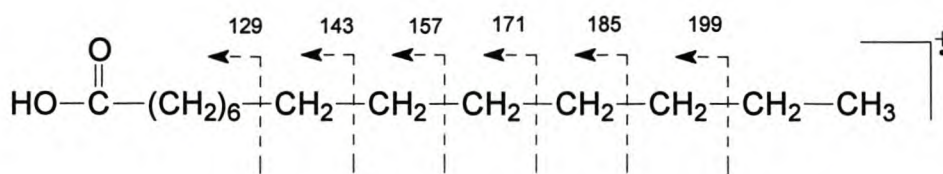
In the same manner, hydrogen migration from C10, followed by β -cleavage, results in the formation of the ion at m/z 185:



The appearance of an ion at $m/z\ 185$ also corresponds to the loss of 43 atomic mass units from the molecular ion, and can be explained by a rearrangement reaction involving the transfer of a hydrogen atom from C6, resulting in the elimination of the fragment containing carbon atoms C2-C4:



The formation of this series of ions at $m/z\ 199\ [M-29]^+$, $185\ [M-43]^+$, $71\ [M-57]^+$..., could also be explained in terms of simple α -cleavage with the charge retained on the oxygen-containing fragments. α -Cleavage with charge retention on the alkyl groups accounts for many of the ions in the lower mass range of the spectrum:



Retention-time comparison with a series of synthetic acids, hexanoic acid through docosanoic acid, confirmed that components 1234, 1565, 2090, 2750, 3137, 3317, 3495, 3657, 3818, 4121 and 4470 are hexanoic, heptanoic, nonanoic, dodecanoic, tetradecanoic, pentadecanoic, hexadecanoic, heptadecanoic, octadecanoic, eicosanoic and docosanoic acid, respectively.

3.2.5 Acids: Aliphatic (Unsaturated)

The EI mass spectra of components 3458 (Fig. 3.91) and 3784 (Fig. 3.92) have ions at m/z 60 and 73 with relative abundance lower than that of a typical saturated aliphatic acid. In addition, it contains a series of prominent ions at m/z 41, 55, 69, 83, 97..., corresponding to the typical formula $[\text{C}_n\text{H}_{2n-1}]^+$, which is characteristic of unsaturated aliphatic acids. These components have retention times slightly shorter (*ca.* 30 s) than their respective saturated acid analogues, which could indicate unsaturation or branching. Evidence supporting the presence of unsaturated acids is the weak ion formed at $[\text{M}-\text{OH}]^+$ (32 (m/z 237 and 265, respectively) and the molecular ion (m/z 254 and 282, respectively). Another significant feature of both spectra is the presence of a $[\text{M}-18]^+$ ion at m/z 236 and 264, respectively, corresponding to the loss of water.

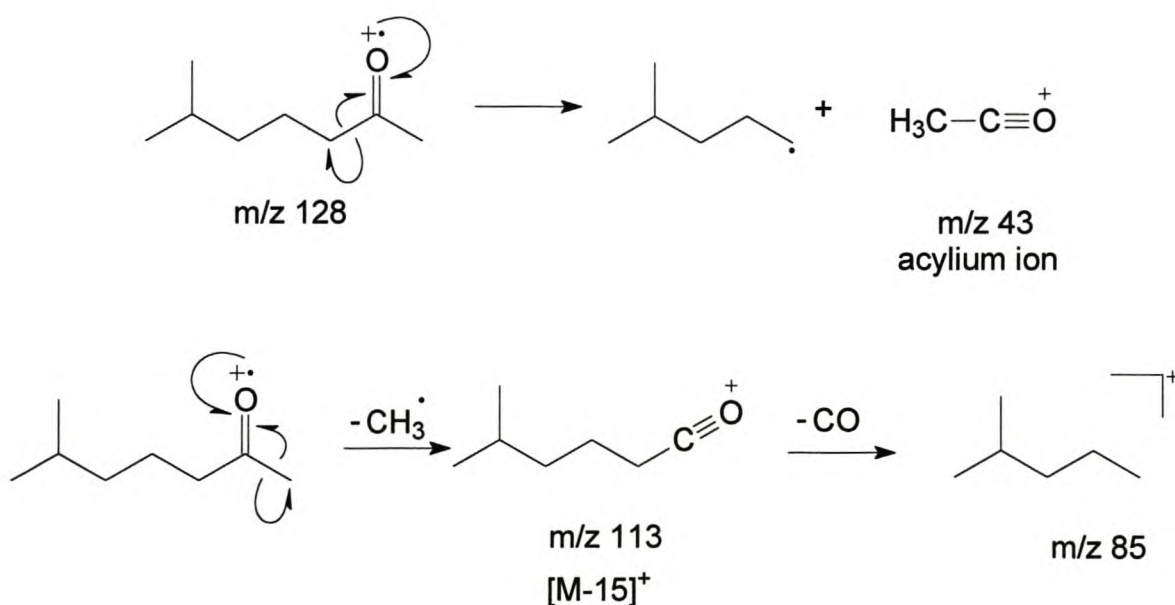
If it is accepted that these two compounds are aliphatic acids, their molecular ions at m/z 254 and 282 indicate the presence of a double bond. The position of the unsaturation cannot be determined by mass spectrometry without using

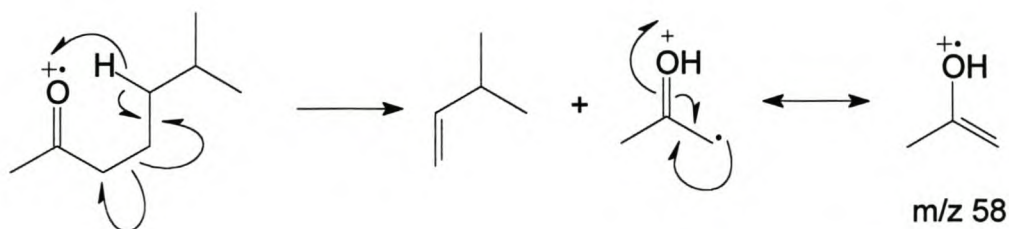
ancillary techniques. It is, however, known that the cell membranes of bacteria consist of Δ_9 -unsaturated acids and that Δ_9 -unsaturated acids are synthesised biologically in bacteria. It was therefore presumed that these unsaturated acids could be 9-hexadecenoic acid and 9-octadecenoic acid.

This assumption was confirmed by retention-time comparison with authentic synthetic samples of the two acids.

3.2.6 Ketones: Aliphatic

In the EI mass spectrum of component 1048 (Fig. 3.93) the base peak at m/z 43 and the prominent ion at even mass m/z 58 are indicative of an acylium ion and a McLafferty rearrangement of a methyl ketone. Further confirmation that this compound could be a ketone are the ions of weak abundance at m/z 128 (the molecular ion) and the $[M-15]^+$ ion at m/z 113. Other significant peaks present in the mass spectrum are m/z 71, 85, 95 and 110 suggesting that component 1048 could be a 2-octanone⁵. Comparison with various methylketones showed component 1048 to be 6-methyl-2-heptanone.





The prominent ions in the EI mass spectrum of component 1900 (Fig. 3.94) are m/z 43, 58 (base peak), and 71. The characteristic ions at m/z 43 and 58 suggest that component 1900 is also methyl ketone. In comparison to the mass spectrum of component 1048, the higher relative abundance of both the molecular ion at m/z 156 and the $[M-15]^+$ ion (m/z 141) suggested that component 1900 could be a straight-chain aliphatic ketone, possibly 2-decanone.

A retention-time comparison confirmed component 1900 to be 2-decanone.

3.2.7 Aromatic compounds

Component 1013 was identified as benzaldehyde on account of its mass spectrum and this was confirmed by retention time comparison. The mass spectrum of benzaldehyde (Fig. 3.57) has already been discussed in Section 3.1.4.

3.2.8 Squalene

The prominent ions in the EI mass spectrum of component 5172 (Fig. 3.95) are the base peak at m/z 69, and the ions at m/z 81, 95, 109, 123, 137 and 149. Other significant, although weak, ions in the mass spectrum of component 5172 are present at m/z 341 and, what was assumed to be the molecular ion,

at m/z 410. A similar spectrum was previously observed in a GC-MS analysis of the dorsal gland of the springbok and was identified as squalene, based on various characterisation methods, namely its mass spectrum and ^{13}C NMR³³. Retention-time comparison of synthetic squalene confirmed that component 5172 was indeed squalene.

The identified metabolites produced by the interdigital micro-organisms in MSM with glucose as a nutrient source are listed in Table 3.3.

Table 3.3: Volatile metabolites of the interdigital microbial community produced in MSM medium.

In TIC Fig. 3.2	Compound	El mass spectrum Fig. No.
1013	benzaldehyde	Fig. 3.57
1034	(Z)-2-heptenal	Fig. 3.76
1048	6-methyl-2-heptanone	Fig. 3.93
1234	hexanoic acid	Fig. 3.80
1276	octanal	Fig. 3.69
1546	1-octanol	Fig. 3.68
1565	heptanoic acid	Fig. 3.81
1646	nonanal	Fig. 3.70
1804	2-nonenal	Fig. 3.77
1902	2-decanone	Fig. 3.94
1937	decanal	Fig. 3.71
2080	(Z)-2-decenal	Fig. 3.78
2090	nonanoic acid	Fig. 3.82
2196	undecanal	Fig. 3.72
2329	2-undecenal	Fig. 3.79
2433	dodecanal	Fig. 3.73
2656	tridecanal	Fig. 3.74
2750	dodecanoic acid	Fig. 3.83
2866	tetradecanal	Fig. 3.75
3137	tetradecanoic acid	Fig. 3.84
3317	pentadecanoic acid	Fig. 3.85
3458	9-hexadecenoic acid	Fig. 3.91
3495	hexadecanoic acid	Fig. 3.86
3657	heptadecanoic acid	Fig. 3.87
3784	9-octadecenoic acid	Fig. 3.92
3818	octadecanoic acid	Fig. 3.88
4121	eicosanoic acid	Fig. 3.89
4470	docosanoic acid	Fig. 3.90
5172	squalene	Fig. 3.95

Sample: MDD COMMUNE F-TSB 30ds: P259; 40(4)-6-220-2-280(30)

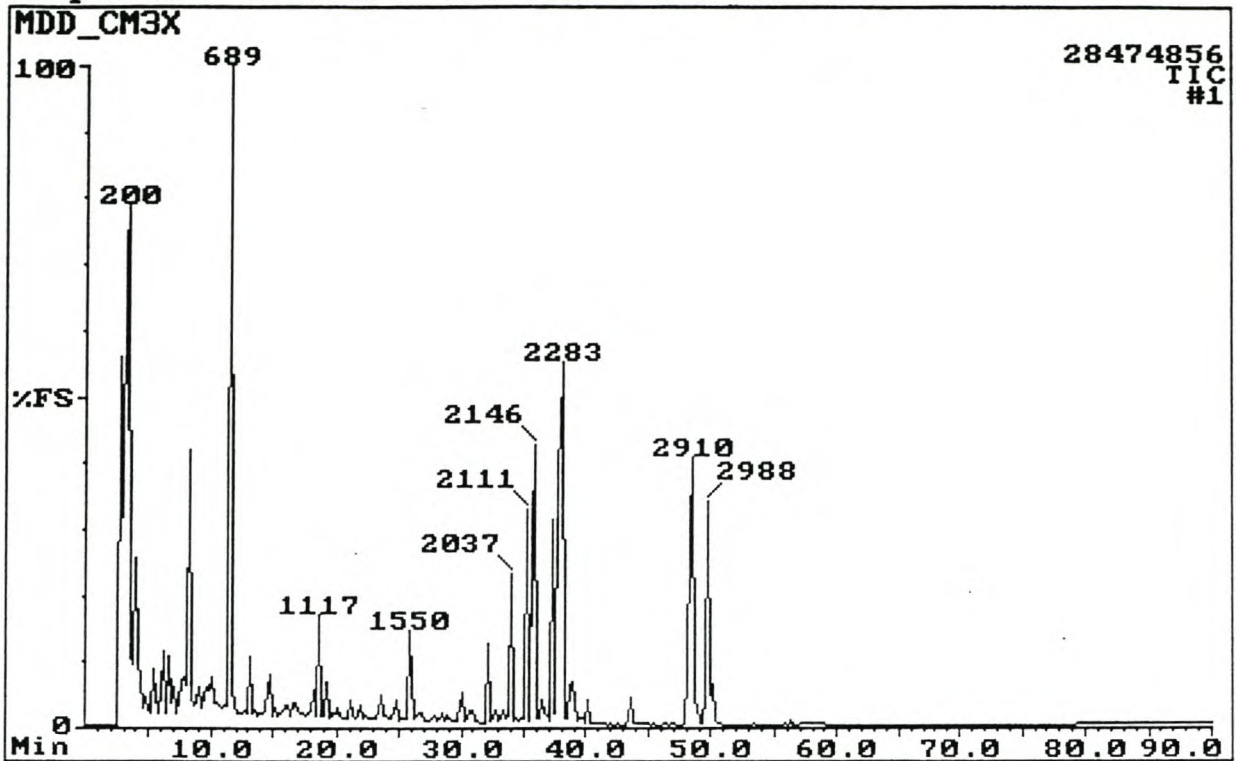


Fig. 3.1: Total ion chromatogram (TIC) of the volatile metabolite extract (30 days) of the total community of bacteria in TSB.

Sample: COMMUNE MSM 3ds: P262; 40C(4min)-4C/min-280(30min)

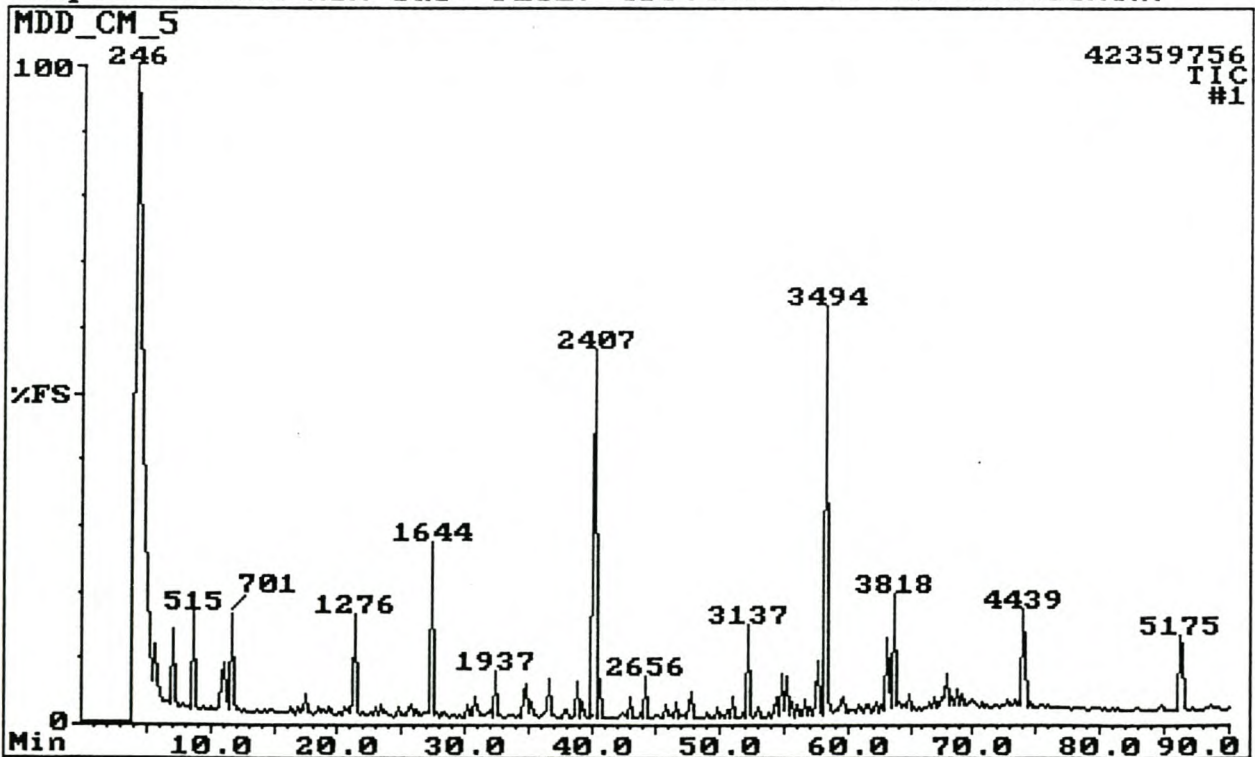


Fig. 3.2: Total ion chromatogram (TIC) of the volatile metabolite extract (3 days) of the total community of bacteria in MSM.

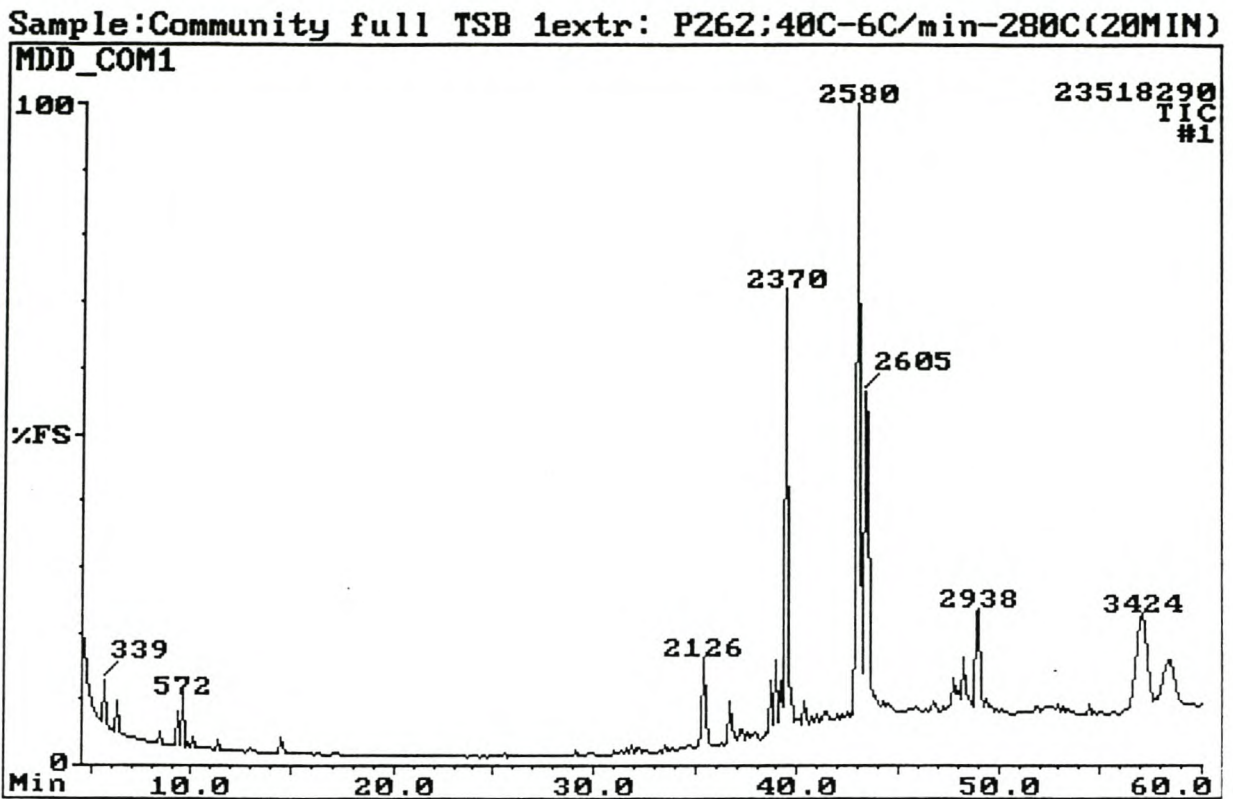


Fig. 3.3: Total ion chromatogram (TIC) of the volatile metabolite extract (3 days) of the total community of bacteria in TSB.

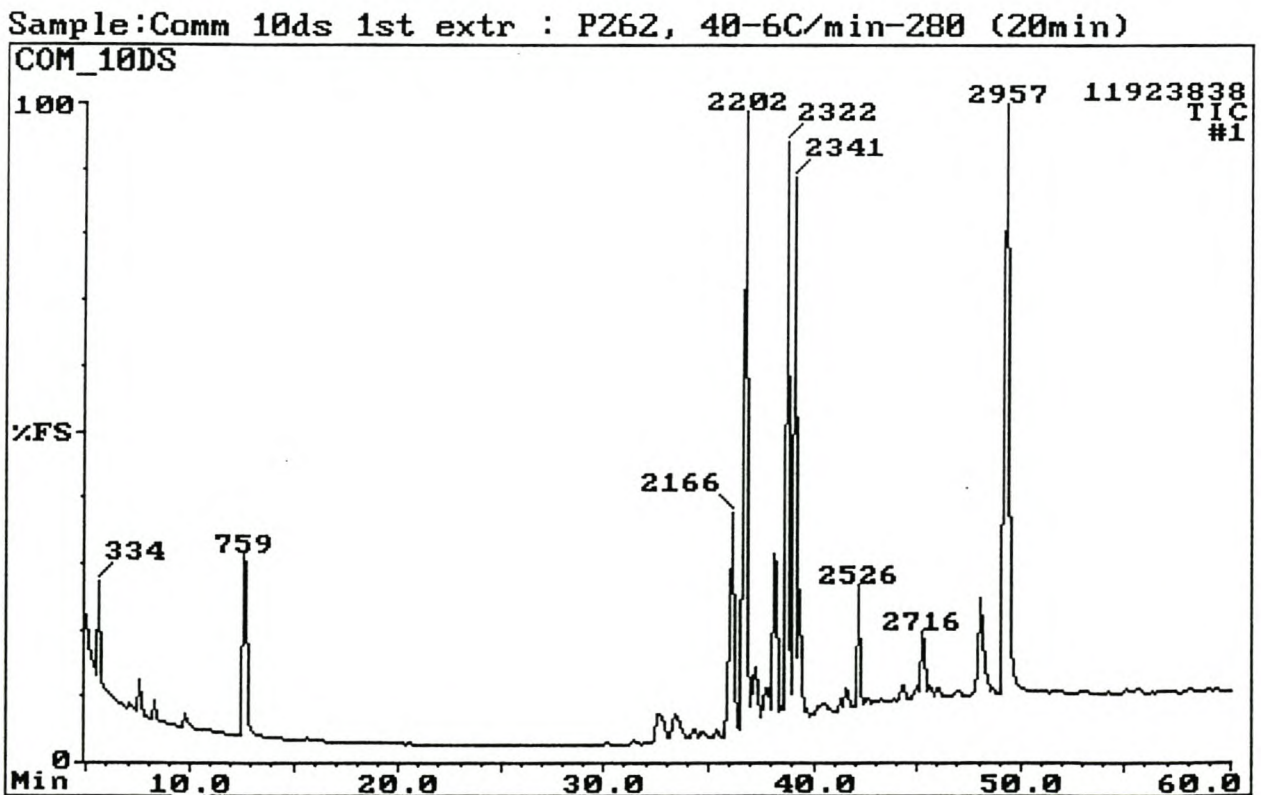


Fig. 3.4: Total ion chromatogram (TIC) of the volatile metabolite extract (10 days) of the total community of bacteria in TSB.

Sample:L1_1 F_TSB 3ds : P262:40C-6C/min-280C(20MIN)

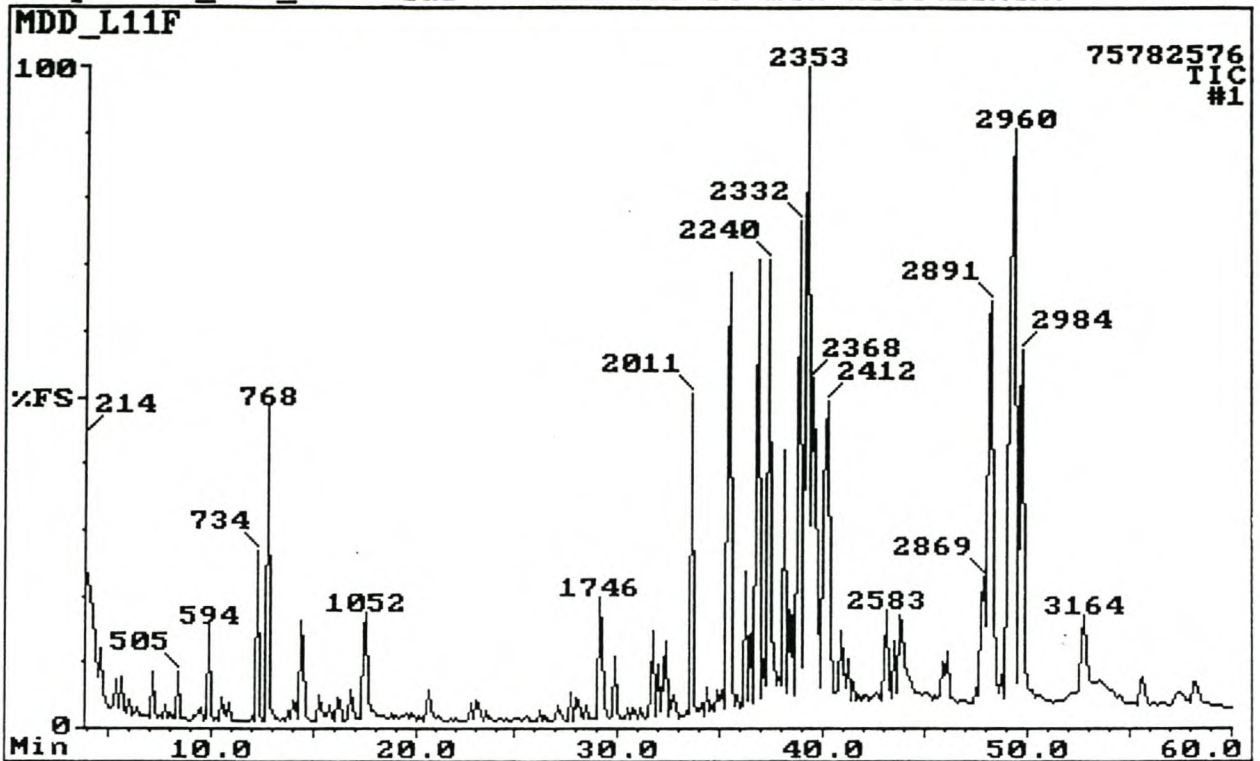


Fig. 3.5: Total ion chromatogram (TIC) of the volatile metabolite extract (3 days) of micro-organism R1.1 in TSB.

Sample:r1_1 F-tsb 10ds 1xtr: P262, 40-4C/min-280C(10min)

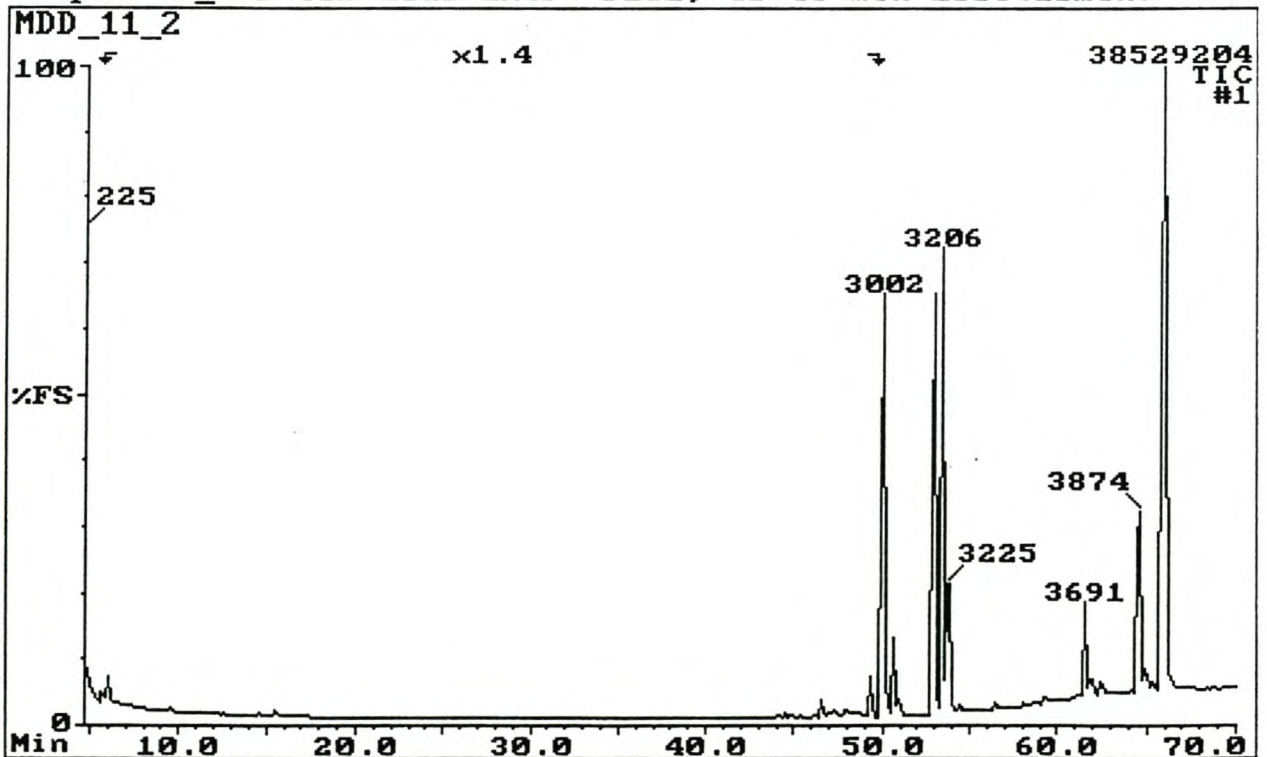


Fig. 3.6: Total ion chromatogram (TIC) of the volatile metabolite extract (10 days) of micro-organism R1.1 in TSB.

Sample:L1.1 F-TSB 30ds RAMPED RUN :P262 40(4)-6-210-2-280(30)

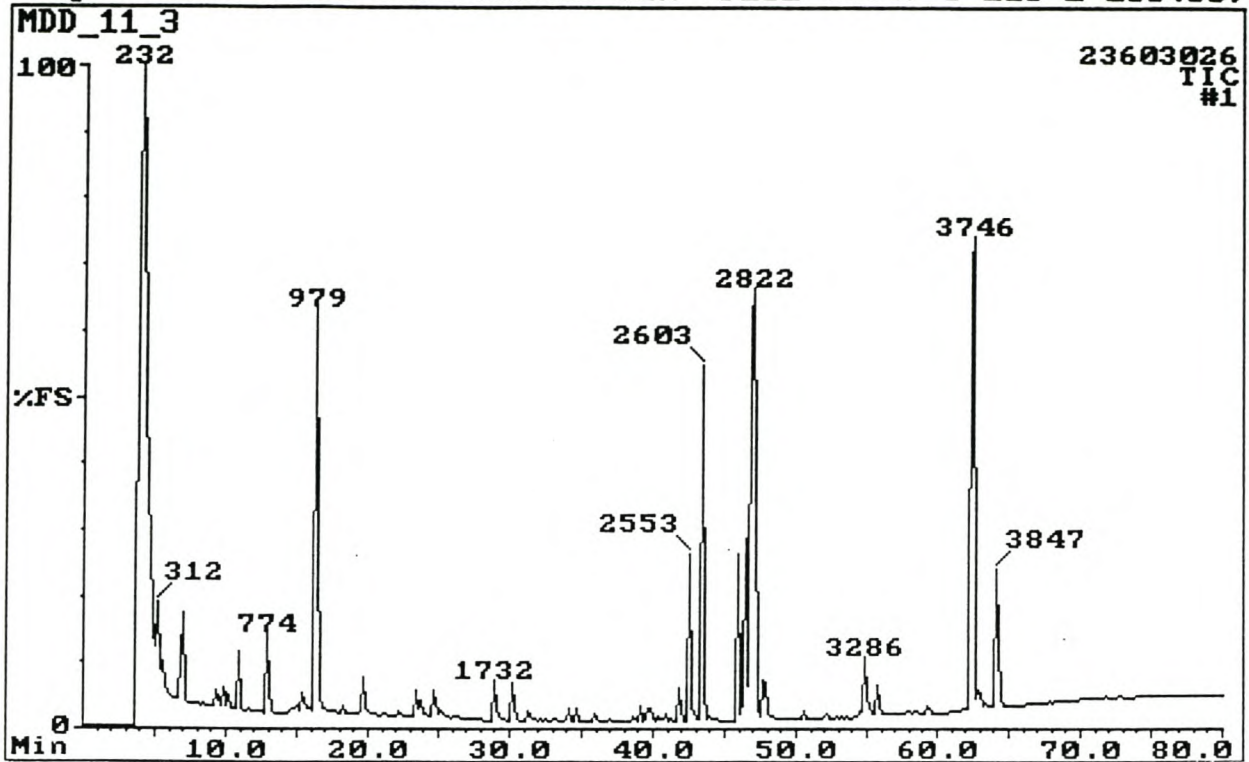


Fig. 3.7: Total ion chromatogram (TIC) of the volatile metabolite extract (30 days) of micro-organism R1.1 in TSB.

Sample:R1_2 F_TSB 1st extr 3ds:P262:40C-6C/min-280C(20min)

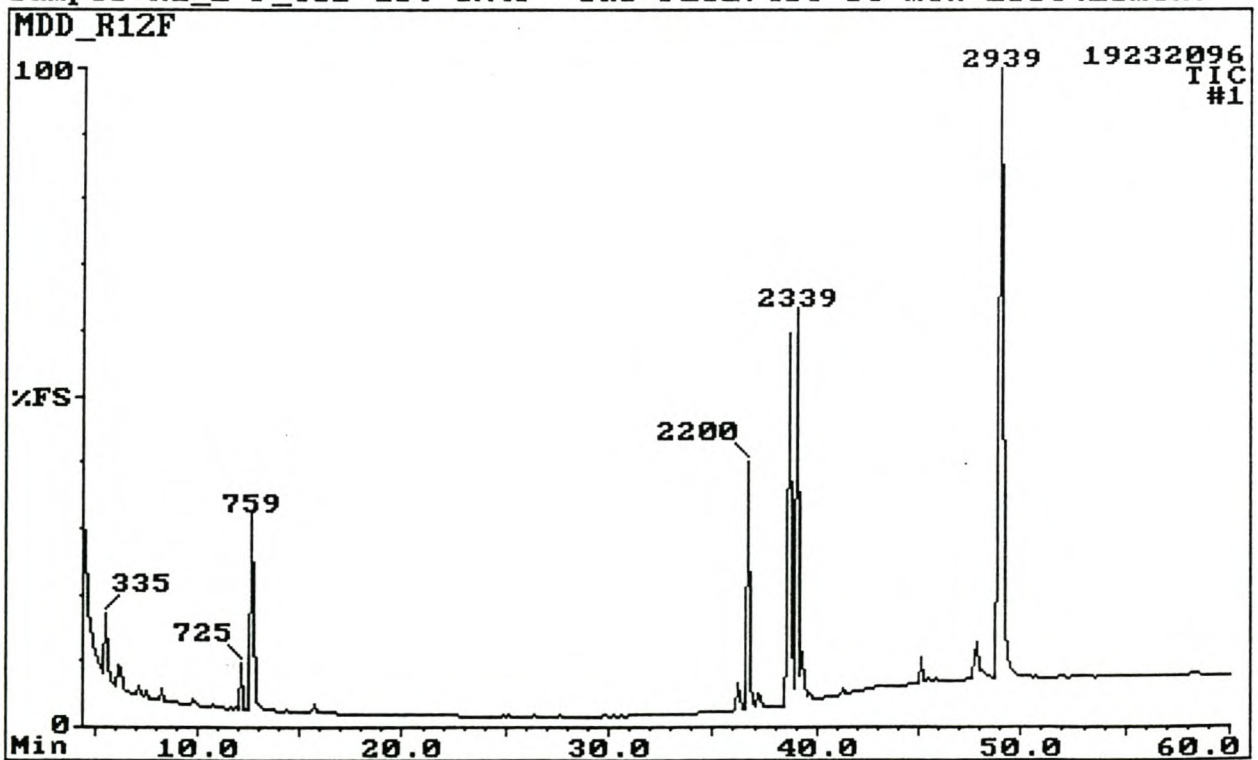


Fig. 3.8: Total ion chromatogram (TIC) of the volatile metabolite extract (3 days) of micro-organism R1.2 in TSB.

Sample: R1_2 F-TSB 10ds 1Xtr: P262;40C-4C/min-280C(10min)

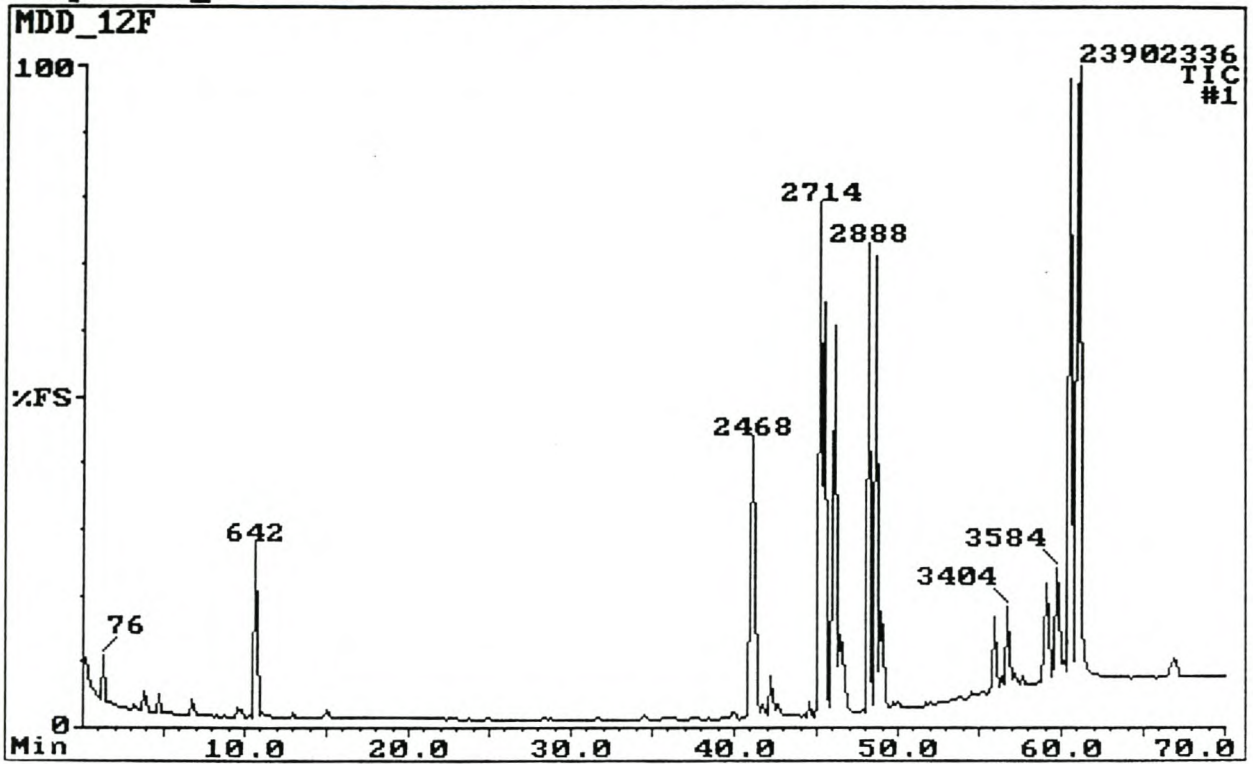


Fig. 3.9: Total ion chromatogram (TIC) of the volatile metabolite extract (10 days) of micro-organism R1.2 in TSB.

Sample: R1.2 30dsF-TSB : P262; 40C(4min)-4C/min-280(30min)

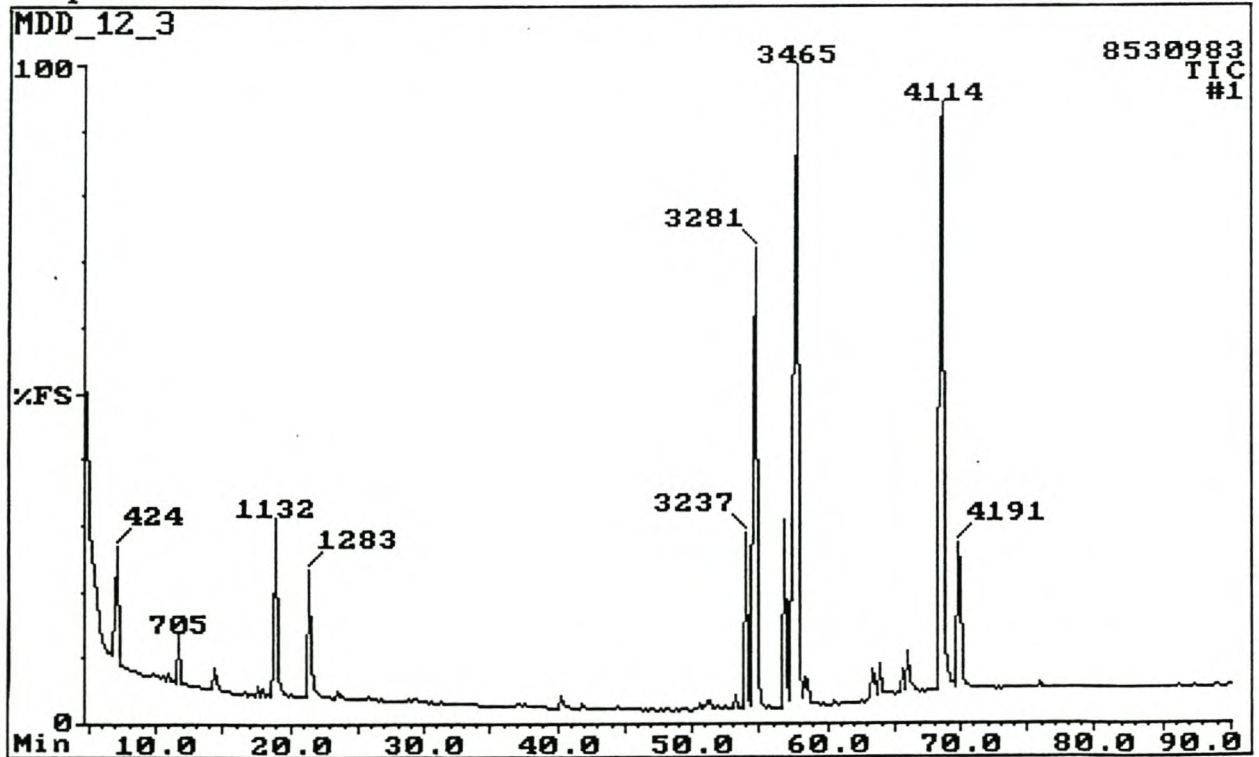


Fig. 3.10: Total ion chromatogram (TIC) of the volatile metabolite extract (30 days) of micro-organism R1.2 in TSB.

Sample:R2_1 f-tsb 3ds 1st extr : P262, 40-6C/min-280 (20min)

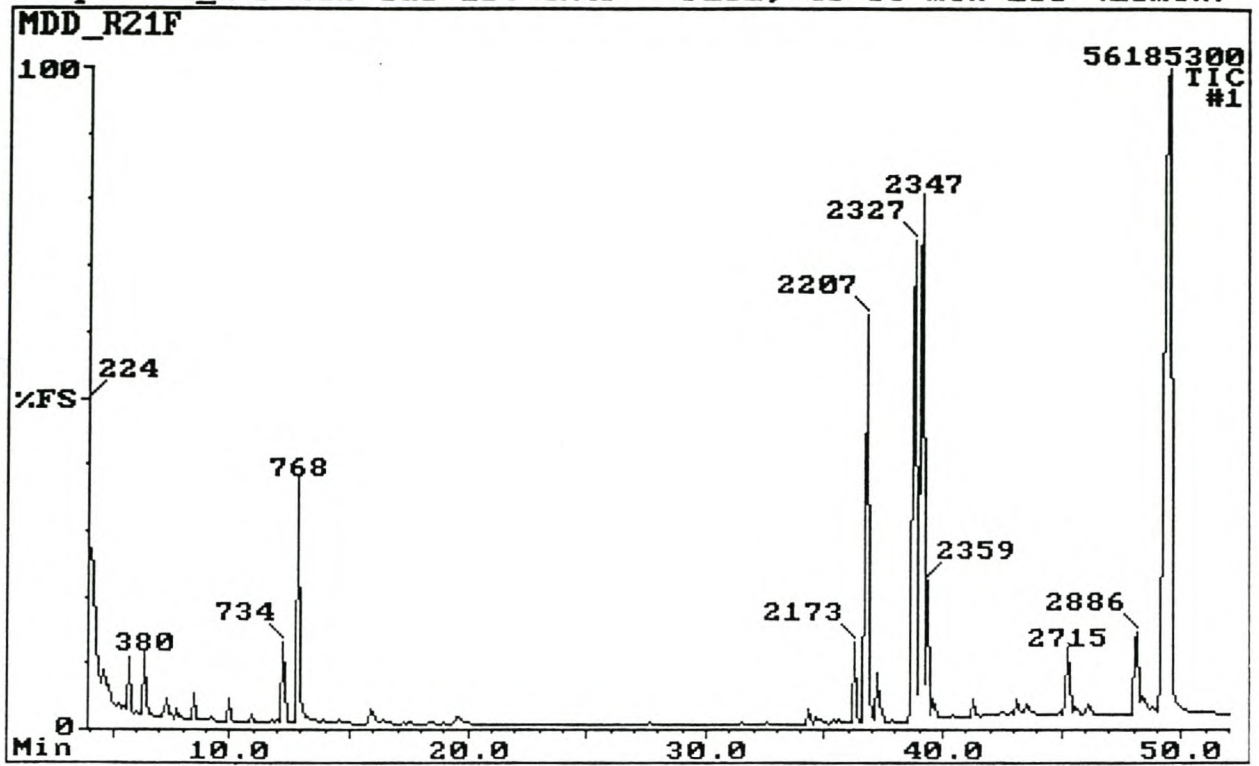


Fig. 3.11: Total ion chromatogram (TIC) of the volatile metabolite extract (3 days) of micro-organism R2.1 in TSB.

Sample:R2_1 F-TSB 10ds 1Xtr: P262;40C-4C/min-280C(10min)

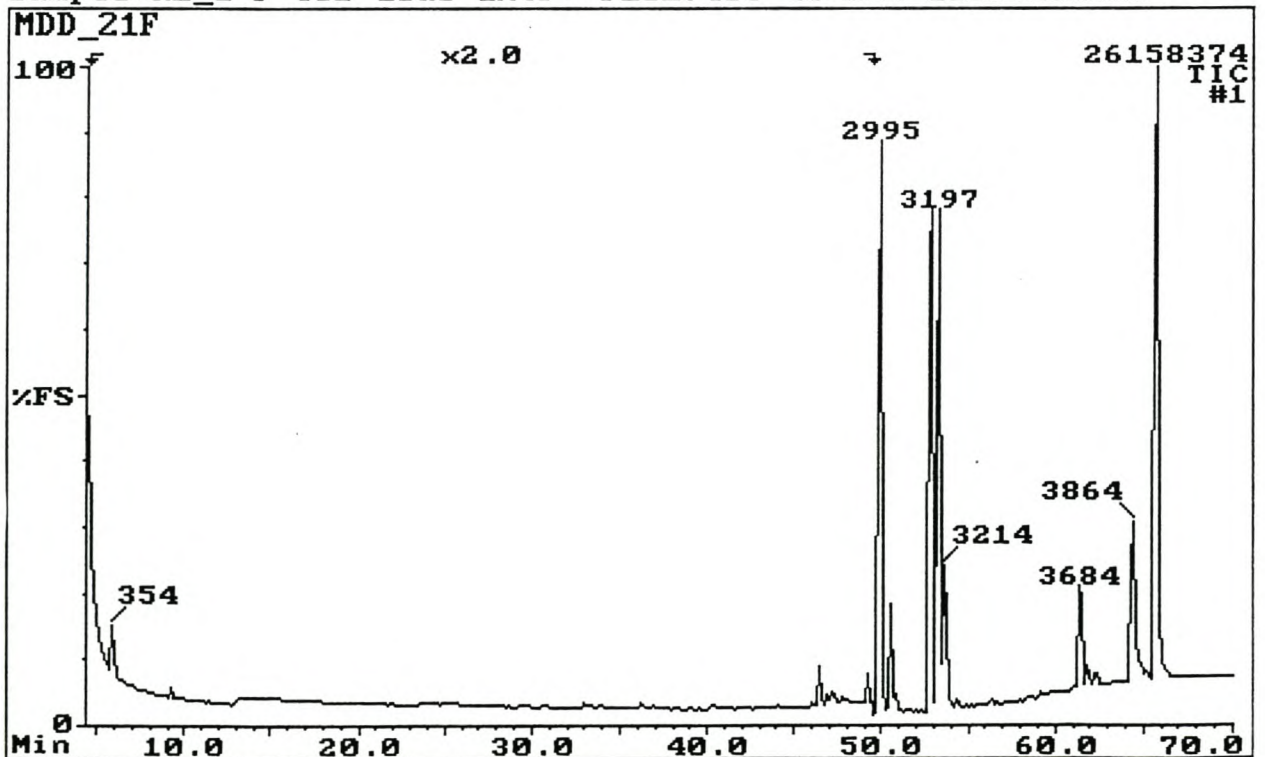


Fig. 3.12: Total ion chromatogram (TIC) of the volatile metabolite extract (10 days) of micro-organism R2.1 in TSB.

Sample:R2.1 F-TSB 30ds:P262; 40C(4min)-4C/min-280C(30min)

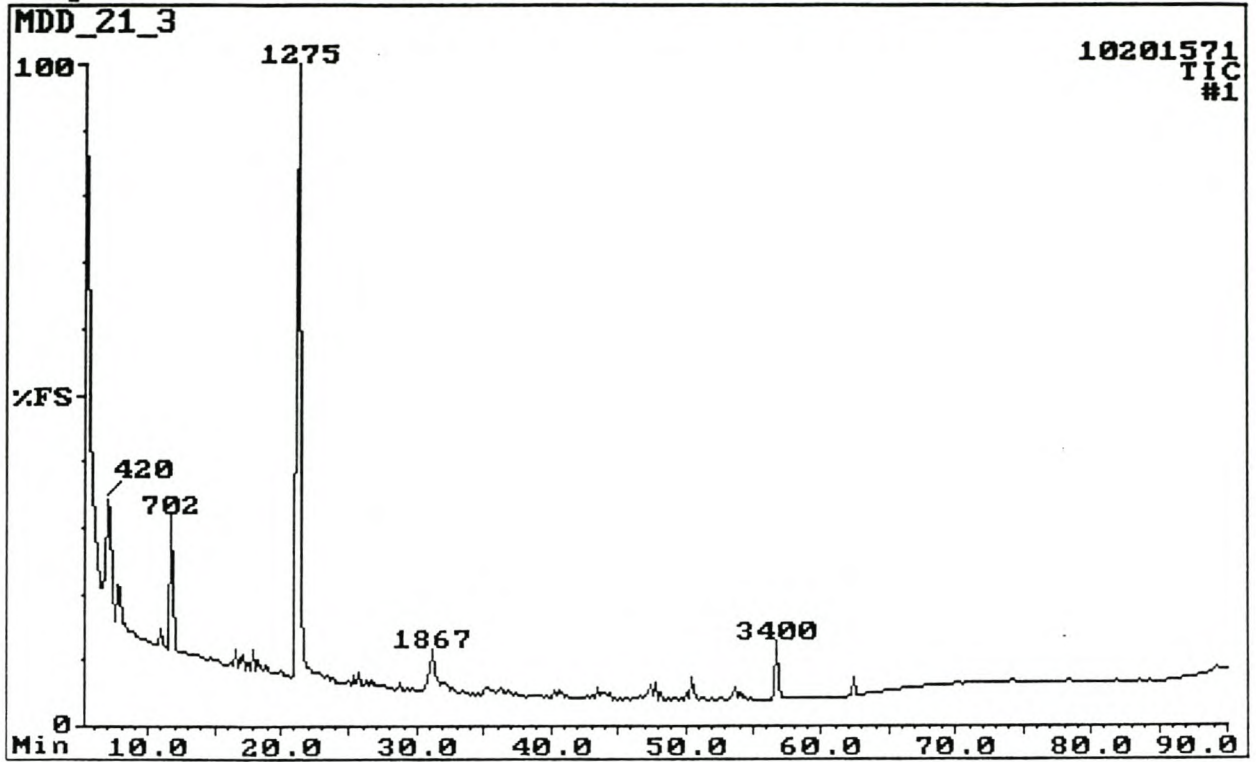


Fig. 3.13: Total ion chromatogram (TIC) of the volatile metabolite extract (30 days) of micro-organism R2.1 in TSB.

Sample:R3_1 f-tsb 3ds conc :P262;40C-6C/min-280C(20min)

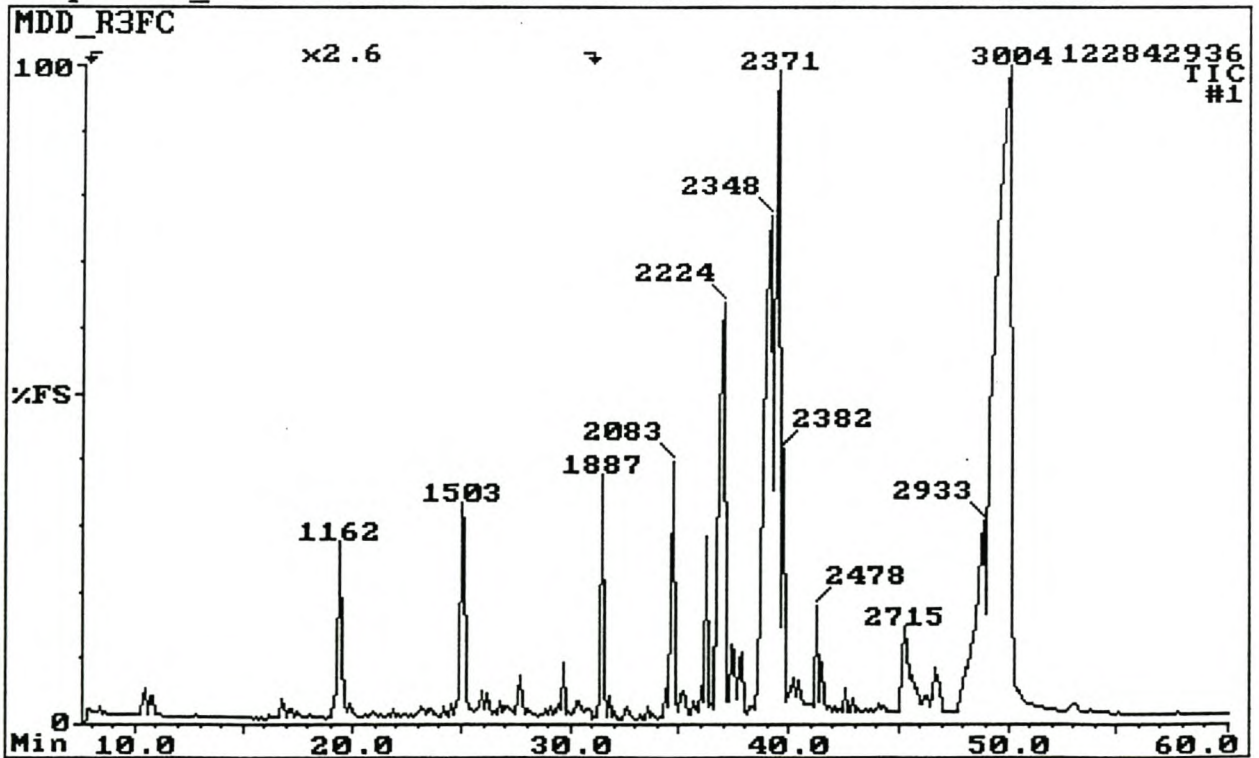


Fig. 3.14: Total ion chromatogram (TIC) of the volatile metabolite extract (3 days) of micro-organism R3.1 in TSB.

Sample:R3_1 F-TSB 10ds 1Xtr: P262;40C-4C/min-280C(10min)

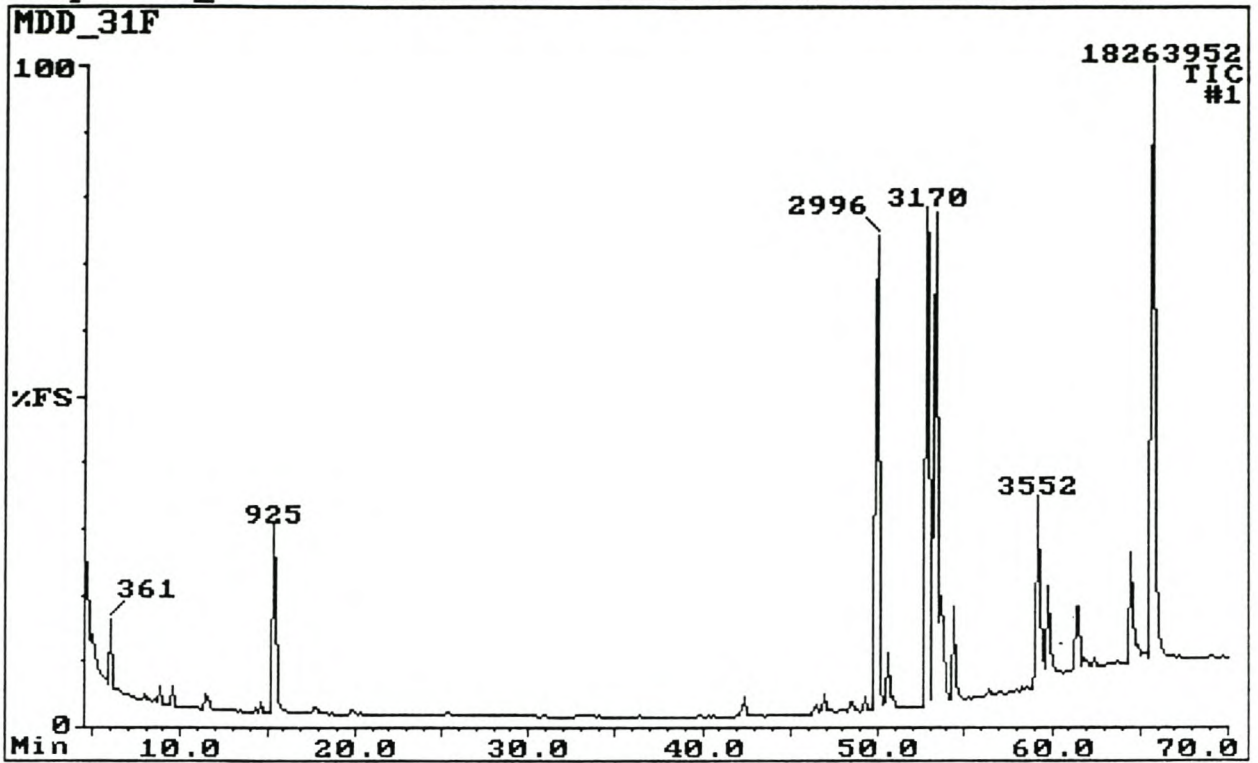


Fig. 3.15: Total ion chromatogram (TIC) of the volatile metabolite extract (10 days) of micro-organism R3.1 in TSB.

Sample:R3.1 F-TSB 30ds : P262; 40-4C/min-280(30min)

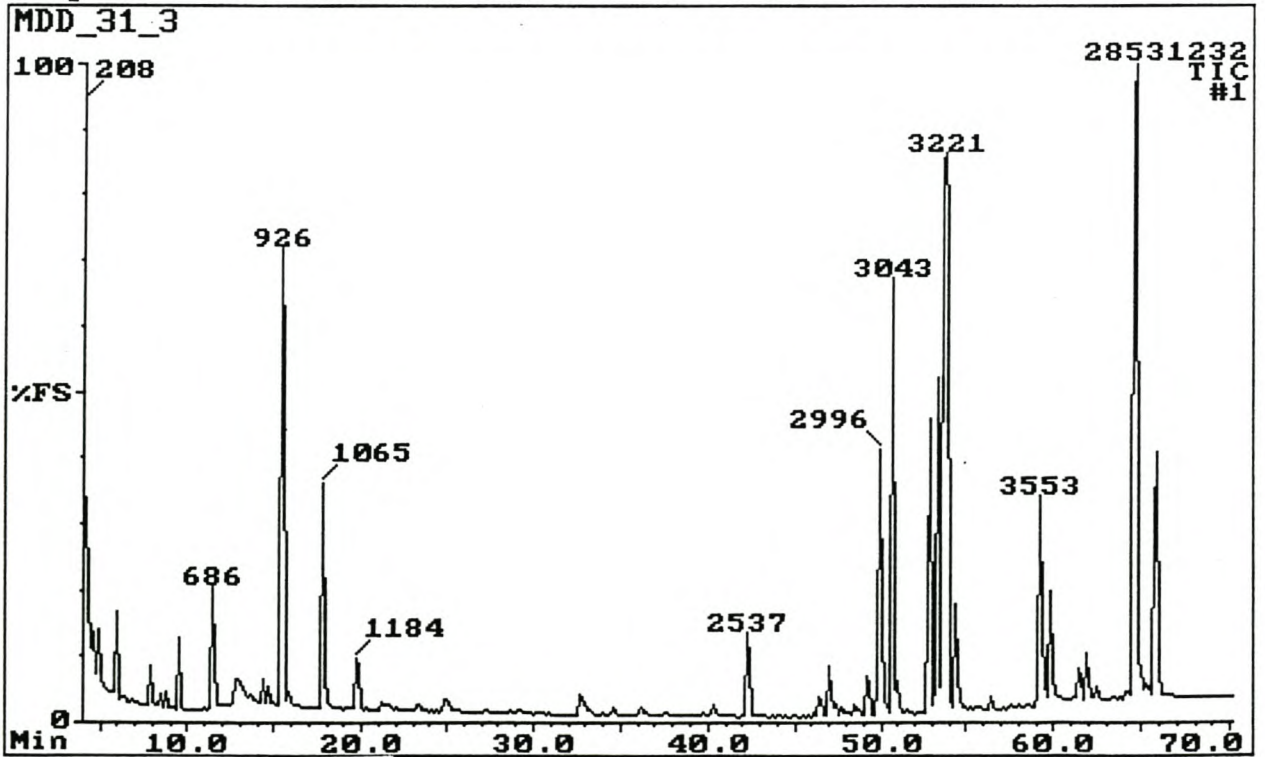


Fig. 3.16: Total ion chromatogram (TIC) of the volatile metabolite extract (30 days) of micro-organism R3.1 in TSB.

Sample:R4_2 F_tsb 3ds 1extr : P262, 40-6C/min-280 (20min)

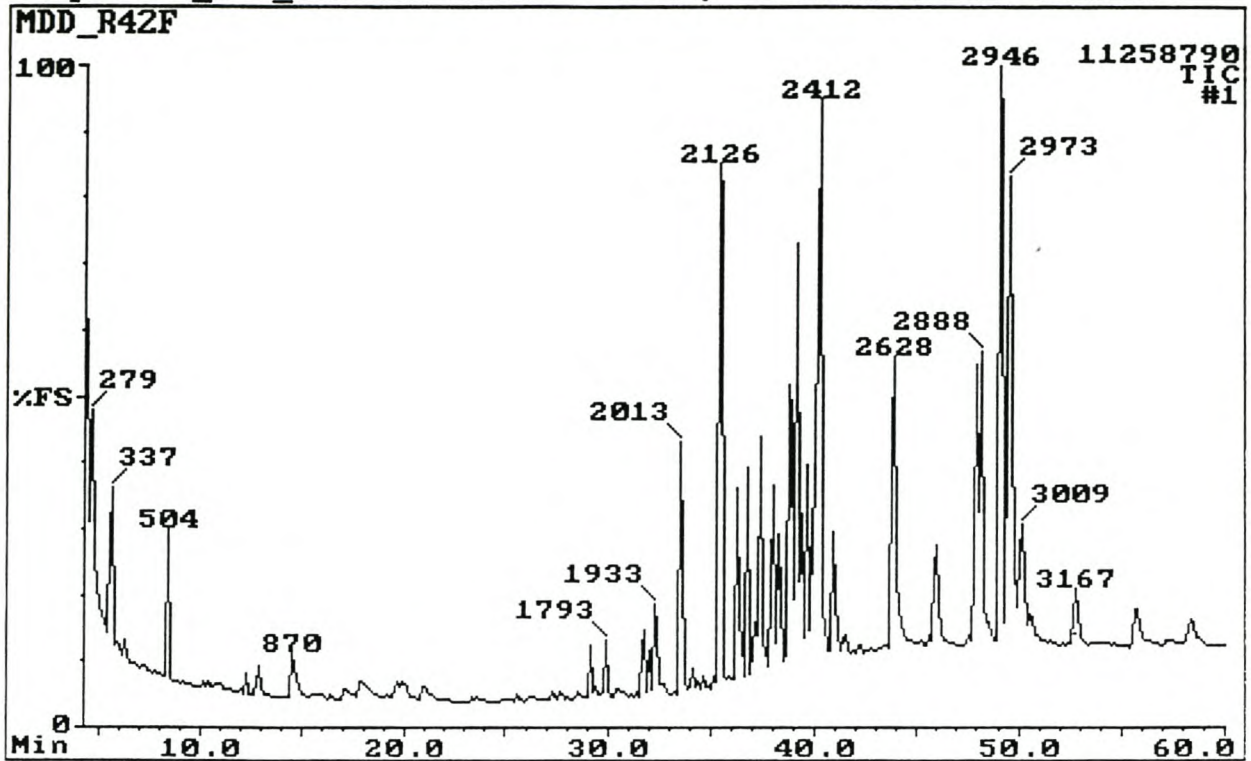


Fig. 3.17: Total ion chromatogram (TIC) of the volatile metabolite extract (3 days) of micro-organism R4.2 in TSB.

Sample:R4_2 F-TSB 10ds 1Xtr: P262;40C-4C/min-280C(10min)

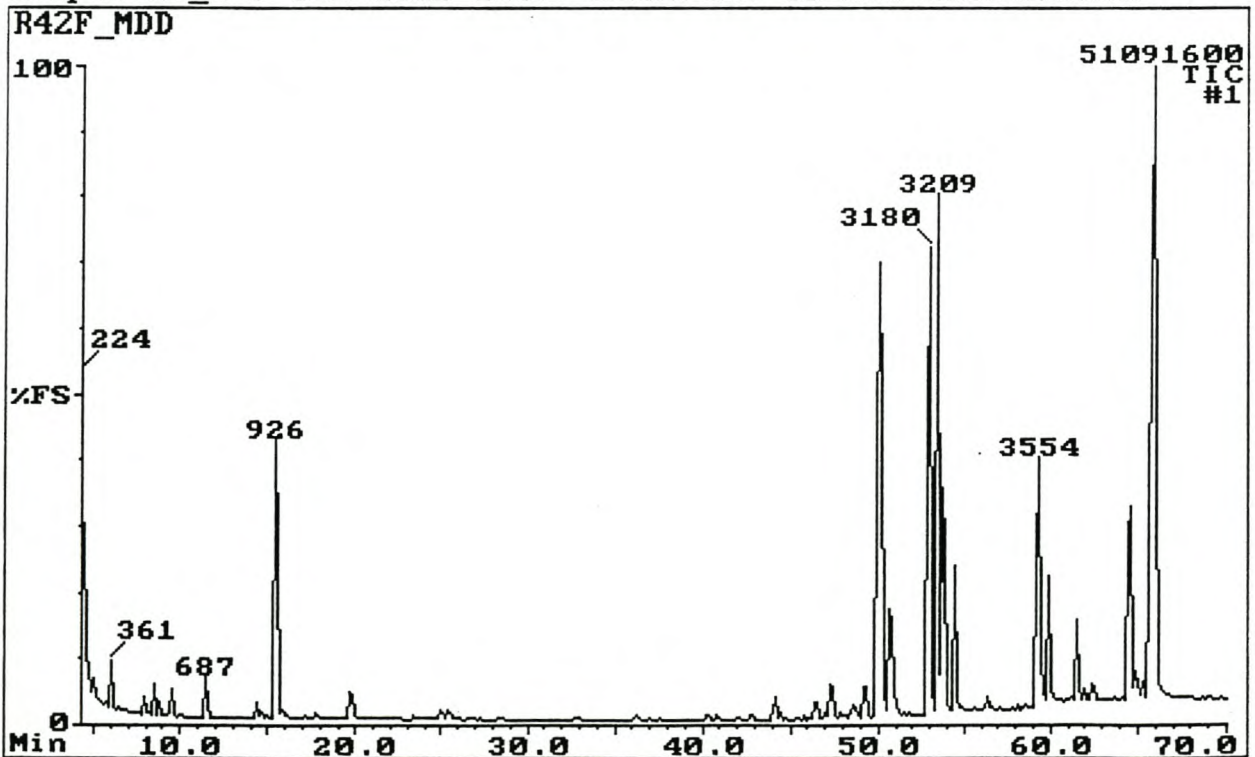


Fig. 3.18: Total ion chromatogram (TIC) of the volatile metabolite extract (10 days) of micro-organism R4.2 in TSB.

Sample:R4.2 30dsF-TSB : P262; 40-4C/min-280(30min)

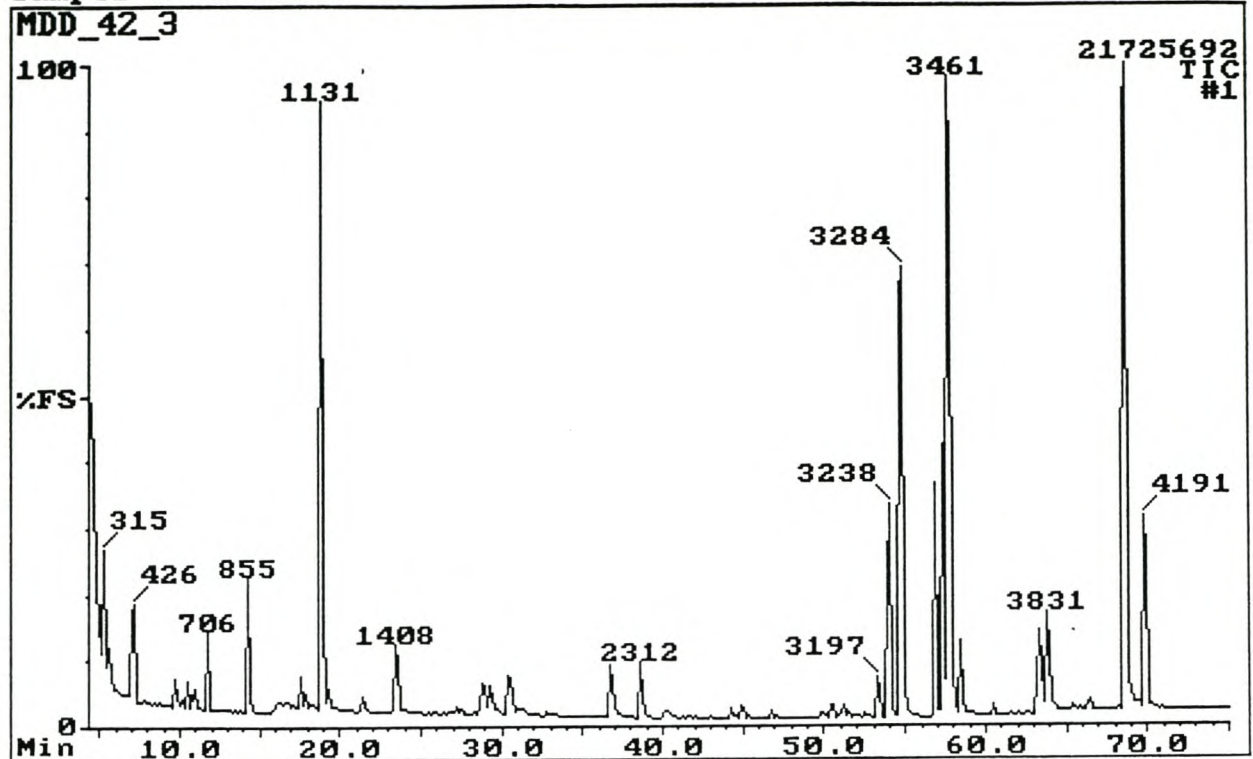


Fig. 3.19: Total ion chromatogram (TIC) of the volatile metabolite extract (30 days) of micro-organism R4.2 in TSB.

Sample:L2_2 F-TSB 3 ds 1Xtr: P262;40C-4C/min-280C(10min)

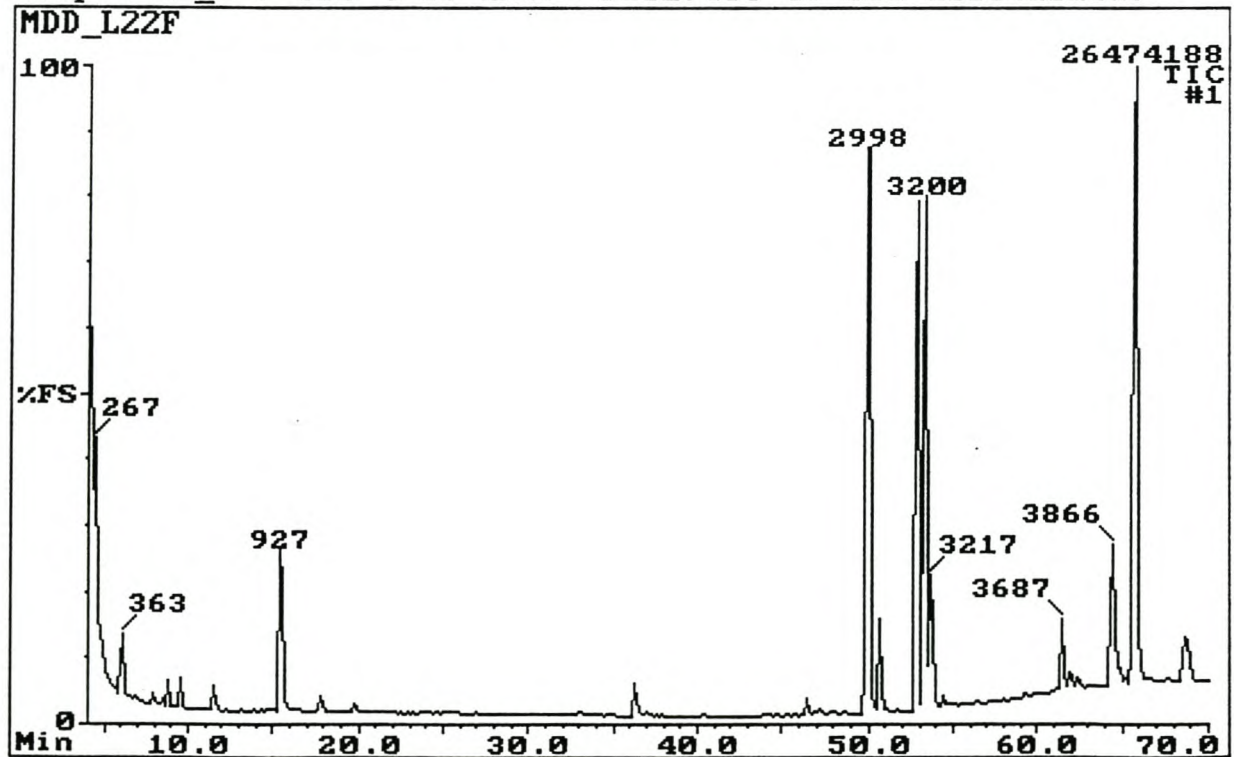


Fig. 3.20: Total ion chromatogram (TIC) of the volatile metabolite extract (3 days) of micro-organism L2.2 in TSB.

Sample: L2_2_F-TSB 2nd Extr: P262; 40C-4C/MIN-280

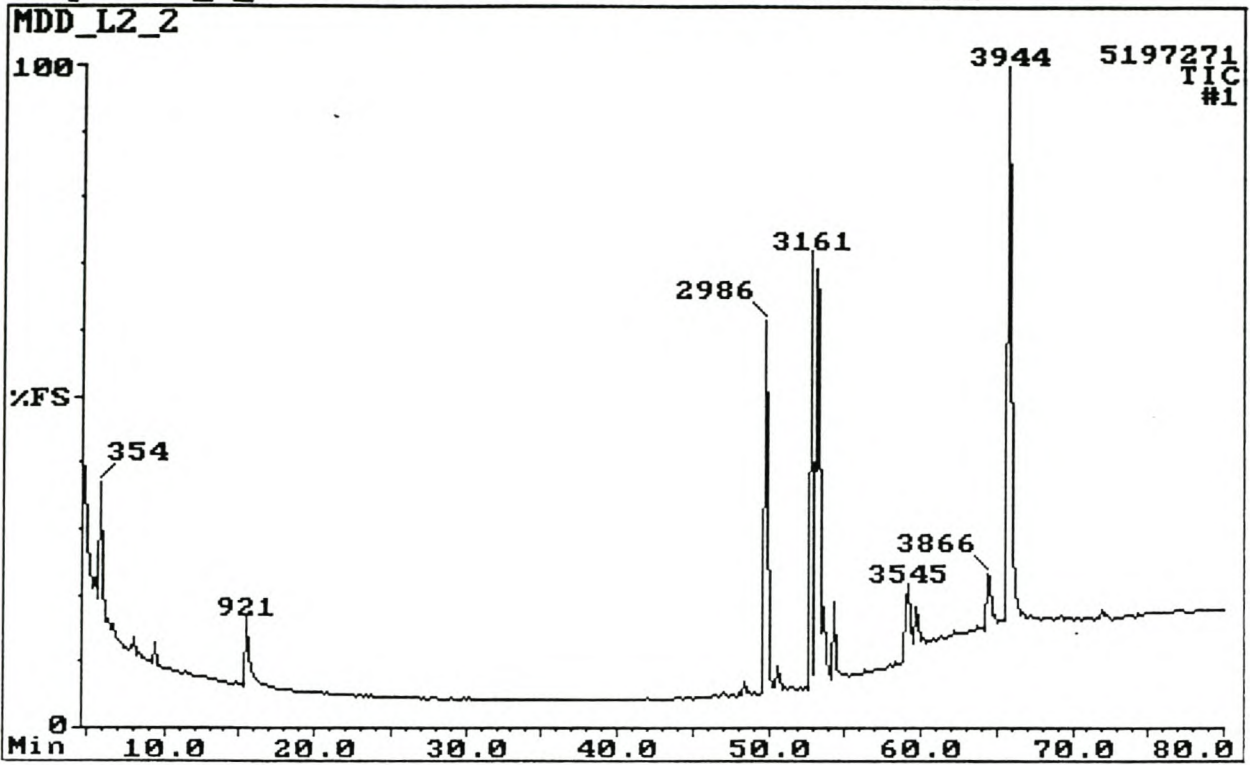


Fig. 3.21: Total ion chromatogram (TIC) of the volatile metabolite extract (10 days) of micro-organism L2.2 in TSB.

Sample: MDD L2.2 f-TSB30ds: P262; 40C-4C/min-280C(10min)

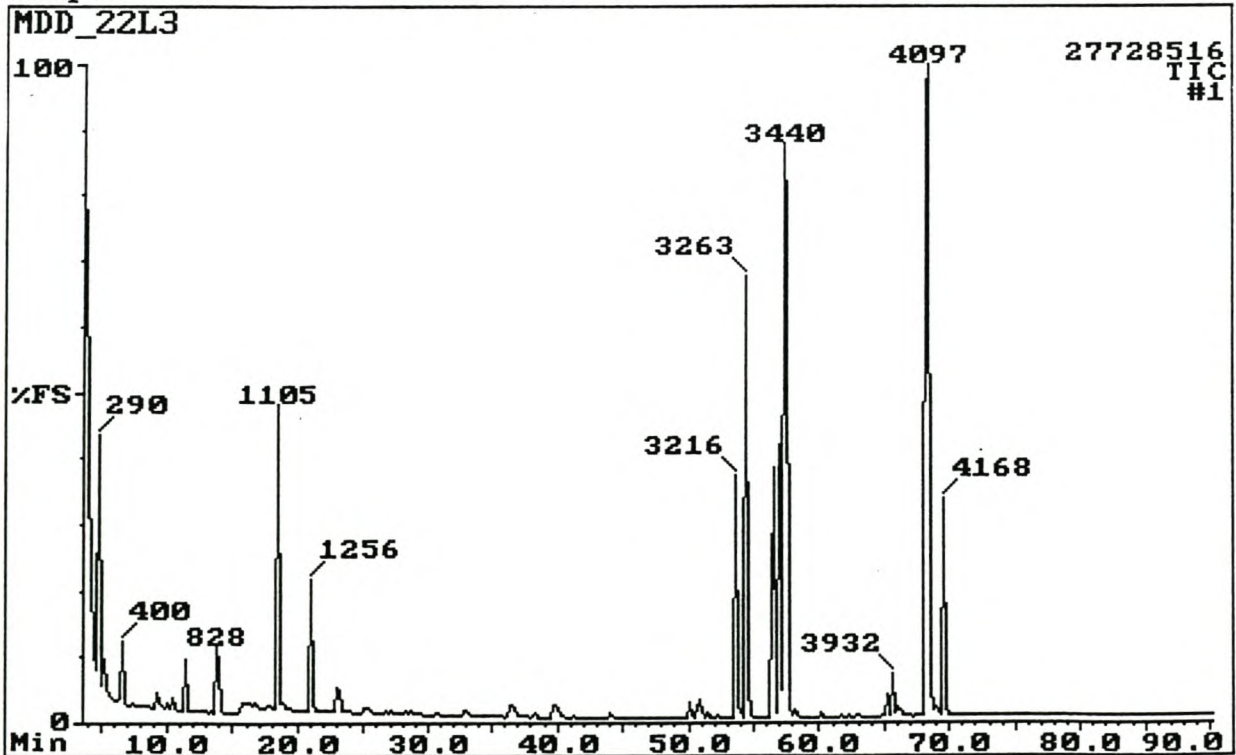


Fig. 3.22: Total ion chromatogram (TIC) of the volatile metabolite extract (30 days) of micro-organism L2.2 in TSB.

Sample: MDD COMMUNE MSM 10ds: P259: 40(4)-6-210-2-280(30)

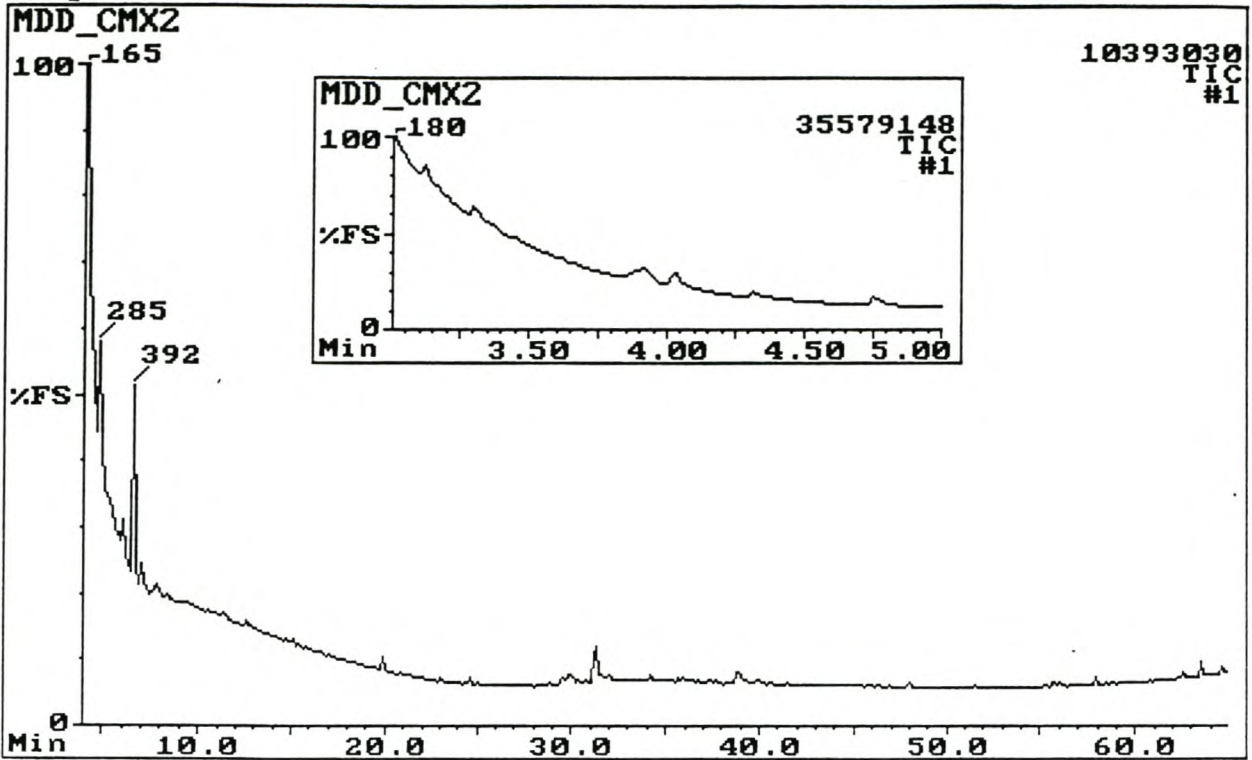


Fig. 3.23: Total ion chromatogram (TIC) of the volatile metabolite extract (10 days) of the total community of bacteria in MSM.

Sample: MDD COMMUNE 30ds MSM P259; 40(4)-6-220-2-280(30)

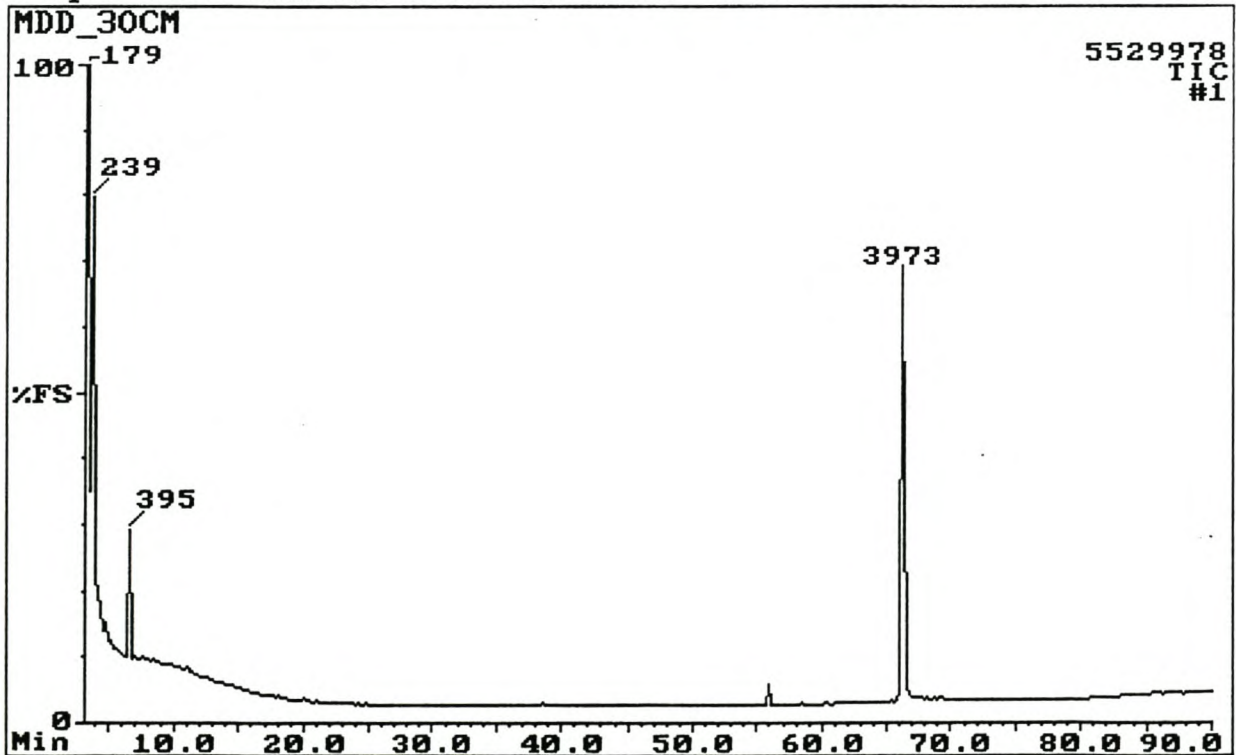


Fig. 3.24: Total ion chromatogram (TIC) of the volatile metabolite extract (30 days) of the total community of bacteria in MSM.

Sample: MDD R1.1 MSM 3ds: P262; 40C(4min)-4C/min-280(30min)

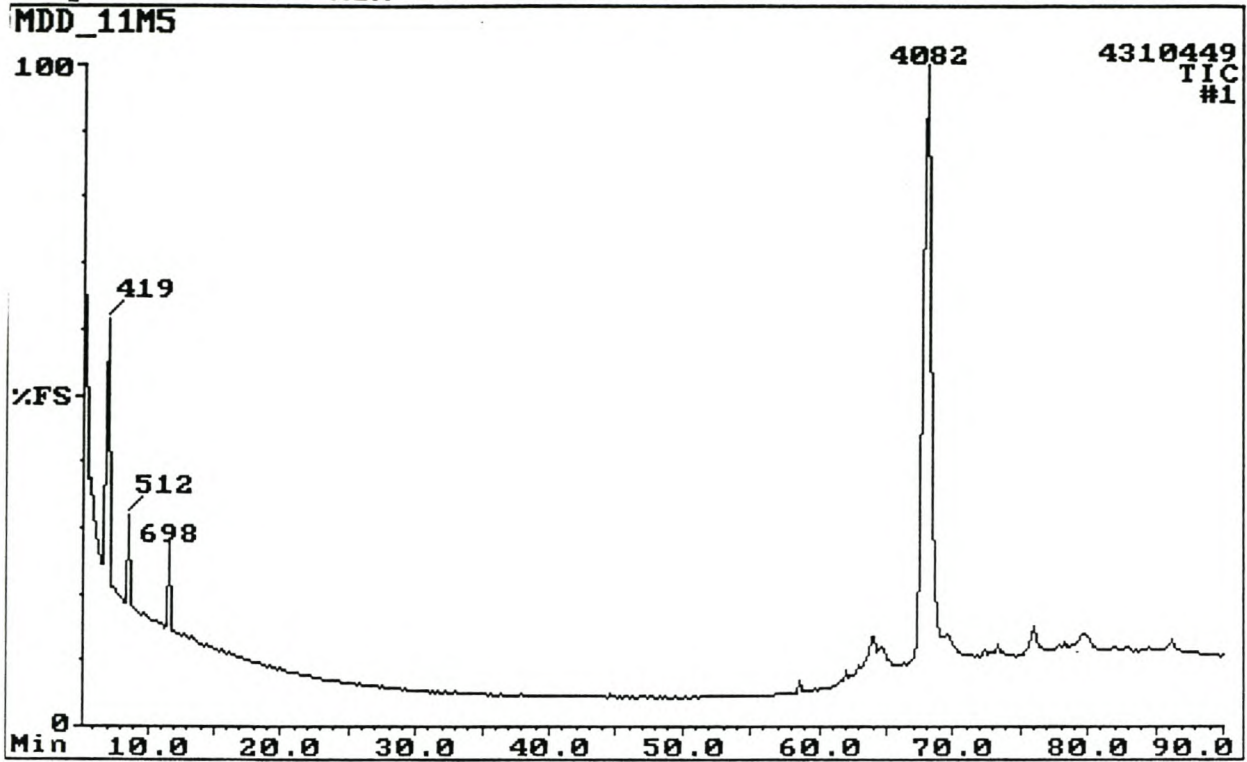


Fig. 3.25: Total ion chromatogram (TIC) of the volatile metabolite extract (3 days) of micro-organism R1.1 in MSM.

Sample: MDD R11 10ds MSM: P259; 40C(4min)-4C/min-280C(30min)

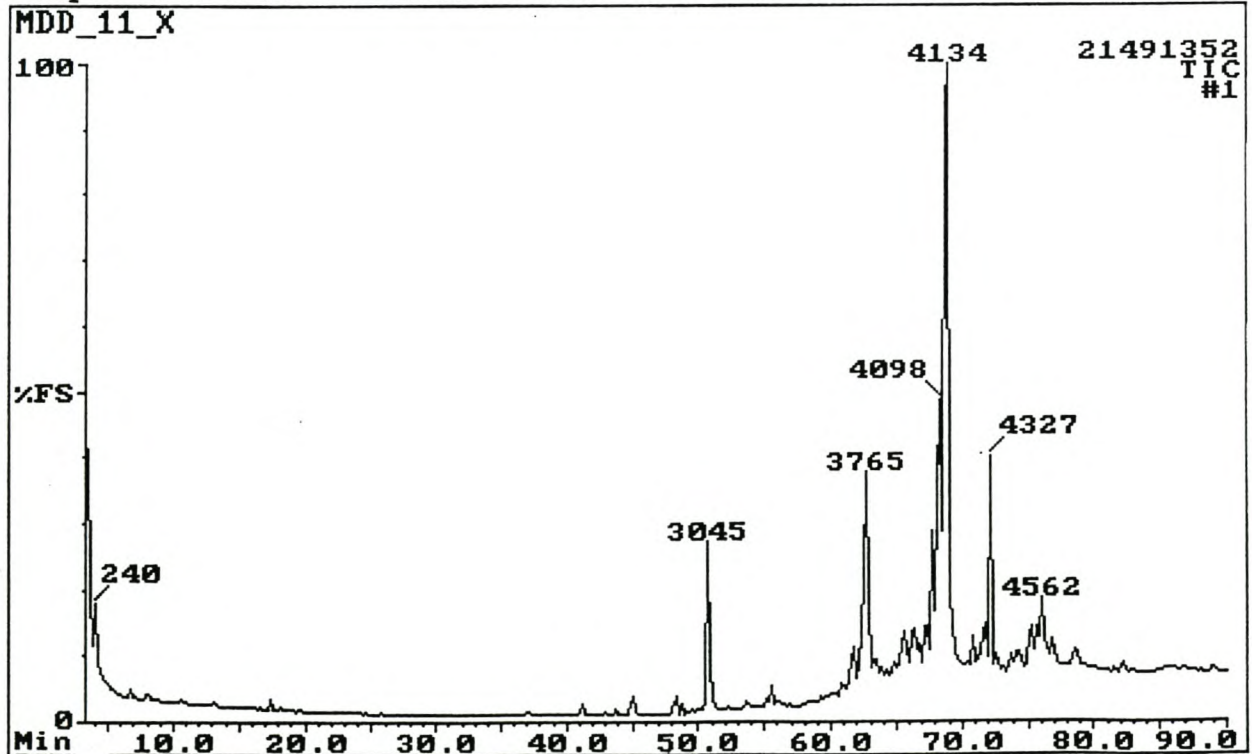


Fig. 3.26: Total ion chromatogram (TIC) of the volatile metabolite extract (10 days) of micro-organism R1.1 in MSM.

Sample: MDD R1.1 MSM 30ds: P259; 40(4)-6-210-2-280(30)

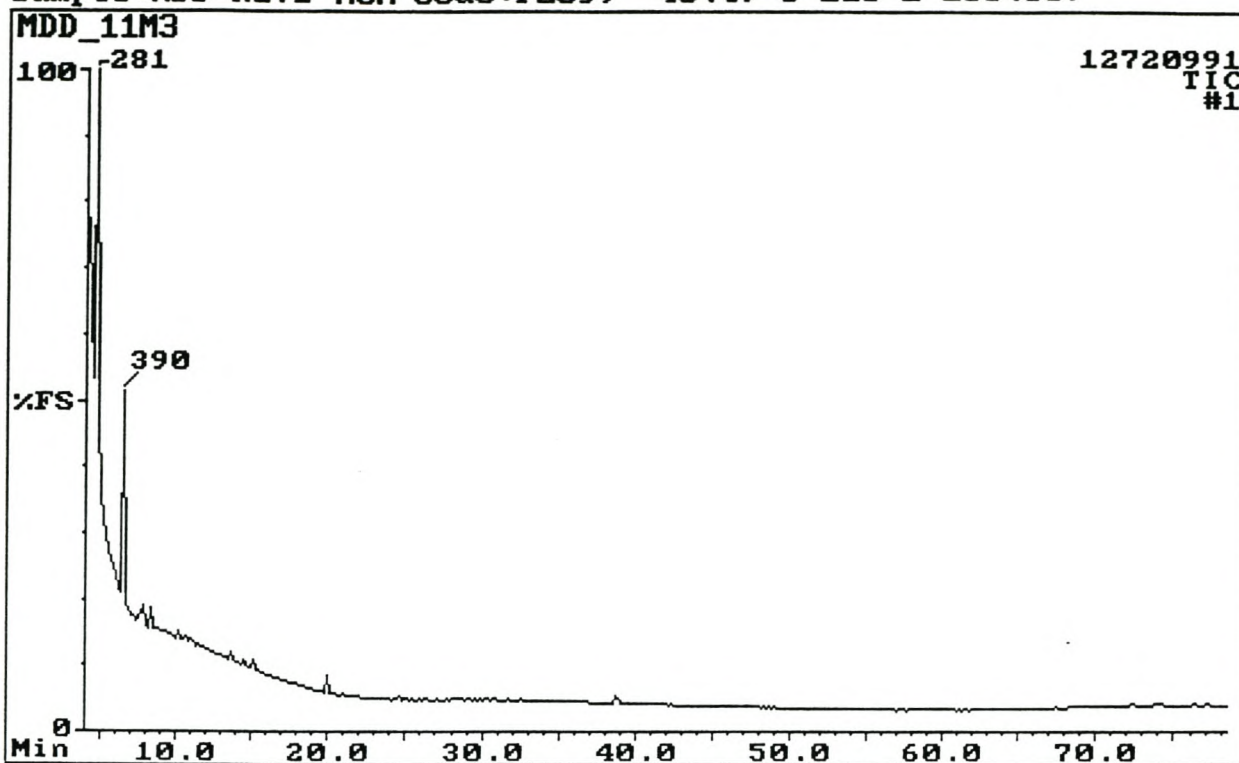


Fig. 3.27: Total ion chromatogram (TIC) of the volatile metabolite extract (30 days) of micro-organism R1.1 in MSM.

Sample: MDD R1.2 MSM 3ds :P259; 40(4)-6-220-2-280(30)

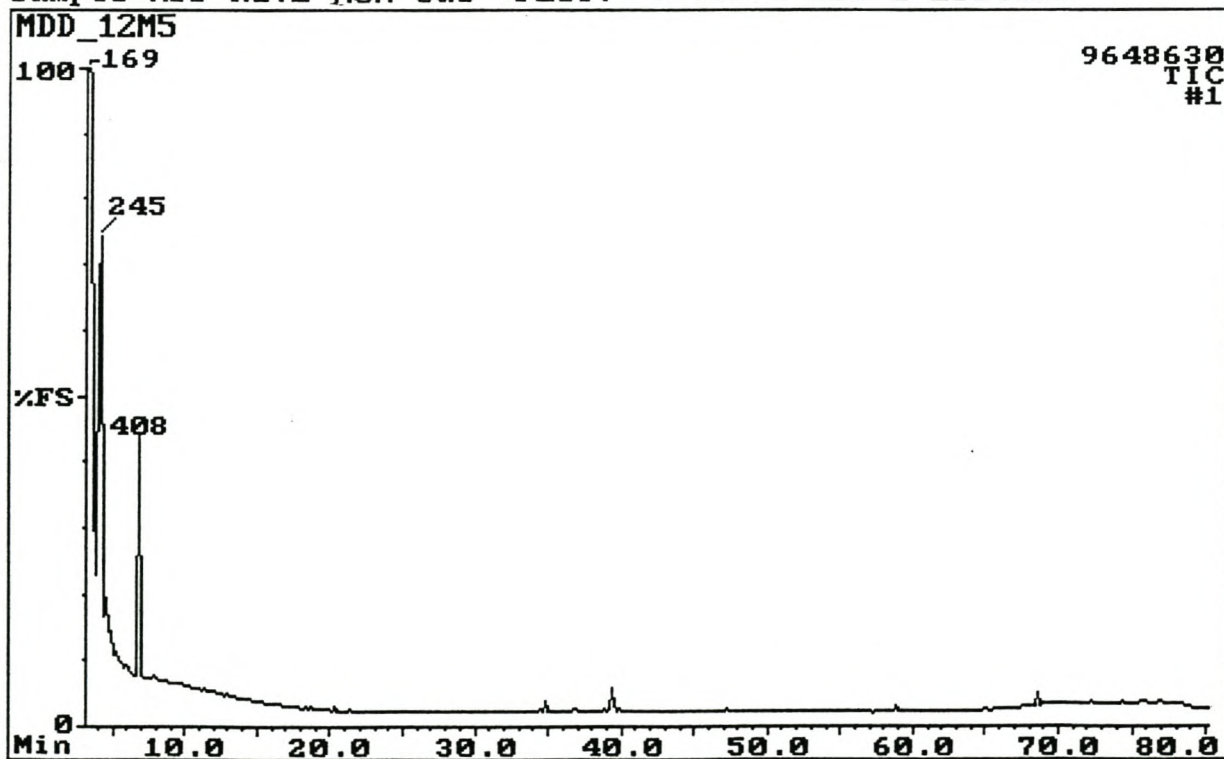


Fig. 3.28: Total ion chromatogram (TIC) of the volatile metabolite extract (3 days) of micro-organism R1.2 in MSM.

Sample: MDD R1.2 MSM 10ds : P259; 40-6-280C(20min)

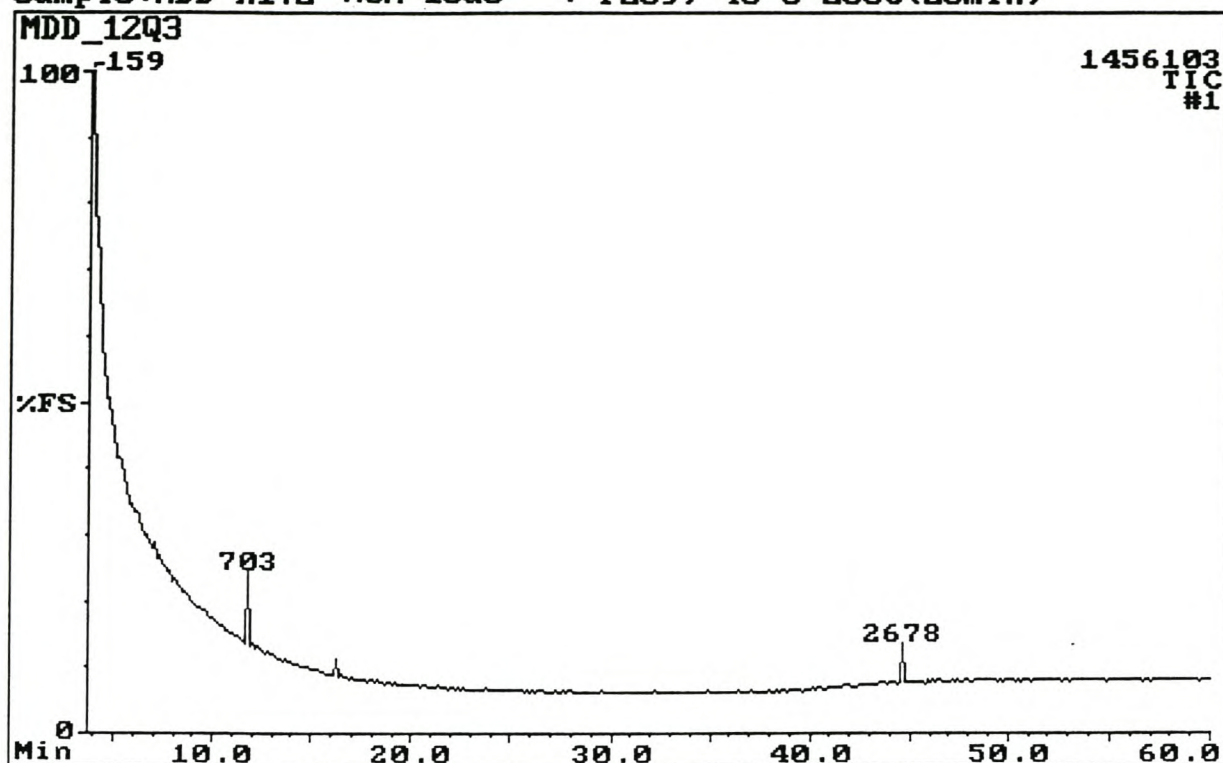


Fig. 3.29: Total ion chromatogram (TIC) of the volatile metabolite extract (10 days) of micro-organism R1.2 in MSM.

Sample: MDD R2.1 MSM 3ds : P259; 40(4)-6-210-2-280(30)

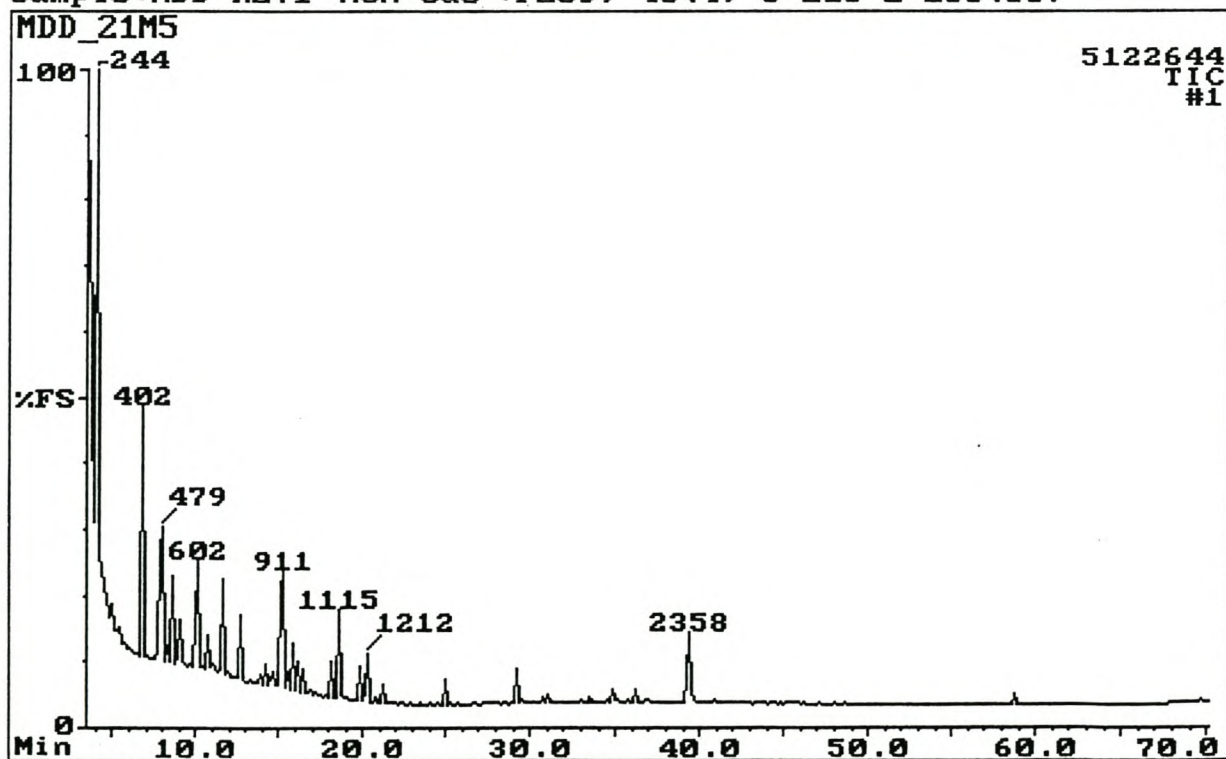


Fig. 3.30: Total ion chromatogram (TIC) of the volatile metabolite extract (3 days) of micro-organism R2.1 in MSM.

Sample: MDD R2.1 MSM 10 ds: P259; 40-6-280(20)

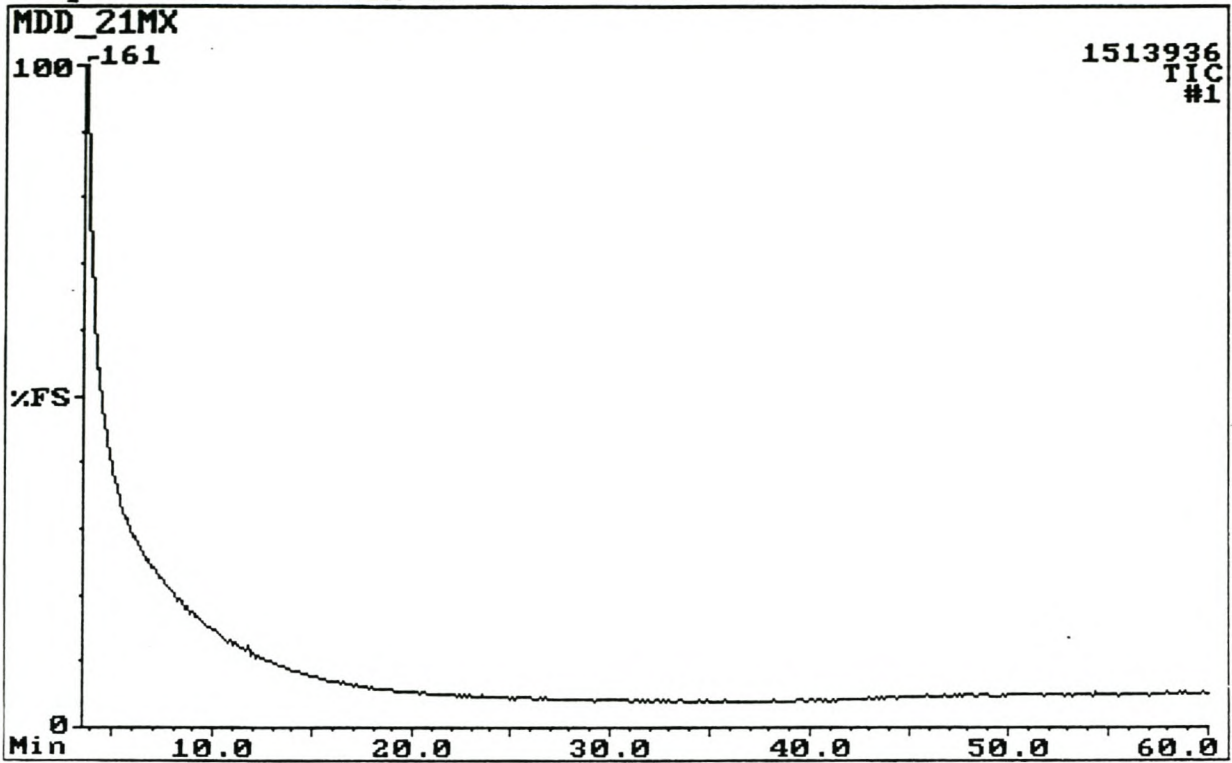


Fig. 3.31: Total ion chromatogram (TIC) of the volatile metabolite extract (10 days) of micro-organism R2.1 in MSM.

Sample: MDD R3.1 MSM 3ds: P259; 40-8-280(10min)

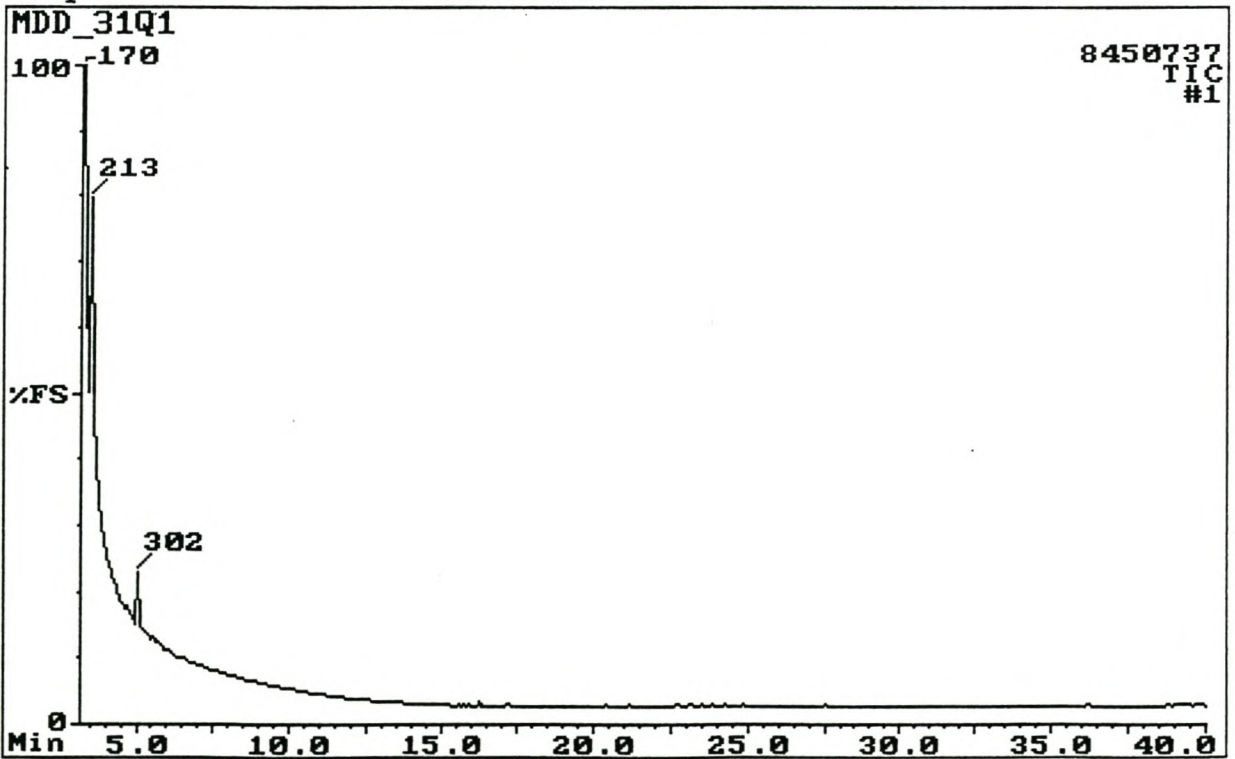


Fig. 3.32: Total ion chromatogram (TIC) of the volatile metabolite extract (3 days) of micro-organism R3.1 in MSM.

Sample: MDD R3.1 MSM 10ds: P259; 40-8-280(20)

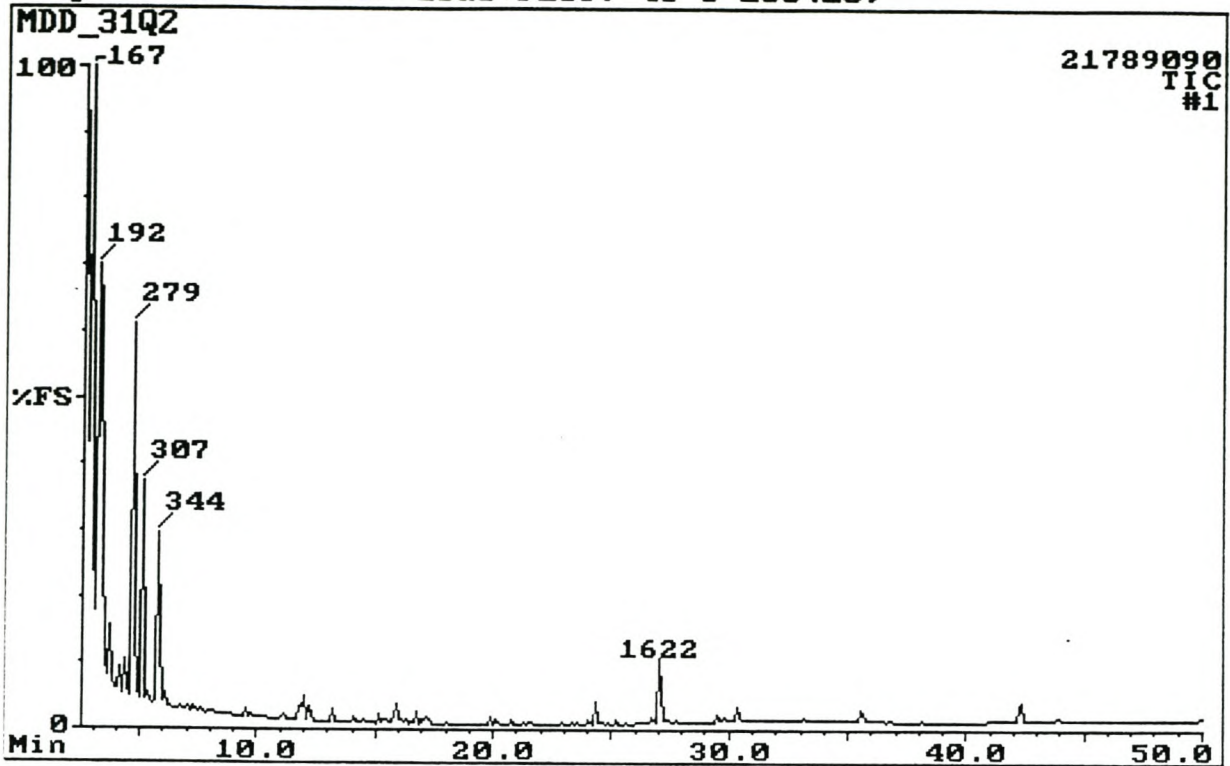


Fig. 3.33: Total ion chromatogram (TIC) of the volatile metabolite extract (10 days) of micro-organism R3.1 in MSM.

Sample: R4.2 MSM 3ds: P262; 40(4min)-4C/min-280C(30min)

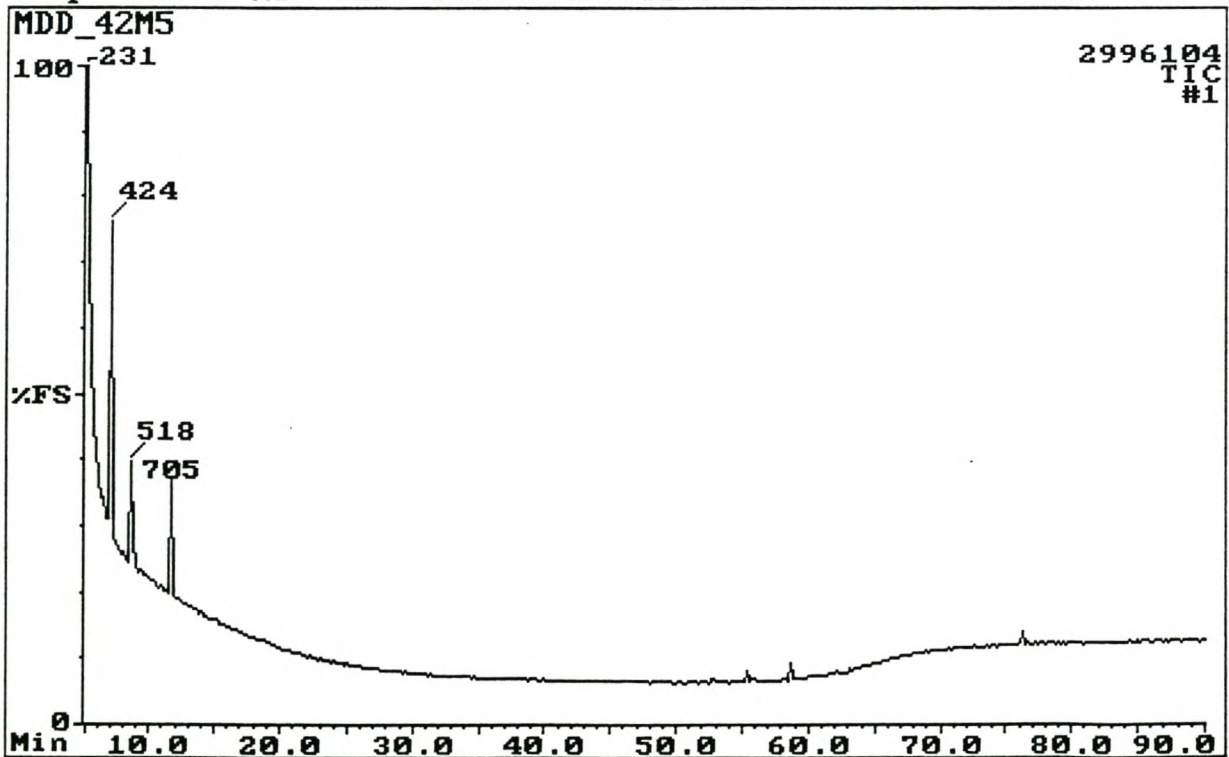


Fig. 3.34: Total ion chromatogram (TIC) of the volatile metabolite extract (3 days) of micro-organism R4.2 in MSM.

Sample: MDD R4.2 MSM 10ds: P259; 40C(4min)-4C/min-280(30min)

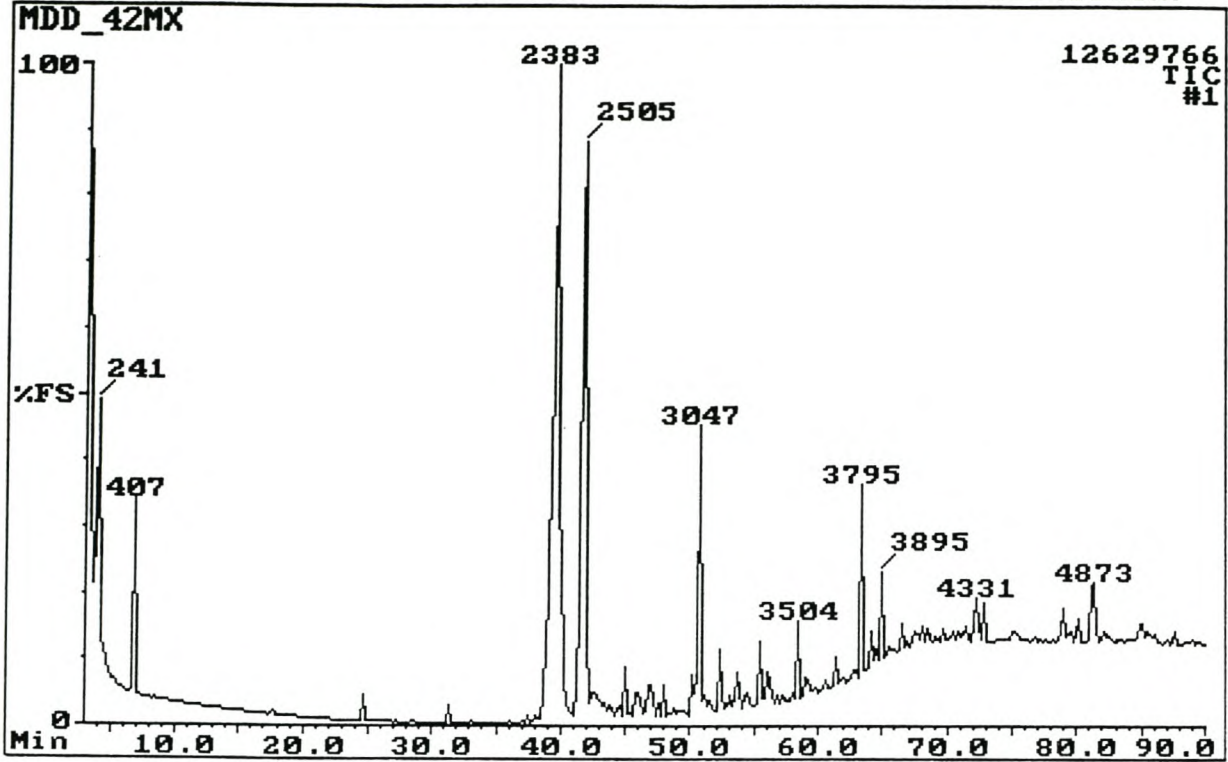


Fig. 3.35: Total ion chromatogram (TIC) of the volatile metabolite extract (10 days) of micro-organism R4.2 in MSM.

Sample: MDD R4.2 MSM 40ds: P259; 40-8-280(10)

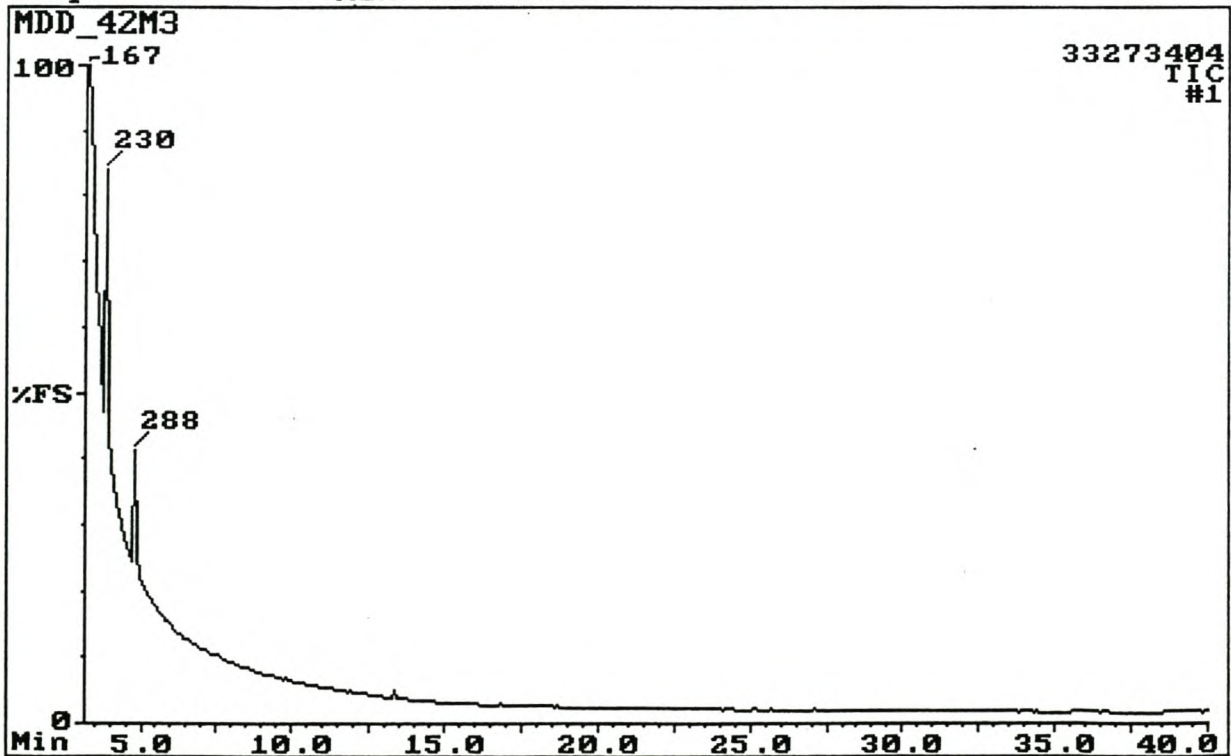


Fig. 3.36: Total ion chromatogram (TIC) of the volatile metabolite extract (30 days) of micro-organism R4.2 in MSM.

Sample: MDD L2.2 MSM 3ds P259; 40(4)-6C/min-210-2C/min-280(30)

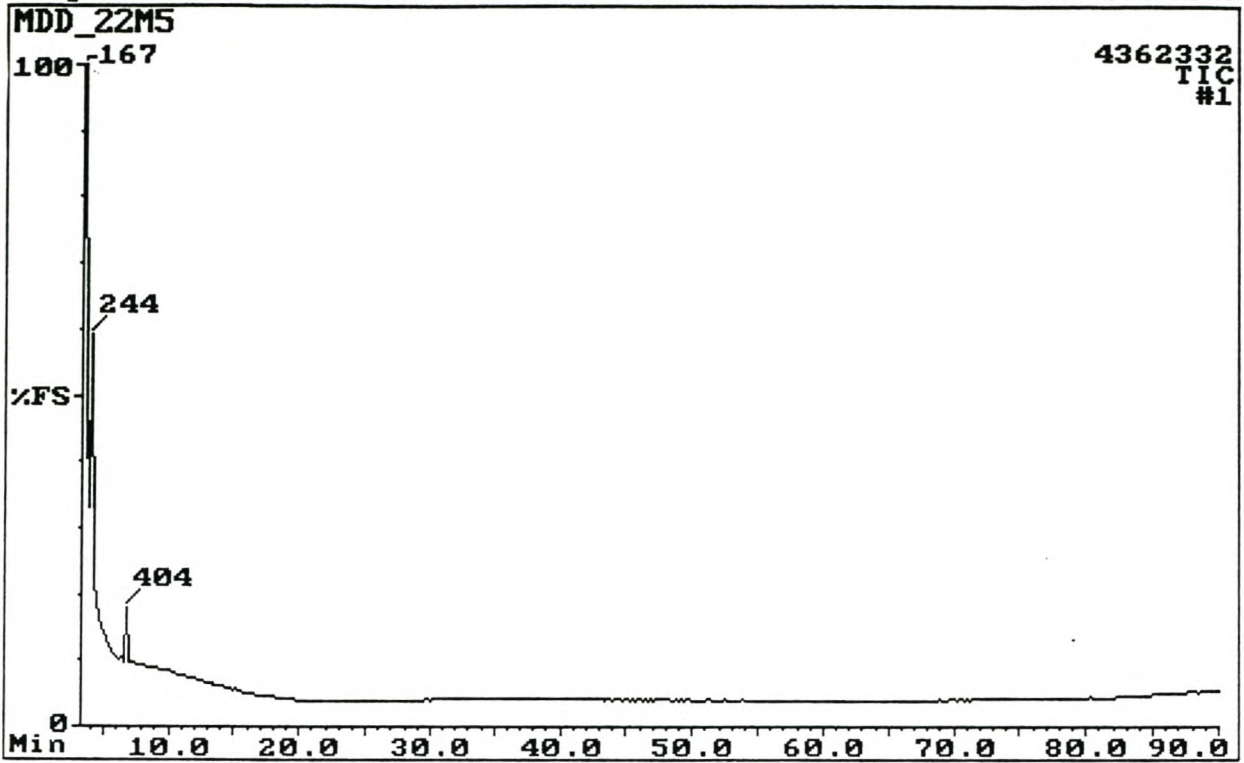


Fig. 3.37: Total ion chromatogram (TIC) of the volatile metabolite extract (3 days) of micro-organism L2.2 in MSM.

Sample: MDD L2.2 MSM 10ds: P259; 40(4min)-6-220-2-280(30min)

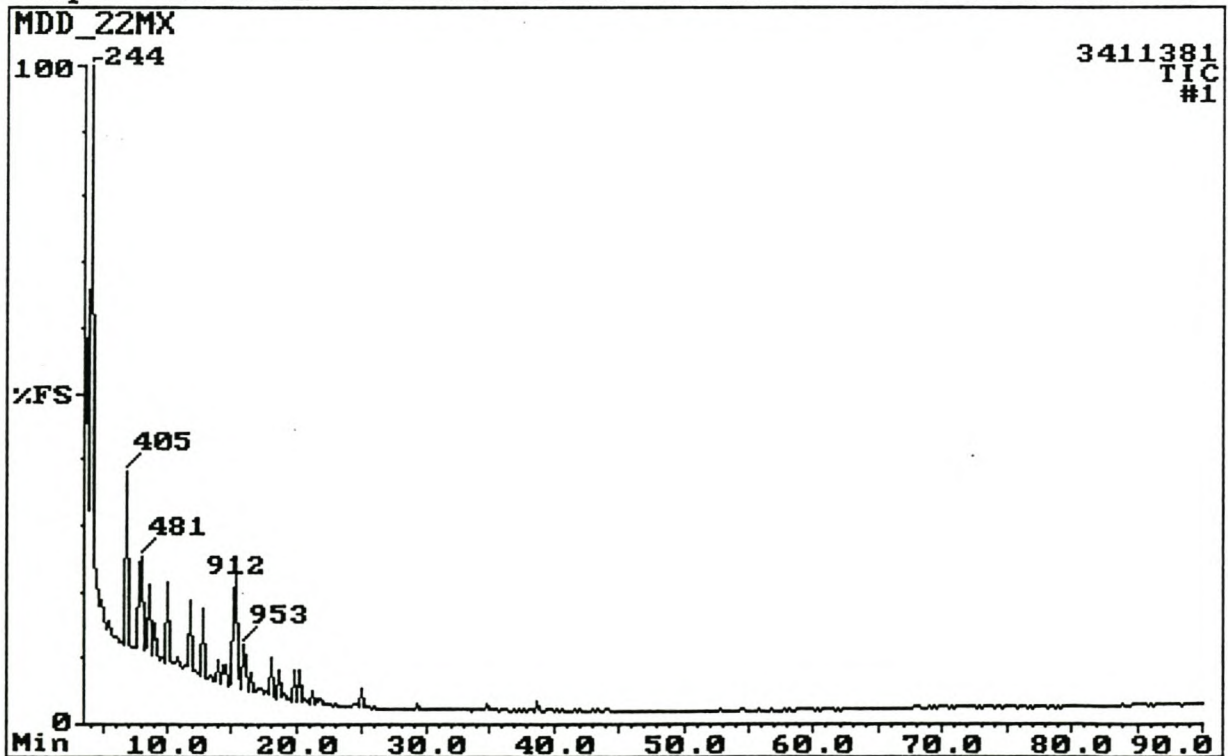


Fig. 3.38: Total ion chromatogram (TIC) of the volatile metabolite extract (10 days) of micro-organism L2.2 in MSM.

Sample: MDD COMMUNE F-TSB 30ds: P259; 40(4)-6-220-2-280(30)

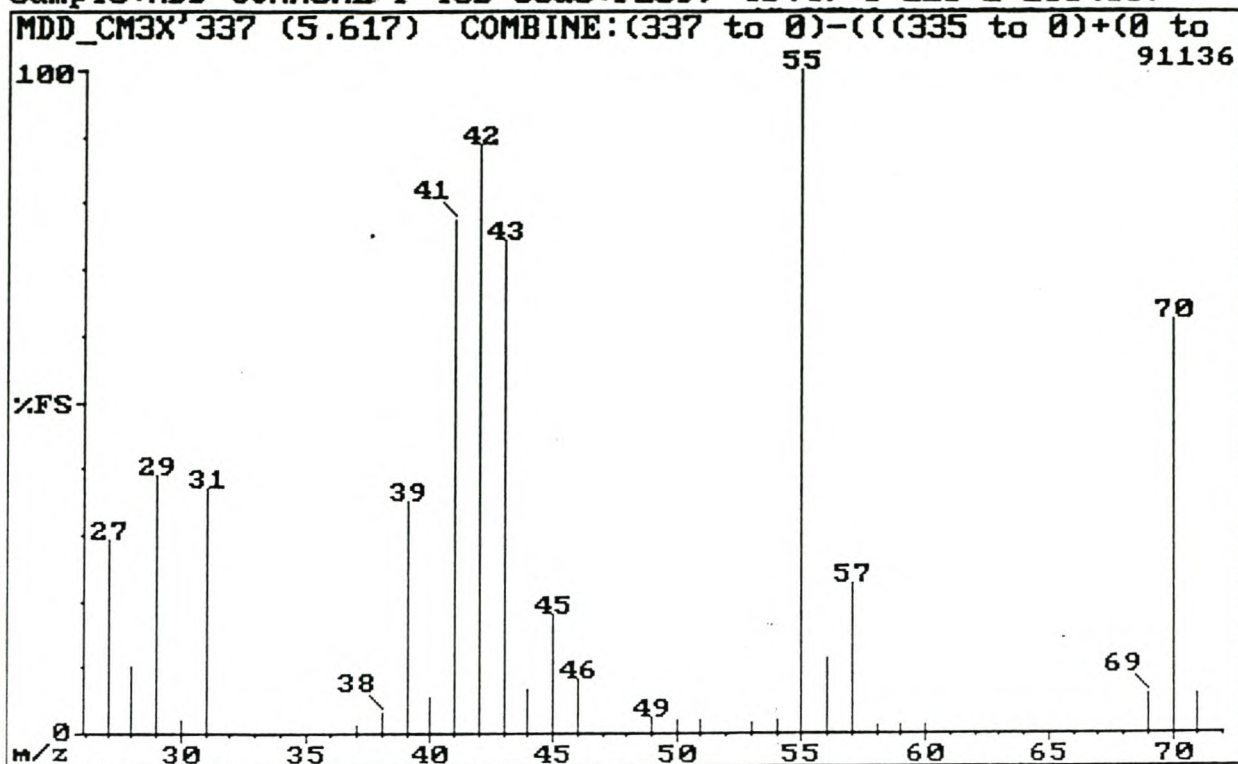


Fig. 3.43: El mass spectrum of component 337 (3-methyl-1-butanol).

Sample: MDD COMMUNE F-TSB 30ds: P259; 40(4)-6-220-2-280(30)

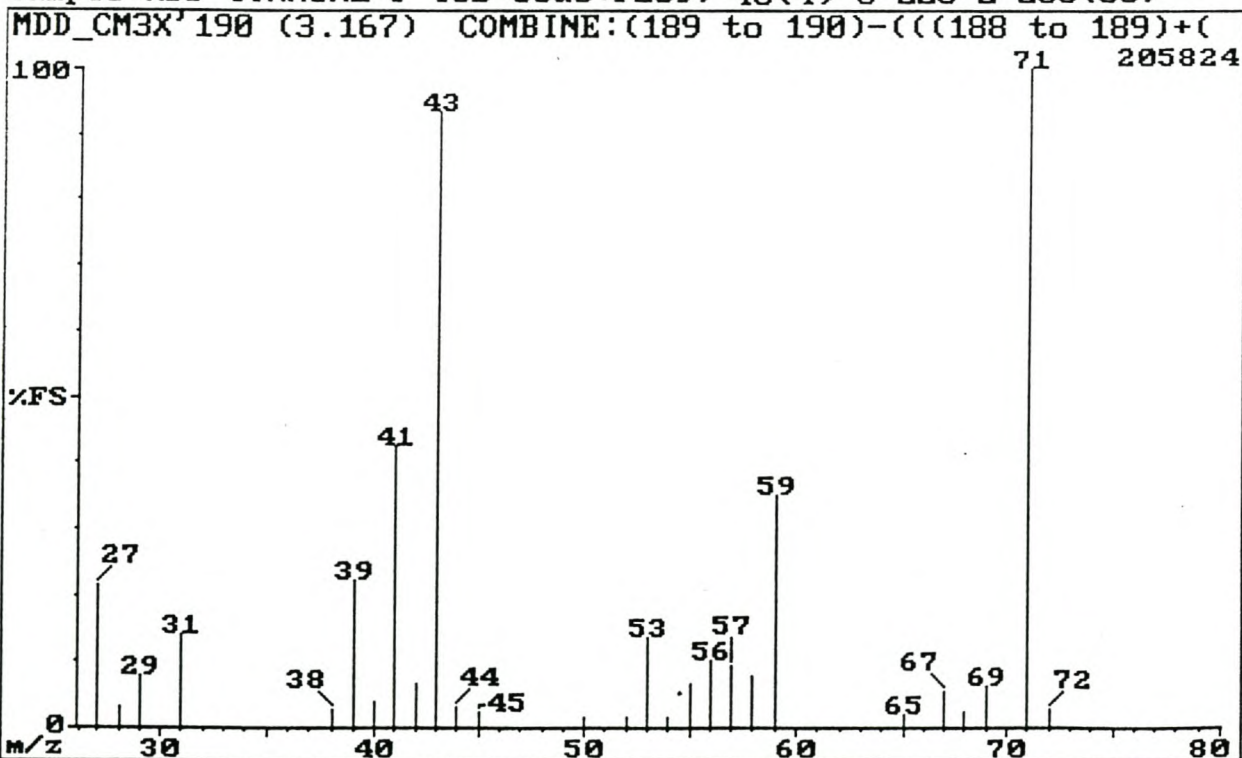


Fig. 3.44: El mass spectrum of component 190 (2-methyl-3-buten-2-ol).

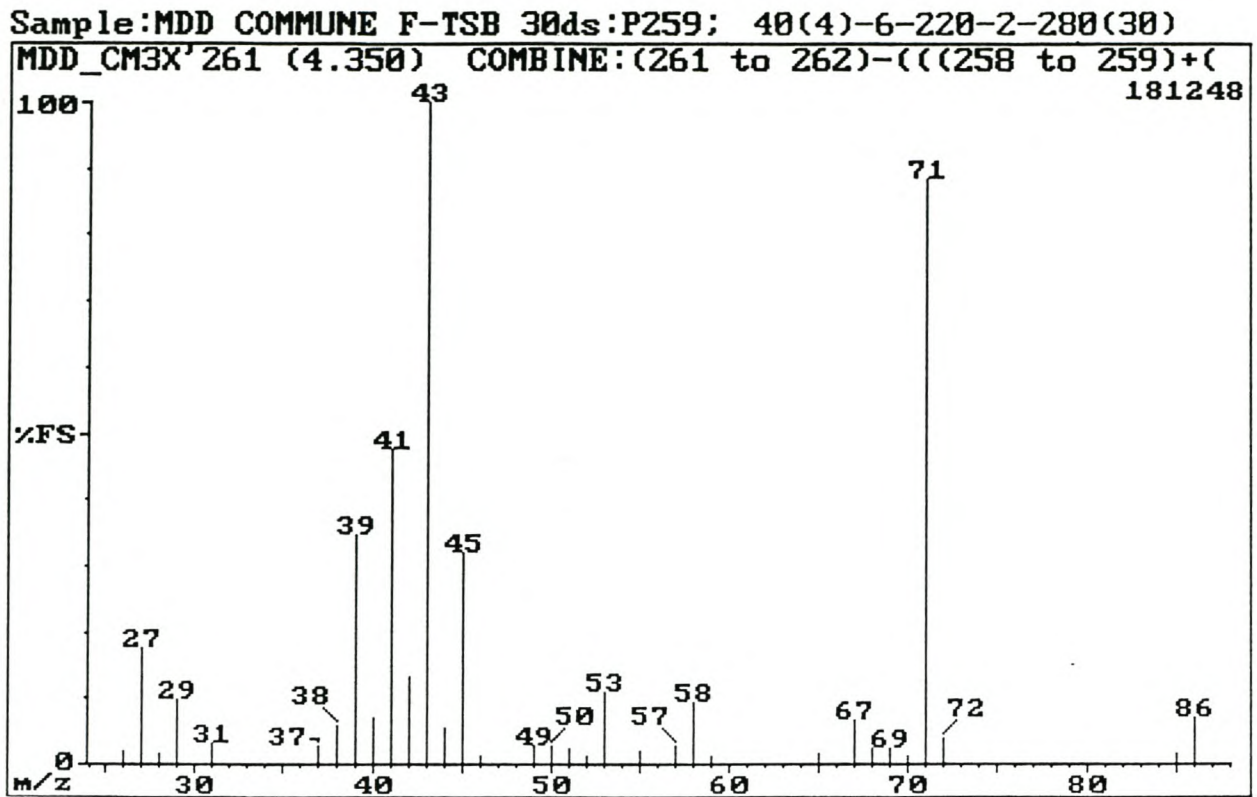


Fig. 3.45: El mass spectrum of component 261 (3-methyl-3-buten-2-ol).

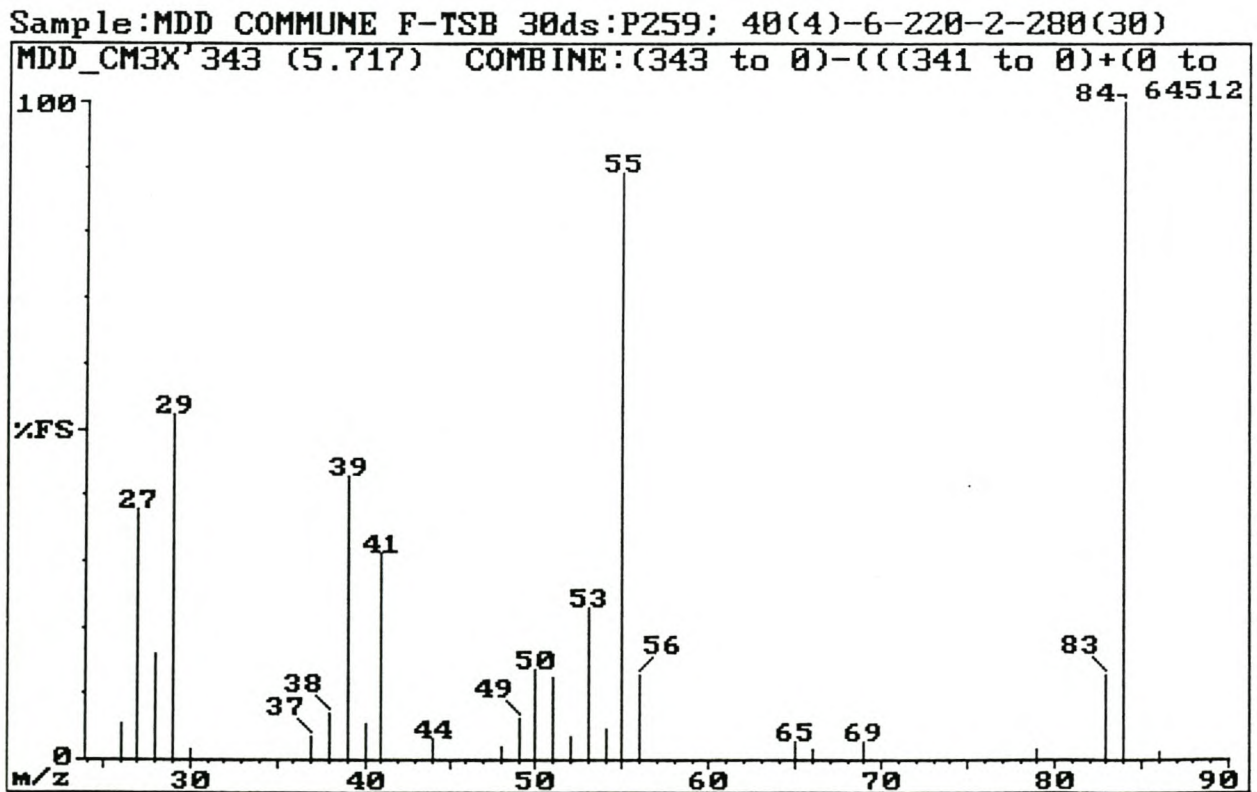


Fig. 3.46: El mass spectrum of component 343 (2-methyl-2-butenal).

Sample: MDD COMMUNE F-TSB 30ds:P259; 40(4)-6-220-2-280(30)

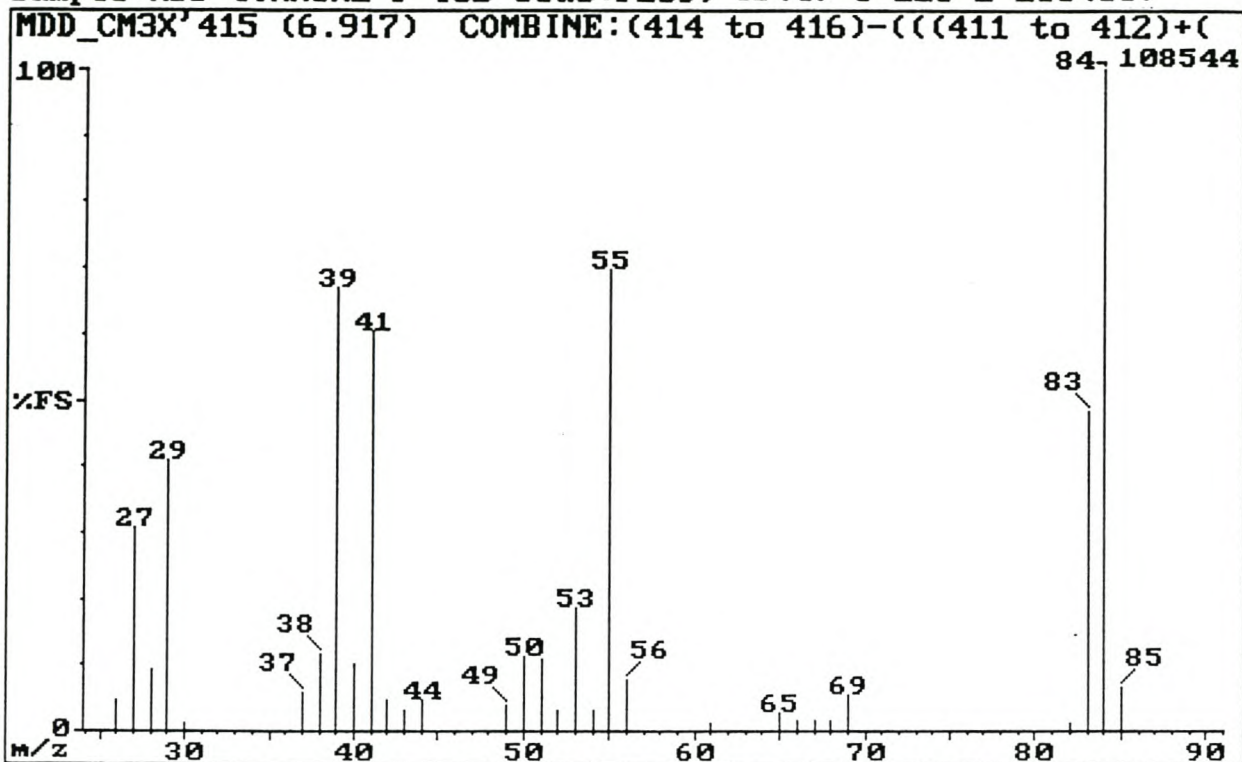


Fig. 3.47: EI mass spectrum of component 416 (3-methyl-2-butenal).

Sample: MDD COMMUNE F-TSB 30ds:P259; 40(4)-6-220-2-280(30)

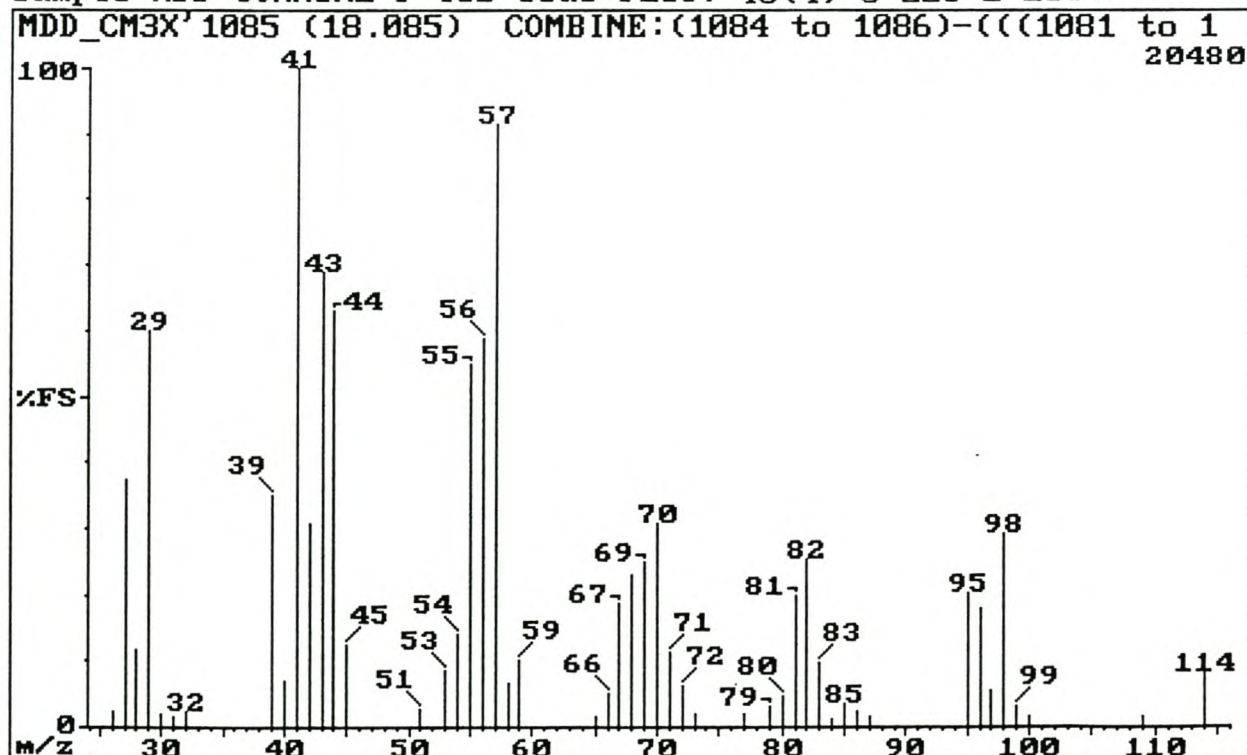


Fig. 3.48: EI mass spectrum of component 1085 (nonanal).

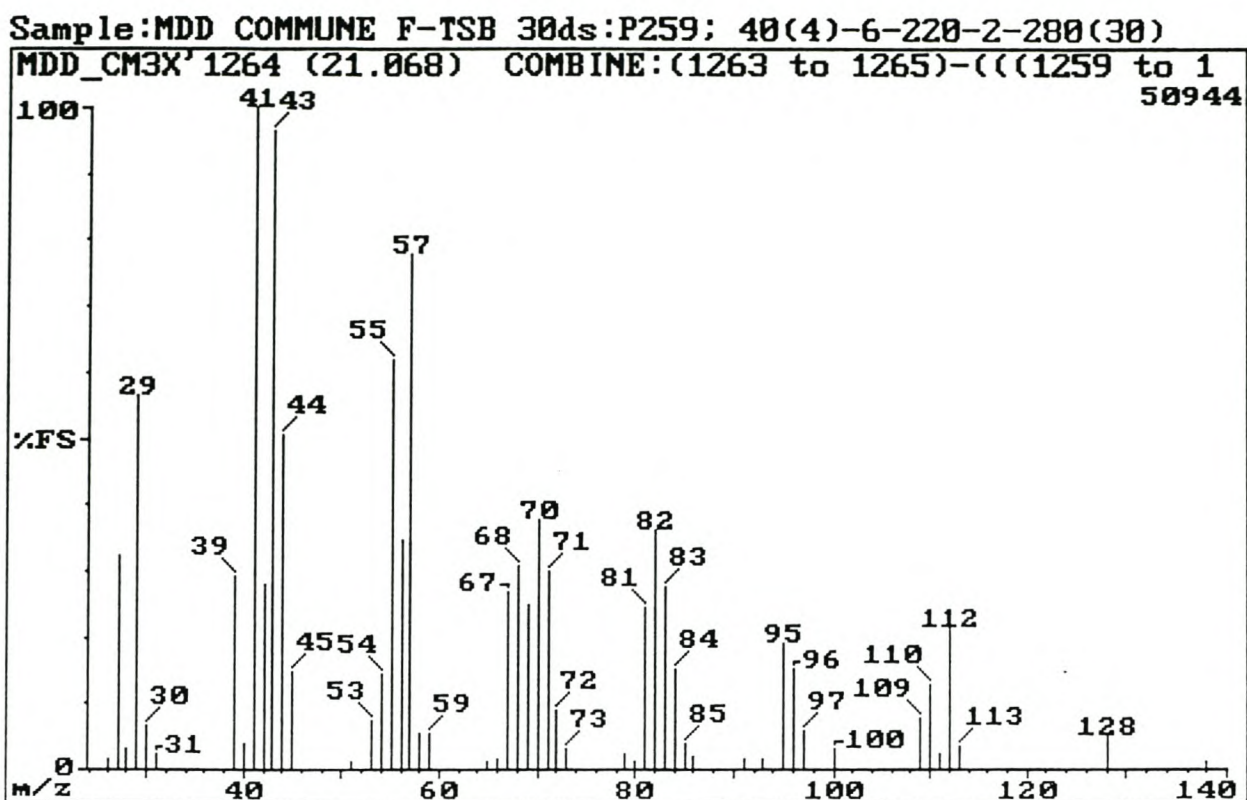


Fig. 3.49: El mass spectrum of component 1264 (decanal).

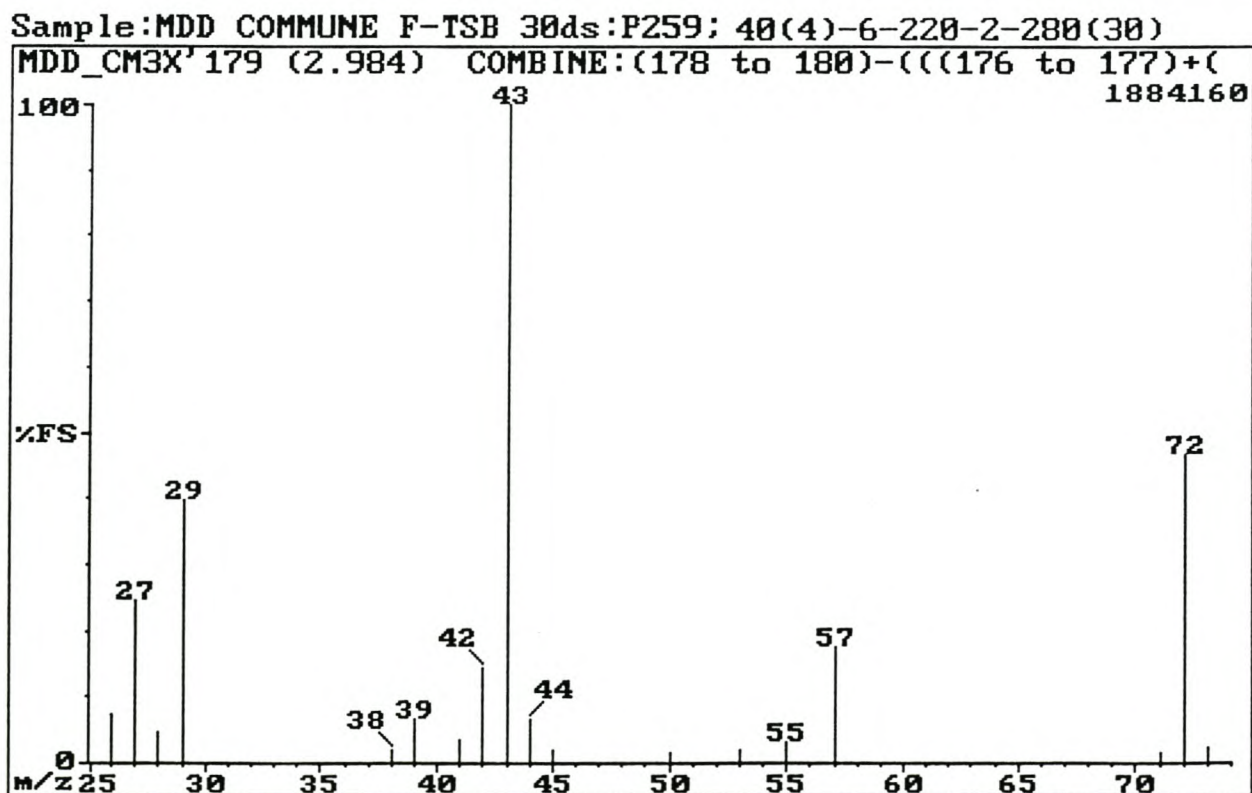


Fig. 3.50: El mass spectrum of component 179 (2-butanone).

Sample: MDD COMMUNE F-TSB 30ds: P259; 40(4)-6-220-2-280(30)

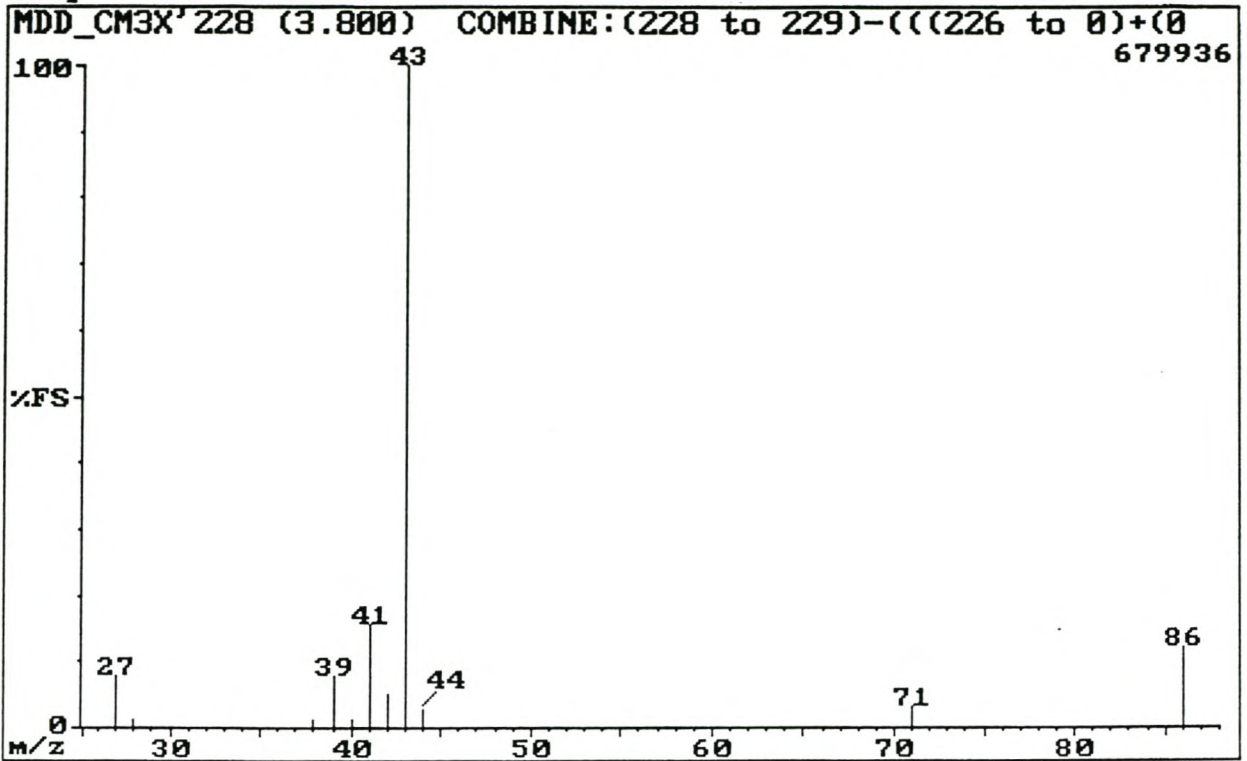


Fig. 3.51: EI mass spectrum of component 228 (3-methyl-2-butanone).

Sample: MDD COMMUNE F-TSB 30ds: P259; 40(4)-6-220-2-280(30)

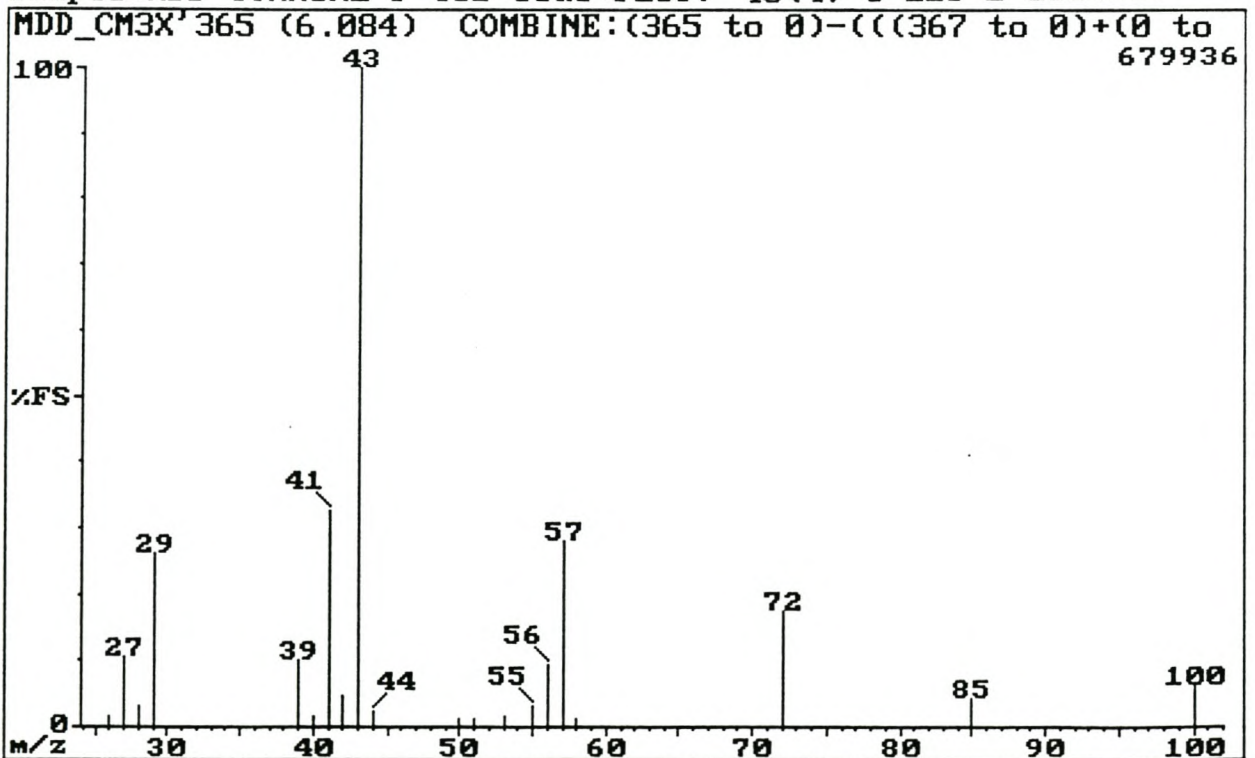


Fig. 3.52: EI mass spectrum of component 364 (3-methyl-2-pentanone).

Sample: MDD COMMUNE F-TSB 30ds: P259; 40(4)-6-220-2-280(30)

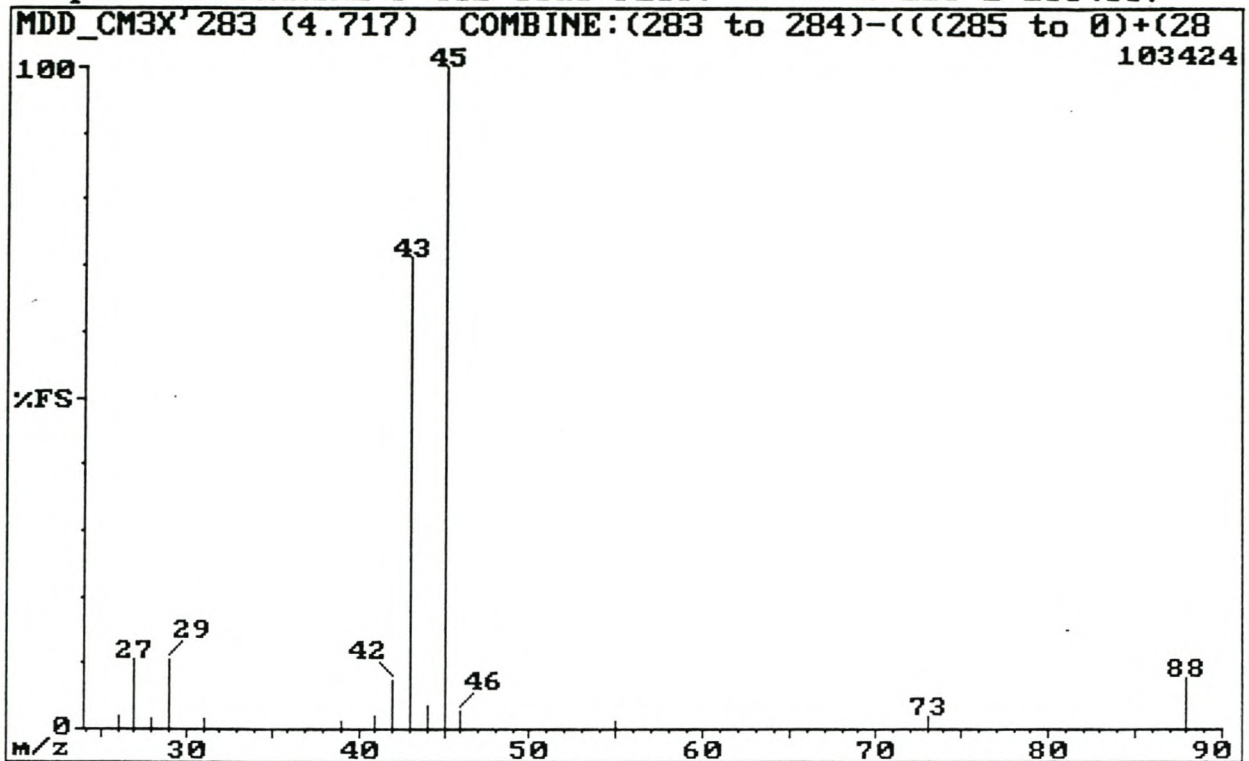


Fig. 3.53: El mass spectrum of component 283 (3-hydroxy-2-butanone).

Sample: MDD COMMUNE F-TSB 30ds: P259; 40(4)-6-220-2-280(30)

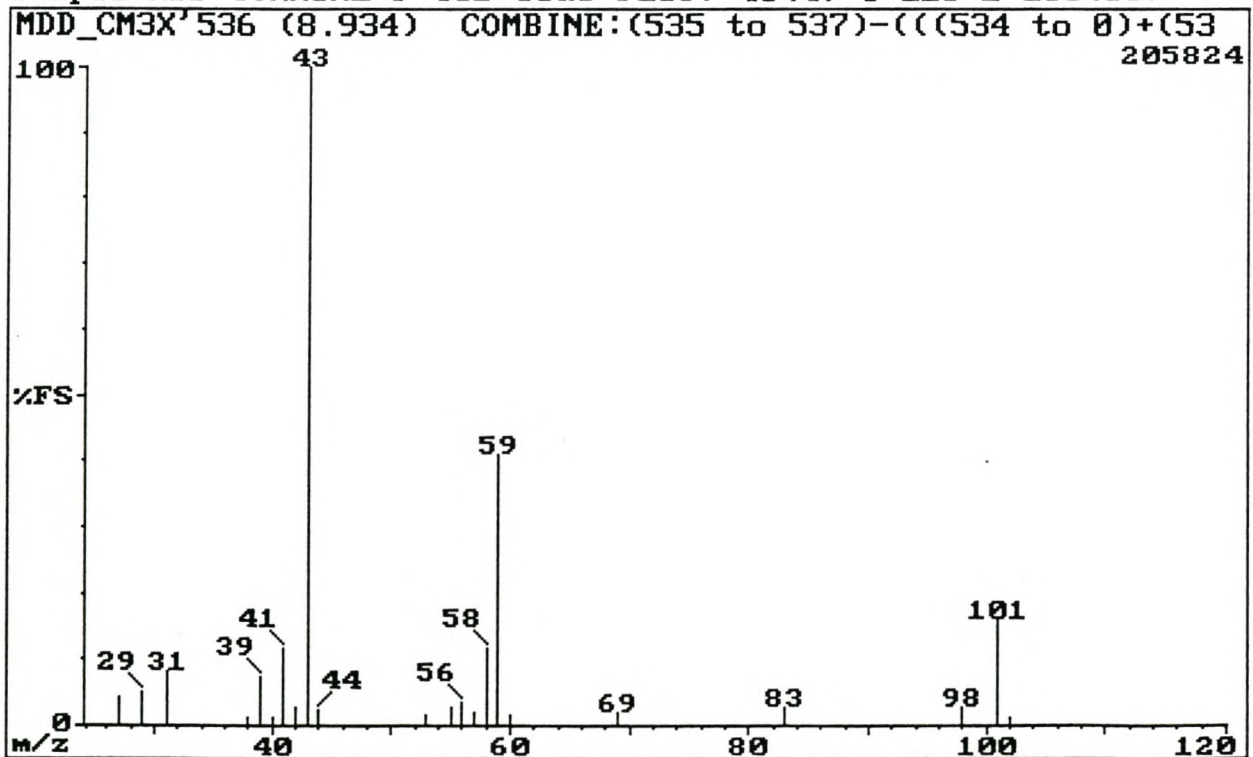


Fig. 3.54: El mass spectrum of component 536 (4-hydroxy-4-methyl-2-pentanone).

Sample: MDD COMMUNE F-TSB 30ds: P259; 40(4)-6-220-2-280(30)

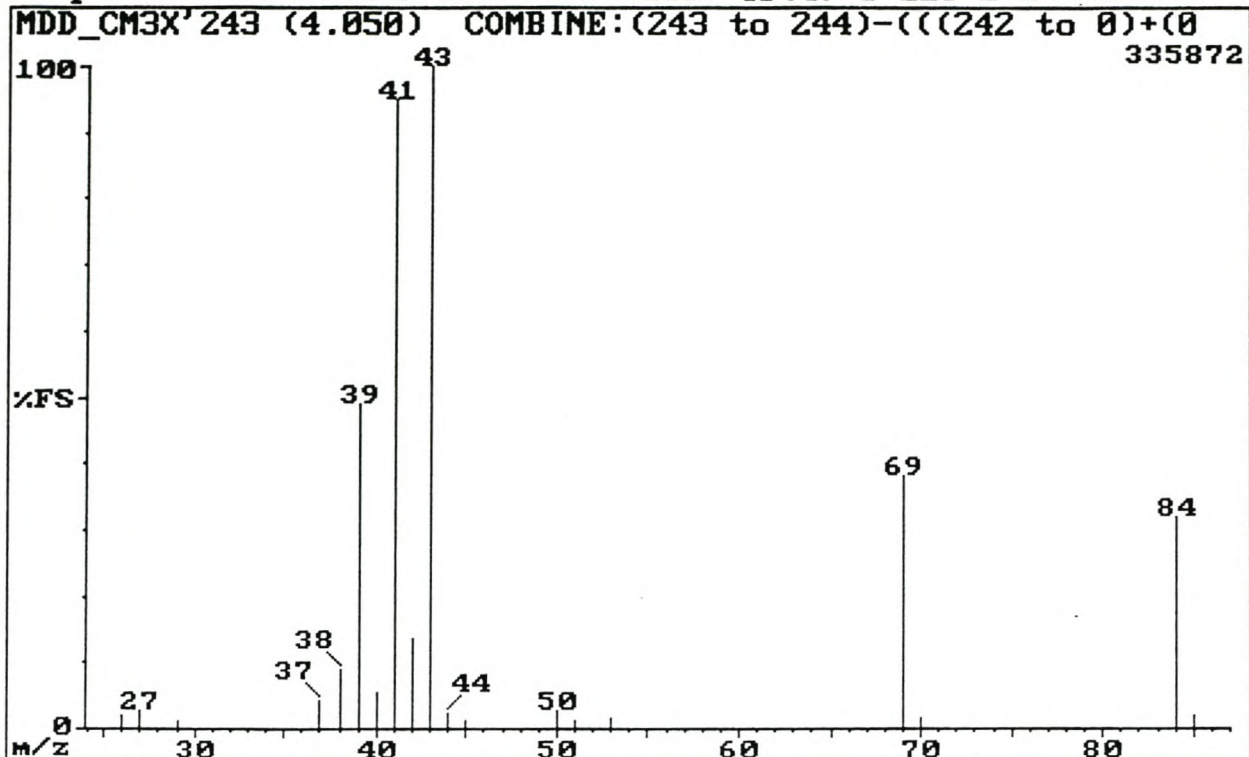


Fig. 3.55: EI mass spectrum of component 243 (3-methyl-3-buten-2-one).

Sample: MDD COMMUNE F-TSB 30ds: P259; 40(4)-6-220-2-280(30)

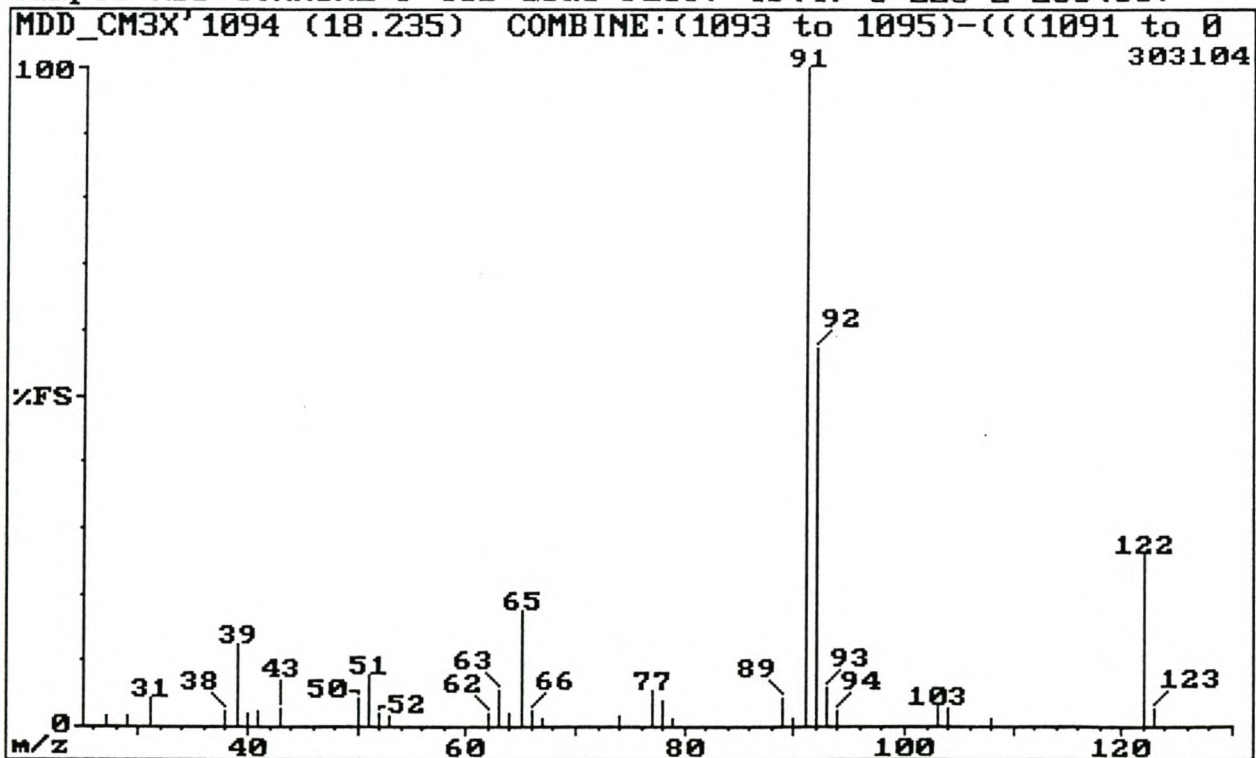


Fig. 3.56: EI mass spectrum of component 1094 (2-phenylethanol).

Sample: MDD COMMUNE F-TSB 30ds:P259; 40(4)-6-220-2-280(30)

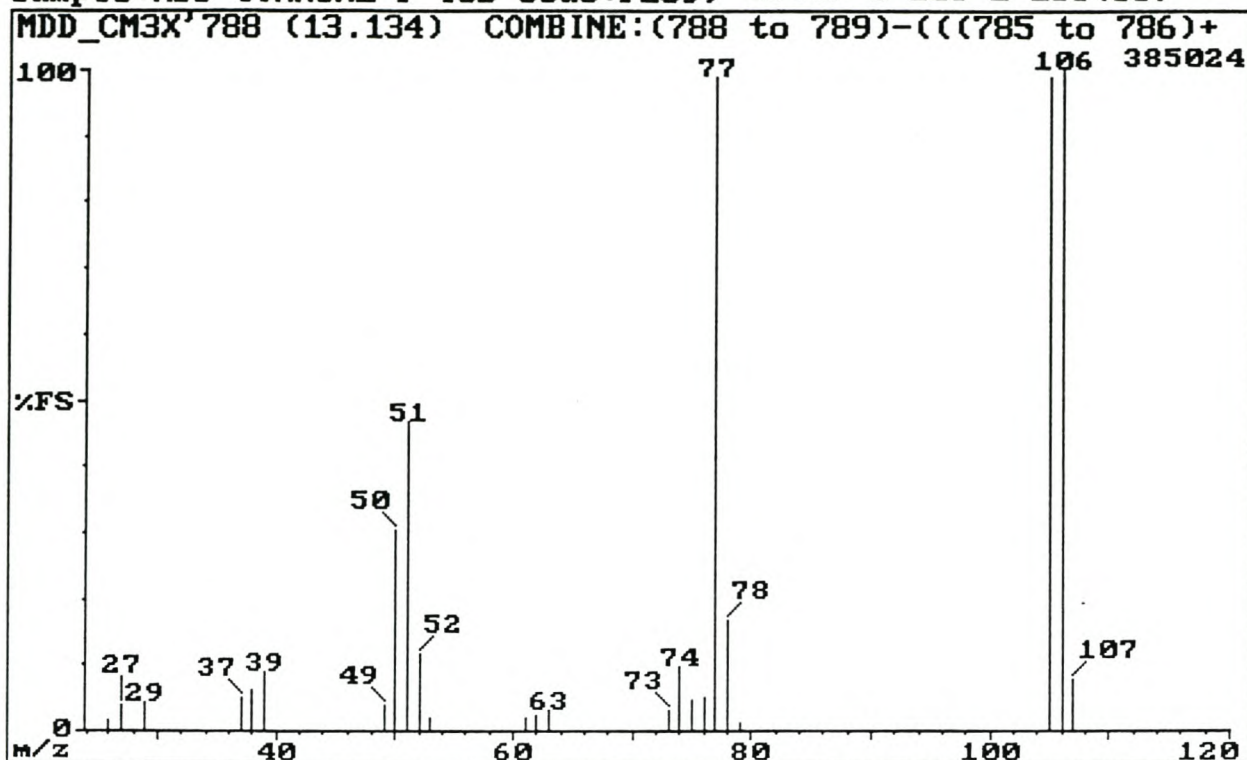


Fig. 3.57: EI mass spectrum of component 788 (benzaldehyde).

Sample: MDD COMMUNE F-TSB 30ds:P259; 40(4)-6-220-2-280(30)

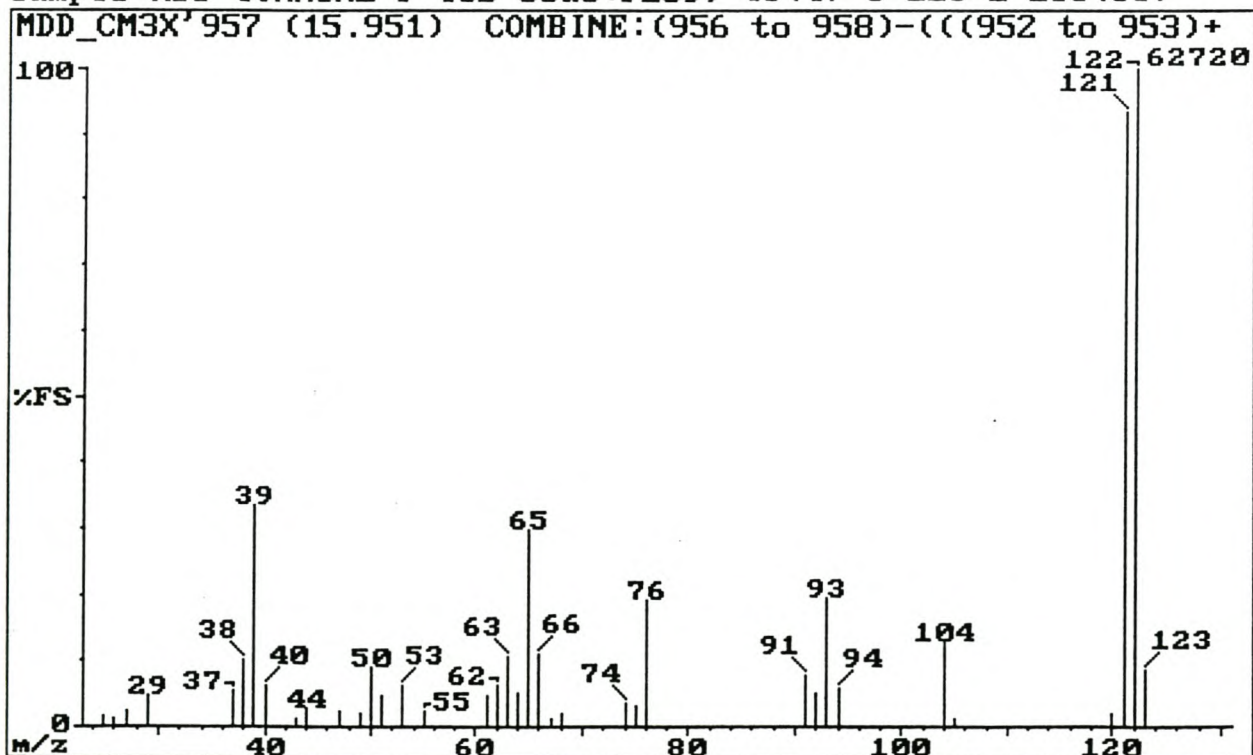


Fig. 3.58: EI mass spectrum of component 957 (2-hydroxybenzaldehyde).

Sample: MDD COMMUNE F-TSB 30ds: P259; 40(4)-6-220-2-280(30)

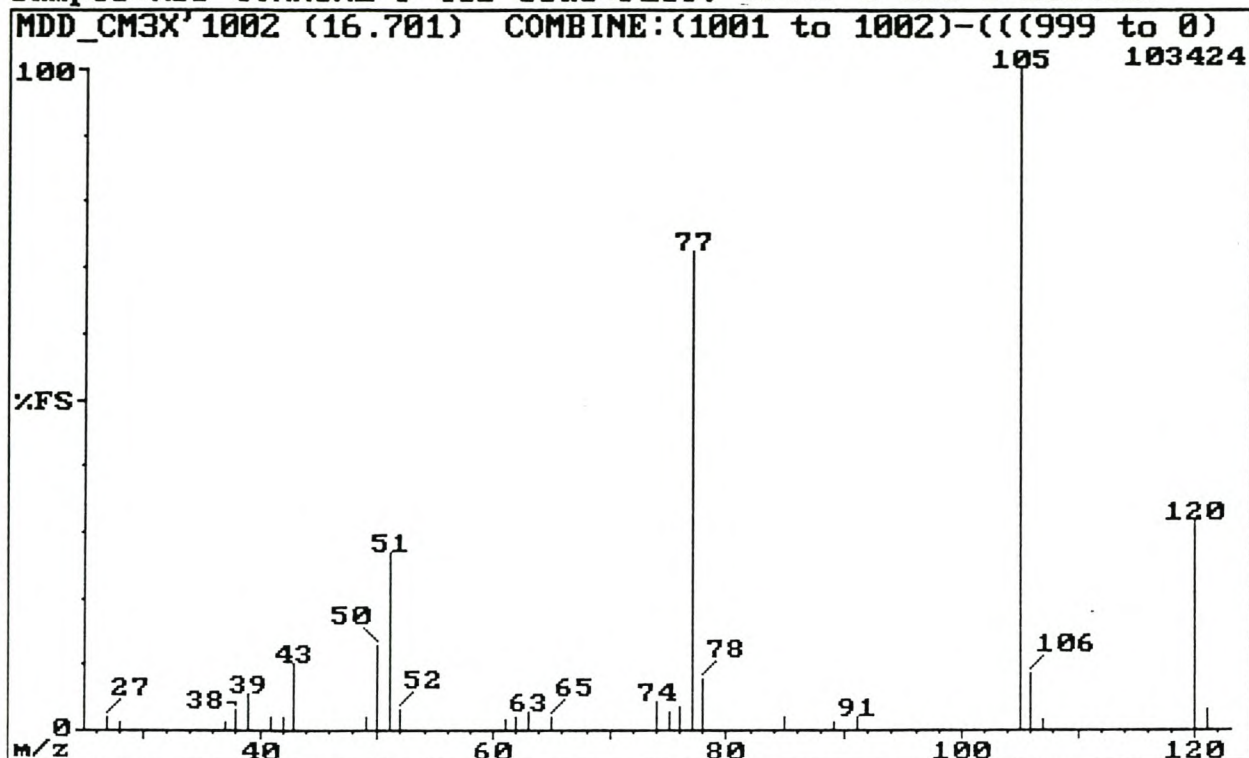


Fig. 3.59: EI mass spectrum of component 1001 (acetophenone).

Sample: MDD COMMUNE F-TSB 30ds: P259; 40(4)-6-220-2-280(30)

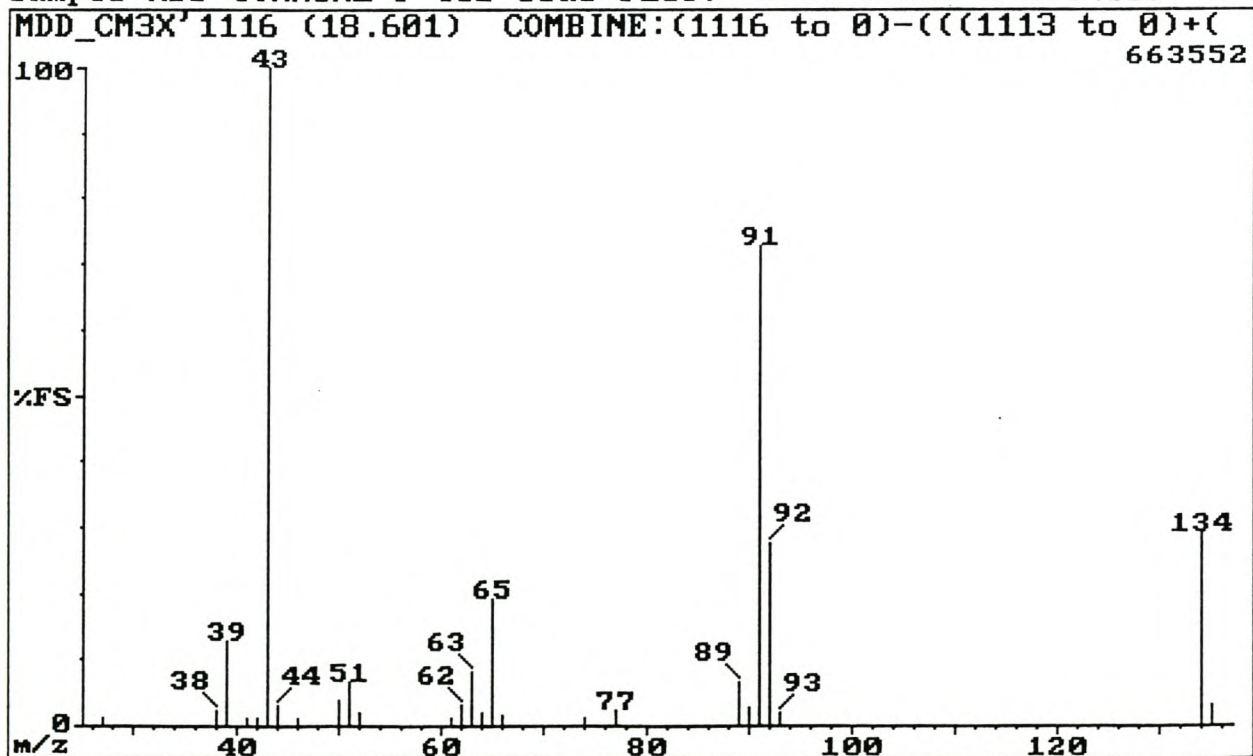


Fig. 3.60: EI mass spectrum of component 1117 (1-phenyl-2-propanone).

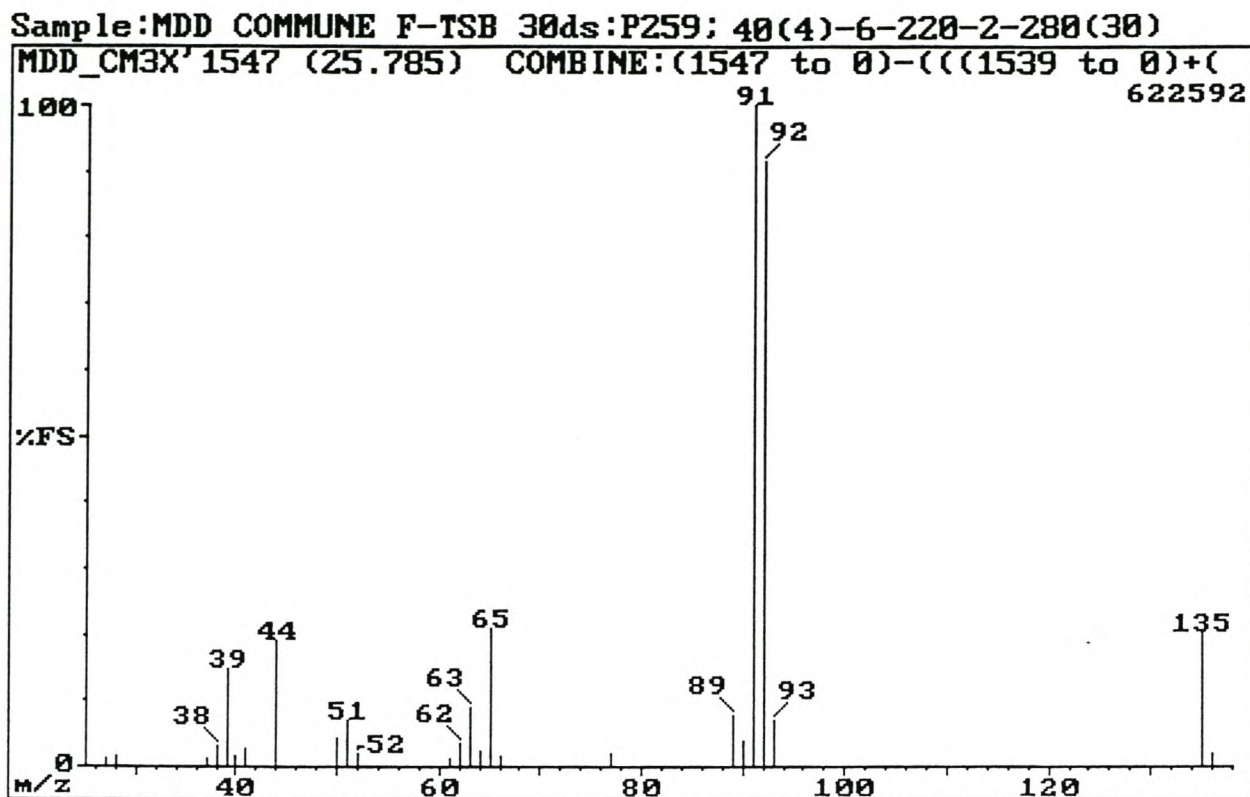


Fig. 3.61: El mass spectrum of component 1550 (phenylacetamide).

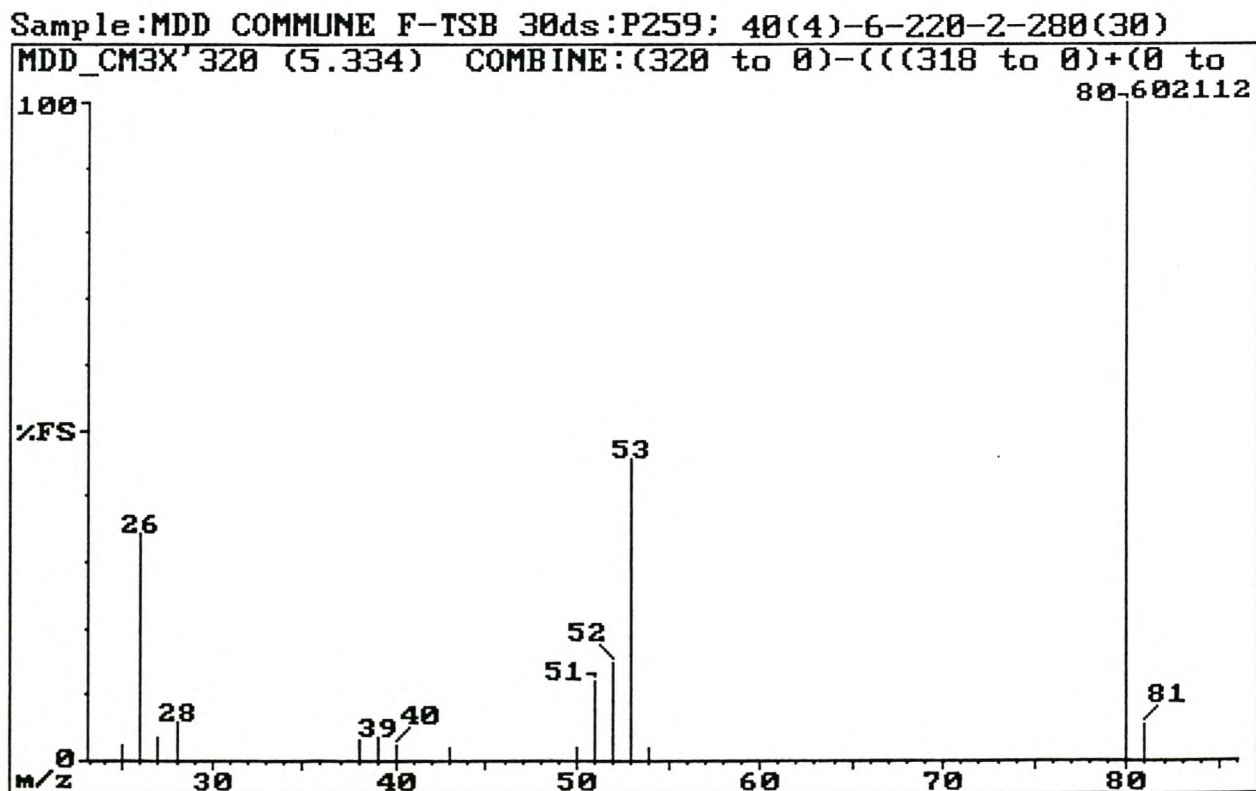


Fig. 3.62: El mass spectrum of component 321 (pyrazine).

Sample: MDD COMMUNE F-TSB 30ds: P259; 40(4)-6-220-2-280(30)

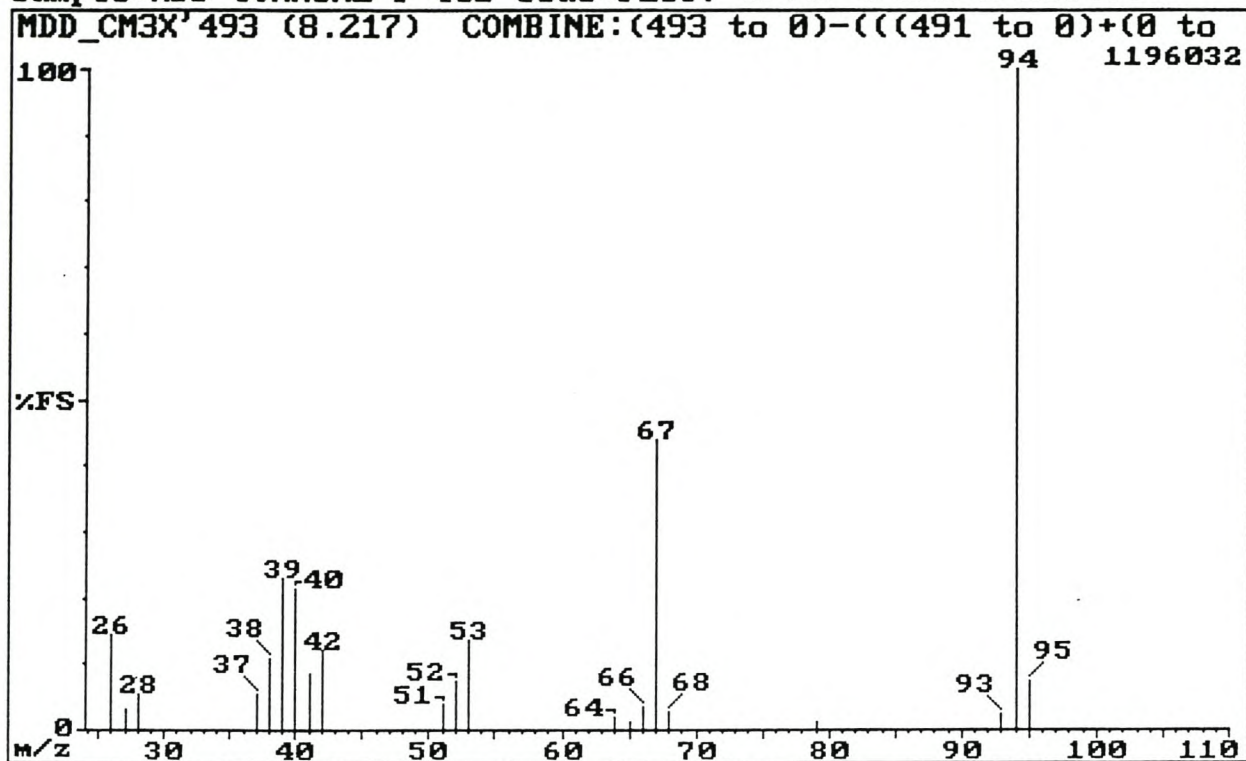


Fig. 3.63: El mass spectrum of component 494 (methylpyrazine).

Sample: MDD COMMUNE F-TSB 30ds: P259; 40(4)-6-220-2-280(30)

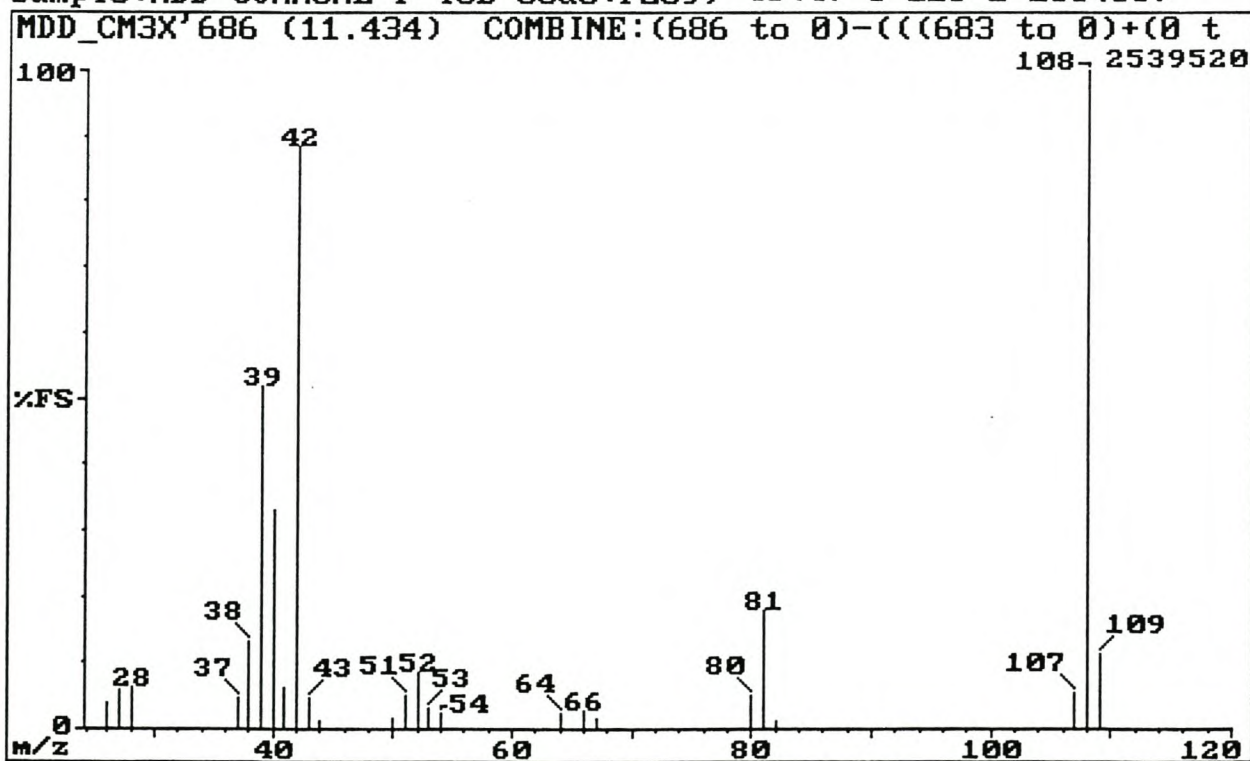


Fig. 3.64: El mass spectrum of component 689 (2,5-dimethylpyrazine).

Sample: MDD COMMUNE F-TSB 30ds: P259; 40(4)-6-220-2-280(30)

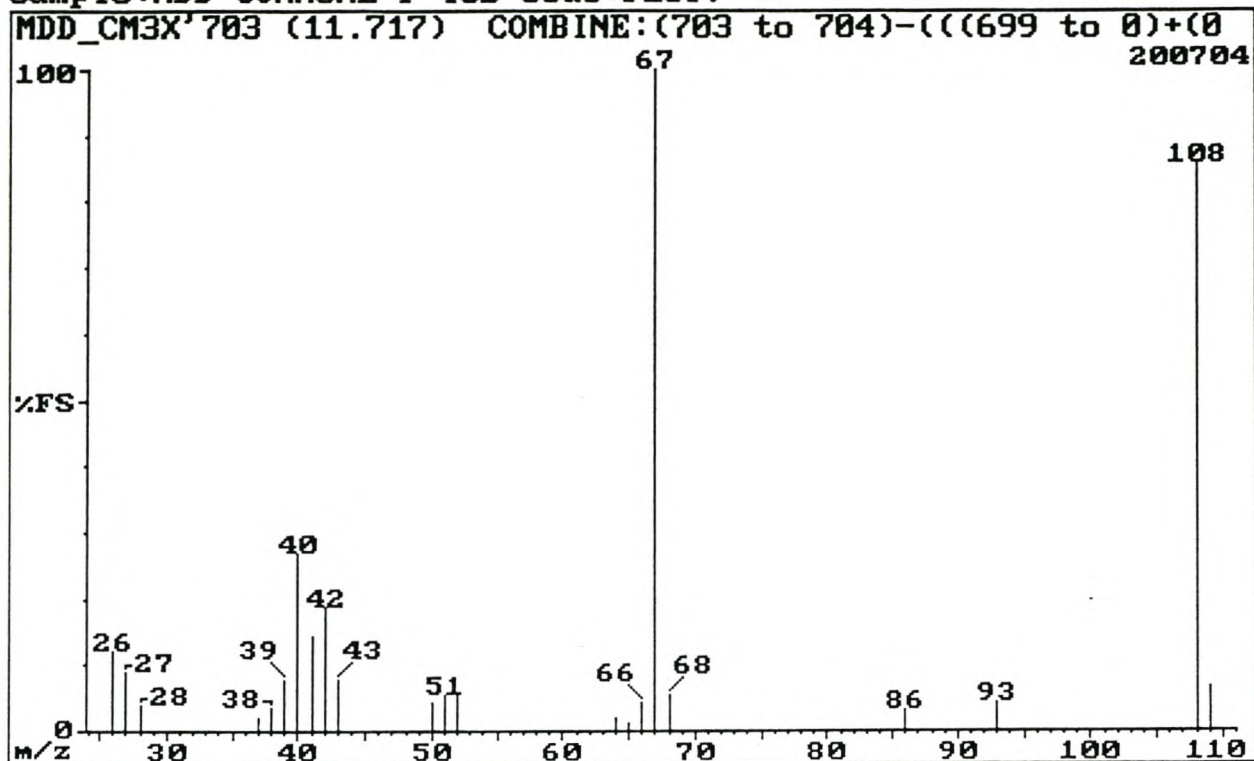


Fig. 3.65: EI mass spectrum of component 703 (2,3-dimethylpyrazine).

Sample: MDD COMMUNE F-TSB 30ds: P259; 40(4)-6-220-2-280(30)

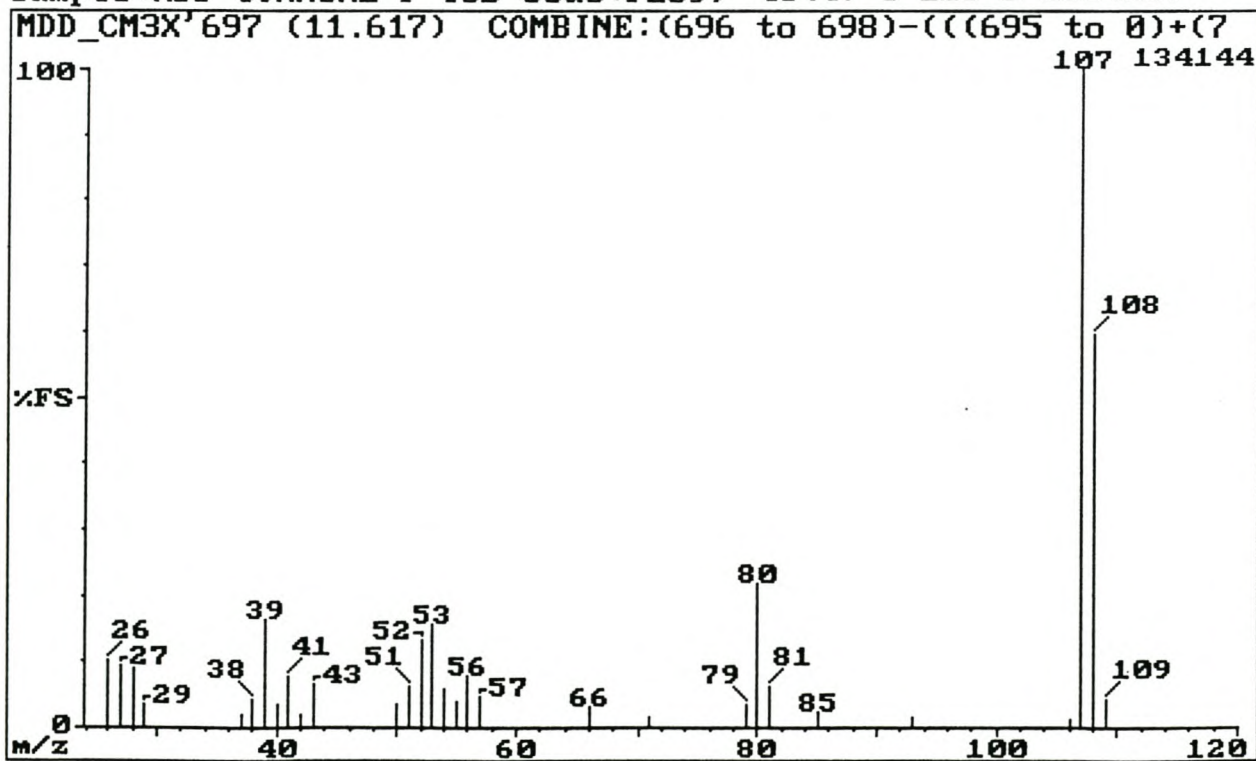


Fig. 3.66: EI mass spectrum of component 697 (ethylpyrazine).

Sample: MDD COMMUNE F-TSB 30ds: P259; 40(4)-6-220-2-280(30)

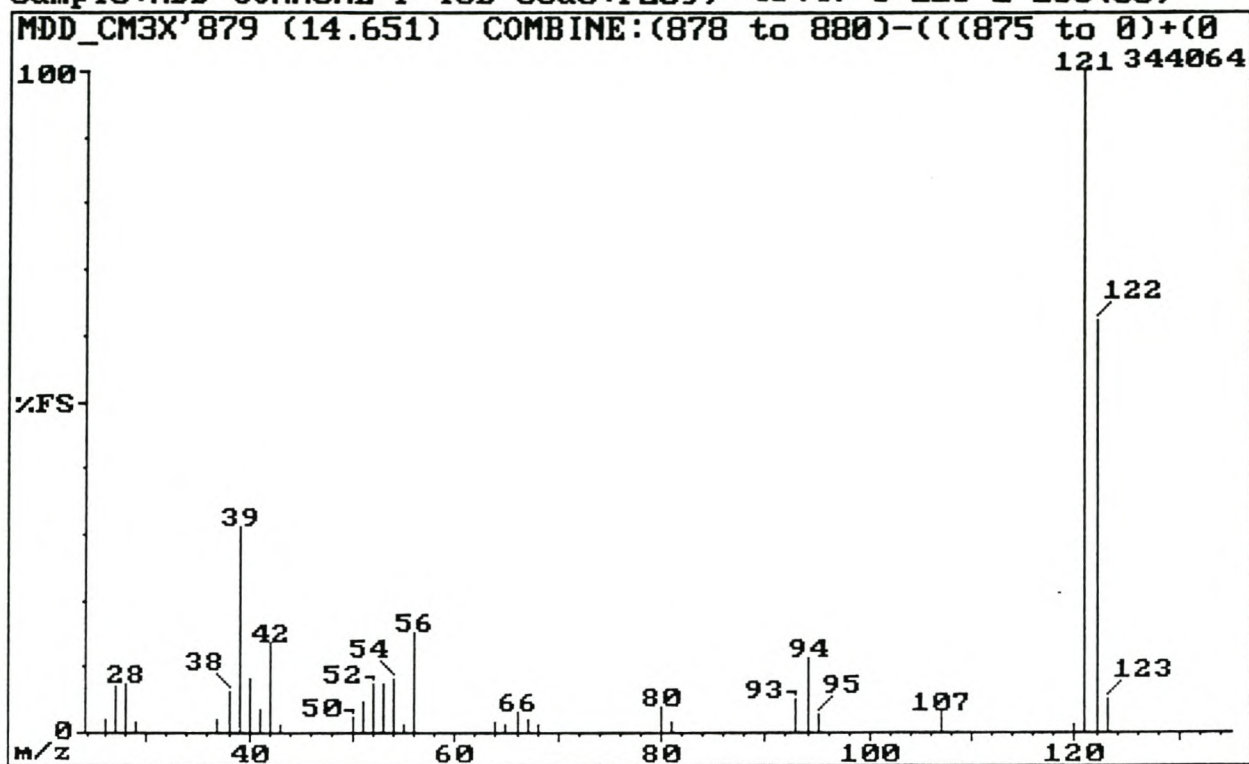


Fig. 3.67: El mass spectrum of component 879 (2-ethyl-5-methylpyrazine).

Sample: COMMUNE MSM 3ds: P262; 40C(4min)-4C/min-280(30min)

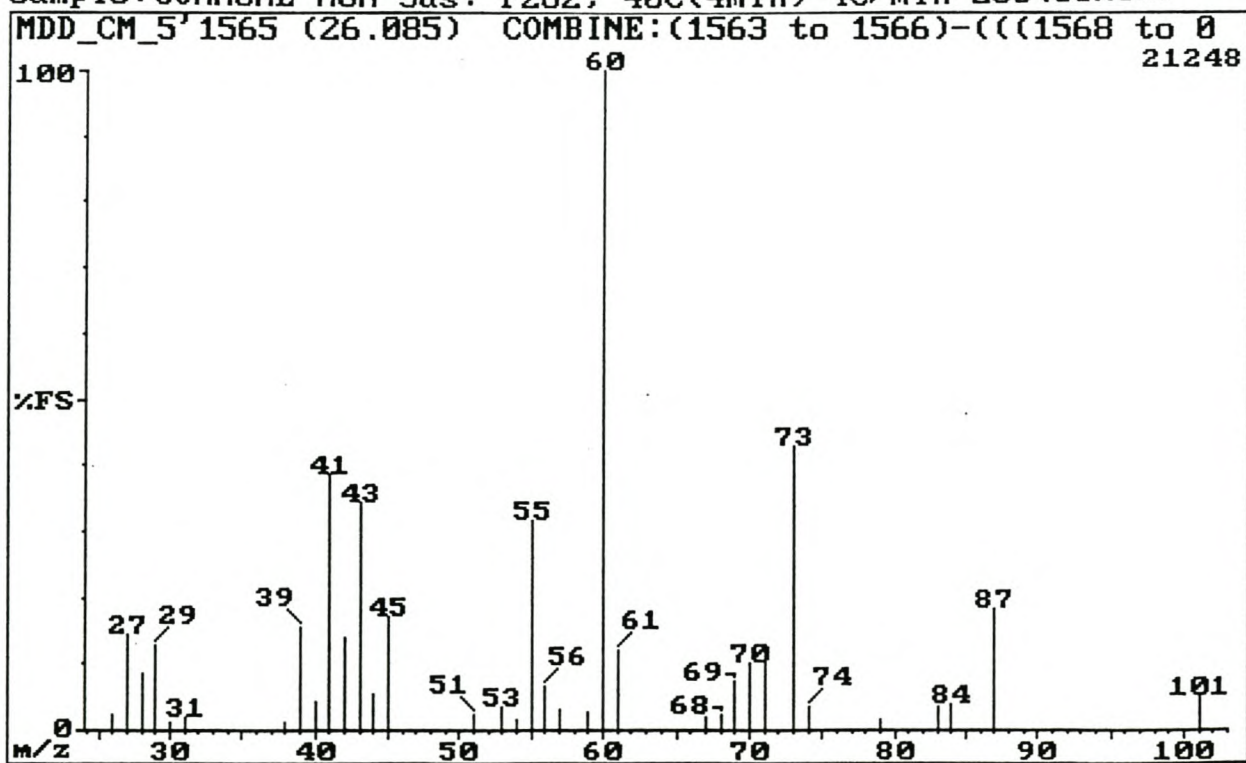


Fig. 3.68: El mass spectrum of component 1546 (1-octanol).

Sample COMMUNE MSM 3ds: P262; 40C(4min)-4C/min-280(30min)

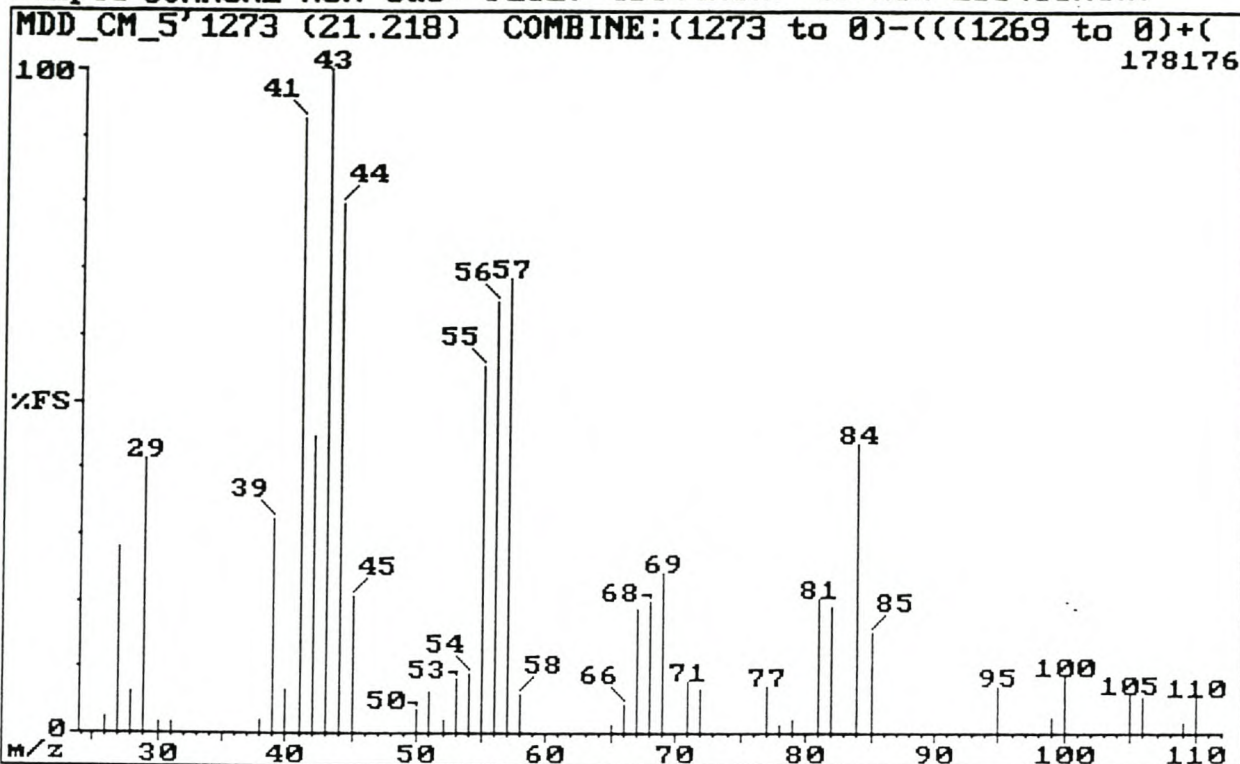


Fig. 3.69: EI mass spectrum of component 1276 (octanal).

Sample:COMMUNE MSM 3ds: P262; 40C(4min)-4C/min-280(30min)

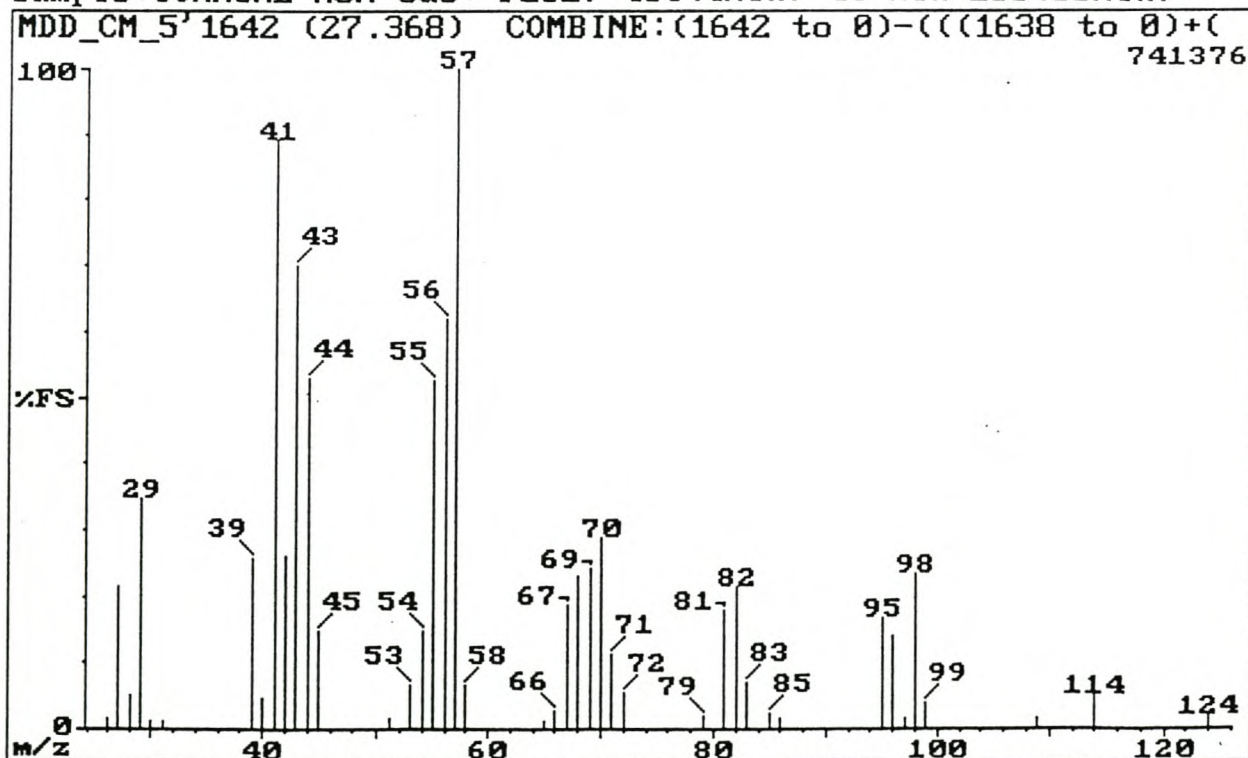


Fig. 3.70: EI mass spectrum of component 1646 (nonanal).

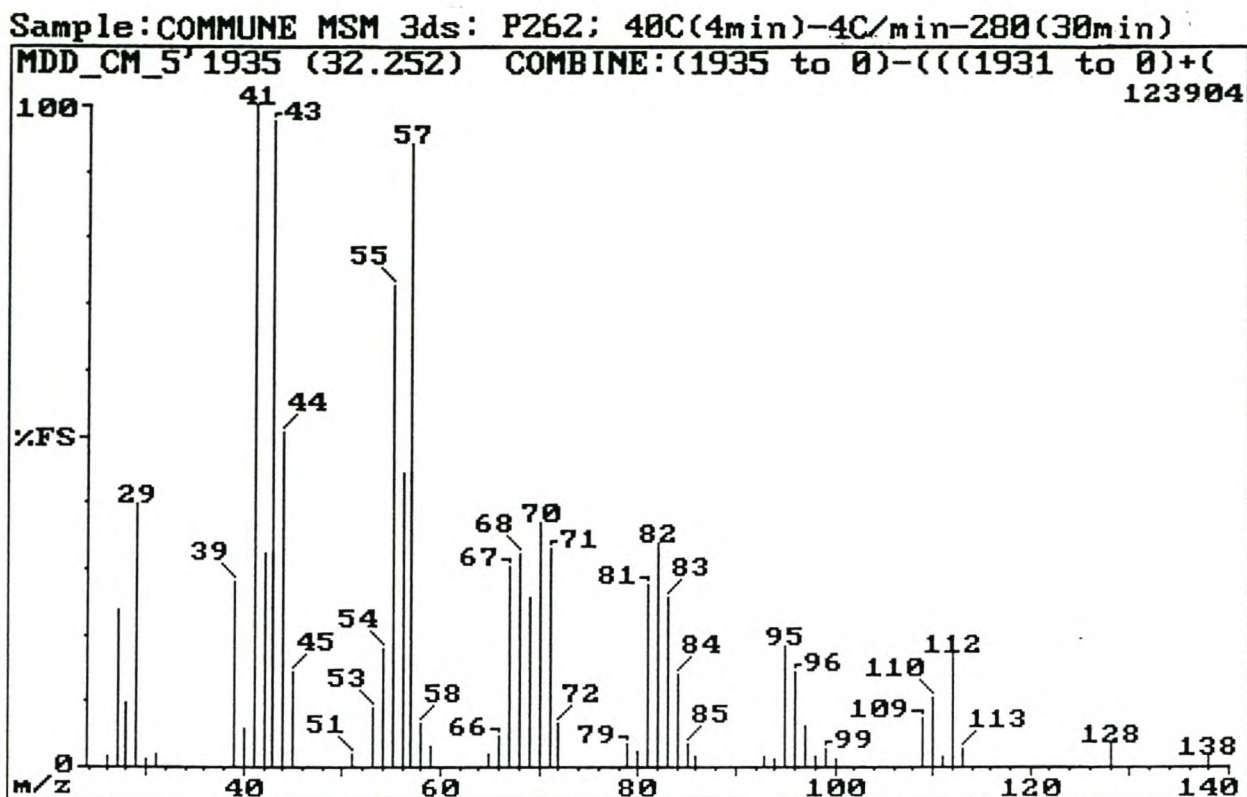


Fig. 3.71: EI mass spectrum of component 1937 (decanal).

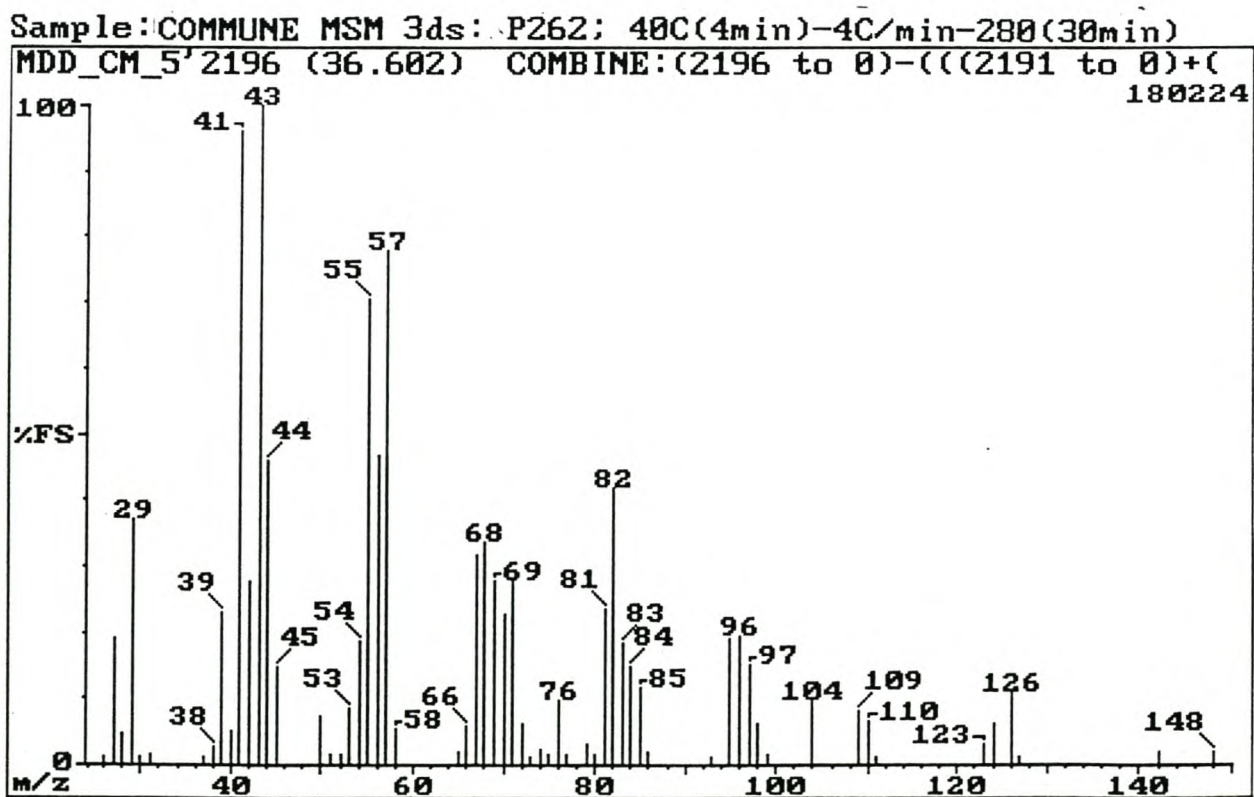


Fig. 3.72: EI mass spectrum of component 2196 (undecanal).

Sample: COMMUNE MSM 3ds: P262; 40C(4min)-4C/min-280(30min)

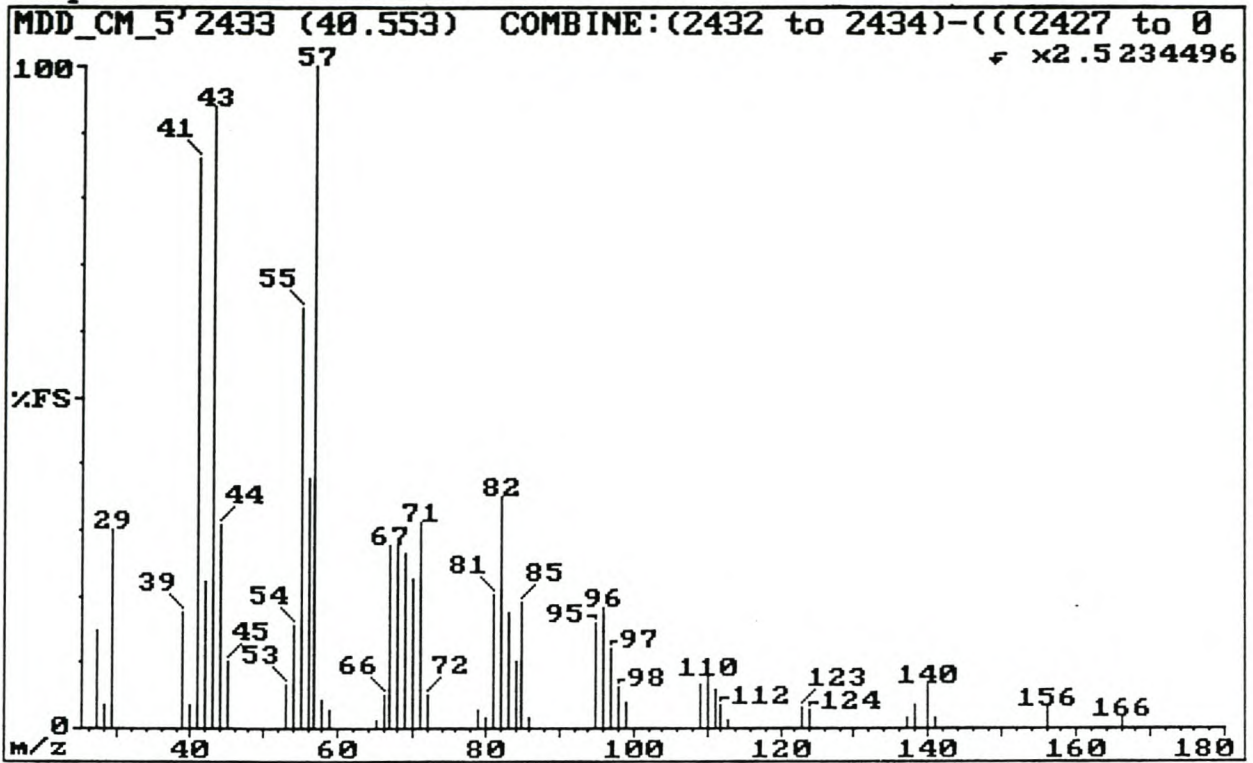


Fig. 3.73: El mass spectrum of component 2433 (dodecanal).

Sample: COMMUNE MSM 3ds: P262; 40C(4min)-4C/min-280(30min)

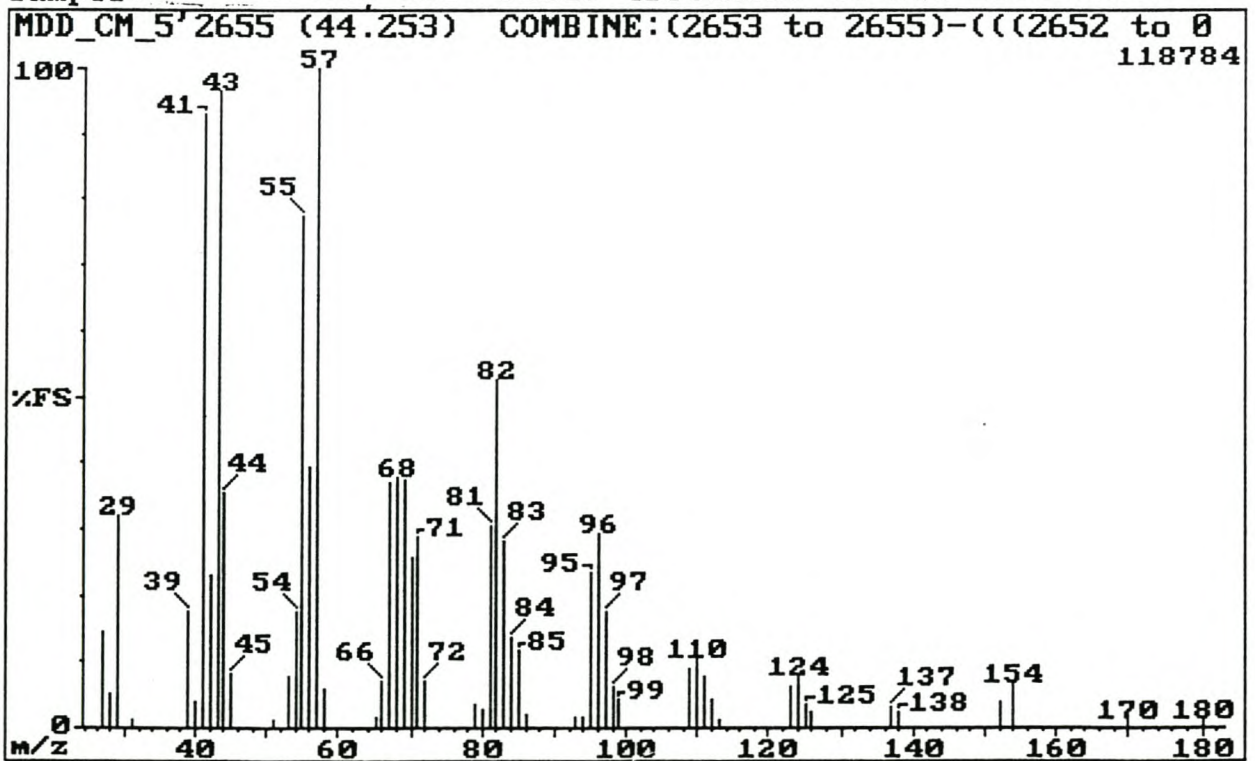


Fig. 3.74: El mass spectrum of component 2656 (tridecanal).

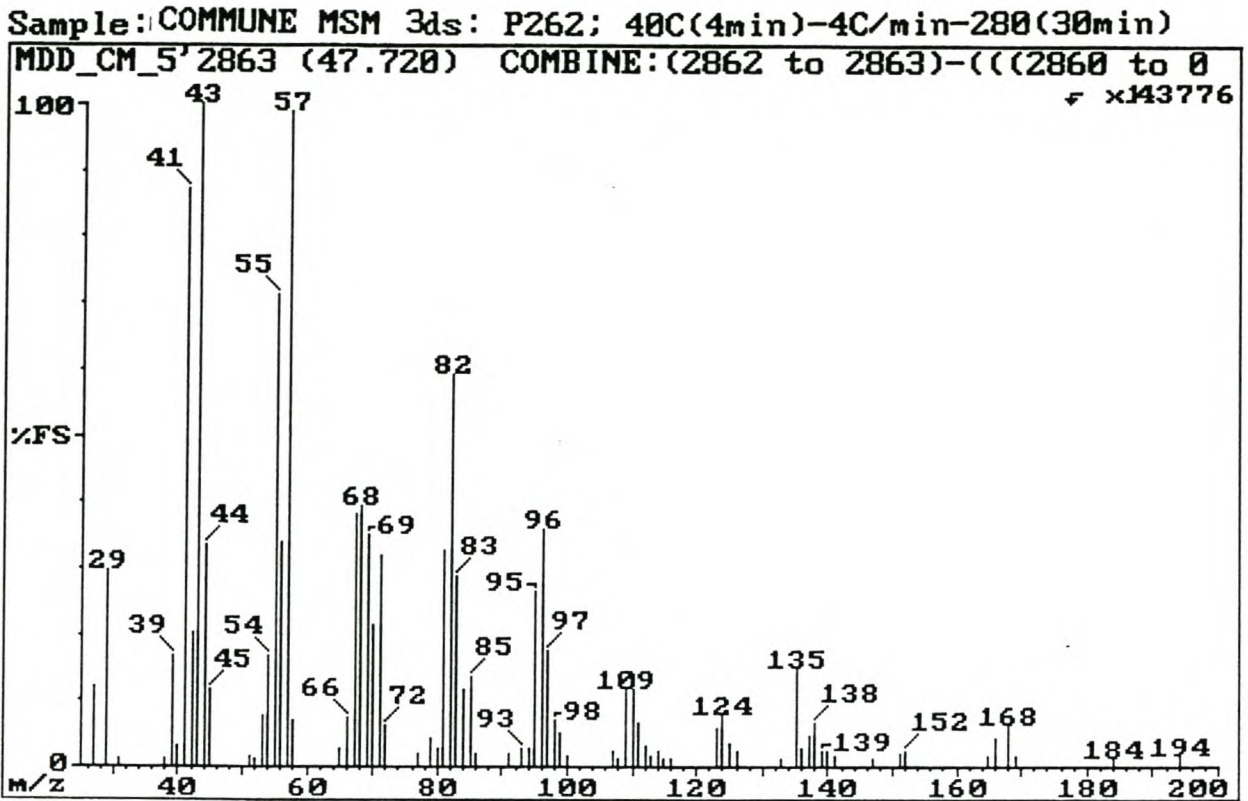


Fig. 3.75: EI mass spectrum of component 2866 (tetradecanal).

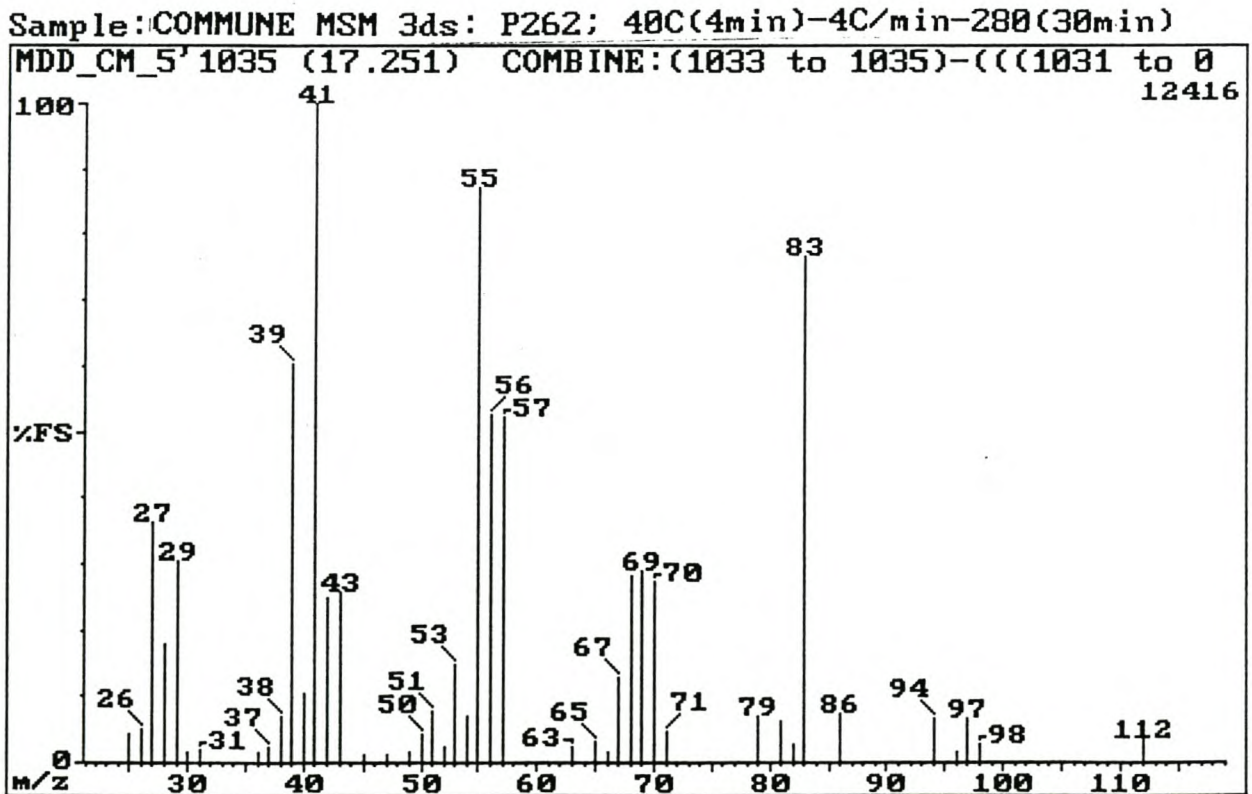


Fig. 3.76: EI mass spectrum of component 1034 [(Z)-2-heptenal].

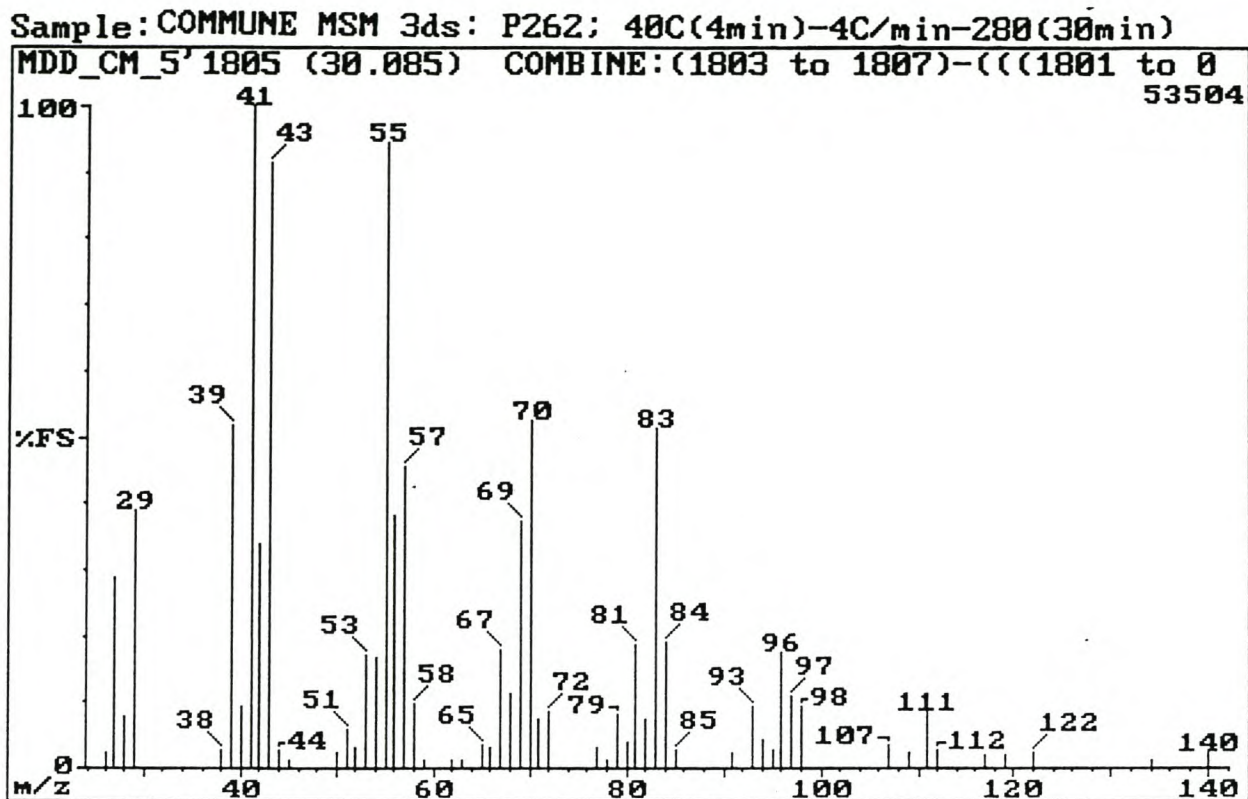


Fig. 3.77: EI mass spectrum of component 1804 (2-nonenal).

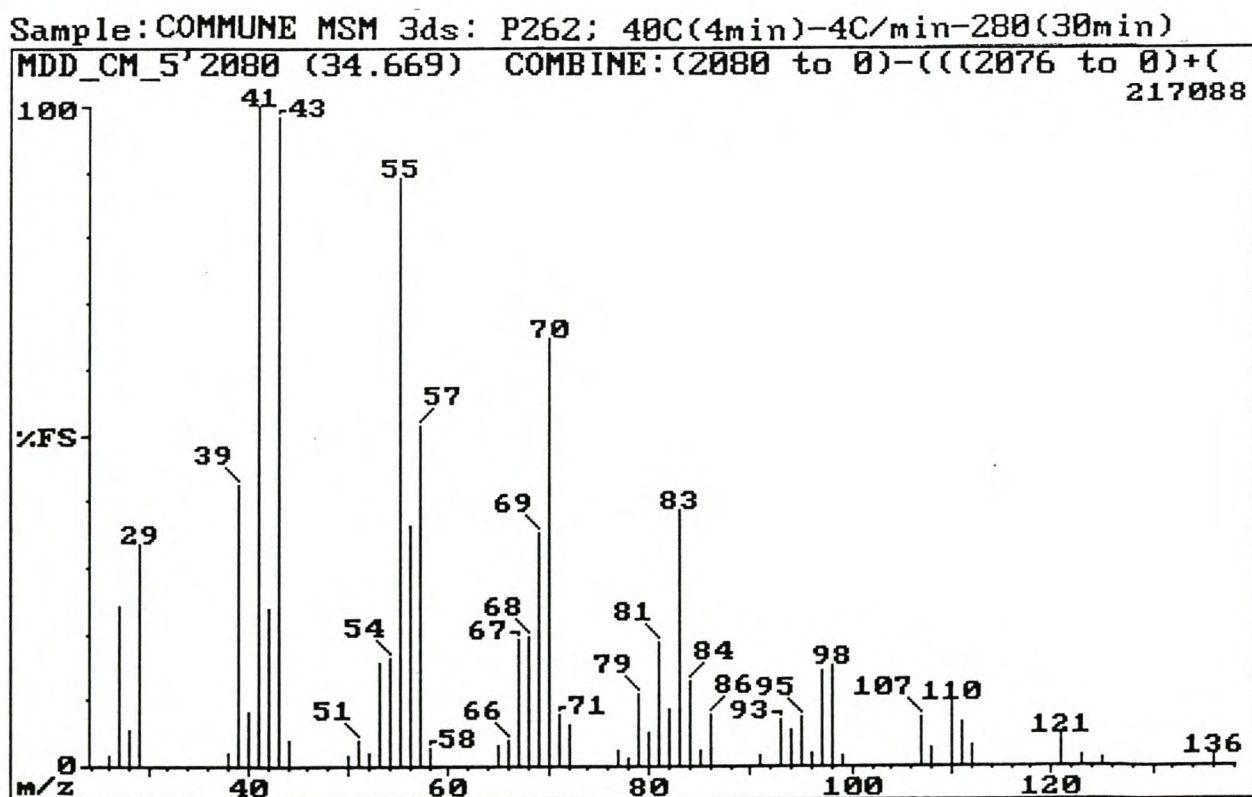


Fig. 3.78: EI mass spectrum of component 2080 [(Z)-2-decenal].

Sample: COMMUNE MSM 3ds: P262; 40C(4min)-4C/min-280(30min)

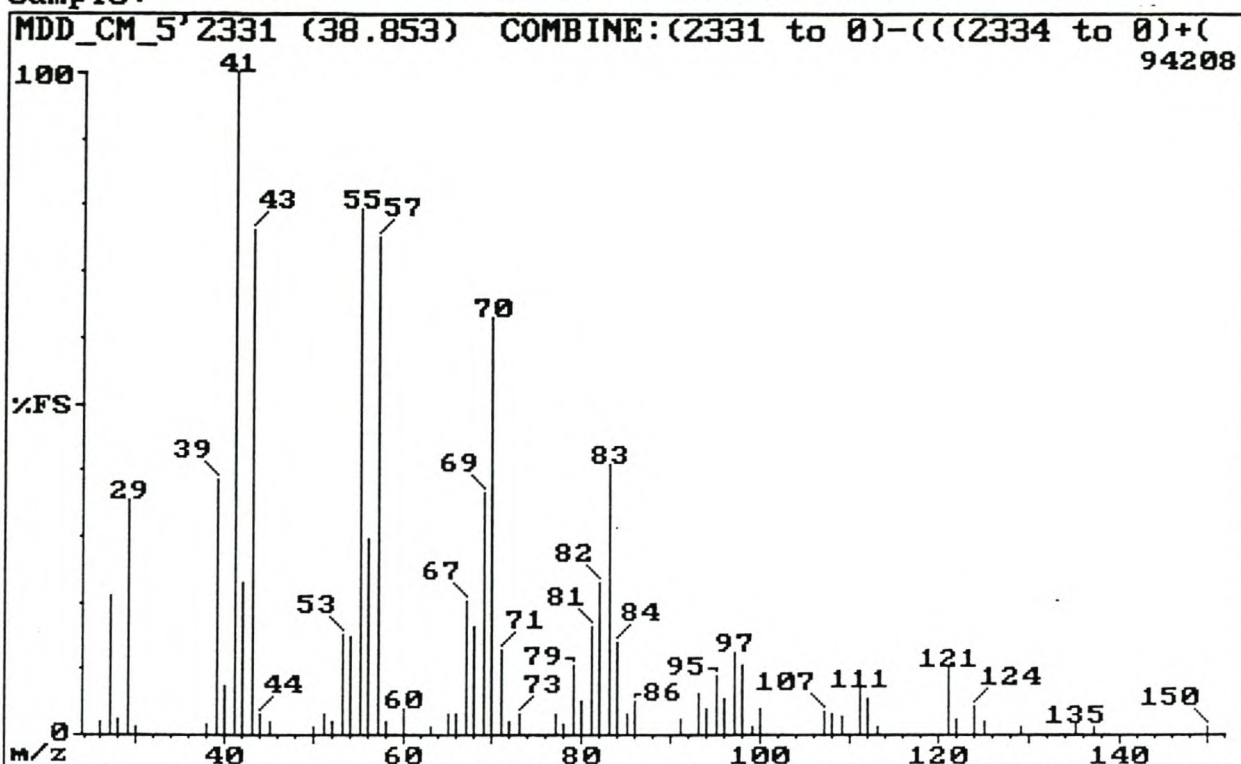


Fig. 3.79: El mass spectrum of component 2329 (2-undecenal).

Sample: COMMUNE MSM 3ds: P262; 40C(4min)-4C/min-280(30min)

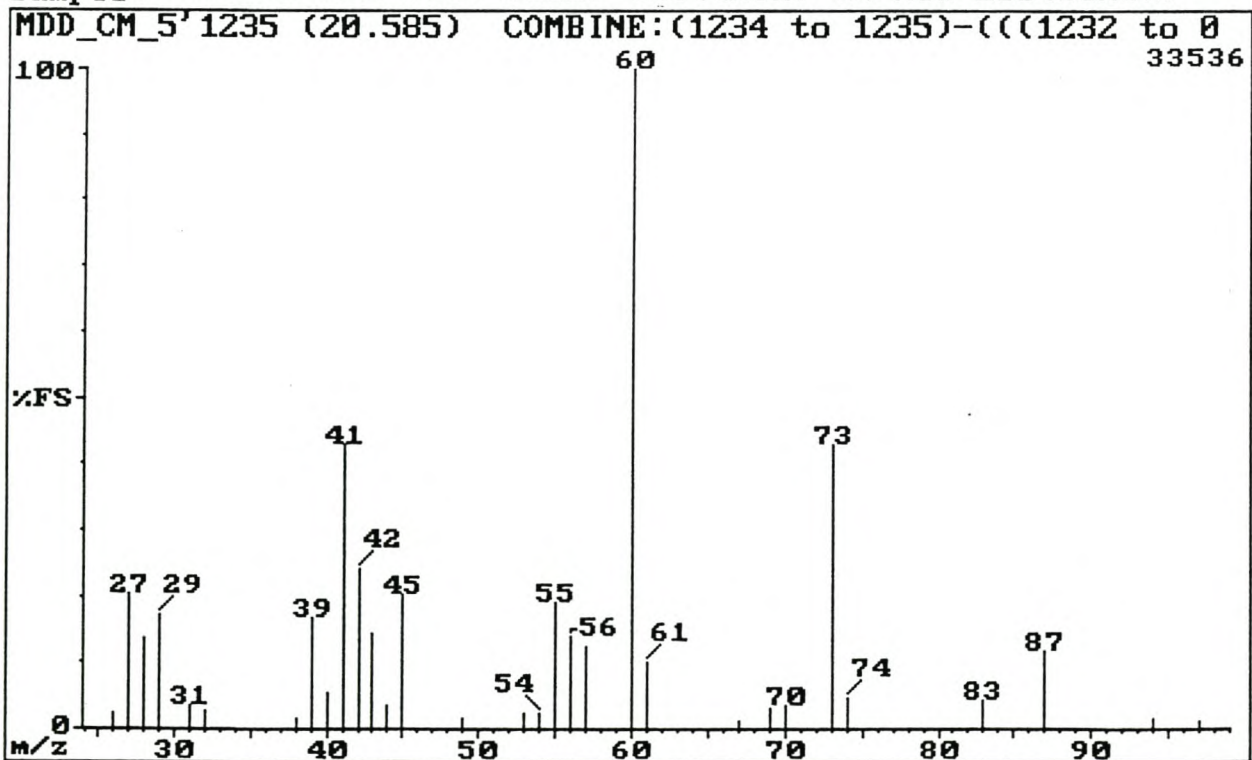


Fig. 3.80: El mass spectrum of component 1234 (hexanoic acid).

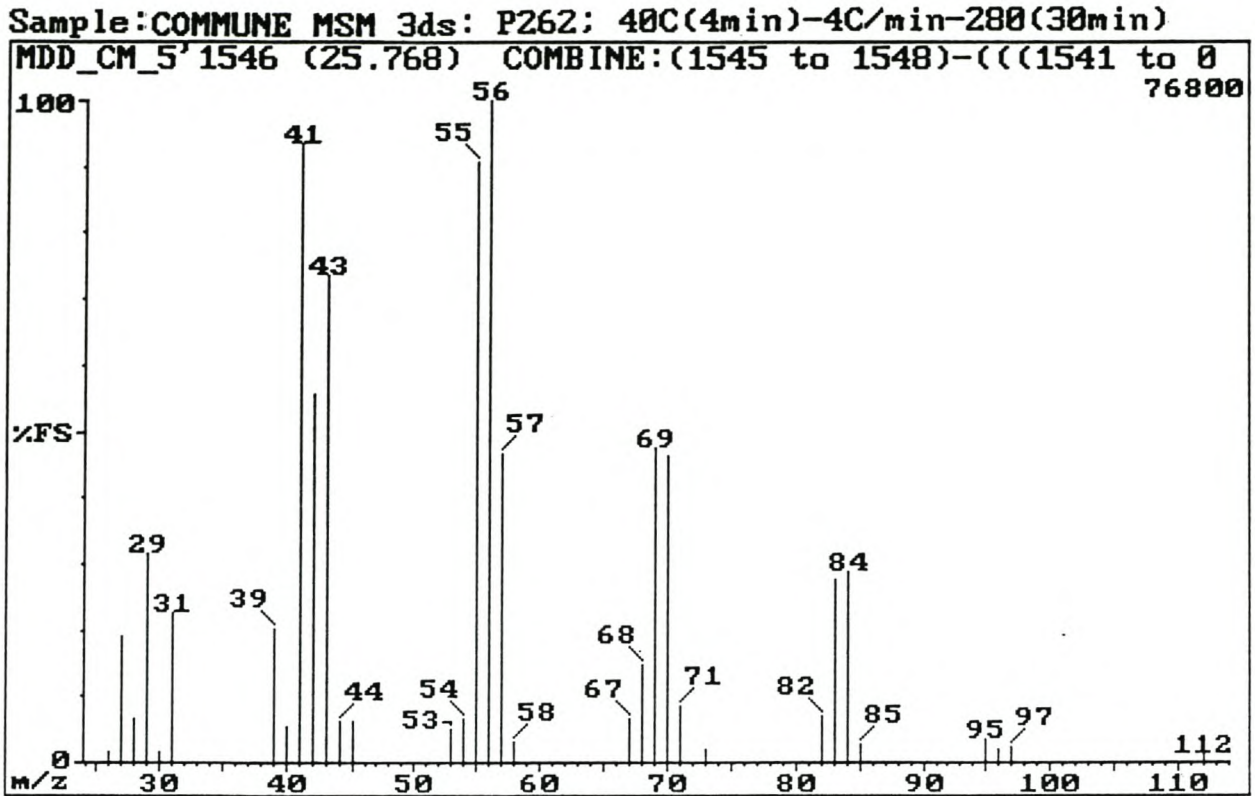


Fig. 3.81: El mass spectrum of component 1565 (heptanoic acid).

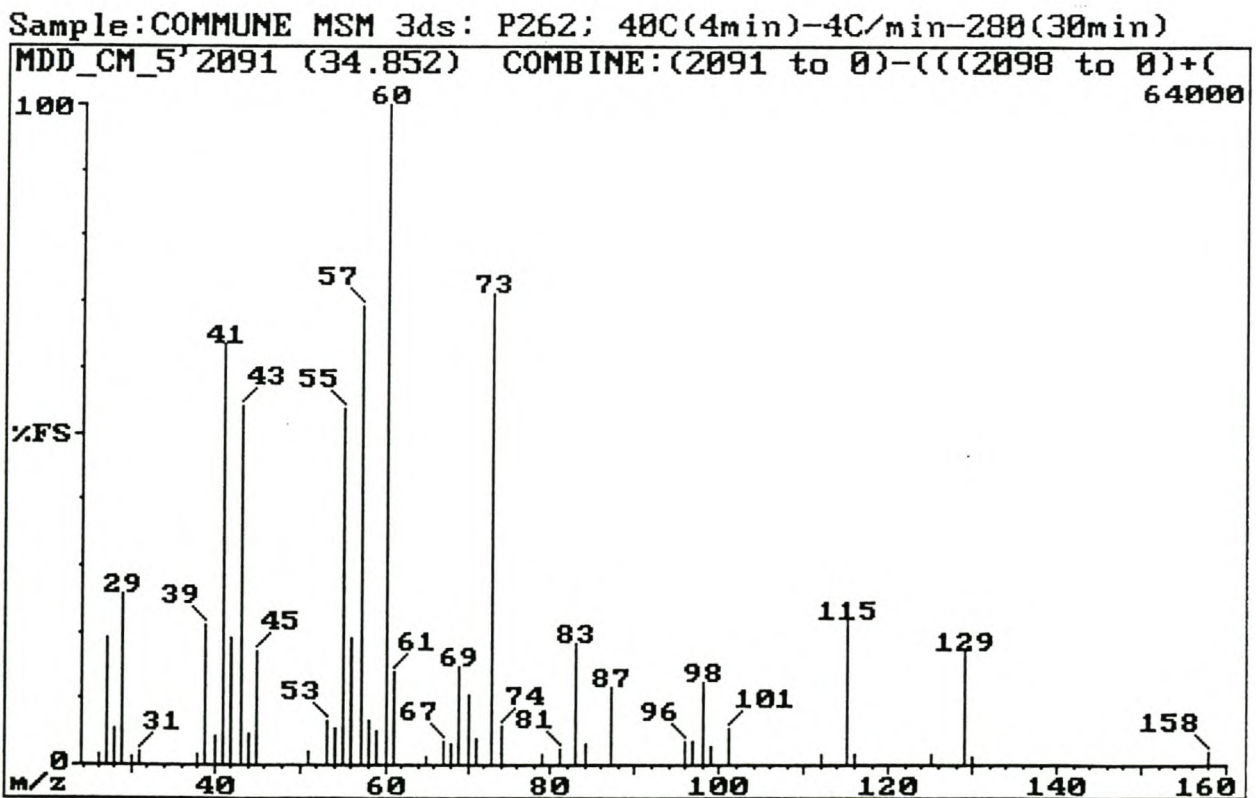


Fig. 3.82: El mass spectrum of component 2090 (nonanoic acid).

Sample: COMMUNE MSM 3ds: P262; 40C(4min)-4C/min-280(30min)

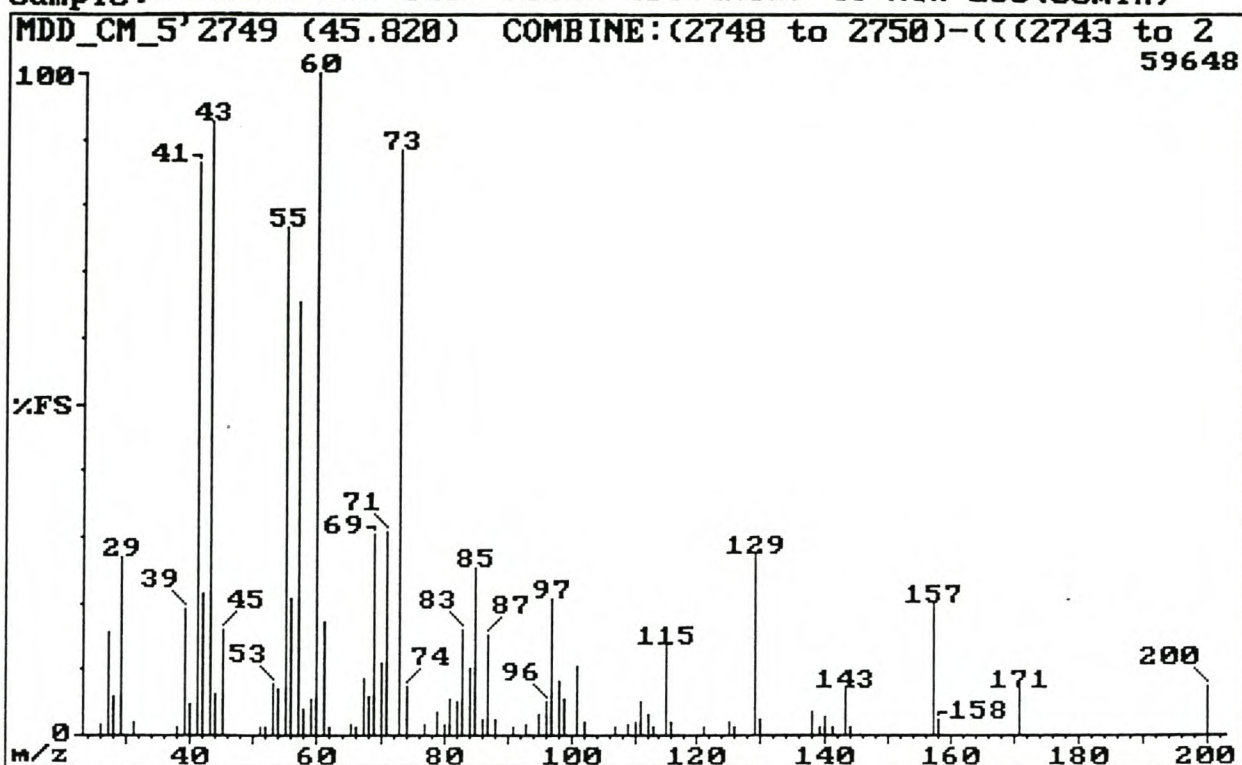


Fig. 3.83: EI mass spectrum of component 2750 (dodecanoic acid).

Sample: COMMUNE MSM 3ds: P262; 40C(4min)-4C/min-280(30min)

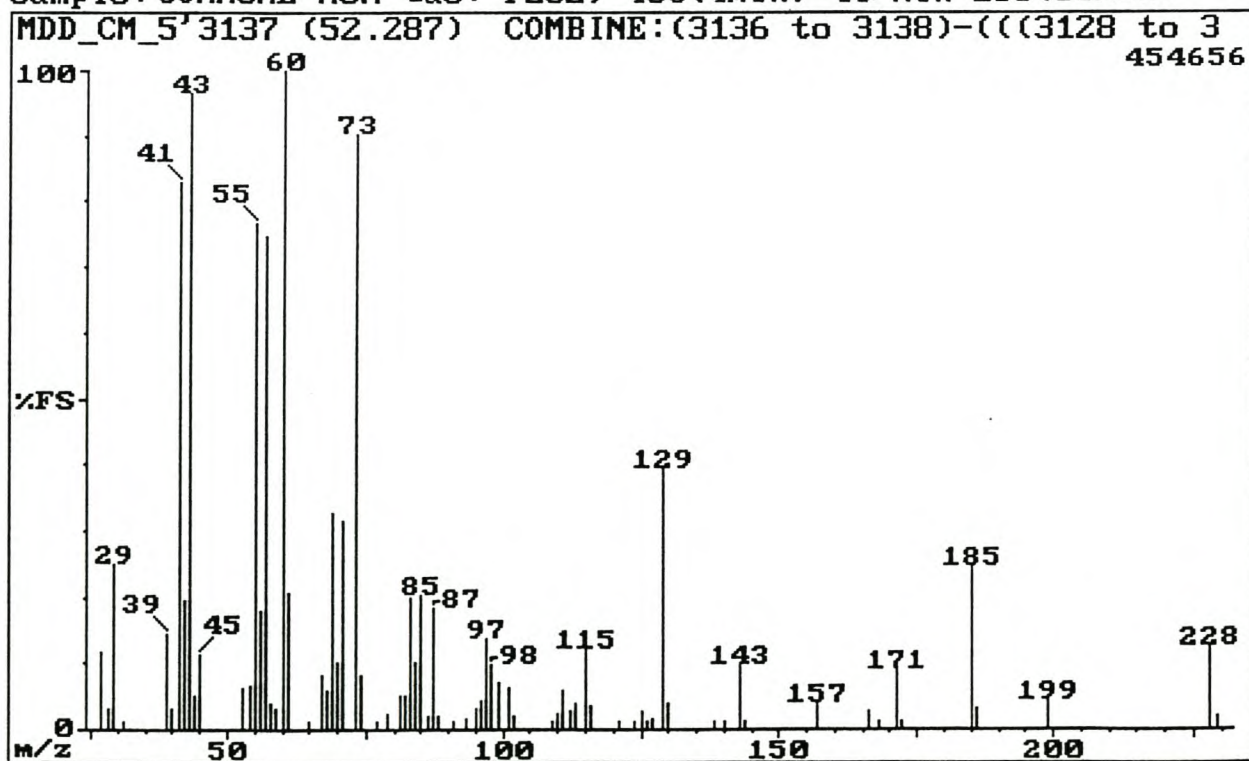


Fig. 3.84: EI mass spectrum of component 3137 (tetradecanoic acid).

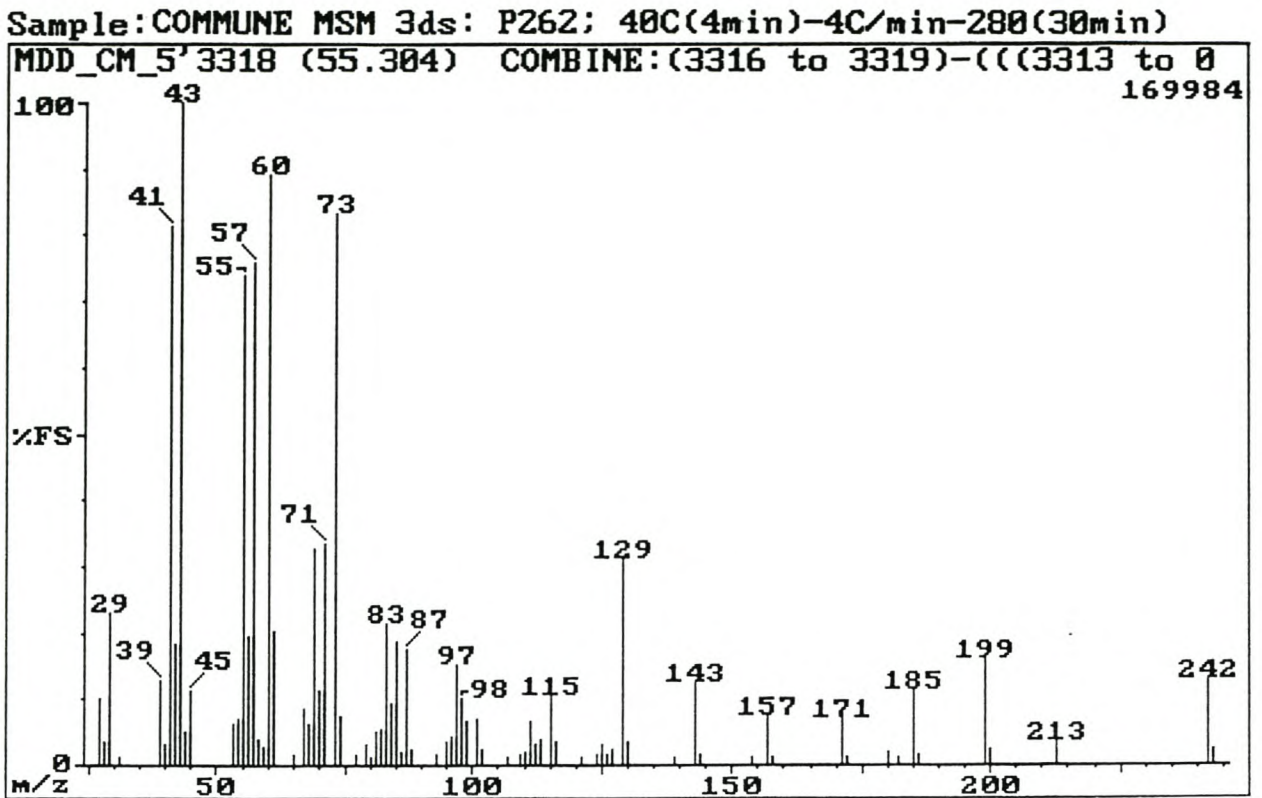


Fig. 3.85: EI mass spectrum of component 3317 (pentadecanoic acid).

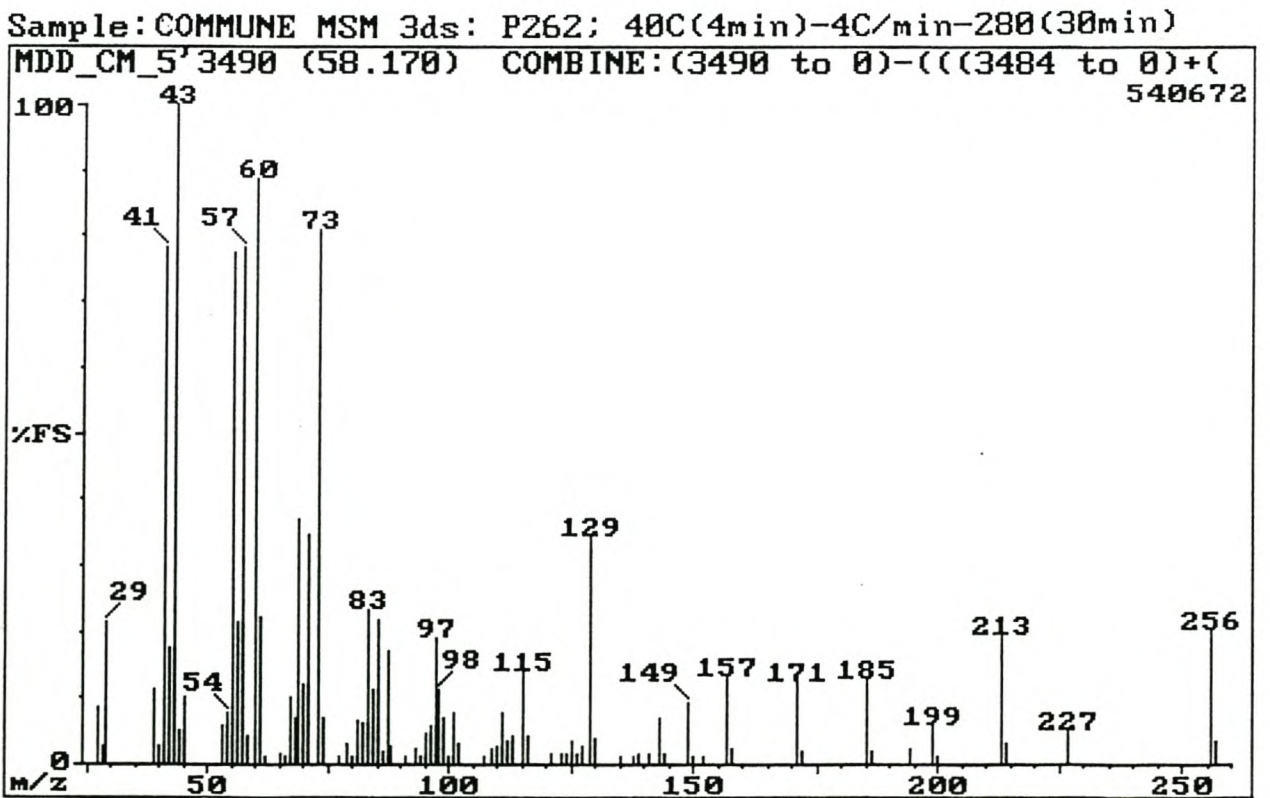


Fig. 3.86: EI mass spectrum of component 3495 (hexadecanoic acid).

Sample: COMMUNE MSM 3ds: P262; 40C(4min)-4C/min-280(30min)

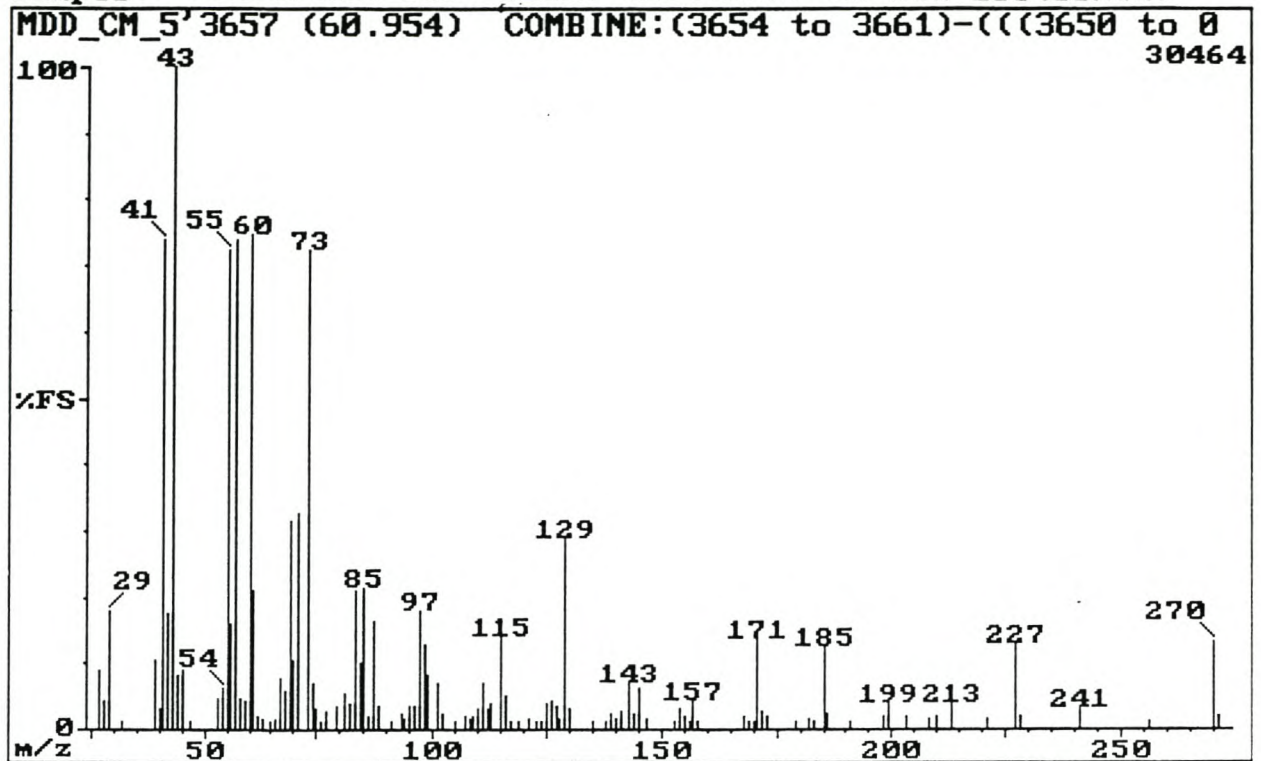


Fig. 3.87: El mass spectrum of component 3657 (heptadecanoic acid).

Sample: COMMUNE MSM 3ds: P262; 40C(4min)-4C/min-280(30min)

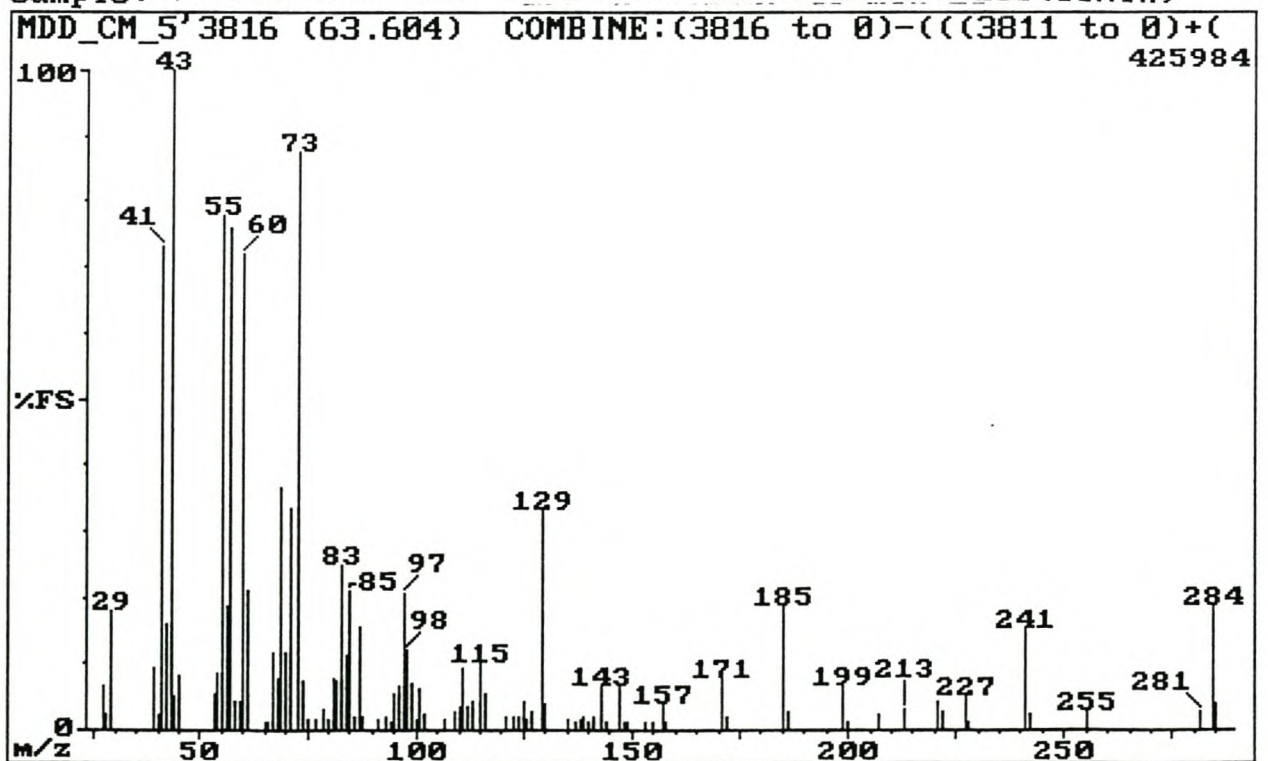


Fig. 3.88: El mass spectrum of component 3818 (octadecanoic acid).

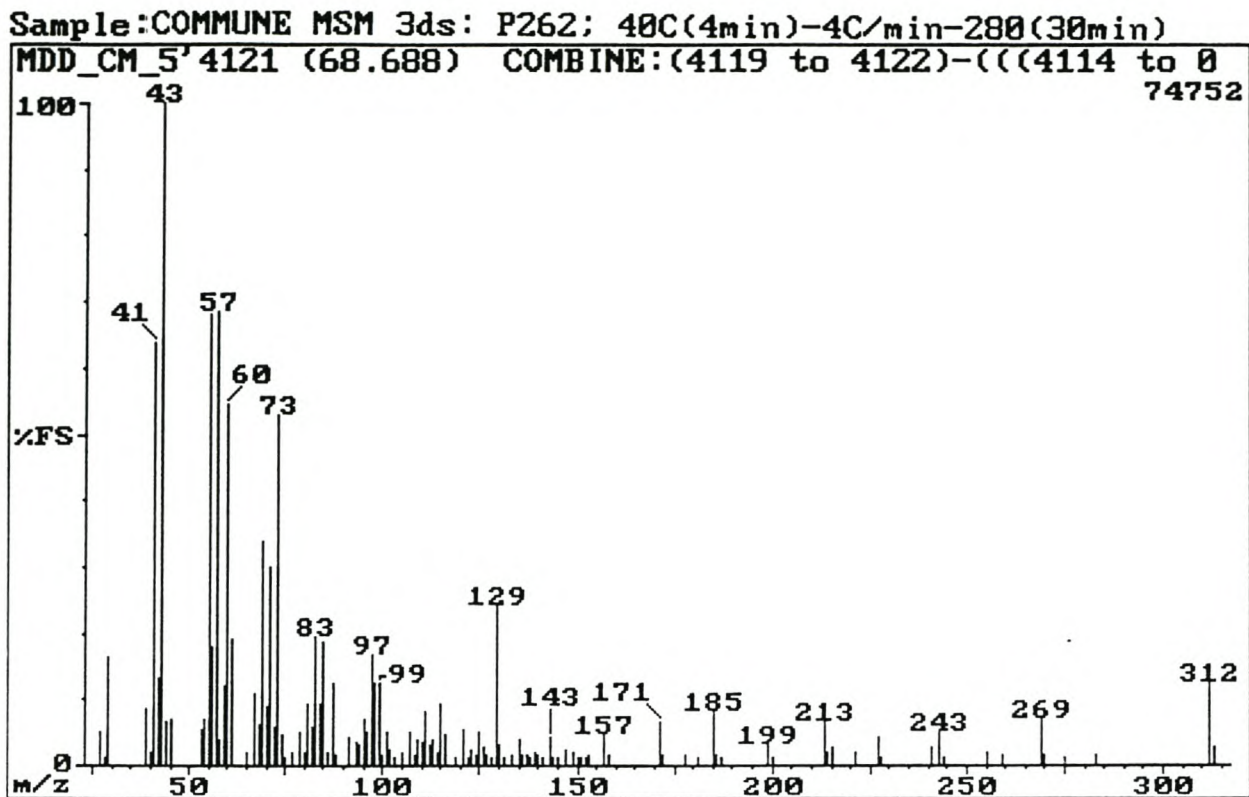


Fig. 3.89: El mass spectrum of component 4121 (eicosanoic acid).

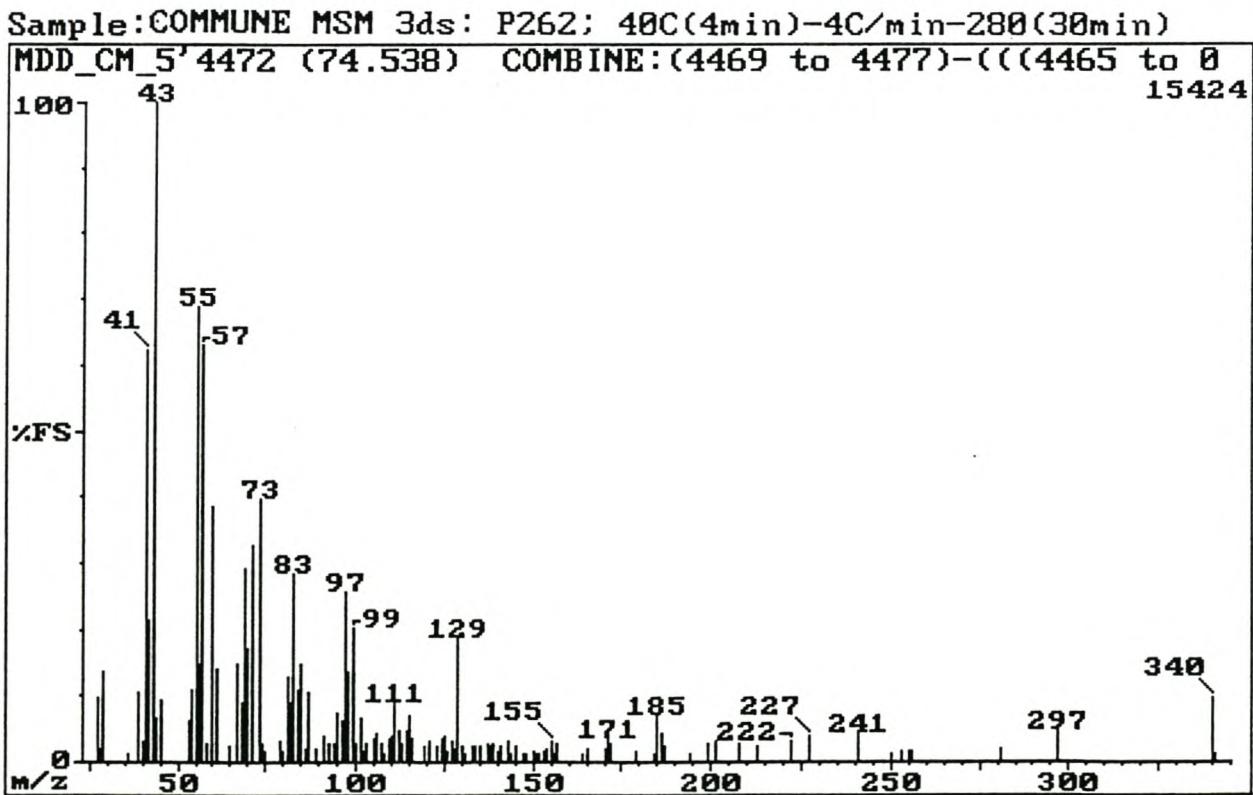


Fig. 3.90: El mass spectrum of component 4470 (docosanoic acid).

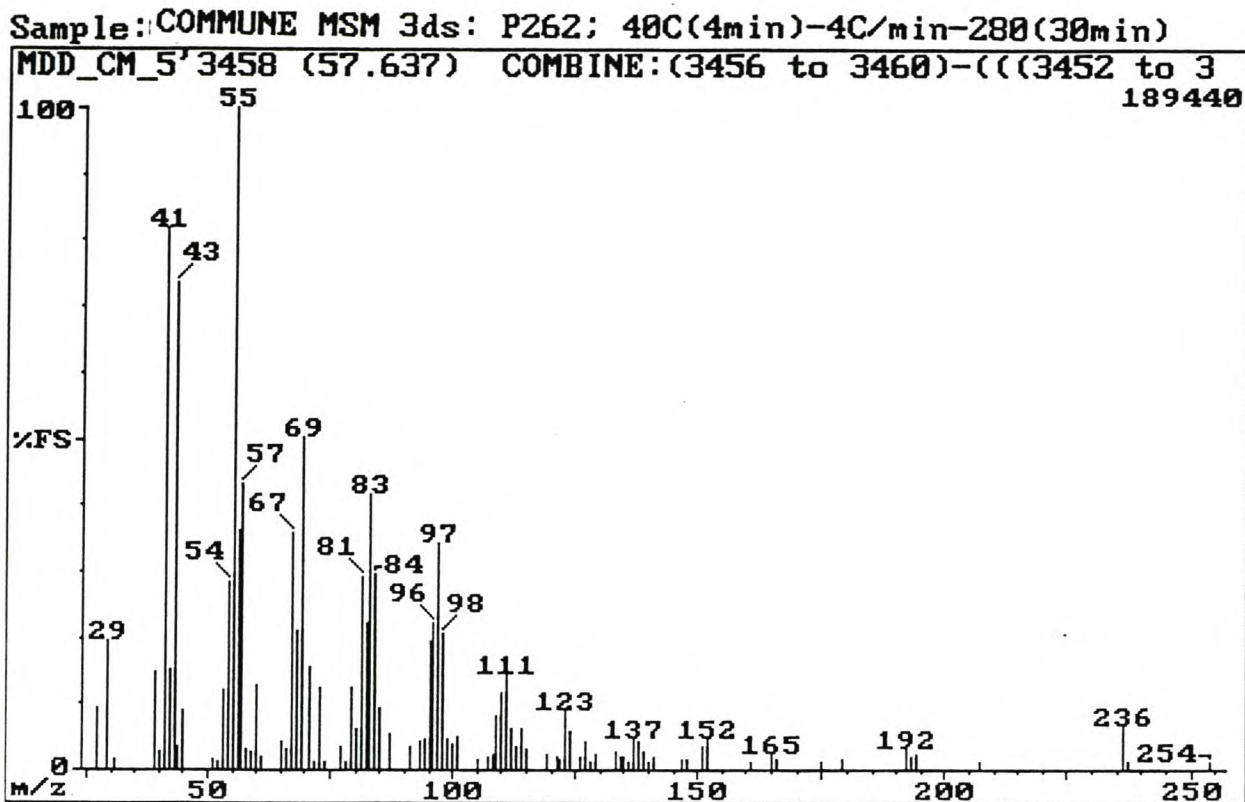


Fig. 3.91: El mass spectrum of component 3458 (9-hexadecenoic acid).

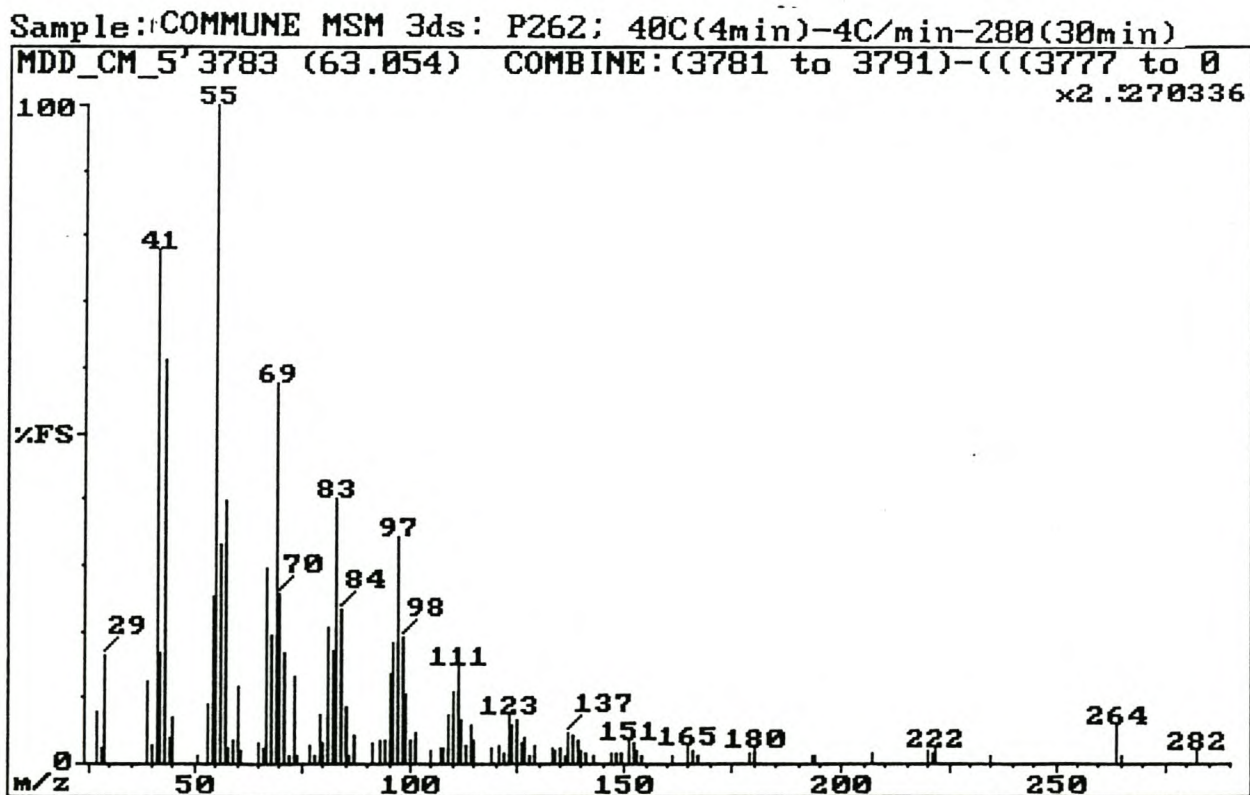


Fig. 3.92: El mass spectrum of component 3784 (9-octadecenoic acid).

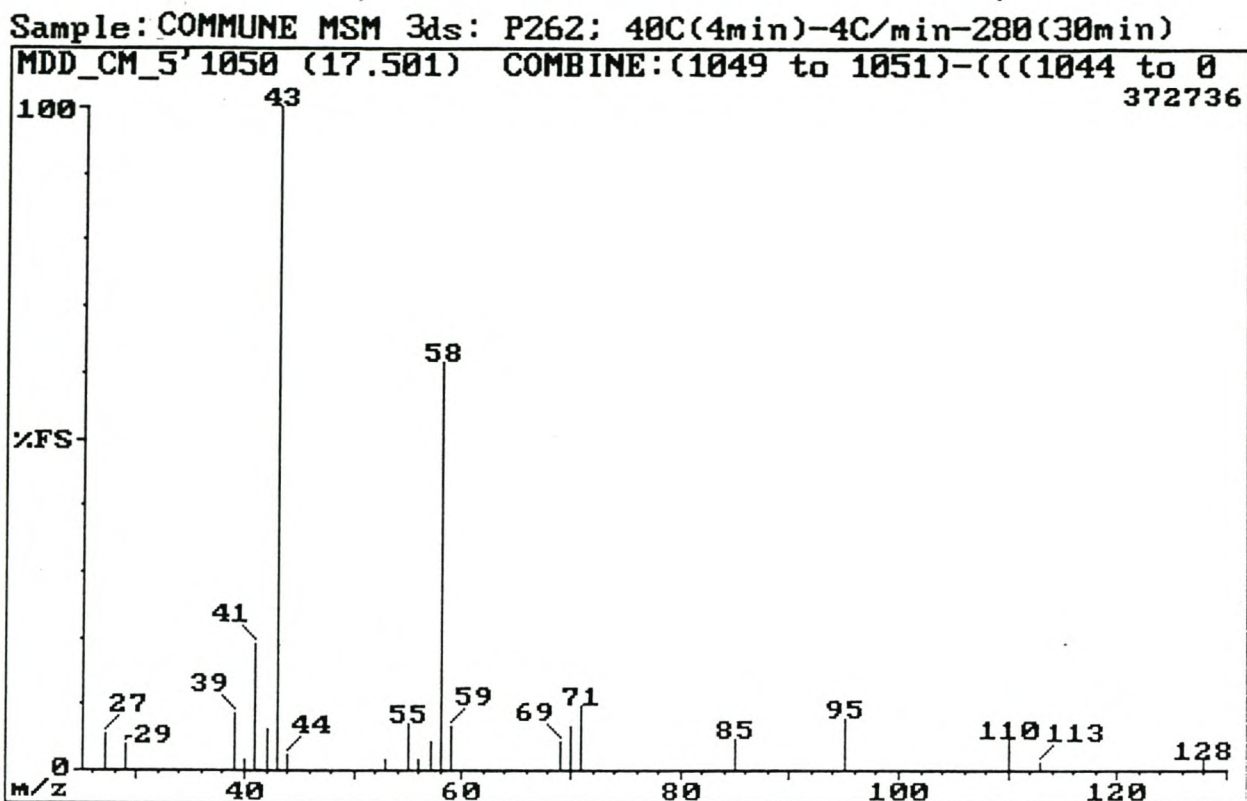


Fig. 3.93: El mass spectrum of component 1048 (6-methyl-2-heptanone).

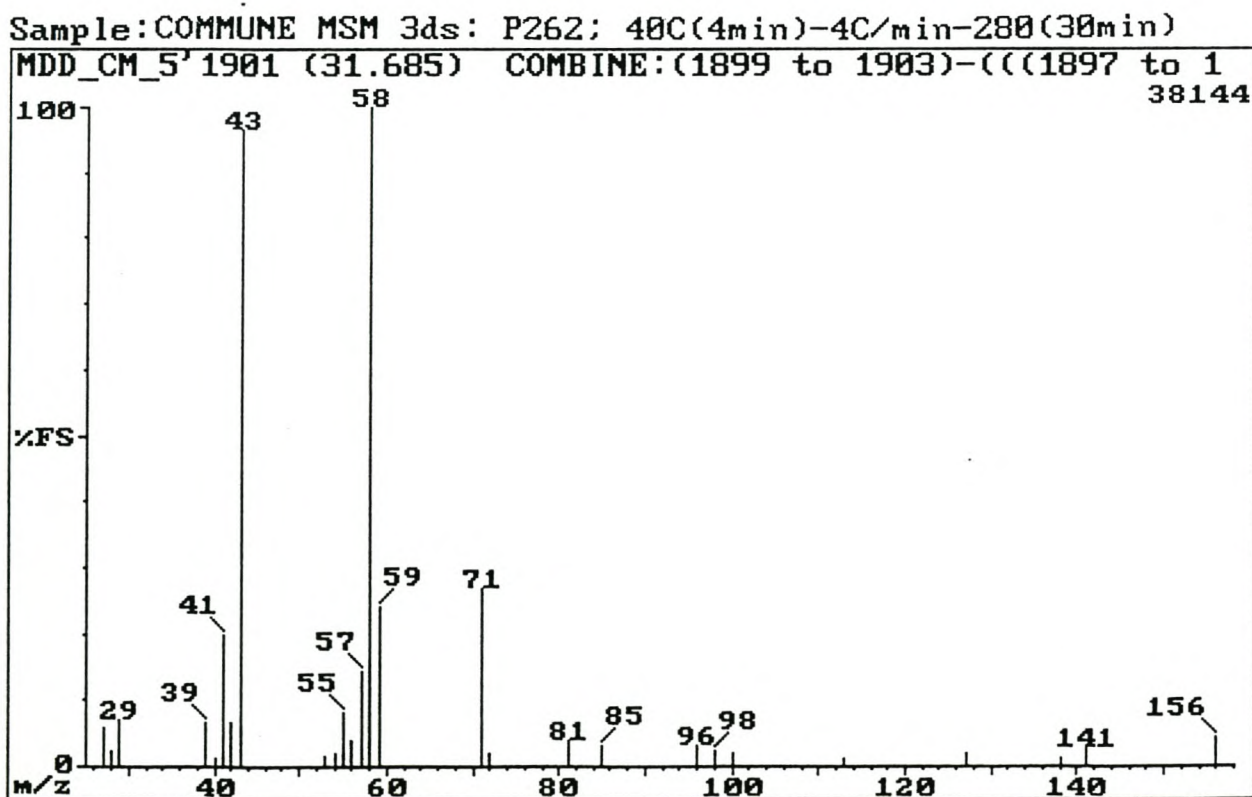


Fig. 3.94: El mass spectrum of component 1902 (2-decanone).

Sample: COMMUNE MSM 3ds: P262; 40C(4min)-4C/min-280(30min)

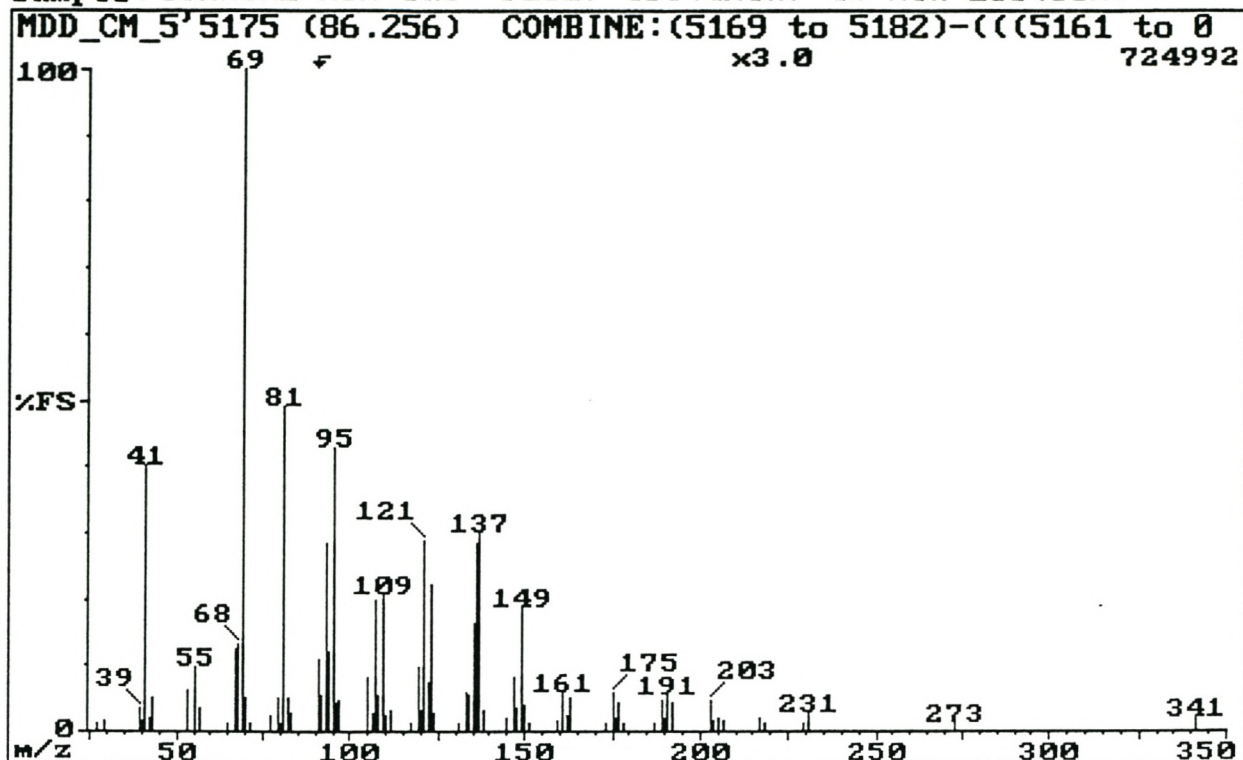


Fig. 3.95: EI mass spectrum of component 5172 (squalene).

References: Chapter 3

1. F.W. McLafferty and F. Tyreček, *Interpretation of mass spectra* (fourth edition), University Science Books, Sausalito, California (1993), pp. 240-246.
2. H. Budzikiewicz, C. Djerassi and D.H. Williams, *Mass spectrometry of organic compounds*, Holden-Day Inc., San Francisco, California (1967), p. 96.
3. Wiley registry of mass spectral data (sixth edition), John Wiley & Sons Inc. and The NIST mass spectral search program, Versions 1.5 and 2.
4. Ref. 2, p. 130.
5. Ref. 1, pp. 247-249.
6. Ref. 1, p. 132.
7. R.J. Liedtke and C. Djerassi, Mass spectrometry in structural and stereochemical problems. CLXXXIII. A study of the electron impact induced fragmentation of aliphatic aldehydes, *J. Am. Chem. Soc.* **91** (14), 6814 (1969).
8. A.G. Sharkey, Jr., J.L. Shultz and R.A. Friedel, Mass spectra of ketones, *Anal. Chem.* **28** (6), 934 (1956).
9. K. Christiansen, V. Mahadevan, C.V. Viswanathan and R.T. Holman, Mass spectrometry of long-chain aliphatic aldehydes, dimethyl acetals and alk-1-enyl ethers, *Lipids* **4** (6), 421 (1969).
10. Ref. 2, pp. 134-138.
11. Ref. 1, p. 247.
12. Ref. 2, p. 76-79.

13. T.A. Lee, *A beginner's guide to mass spectral interpretation*, John Wiley & Sons, New York (1998), p. 46.
14. Ref. 2, p. 162.
15. Ref. 2, p. 163.
16. S.F. Dyke, A.J. Floyd, M. Sainsbury and R.S. Theobald, *Organic Spectroscopy: An introduction*, Penguin, Baltimore (1971), pp. 190-191.
17. Ref. 2, p. 336.
18. Ref. 2, pp. 582-584.
19. Ref. 2, 569.
20. Ref. 2, 571 and 582-584.
21. Ref. 1, 239-241.
22. Ref. 1, 249.
23. Ref. 2, 131.
24. A.G. Harrison, The high-resolution mass spectra of aliphatic aldehydes, *Org. Mass. Spectrom.* **3**, 549 (1970).
25. Y.S. Shiekh, A.M. Duffield and C. Djerassi, Mass spectrometry in structural and stereochemical problems. CXCVIII: A study of the fragmentation process of some α,β -unsaturated aliphatic ketones, *Org. Mass. Spectrom.* **4**, 273 (1970).
26. Ref. 1, p. 145.
27. Ref. 2, p. 214.
28. Ref. 1, p. 142.

29. A. Maccoll, Low-energy, low-temperature mass spectra, *Org. Mass. Spectrom.* **23**, 381 (1988).
30. W-P Mo, *Olfactory communication: Chemical characterisation of the preorbital secretion of the oribi, Ourebia ourebi*, Ph. D. Thesis, Stellenbosch University (1994), p. 108.
31. G. Spiteller, *Interpretation of mass spectra obtained from natural sources, especially those of aliphatic compounds*, Course given at Stellenbosch University (1994), p. 24.
32. Ref. 1, p. 259.
33. M. le Roux, *Reuksintuiglike kommunikasie: Chemiese samestelling van eksokriene klierafskeidings van die bontebok (Damaliscus dorcas dorcas), springbok (Antidorcas marsupialis) en grysbok (Raphicerus melanotis)*, Ph. D. Thesis, Stellenbosch University (1980), p. 62.

CHAPTER 4

DISCUSSION AND COMPARISON OF RESULTS

4.1 COMPARISON OF THE RESULTS OBTAINED WITH DIFFERENT GROWTH MEDIA

As a first approach, tryptic soy broth (TSB), which consists of nitrogen and carbon sources, was chosen as medium for the incubation of the interdigital microbes, since it was considered to closely resemble the natural growth environment existing in the interdigital cavity. However, GC-MS analyses of the dichloromethane extracts of the microbial metabolites produced in and extracted from this medium were greatly complicated by the presence in the extracts of a large number of organic compounds which originated from the TSB medium itself, and which were present in relatively high concentrations in the extracts. The problem of these interfering 'background' peaks in the chromatograms, which rendered the metabolite peaks almost undetectable, was overcome by using the more selective minimal salts medium (MSM) with glucose as sole nutrient source.

It was therefore concluded that MSM was a more suitable medium for the study of volatile metabolites of interdigital micro-organisms than TSB and further studies with MSM as growth medium and various other nutrient sources are envisaged.

4.2 COMPARISON OF THE METABOLITE PROFILES PRODUCED BY THE INDIVIDUAL INTERDIGITAL MICRO-ORGANISMS AND BY THE TOTAL COMMUNITY OF MICRO-ORGANISMS

The results of the chemical characterisation of the metabolites isolated from each of the media that was inoculated and incubated for 3 days with the individual bacteria as well as with the total community, are used as reference data in the discussion in this section.

4.2.1 TSB as growth medium

Table 4.1: The volatile organic metabolites produced by the individual bacterial species and the total community of bacteria in TSB analysed after incubation for 3 days.

Compound		Micro-organism						
No.	Name	Community	R1.1	R1.2	R2.1	R3.1	R4.2	L2.2
1	1-butanol		+					
2	(R)-2-butanol		+				+	
3	3-methyl-1-butanol	+	+	+	+		+	
4	3-penten-2-ol		+	+			+	
5	2-methyl-3-buten-2-ol	+	+	+	+			
6	3-methyl-3-buten-2-ol	+						
7	2-butanone	+	+	+	+		+	+
8	3-hydroxy-2-butanone	+	+					
9	3-methyl-2-butanone	+						
10	2-pentanone				+			
11	4-methyl-2-pentanone		+					
12	3-methyl-2-pentanone	+	+					+

Table 4.1 continued:

Compound		Micro-organism						
No.	Name	Community	R1.1	R1.2	R2.1	R3.1	R4.2	L2.2
13	4-hydroxy-4-methyl-2-pentanone	+						
14	3-methyl-3-buten-2-one	+						
15	dimethyldisulphide			+	+			+
16	3-methylbutanal		+	+	+			
17	2-methylbutanal			+				
18	3-methyl-2-butenal	+						
19	2-methyl-2-butenal	+						
20	nonanal	+						
21	decanal	+						
22	pyrazine	+	+	+	+			+
23	methylpyrazine	+	+	+	+			+
24	ethylpyrazine	+	+					
25	2,3-dimethylpyrazine	+	+					
26	2,5-dimethylpyrazine	+	+	+	+	+	+	+
27	2-ethyl-5-methylpyrazine	+	+					
28	trimethylpyrazine				+			+
29	3-methylbutanoic acid		+			+		
30	2-methylbutanoic acid		+			+		
31	octanoic acid		+					
32	nonanoic acid		+					
33	tetradecanoic acid				+			+
34	hexadecanoic acid		+		+			
35	(Z)-9-octadecenoic acid		+		+			
36	octadecanoic acid		+		+			
37	ethylbenzene				+			+
38	benzaldehyde	+	+	+		+	+	+
39	2-hydroxybenzaldehyde	+						
40	benzoic acid		+				+	

Table 4.1 continued:

Compound		Micro-organism						
No.	Name	Community	R1.1	R1.2	R2.1	R3.1	R4.2	L2.2
41	phenylacetic acid		+				+	
42	phenylacetamide	+	+				+	
43	acetophenone	+	+					
44	1-phenyl-2-propanone	+						
45	phenylmethanol		+			+	+	
46	2-phenylethanol	+			+	+	+	+
47	p-cresol					+		

In general (see Table 4.1) it appears that the total community of bacteria have a unique metabolite profile of volatile organic compounds in comparison to the individual species of bacteria (isolates). With certain exceptions, bacteria do not exist by themselves in a natural environment, therefore interaction between bacteria is unavoidable. This would suggest that the results obtained with the total community should be more significant than those obtained with the respective isolates. The differences in the profiles are visualised in the form of the histogram in Figure 4.1 for TSB.

The most notable difference between the total community of bacteria and the individual species of bacteria is the lack of any organic acids in the profile of the metabolites produced by the total community. Another difference is that aldehydes were only produced by the total community of bacteria.

In the profile of the micro-organism labelled R1.1, a wide variety of organic compounds was found. When the profile of R1.1 is compared to that of the total community, it becomes apparent that many of the compounds produced by R1.1 do not occur in the profile of the total community. A possible explanation could be that R1.1 is inhibited by the other micro-organisms present in the total

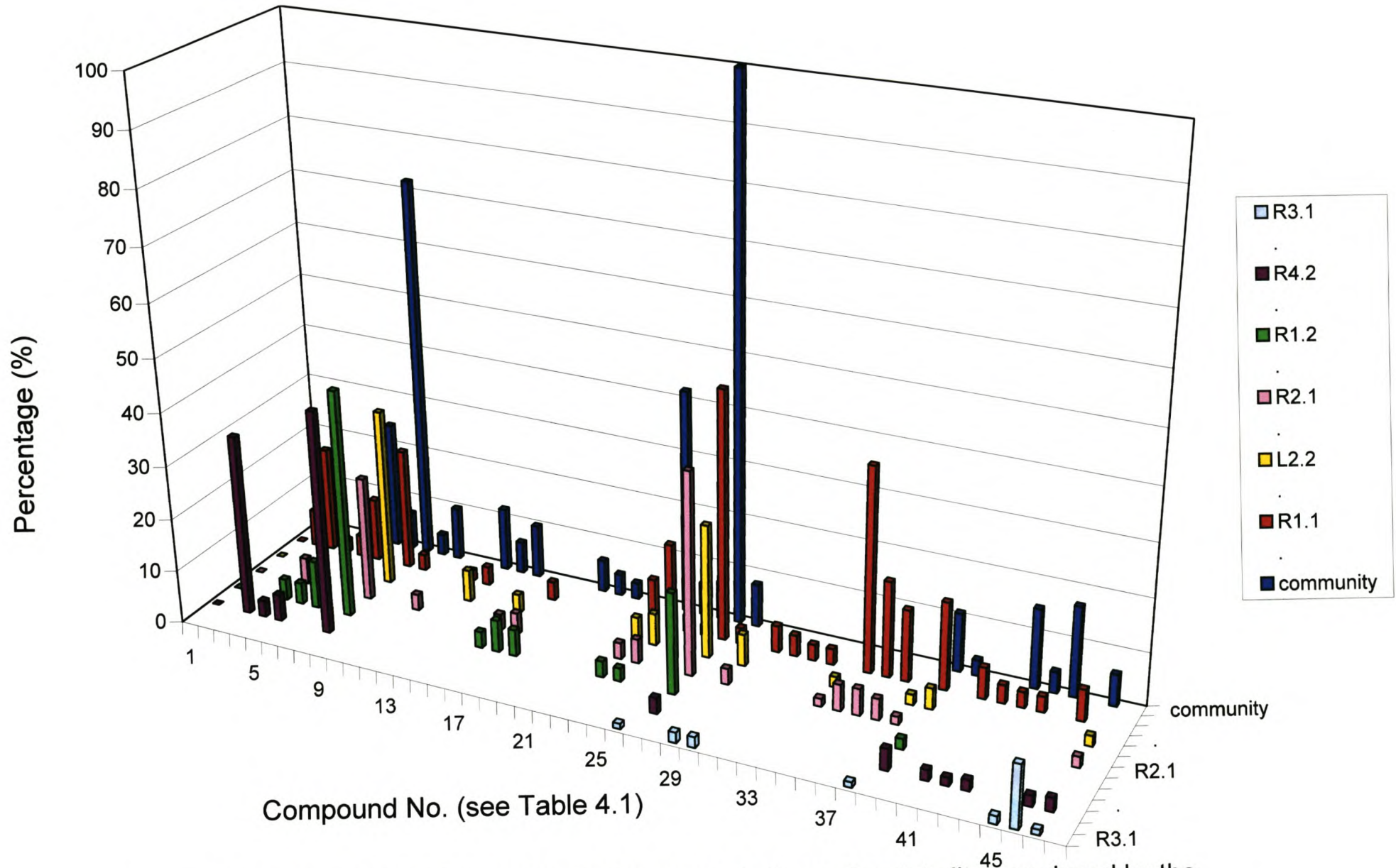


Fig. 4.1 Graphic presentation of the relative concentrations of metabolites produced by the individual species of bacteria and the total community of bacteria in TSB.

community. This was confirmed by anti-microbial tests, which showed that R1.1 is partially inhibited by in the presence of all the other isolates¹. None of the other micro-organisms exhibited any anti-microbial effects with regard to the other. It is also possible that the compounds produced by R 1.1 were metabolised by other members of the community, because quite often these compounds were also produced by other isolates (for example, compounds numbered 16, 34-36, 40, 42 and 45).

4.2.2 MSM as growth medium and glucose as carbon source

From Table 4.2 it is clear that the isolates do not grow well by themselves in MSM plus glucose, although it has to be noted that all the bacteria did show visible growth in their respective vessels. In the cases of the micro-organisms labelled R3.1, R4.2 and L2.2, no metabolites, of those that were analysed in this study, were observed at all. The absence of metabolites could be due to the likelihood that the isolates do not produce these metabolites in the first place, but rather convert glucose to biomass (cell growth) and carbon dioxide.

Table 4.2: The volatile organic metabolites produced by the individual bacterium species and the total community of bacteria in MSM, with glucose as carbon source, analysed after incubation for 3 days.

Compound		Micro-organism						
No.	Name	Community	R1.1	R1.2	R2.1	R3.1	R4.2	L2.2
1	1-octanol	+						
2	2-methyl-3-buten-2-ol			+				
3	3-methyl-3-buten-2-ol			+				
4	3-methyl-1-butanol			+				
5	3-methyl-2-butanone				+			
6	3-methyl-3-buten-2-one			+				
7	6-methyl-2-heptanone	+						
8	2-decanone	+						
9	octanal	+						
10	nonanal	+						
11	decanal	+						
12	undecanal	+						
13	dodecanal	+						
14	tridecanal	+						
15	tetradecanal	+						
16	(Z)-2-heptenal	+						
17	2-nonenal	+						
18	(Z)-2-decenal	+						
19	2-undecenal	+						
20	hexanoic acid	+						
21	heptanoic acid	+						
22	nonanoic acid	+						
23	dodecanoic acid	+						
24	tetradecanoic acid	+		+	+			
25	pentadecanoic acid	+						
26	9-hexadecenoic acid	+						

Table 4.2 continued:

Compound		Micro-organism						
No.	Name	Community	R1.1	R1.2	R2.1	R3.1	R4.2	L2.2
27	hexadecanoic acid	+		+	+			
28	heptadecanoic acid	+						
29	9-octadecenoic acid	+						
30	octadecanoic acid	+						
31	eicosanoic acid	+						
32	docasanoic acid	+						
33	benzaldehyde	+						
34	squalene	+						
35	cholesterol		+					

An important feature observed in MSM is that the metabolic ability of the community is much greater than that of the individual species (see Table 4.2 and Fig. 4.2). In the case of MSM it can be clearly seen that virtually all of the metabolites, with the exception of a few alcohols, are produced in a communal setting.

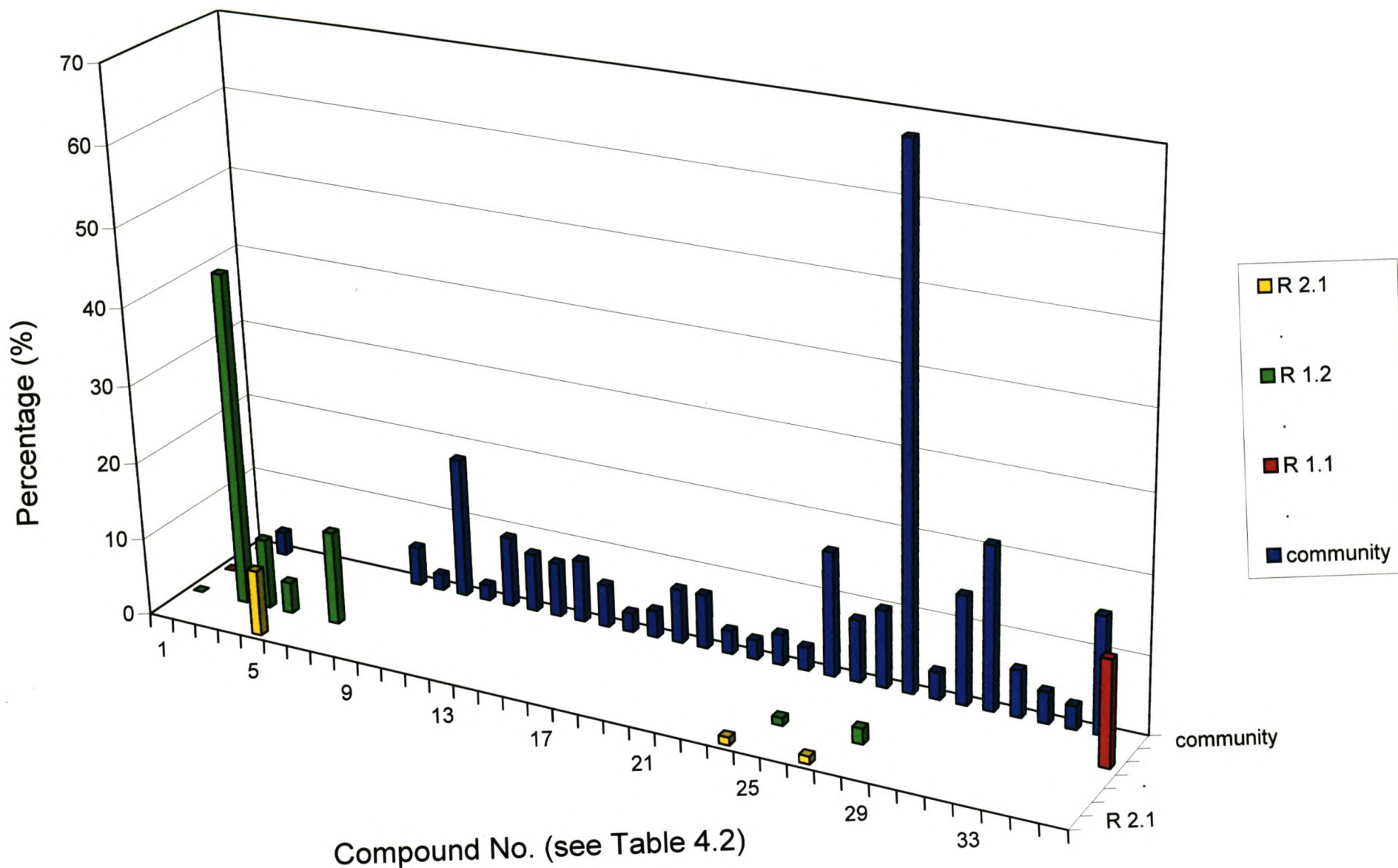


Fig. 4.2 Graphic presentation of the relative concentrations of metabolites produced by the individual species of bacteria and the total community of bacteria in MSM.

4.3 COMPARISON OF THE COMPOUNDS PRESENT IN THE INTERDIGITAL GLAND SECRETION AND THE METABOLITES PRODUCED BY THE TOTAL COMMUNITY OF MICRO-ORGANISMS (IN TSB AND MSM)

For the discussion in this section, the results reported in Chapter 3 for the total bacterial community in TSB (Fig. 3.1, Table 3.2) and in MSM (Fig. 3.2, Table 3.3) are used as reference. These results are compared with those obtained in a previous study of the chemical composition of the interdigital secretion of the bontebok². In order to make a direct comparison of results possible, only the corresponding compounds in the interdigital secretion and in the total community of bacteria in MSM have been presented (Table 4.3) for easier visual comparison. It was found that total community of bacteria incubated in TSB only had one compound, which corresponded to the interdigital secretion and as a result it was not included in Table 4.3.

Table 4.3: The volatile compounds identified in both the interdigital secretion and in the total microbial community in MSM medium supplemented with glucose as carbon source.

Compound
2-heptenal
hexanoic acid
octanal
heptanoic acid
(E)-2-nonenal
dodecanoic acid
tetradecanoic acid
pentadecanoic acid
(Z)-9-hexadecanoic acid
hexadecanoic acid
heptadecanoic acid
(Z)-9-octadecanoic acid
squalene

A large number of compounds found in the extract of the metabolites produced in MSM plus glucose, have also previously been identified in the interdigital secretion of the bontebok. These were mainly carboxylic acids, but also included a number of aldehydes.

The chemical composition of the TSB metabolite extract differs from that of the MSM extract and also from that of the interdigital secretion, with the exception of 3-methyl-2-butanone, which is a compound also identified in the interdigital secretion. The TSB extract was found to contain a number of pyrazines. These compounds were not observed in the MSM metabolite extracts and have also not been observed in previous interdigital microbial studies³ in which other microbial selective media, with only carbon sources, were employed.

Three substituted pyridines have, however, been identified in the interdental secretion. The presence of these nitrogen-containing compounds in the TSB metabolite extract could be attributed to the fact that this medium contains nitrogen sources that can be converted into pyridines by the micro-organisms.

References: Chapter 4

1. L.J. Farr, *The possible influence bacterial interactions have on the composition of the interdigital gland exudates of the bontebok, Damaliscus dorcas dorcas*, BSc. honours symposium report, Stellenbosch University (2002), pp. 1-12.
2. A.E. Nell, *Reuksintuiglike Kommunikasie: Chemiese Karakterisering van die Bontebok, Damaliscus dorcas dorcas en die Blesbok, Damaliscus dorcas phillipsi*, Ph. D. Thesis, Stellenbosch University (1992)., pp. 163-169
3. Ref. 2, pp. 183-192.

CHAPTER 5

EXPERIMENTAL

5.1 GENERAL

All Pyrex glassware used in the preparation and handling of biological material, microbiological samples and extracts were heated to 500°C in an annealing oven to remove trace amounts of organic matter that cannot be removed by conventional methods. Dichloromethane (Riedel-de Haën, Pestanal®) was used for extraction purposes and all syringes were cleaned using this solvent.

5.2 INSTRUMENTATION

Electron impact (EI) mass spectra were recorded at 70 eV on a Carlo Erba QMD 1000 gas chromatograph-mass spectrometer (GC-MS quadropole system) with VG Analytical Lab-Base software. The gas chromatograph was equipped with a Grob split-splitless injector and a 40 m × 0.25 mm glass capillary column coated with a 0.25 µm layer of PS 089, manufactured by the Laboratory for Ecological Chemistry, University of Stellenbosch. All analyses were done with helium as the carrier gas at a linear velocity of 38 cm per second at a column temperature of 40°C. The injector temperature was 220°C and samples were injected in the split mode and analytes thermally focussed at 30°C. Samples (1 µl) were analysed using a temperature program of 4°C per minute from 40-280°C (hold for 30 min).

An interface temperature of 250°C was used. The ion source temperature was set at 180°C and the pressure in the source was approximately 1×10^{-3} mbar at a column temperature of 40°C, decreasing to approximately 5×10^{-4}

mbar towards the end of the temperature programme. A scan rate of 0.9 scan per second, with an interval of 0.1 seconds between scans, was employed.

5.3 SAMPLING OF BIOLOGICAL MATERIAL

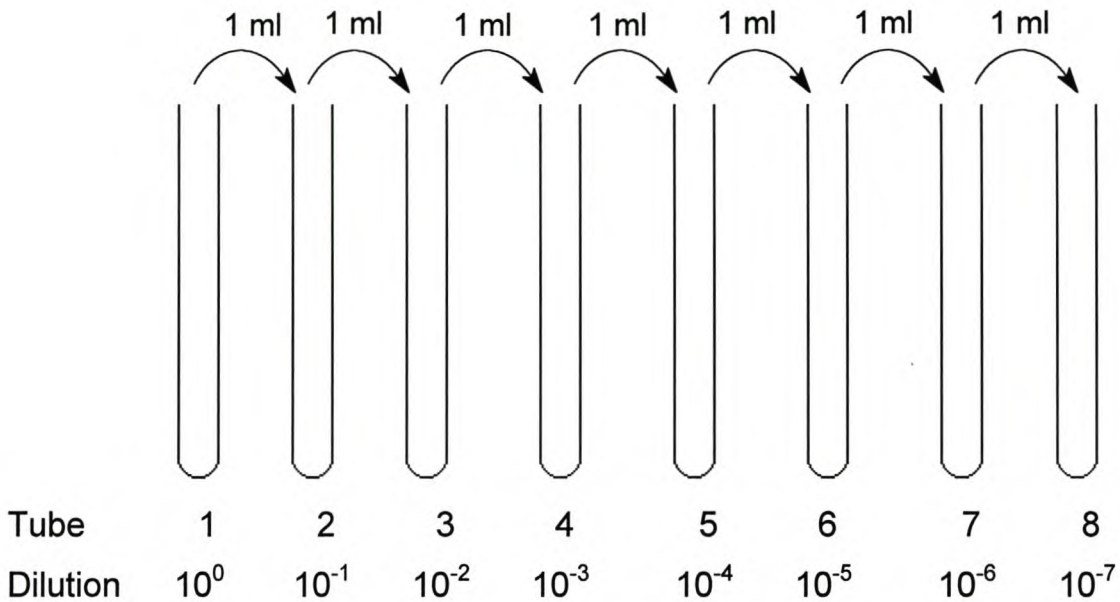
Interdigital secretions were collected from bontebok at two sites in the Western Cape, namely at Somchem in Somerset West (on the property of AE & CI) and the Tygerberg Zoo.

Interdigital secretions were collected from male bontebok with 150 cm sealed sterile swabs (Copan). Two samples were taken from each interdigital gland and one from the ground, close to the where the animal had been immobilised. The swab seals were broken moments before the samples were taken and inserted into the interdigital cavity. A twisting motion¹ coupled with forward and backward motion was employed to ensure thorough transfer of the secretion onto the swab. After the swab was sufficiently loaded with biological material, it was inserted into its original sterile closure and appropriately labelled. Samples were incubated, enriched and micro-organisms isolated.

5.4 ISOLATION OF MICRO-ORGANISMS AND INOCULATION OF MICRO-ORGANISMS INTO LIQUID BROTHS

The collected samples were placed in separate test tubes, each containing sterilised Ringer solution (first tube containing 10 ml and the rest 9 ml each) and mixed with a vortex mixer to release microbes from the swabs into the solution¹. One millilitre of this solution was transferred by pipette to another test tube containing 9 ml of Ringer solution (as shown below). From the diluted solution, another millilitre was transferred to the next test tube

containing 9 ml of solution. This process of dilution was repeated to obtain a dilution series from 10^0 to 10^{-7} .



A volume of 100 μ l of the contents of each of the test tubes was plated out onto different media, using the pour-plate technique, to determine which growth media would be ideal for the organism². The media used to determine the necessary growth conditions were Tryptic Soy Agar (TSA), R2A, MRS and MacConkey. A blank test tube only containing Ringer solution was streaked out, as a control to ensure that contamination of the sample did not occur. These plated samples were allowed to incubate overnight at room temperature under aerobic conditions³. All the isolates exhibited sufficient growth when grown on either TSA or R2A.

Each colony that grew and was observed to be visibly different was considered an individual microbial species. The respective microbial colonies were streaked out onto an agar plate using the streak-plate technique¹. These plates were then incubated and purified microbial colonies were obtained³.

Once sufficient enrichment of the purified microbes had been obtained, the different organisms were inoculated into a specific broth and incubated with stirring.

5.5 ISOLATION OF MICROBIAL METABOLITES

5.5.1 Incubation in tryptic soy broth (TSB) media

The TSB medium was sterilised by autoclaving it in the container that was to be used for incubation⁴. The individual microbes as well as the combined community were incubated at 30°C in 1%, 10% and full strength TSB (no agar was added, see Table 5.1) for three days, 10 days and 30 days, after which the metabolites were extracted from the broth with dichloromethane. It is important to note that the composition of TSB is largely dependent on the commercial source.

Table 5.1 Ingredients of tryptic soy broth¹

Ingredients	Concentration (g/l)
Tryptic (pancreatic digest of casein)	17
Peptone	3
Glucose	2.5
Sodium chloride	5
Dipotassium phosphate	2.5

Samples (100 ml) of the respective microbe-containing broths were centrifuged in a conical sample bottle (Fig 5.1) at 2500 rpm. The conical vessel was specifically fabricated for this purpose in order to concentrate the bacteria in the broth in the form of a pellet in the bottom of the cone, thus achieving an effective separation of the micro-organisms from the broth. The supernatant, containing the metabolites, was decanted into a separating funnel (250 ml) and the metabolites were extracted with dichloromethane (three 0.33 ml portions). The supernatant was carefully run off and collected in

a 2 ml screw-capped vial to ensure complete separation of the aqueous and organic layers. GC-MS analysis of the extracts showed that the metabolites were present in extremely low concentrations and all extracts were subsequently concentrated, by allowing the dichloromethane to evaporate at room temperature to approximately 1 μ l. The concentrated samples (1 μ l) were then subjected to GC-MS analysis.

5.5.2 Incubation in minimal salts medium (MSM) with glucose as the carbon source

Two solutions containing the ingredients shown in Table 5.2 were autoclaved separately, then cooled and pooled. The carbon source (0.5% m/V of glucose) was added to solution A before autoclaving. The microbes were subjected to the same growth conditions (duration and temperature) and extracted as described for the experiments with TSB as medium.

Table 5.2 Ingredients of minimal salt medium

Solution A	
Ingredients	Concentration (g/l)
NaCl	2
NH ₄ Cl	1
MgSO ₄ ·7H ₂ O	0.12
EDTA	5
CaCl ₂	0.0015
FeSO ₄ ·7H ₂ O	0.001
MnSO ₄ ·2H ₂ O	0.00035
Na ₂ MoO ₄ ·2H ₂ O	

Solution B	
Ingredients	Concentration (g/l)
Na ₂ HPO ₄	4.24
KH ₂ PO ₄	2.7

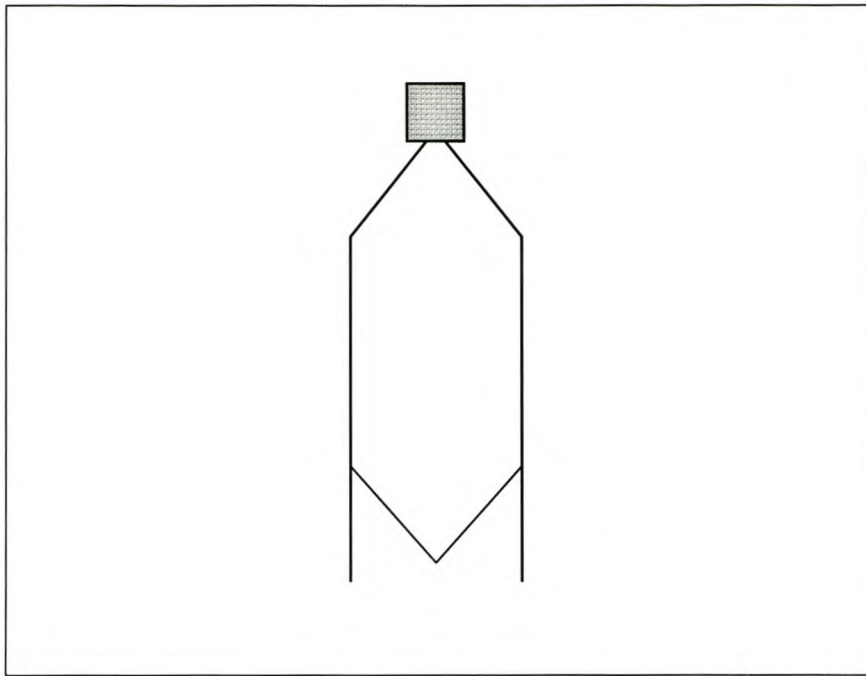


Fig. 5.1 The schematic representation of the glass container utilised to centrifuge the bacterium suspension.

5.6 DETERMINATION OF THE GROWTH CURVES

All of the preparation and sampling of each individual micro-organism was performed in a laminar flow cabinet under sterile conditions. The medium utilised for the determination of the growth curve was MSM with 0.1% glucose as nutrient source.

The containers required for the measurement of the growth was autoclaved (121°C at 15 PSI) prior to commencing with the determination of the growth curve. The containers required was a volumetric cylinder (200 ml), seven Erlenmeyer flasks (100 ml), 14 test tubes, 5 ml and 1 ml tips for Ependorff[®] pipette and Solutions A and B of MSM.

The MSM (5 ml) was pipetted into the test tubes and allowed to stand overnight to ensure that the growth of any contaminants would be excluded. Each individual microbe was inoculated in a separate test tube and again

left overnight. To ensure that the inadvertent introduction of a contaminant would not jeopardise the experiment, the inoculations were performed in duplicate. On the same day MSM (100 ml) was poured into the Erlenmeyer flasks and left overnight. After sufficient growth of microbes had occurred in the respective test tubes, the overnight cultures were inoculated (100 μ l, diluted 100 fold) into separate Erlenmeyer flasks and incubated on a stirrer at 30°C.

Samples (1 ml) were taken from each flask periodically (every hour) and pipetted into separate polyethylene cuvettes. An ultra violet/visible (UV/Vis.) spectrophotometer was utilised to determine the optical density, which is directly proportional to the growth that had taken place in the flasks⁵. The optical density (at 600 nm) of each cuvette was measured and the measurement recorded (see example in Section 2.2 in Table 2.1).

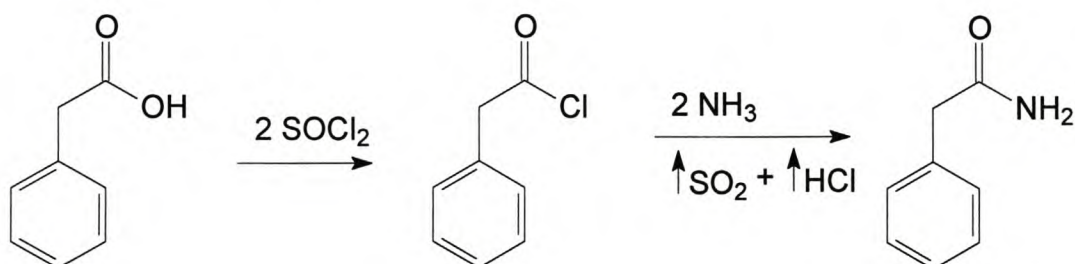
After 36 hours, several of the bacteria were only entering the logarithmic (log) phase of the growth curve, whilst the remainder of the microbes did not yet enter the log phase. Therefore, the method of performing the experiment had to be revised. Because all of the organisms grew very slowly, it was decided to start the measurement of optical densities 20 hours after inoculation and to repeat the measurements every hour until the microbes entered the stationary phase.

5.7 SYNTHESIS OF REFERENCE COMPOUNDS

All the chemicals used for synthetic work were obtained from Aldrich Chemical Co., Sigma Chemical Co. or Riedel-de Haën Co. or Saarchem Co. and the syntheses were performed in fume cupboard.

5.7.1 Preparation of phenylacetamide

Phenylacetamide was prepared from phenylacetic acid according to the following reaction scheme:



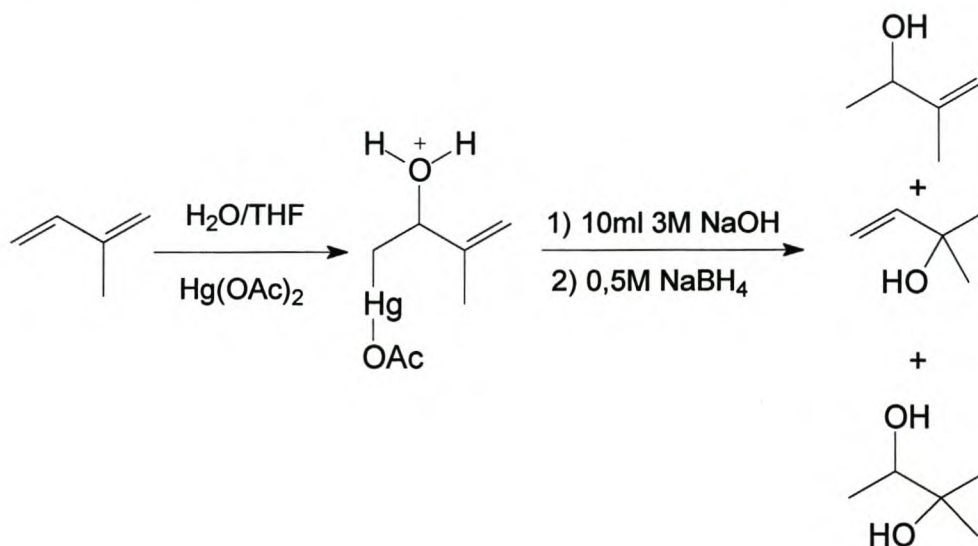
Thionyl chloride (1,07 ml, 1.7g, 14,2 mmol) was slowly added to magnetically stirred phenylacetic acid (1 g, 7.34 mmol) in a round-bottomed flask in an oil bath at 90°C⁶. The reaction mixture was refluxed for 30 minutes. The resulting phenylacetyl chloride was added cautiously poured into an excess (125 ml) of ice cold 3M ammonia solution in a beaker (600 ml)⁷. The reaction mixture was allowed to stand for 15 minutes, after which the solid material was filtered off under suction on a sintered-glass filter and spread out on filter paper to dry. Phenylacetamide (0.72 g, mp. 155-159°C) was obtained in a yield of 72%.

5.7.2 Preparation of 3-methyl-3-buten-2-ol

If suitable experimental conditions are used the oxymercuration-demercuration of dienes with one mole of mercuric acetate per mole could provide a convenient method for the Markovnikov monohydration of one of the two double bonds of some dienes^{8,9}, although certain by-products such as diols as well as some unchanged diene can be expected. Furthermore, the hydroboration-oxidation provides a convenient method for the anti-

Markovnikov hydration of the carbon-carbon double bonds in olefins and dienes.

Isoprene (1,36 g, 20 mmol) was added to a round-bottomed flask (250 ml) containing water (10 ml) and tetrahydrofuran (THF, 20 ml). The reaction was allowed to proceed at room temperature, as very little success was achieved at 0°C. Mercuric acetate (6.38 g, 20 mmol) was added to the contents of the flask and the mixture was stirred for 3 hours. After 3 hours sodium hydroxide (10 ml, 3,0 M solution) was added to the reaction mixture, followed by the rapid addition of sodium borohydride (10 ml, 0,5 M solution of NaBH₄ in 3,0 M NaOH). The reaction mixture was stirred for 30 minutes and then the aqueous phase was saturated with potassium carbonate. This caused the water-soluble THF to form a supernatant layer containing the organic material. The THF layer was separated from the saturated water/carbonate layer, dried over anhydrous magnesium sulphate and analysed by GC-MS.

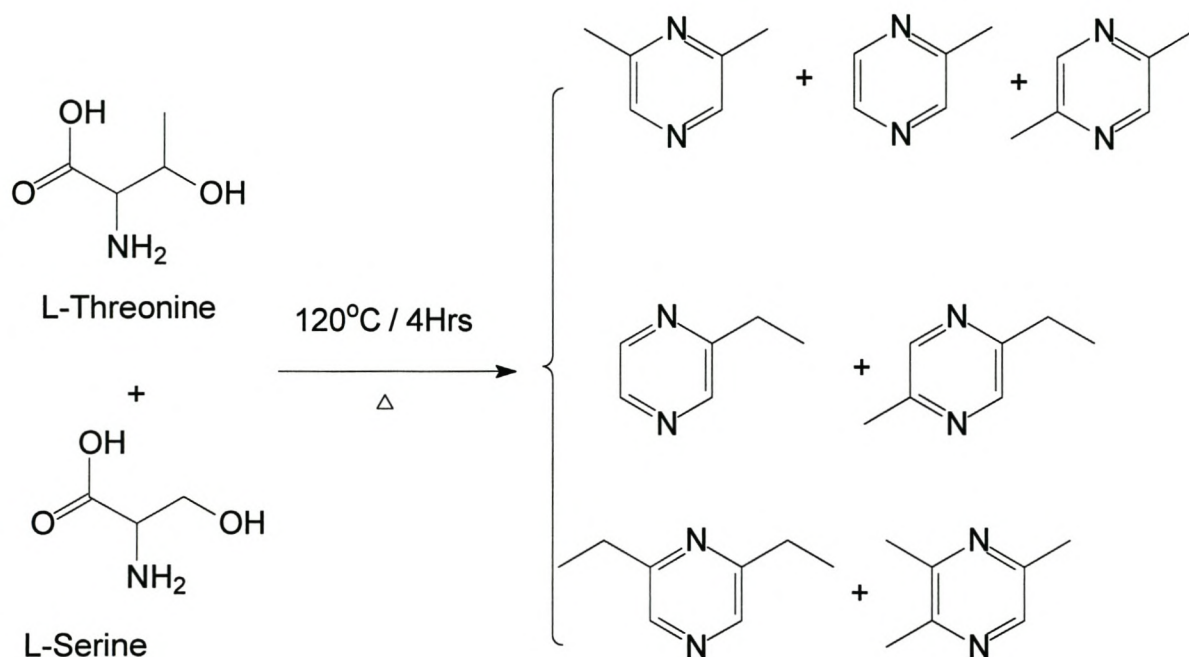


5.7.3 Preparation of alkylpyrazines

A small volume of water (36 μl) was added to mixture of L-serine (150 g) and L-threonine (150 g) in a round-bottomed flask, the flask was sealed gas-tight and the reaction mixture was heated in an oven at 120°C for four

hours¹⁰. The reaction mixture was allowed to cool down to room temperature and the solid material of the flask was extracted with four portions (5 ml) of dichloromethane. The combined extracts were analysed by GC-MS.

The formation of various pyrazines from the two amino acids can be rationalised as follows:



References: Chapter 5

1. L.M. Prescott, J.P. Harley and D.A. Klein, *Microbiology* (fourth edition), McGraw-Hill, New York (1999), pp. 105-110.
2. Ref. 1, pp. 123-132.
3. L.J. Farr, *The possible influence bacterial interactions have on the composition of the interdigital gland exudates of the bontebok, Damaliscus dorcas dorcas*, BSc. honours symposium, Stellenbosch University (2002), pp. 1-12.
4. Ref. 1, pp. 139-141.
5. Ref. 1, pp. 114-117.
6. B.S. Furniss, A.J. Hannaford, P.W.G. Smith and A.R. Tatchell, *Vogel's textbook of practical organic chemistry* (fifth edition), Longman Scientific & Technical, Harlow, England (1989), pp. 692-693 and 1073
7. Ref. 9, pp. 1261-1262.
8. H.C. Brown, P.J. Geoghegan, Jr., G.J. Lynch and J.T. Kurek, Solvomercuration-demercuration. IV. The monohydration of representative dienes *via* oxymercuration-demercuration, *J. Org. Chem.* **37** (12), 1941 (1972).
9. H.C. Brown and W.J. Hammer, The oxymercuration-demercuration of representative olefins. A convenient, mild procedure for the Markovnikov hydration of the carbon-carbon double bond, *J. Am. Chem. Soc.* **89** (6), 1522 (1967).
10. Chi-Kuen Shu, Pyrazine formation from serine and threonine, *J. Agric. Food Chem.* **47**, 4332 (1999).

ADDENDUM A

Table 3.4: Volatile metabolites identified in the microbial extract of the total microbial community in TSB (3 days).

In TIC Fig 3.3	Compound
561	3-hydroxy-3-methyl-2-butanone
572	4-penten-2ol
607	benzaldehyde
2127	tetradecanoic acid
2349	9-hexadecenoic acid
2371	hexadecanoic acid
2573	(Z,Z)-9,12-octadecadienoic acid
2575	(Z)-9-octadecenoic acid
2580	octadecanoic acid
3600	eicosanoic acid

Table 3.5: Volatile metabolites identified in the microbial extract of the total microbial community in TSB (10 days).

In TIC Fig 3.4	Compound
462	3-methyl-2-pentanone
587	methyl-pyrazine
759	2,6-dimethyl-pyrazine
1497	phenyl ethyl alcohol
2522	dodecanoic acid
2911	tetradecanoic acid
3234	9-hexadecenoic acid
3265	hexadecanoic acid
3548	(Z,Z)-9,12-octadecadienoic acid
3558	9-octadecenoic acid
3593	octadecanoic acid
3920	eicosanoic acid

Table 3.6: Volatile metabolites identified in the microbial extract of micro-organism R1.1 in TSB (3 days).

In TIC Fig. 3.5	Compound
245	2-butanone
251	(R)-2-butanol
263	2-methyl-3-buten-2-ol
313	3-methyl-butanal
327	1-butanol
358	3-penten-2-ol
384	3-hydroxy-2-butanone
427	pyrazine
437	3-methyl-1-butanol
445	4-methyl-2-pentanone
469	3-methyl-2-pentanone
594	methylpyrazine
633	3-methyl-butanoic acid
653	2-methyl-butanoic acid
767	2,5-dimethylpyrazine
776	ethylpyrazine
783	2,3-dimethylpyrazine
867	benzaldehyde
947	2-ethyl-5-methylpyrazine
1009	benzenemethanol
1071	acetophenone
1236	benzoic acid
1247	octanoic acid
1380	phenyl-acetic acid
1412	nonanoic acid
2374	hexadecanoic acid
2583	(Z)-9-octadecenoic acid
2608	octadecanoic acid

Table 3.7: Volatile metabolites identified in the microbial extract of micro-organism R1.1 in TSB (10 days).

In TIC Fig. 3.6	Compound
928	2,5-dimethyl-pyrazine
2665	tridecanoic acid
2911	tetradecanoic acid

Table 3.8: Volatile metabolites identified in the microbial extract of micro-organism R1.1 in TSB (30 days).

In TIC Fig. 3.7	Compound
416	pyrazine
458	3-methyl-2-pentanone
594	methyl-pyrazine
803	2,6-dimethyl-pyrazine
2247	N-(2-phenylethyl)-acetamide
2460	(Z)-9-hexadecenoic acid
2745	tetradecanoic acid
3090	hexadecanoic acid
3387	9-octadecenoic acid
3421	octadecanoic acid

Table 3.9: Volatile metabolites identified in the microbial extract of micro-organism R1.2 in TSB (3 days).

In TIC Fig. 3.8	Compound
311	3-methyl-butanal
324	2-methyl-butanal
431	3-methyl-1-butanol
453	dimethyl disulphide
590	methyl-pyrazine
759	2,5-dimethyl-pyrazine
859	benzaldehyde
940	2-ethyl-5-methylpyrazine

Table 3.10: Volatile metabolites identified in the microbial extract of micro-organism R1.2 in TSB (10 days).

In TIC Fig. 3.9	Compound
347	3-methyl-butanone
479	pyrazine
500	4-methyl-2-pentanone
515	dimethyl disulphide
529	3-methyl-2-pentanone
694	methyl-pyrazine
819	ethylbenzene
929	2,5-dimethylpyrazine
954	2,3-dimethylpyrazine
1069	benzaldehyde
1177	trimethylpyrazine
1530	2-phenylethanol
2183	phenylacetamide
2848	tetradecanoic acid

Table 3.11: Volatile metabolites identified in the microbial extract of micro-organism R1.2 in TSB (30 days).

In TIC Fig. 3.10	Compound
653	3-methyl-2-pentanone
858	methyl-pyrazine
1002	ethylbenzene
1132	2,6-dimethyl-pyrazine
1283	benzaldehyde
1410	trimethylpyrazine
3510	hexadecanoic acid
3801	(Z)-9-octadecenoic acid
3830	octadecanoic acid

Table 3.12: Volatile metabolites identified in the microbial extract of micro-organism R2.1 in TSB (3 days).

In TIC Fig. 3.11	Compound
247	2-butanone
266	2-methyl-3-buten-2-ol
315	3-methyl-butanal
361	2-pentanone
430	pyrazine
439	3-methyl-1-butanol
461	dimethyl disulphide
596	methyl-pyrazine
688	ethylbenzene
768	2,5-dimethyl-pyrazine
950	2-ethyl-5-methyl-pyrazine
1173	2-phenylethanol
2132	tetradecanoic acid
2373	hexadecanoic acid
2585	9-octadecenoic acid
2610	octadecanoic acid

Table 3.13: Volatile metabolites identified in the microbial extract of micro-organism R2.1 in TSB (10 days).

In TIC Fig. 3.12	Compound
1507	2-phenylethanol
2172	benzeneacetamide

Table 3.14: Volatile metabolites identified in the microbial extract of micro-organism R2.1 in TSB (30 days).

In TIC Fig. 3.13	Compound
402	3-methyl-2-butanone
649	3-methyl-2-pentanone
996	ethylbenzene
1023	o-xylene
1094	p-xylene
1129	2,5-dimethyl-pyrazine
1274	benzaldehyde
2132	nonanoic acid

Table 3.15: Volatile metabolites identified in the microbial extract of micro-organism R3.1 in TSB (3 days).

In TIC Fig. 3.14	Compound
625	3-methylbutanoic acid
646	2-methylbutanoic acid
768	2,5-dimethylpyrazine
867	benzaldehyde
1008	benzyl alcohol
1083	p-cresol
1161	2-phenylethanol

Table 3.16: Volatile metabolites identified in the microbial extract of micro-organism R3.1 in TSB (10 days).

In TIC Fig. 3.15	Compound
474	pyrazine
509	dimethyl disulphide
525	3-methyl-2-pentanone
689	methylpyrazine
926	2,5-dimethylpyrazine
1065	benzaldehyde
1184	trimethyl-pyrazine
2648	tridecanoic acid
2908	tetradecanoic acid
3022	pentadecanoic acid
3261	hexadecanoic acid
3551	9-octadecenoic acid
3587	octadecanoic acid

Table 3.17: Volatile metabolites identified in the microbial extract of micro-organism R3.1 in TSB (30 days).

In TIC Fig. 3.16	Compound
470	pyrazine
509	dimethyl-disulphide
525	3-methyl-2-pentanone
686	methyl-pyrazine
926	2,5-dimethyl-pyrazine
1065	benzaldehyde
1184	trimethyl-pyrazine
3261	hexadecanoic acid
3587	octadecanoic acid

Table 3.18: Volatile metabolites identified in the microbial extract of micro-organism R4.2 in TSB (3 days).

In TIC Fig. 3.17	Compound
249	2-butanol
358	3-penten-2-ol
436	3-methyl-1-butanol
769	2,5-dimethylpyrazine
870	benzaldehyde
1023	benzenemethanol
1173	2-phenylethanol
1251	benzoic acid
1402	phenylacetic acid
1633	phenylacetamide

Table 3.19: Volatile metabolites identified in the microbial extract of micro-organism R4.2 in TSB (10 days).

In TIC Fig. 3.18	Compound
254	2-butanone
471	pyrazine
509	dimethyl disulphide
525	3-methyl-2-pentanone
687	methyl-pyrazine
926	2,5-dimethyl-pyrazine
1183	trimethyl-pyrazine

Table 3.20: Volatile metabolites identified in the microbial extract of micro-organism R4.2 in TSB (30 days).

In TIC Fig. 3.19	Compound
280	2-butanone
629	dimethyl disulphide
653	3-methyl-pentanone
580	pyrazine
855	methyl-pyrazine
1131	2,5-dimethyl-pyrazine
1155	2,3-dimethyl-pyrazine
1282	benzaldehyde
1408	trimethyl-pyrazine
1727	benzene-ethanol
1754	1-phenyl-2-propanone
1963	decanal
3150	tetradecanoic acid
3331	pentadecanoic acid
3505	hexadecanoic acid
3800	octadecenoic acid
3831	octadecanoic acid

Table 3.21: Volatile metabolites identified in the microbial extract of micro-organism L2.2 in TSB (3 days).

In TIC Fig. 3.20	Compound
254	2-butanone
474	pyrazine
510	dimethyl disulphide
525	3-methyl-pentanone
689	methyl-pyrazine
813	ethylbenzene
926	2,5-dimethyl-pyrazine
1068	benzaldehyde
1509	2-phenylethanol
1786	trimethyl-pyrazine
2907	tetradecanoic acid

Table 3.22: Volatile metabolites identified in the microbial extract of micro-organism L2.2 in TSB (10 days).

In TIC Fig. 3.21	Compound
479	3-methyl-1-butanol
920	2,5-dimethylpyrazine
2900	tetradecanoic acid
3251	hexadecanoic acid
3543	octadecenoic acid
3580	octadecanoic acid

Table 3.23: Volatile metabolites identified in the microbial extract of micro-organism L2.2 in TSB (30 days).

In TIC Fig. 3.22	Compound
555	pyrazine
565	3-methyl-3-buten-1-ol
579	3-methyl-1-butanol
602	dimethyl disulphide
625	3-methyl-pentanone
828	methyl-pyrazine
974	ethylbenzene
1105	2,5-dimethyl-pyrazine
1128	2,3-dimethylpyrazine
1256	benzaldehyde
1383	trimethylpyrazine
1560	butylbenzene
1717	2-phenylethanol
2328	benzeneacetamide
3479	hexadecanoic acid

Table 3.24: Volatile metabolites identified in the microbial extract of the total microbial community in MSM (10 days).

In TIC Fig. 3.23	Compound
259	3-penten-2-ol

Table 3.25: Volatile metabolites identified in the microbial extract of the total microbial community in MSM (30 days).

In TIC Fig. 3.24	Compound
243	3-methyl-3-buten-2-one
260	3-penten-2-ol
3972	squalene

Table 3.26: Volatile metabolites identified in the microbial extract of micro-organism R1.1 in MSM (3 days).

In TIC Fig. 3.25	Compound
4060	cholesterol

Table 3.27: Volatile metabolites identified in the microbial extract of micro-organism R1.1 in MSM (10 days).

In TIC Fig. 3.26	Compound
2698	tetradecanoic acid
3044	hexadecanoic acid
3357	octadecanoic acid

Table 3.28: Volatile metabolites identified in the microbial extract of micro-organism R1.1 in MSM (30 days).

In TIC Fig. 3.27	Compound
256	3-penten-2-ol

Table 3.29: Volatile metabolites identified in the microbial extract of micro-organism R1.2 in MSM (3 days).

In TIC Fig. 3.28	Compound
191	2-methyl-3-buten-2-ol
249	3-methyl-3-buten-2-one
269	3-methyl-3-buten-2-ol
350	3-methyl-1-butanol
2068	tetradecanoic acid
2364	hexadecanoic acid

Table 3.30: Volatile metabolites identified in the microbial extract of micro-organism R1.2 in MSM (10 days).

In TIC Fig. 3.29	Compound
248	3-hydroxy-2-butanone

Table 3.31: Volatile metabolites identified in the microbial extract of micro-organism R2.1 in MSM (3 days).

In TIC Fig. 3.30	Compound
235	3-methyl-butan-2-one
2068	tetradecanoic acid
2364	hexadecanoic acid

Table 3.32: Volatile metabolites identified in the microbial extract of micro-organism R3.1 in MSM (10 days).

In TIC Fig. 3.33	Compound
160	2-methyl-3-buten-2-ol
182	3-methyl-butanal
203	3-penten-2-ol
249	2-methyl-2-butenal
287	3-methyl-2-butenal
344	3-methyl-3-buten-2-ol
353	4-hydroxy-4-methyl-2-pentanone
434	heptanal
573	octanal
710	nonanal
842	decanal
910	2-decenal
1033	2-undecenal
1441	tetradecanoic acid
1623	hexadecanoic acid
1769	9-octadecenoic acid
1788	octadecanoic acid
2535	squalene

Table 3.33: Volatile metabolites identified in the microbial extract of micro-organism R4.2 in MSM (10 days).

In TIC Fig. 3.35	Compound
267	3-penten-2-ol
2703	tetradecanoic acid
2878	pentadecanoic acid
3010	9-hexadecenoic acid
3046	hexadecanoic acid
3323	9-octadecanoic acid
3361	octadecanoic acid

Table 3.34: Volatile metabolites identified in the microbial extract of micro-organism R4.2 in MSM (30 days).

In TIC Fig. 3.36	Compound
214	3-penten-2-ol

Table 3.35: Volatile metabolites identified in the microbial extract of micro-organism R2.1 in MSM (3 days).

In TIC Fig. 3.38	Compound
214	3-penten-2-ol